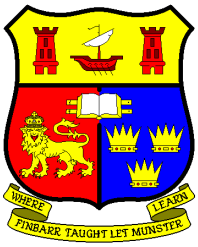
CORA Cork Open Research Archive
Cartlann Taighde Oscailte Chorcaí

Title	Engineering design of an integrated sustainable process system for cassava biobased materials
Authors	Tumwesigye, Kashub S.
Publication date	2016
Original Citation	Tumwesigye, K. S. 2016. Engineering design of an integrated sustainable process system for cassava biobased materials. PhD Thesis, University College Cork.
Type of publication	Doctoral thesis
Rights	© 2016, Kashub Steven Tumwesigye. - http://creativecommons.org/licenses/by-nc-nd/3.0/
Download date	2026-11-06 15:31:58
Item downloaded from	https://hdl.handle.net/10468/3301



UCC
University College Cork, Ireland
Coláiste na hOllscoile Corcaigh

National University of Ireland, Cork



University College Cork

ENGINEERING DESIGN OF AN INTEGRATED SUSTAINABLE PROCESS SYSTEM FOR CASSAVA BIOBASED MATERIALS

Kashub Steven Tumwesigye

A thesis presented to the National University of Ireland for the Doctor of Philosophy (PhD, Engineering) degree

With the supervisory guidance of

Dr. Maria J. Sousa Gallagher

Dr. Jorge C. Oliveira



Process & Chemical Engineering,
School of Engineering,
College of Science, Engineering and Food Science

June, 2016

DECLARATION

I declare that the thesis submitted is my own work and has not been submitted in entity for another degree, either at University College Cork or elsewhere. I certify that the thesis contents are the research efficacy and effectiveness except where otherwise indicated. I declare that all external references and sources are clearly acknowledged and identified within the contents. I have read and understood the regulations of University College Cork concerning plagiarism.



This thesis is dedicated to my late father Kosia Kashubiriro and mother Edith Kashubiriro, whose incessant work and sweat to ensure that I belong to educated elites of Kashenyi village community, has been an inspiration for my education.

My further thesis dedication goes to my lovely son, Alvin Ayesigye, and my wife, Mrs. Edith Tumwesigye, whose care and encouragement I cannot overemphasize.

EXECUTIVE SUMMARY

Cassava (*Manihot esculenta* Crantz) is an important crop for biobased material development globally. In the broad area of biobased material development, sweet cassava constitutes the biggest portion of the natural biomaterial sources than bitter cassava. Bitter Cassava has lagged behind, and employed mainly as an emergency famine crop, but can also be used as a value added biomaterial material for broad range application. The conventional approach for production of cassava biopolymer derivatives (BPD) is accompanied by significant wastes with potential negative environmental impact. Among the BPD, starch has been used as lone additive in most formulations. However, starch matrices have been the most challenging, causing difficulties in the development of uniform tailored materials and limiting industrial applications. Attempts have been made to reinforce and modify starch formulations in order to improve their functional properties, but also counteract its deficits and improve material development and foster applications. However, variability in starch properties implied high production costs as well as adding wastes to the environment during its processing, limit cassava applications for industrial development of biomaterials. This challenge has been compounded by the increasing use of bitter cassava varieties with high toxic total cyanogens. Thus, transforming waste cassava into a sustainable resource requires a new approach and redesign of the current processing methodologies. Exploiting integrated sustainable engineering process design of all BPD, is a novel approach in designing efficient system of cassava biobased materials for food and non-food applications. Exploring possibilities for tapping advantages inherent in cassava root should be prioritised in order to address, synergistically, intrinsic cassava issues so as to indirectly provide solutions to increasing environment wastes and associated management costs. Harnessing innovations in downstream processes and new biomaterials which are unexplored, underutilized or region-specific, can facilitate low-cost and energy-efficient material production, indirect waste management and lead to zero environmental footprints. Simultaneous release recovery cyanogenesis (SRRC) is hereby proposed as a novel downstream process improvement that can result in necessary modifications of cassava processing.

The ultimate goal of this study was to propose an integrated sustainable process system for cassava biobased materials development, and demonstrate its potential broad application. Processing of intact bitter cassava can minimise waste, and produce low-

cost added value biopolymer packaging films for targeted applications. This aim was achieved through: (i) development and (ii) standardisation of a methodology for elimination of waste and production of widely applicable cassava-rich biopolymer derivatives material. This presents a novel downstream processing method for intrinsic modification of intact root via simultaneous release recovery cyanogenesis (SRRC); (iii) formulation of biopolymeric film prototypes and assessment of their properties for food application. Besides, an attempt was made to evaluate them for different applications, such as non-food uses; (iv) quantification of film mass transport behaviour simulating different relative humidity and temperatures during supply chain. The purpose was to gain an understanding of film performance and resilience when they are placed in the distribution chain environments; (v) optimisation of film prototypes for desirable properties; (vi) development of an integrated process design for effective use of cassava wastes, and development of sustainable packaging materials; and (vii) demonstration of application of biopolymer flexible films for the development of desired atmosphere packaging to extend shelf life of products; (viii) derivatives for the development of nutraceutical excipient micronutrient carrier tablet for fast delivery systems; and (ix) coatings for antifungal active food packaging.

An extensive critical review was performed on the progress of cassava biobased packaging research applications, the current and emerging technologies to solve cassava wastes, and cassava biobased packaging research application challenges were highlighted, and possible revisions suggested. The potential of integrated sustainable engineering process design framework for packaging system was also discussed.

A novel SRRC downstream processing methodology for sustainable reduction of intact bitter cassava waste was developed, along with biopolymer derivatives (BPD) and films packaging material. The peeled (BP) and intact (BI) bitter cassava biopolymer derivatives were produced and analysed for waste reduction, yield, and total cyanogen and amylose contents. The standardisation of the methodology for production of BPD was demonstrated by desirability optimisation of the SRRC process. The parameters used in the optimisation were buffer, 0, 2, 4 % v/v, cassava waste solids, 15, 23, 30 % w/w, and extraction time, 4, 7, 10 minutes, and the responses included yield and colour. The global desirability (0 to 1) was used in the prediction of material balances to produce the desired yield and colour. The optimal conditions were validated experimentally using buffer, 3.3 % w/v, cassava waste solids, 30 % w/w and extraction

time, 10 minutes. Validated BPD was characterised using SEM, DSC, TGA, FTIR and moisture barrier analyses. The BPD was used in producing films, which were characterised in terms of transparency, homogeneity, solubility, permeability to moisture, oxygen and carbon-dioxide, less hydrophilicity and sealing ability for food application.

Mechanistically fluid-phase solvent mass transport in IBC packaging films was quantified under variable RH and temperature. IBC films were tested for solvent solubility, swelling ratio, sorption and permeability to water vapour and oxygen at 10-40°C, 10-90 % RH (adsorption) and 75, 85, 95% RH (transfer rates). Film's structural alterations were characterised by their thermal and chemical properties.

The optimal processing conditions, which define the most desirable properties, were determined, and films were developed following a Box-Behnken response surface design, and optimised using multi-response desirability. The parameters and conditions used included cassava (2, 3, 4 % w/v), glycerol (20, 30, 40 % w/w), and drying temperature (30, 40, 50°C).

In order to use cassava wastes effectively, and develop sustainable packaging materials, an integrative seven-unit process model flow was considered in the process design. Individual processes, within the SRRC, were modelled, optimised and integrated.

The effect of equilibrium atmosphere packaging (EMAP) design parameters on gas composition for cherry tomatoes was assessed and optimised, using an experimental design with 4 factors and 2 levels (bio-based, non-bio-based films; 0, 1 perforation; 10, 20°C; 75, 95 % RH). Package oxygen composition was analysed in duplicate using a non-invasive optical oxygen sensor until the equilibrium was reached. The performance of bio-based IBC film was compared with non-bio-based oriented polypropylene (OPP) film for EMAP.

The properties of SRRC-processed peeled and intact bitter cassava powders suitable for making iron and zinc tablet excipients were determined, as well as disintegration time and in-vitro dissolution rate. A preliminary screening, designed to select the powder derivative, with best tableting properties for fast Iron (Fe) and zinc (Zn) delivery was conducted. Microcrystalline cellulose was used as a reference material with known properties for developing drug excipients. Peeled and intact bitter cassava derivatives (PD) were characterised for properties suitable for making tablets. Wet granulation of PD were used for tablet formulation with Fe and Zn. Disintegration and in-vitro release

were performed in deionized water, pH 1.2 and pH 6.8 media, at 37°C. Kinetic models were used for describing matrix dissolution and Fe/Zn release mechanisms.

Application of biopolymer coatings for antifungal active food packaging was demonstrated, by evaluating the capacity of intact bitter cassava polysaccharide-rich derivatives (PD) to encapsulate thymol, and their antifungal effect and strength on stored strawberries using qualitative methods. Four coatings were formulated with intact bitter cassava polysaccharide-rich derivative (2 % w/v), glycerol (40 % w/w) and thymol (0.25, 0.5, 0.75 and 1.0 % w/v), and analysed by their encapsulation efficiency, permeability to water vapour, surface energy and wetting, and antifungal activity.

Previous work showed that sweet cassava starch is extensively used in biobased materials, and its production using conventional methods (at all processing levels) generated significant wastes (20-30% w/w). In addition, the shortfalls in starch resulted in their matrix physical & chemical modifications. Together, with multiple processes applied to add value to wastes caused high cost & high energy of material production, and limited their commercial use. Furthermore, the review revealed that there is scanty information on research that attempted to validate starch based packaging materials in real conditions of the supply chain. There is potential of using holistic approaches to cassava biobased material development.

This study showed that using this novel SRRC process, intact bitter cassava (BI) produced significantly higher biopolymer derivative yields than peeled (BP), guaranteeing 16 % waste decrease with no environmental impact caused by discard residues. SRRC reduced effectively the total cyanogen content to within Codex minimum safety limits, demonstrating that the peeling of bitter Cassava process can be avoided. An integrated process methodology transformed nearly all the intact root into BPD with higher yield, 41 % w.b. and colour difference, 1.3 in contrast to 26 % w.b. yield and 28 colour difference when cassava starch was extrinsically processed. Efficient material balance was predicted at optimal global desirability, 1.0 in order to produce BPD with yield, 38.8 % w.b. when using buffer, 4.0 % w/v, cassava waste solids, 23 % w/w and extraction time, 10 minutes, for producing BPD with yield, 38.8 % w.b. Experimental validation, with buffer, 3.3 % w/v, cassava waste solids, 30 % w/w and extraction time, 10 minutes, produced BPD with 40.7 % w.b. yield. The BPD produced films which were more transparent and homogeneous, less soluble, less permeable to moisture, less hydrophilic, more permeable to oxygen and carbon-dioxide,

sealable, lower cost, than the BP. The uniform microstructure and high thermal stability of BPD and film demonstrated efficient performance of the standardised integrated methodology.

Processing intact bitter cassava root using a standardised integrated SRRC can be used to produce sustainable low cost BPD and films for a broad range of applications. Methodologies designed around standard integrated procedures, matching zero-based approach to contamination elimination, are novel strategies, and if they are used effectively and widely can provide better avenues to eliminate cassava wastes and recover BPD resources as sustainable biomaterials.

Modified-BET (R^2, 1.0; deviation, 3-4%) and Peleg (R^2, 1.0; deviation, 3-5%) models best described the sorption data. The temperature dependence of permeability for water vapour through films is best simulated by Arrhenius and WLF models (R^2, 0.999), while that of oxygen was influenced by crystalline and high RH. The diffusion of non-organic and organic solvents through films followed case II non-diffusional and Fickian patterns, respectively. Solvents through films induce structural changes in IBC films with concentration-dependent diffusion.

Developed models predicted impact of processing conditions on film properties. Desirable film properties for food packaging were produced using the optimised processing conditions, 2 % w/v cassava, 40.0 % w/w glycerol, and 50°C drying temperature. These processing conditions produced films with 0.3 %; transparency, 3.4 %; solubility, 21.8 %; water-vapour-permeability, 4.2 $gmm.M^{-2}.day^{-1}kPa^{-1}$; glass transition, 56°C; melting temperature, 212.6°C; tensile strength, 16.3 MPa; elongation, 133.3%; elastic modulus, 5.1 MPa; puncture resistance, 57.9 J, which are adequate for packaging applications.

The release process models, predicted the maximum yield (45.8 %) and the maximum total cyanogens (0.6 ppm) and colour difference (4.0) needed to avoid wastes and unsafe biopolymer derivatives. The process design allowed saving on the energy and water due to its ability to reuse wastewaters in the reactions and release processes. Drying rates, Scanning Electron Micrograph, Differential Scanning Calorimetry, Water vapour transmission rate and Fourier transmission infrared spectroscopy analyses have demonstrated the practical advantage of laminar flow hood air systems over oven-drying heat for an integrated design process. Thus, integrated design process could be used as a green tool in production of cassava products with near zero environmental waste disposal.

Intact bitter cassava film (IBCF) in-package O_2 composition reached equilibrium at 2 % and 3 %, after 180 h (over 7 days) at 10°C, with 0 or 1 perforation, for 75% and 95% RH respectively. This ensured that the mould growth on cherry tomato surface was inhibited until 15-19 days of storage at 10^0C. The similarities in the equilibrium O_2 composition of 2 % between perforated and non-perforated suggest that there would not be need to perforate IBCF. Besides, there is need to establish the possible structural changes likely to occur in IBCF at high RH. Factorial analysis on package performance showed that film type, perforations, temperature, relative humidity, and their interaction had varying significant ($p \leq 0.05$) effects on O_2 composition. Temperature and RH influenced IBCF significantly, whereas perforations, temperature and their interaction impacted on OPP significantly. Desirable O_2 and CO_2 composition of 3.11 and 4.73 % for IBCF EMAP of cherry tomatoes was achieved with optimised design parameters, 10°C, 75 %RH, 0 mm, while one of OPP (7.65 % and 11.39%) did not fall within the recommended 3-5 % O_2 composition; hence, IBCF can be an alternative film for EMAP. Demonstration of the potential application of IBC film for EMAP was shown.

Application of biopolymer derivatives for the development of nutraceutical excipient micronutrient carrier tablet for fast delivery systems was demonstrated. Intact bitter cassava PD allowed formulation of tablets, showing better properties than peeled cassava PD, to which the tablets were selected for in vitro dissolution studies. Tablet excipient matrices demonstrated faster dissolution and Fe/Zn release within 30 to 45 min, across all tablet weights, with dissolution rates of about 90%. All the kinetic models described the release mechanism, with best fits ($R^2 > 0.85$). The study highlights potential of intact bitter cassava polysaccharide-rich derivatives as an excipient that can enhance fast releases of Iron and zinc. The recovered biomaterial from waste cassava may provide broader applications as potential alternative nutraceutical excipients.

All the four coatings developed had higher encapsulation efficiency (> 95%), which was concentration-dependent. Coating permeability to water vapour was in the range of 4.89-0.02 g mm / (m^2 day kPa), and was inversely proportional to coating concentration. Coating wettability occurred at medium to high contact angles (88.71-111.26^0) and decreased as thymol concentration increased, and this facilitated better and smooth coating of the strawberries. Coatings demonstrated efficient antifungal activity in strawberries, with mould-growth inhibition reaching beyond 14 days of storage. These results have significant implications for the design of antifungal systems based on intact bitter cassava/natural bioactive-coating dispersions.

Cassava biobased materials should be improved using a holistic approach reflecting the target products, variable environment, minimising production costs and energy. Use of novel material resources, eliminating waste, and employing a standardised methodology via desirability optimisation, present a promising process integration tool for development of sustainable cassava biobased systems. The outcomes of this research through an integrated process design have potential applications:

1. Mitigating the challenging issue of cyanogens in bitter cassava provides a path for use in bioderivatives development and other applications, but also a paradigm of economic and well-being of communities which use bitter cassava.
2. Intact bitter cassava use leads to zero waste, and will help to reshape the current style one-way processing designs into circular designs modelled on nature's effective approaches. This will also benefit SME processing units achieve a local system that functions efficiently, sustains the environment, and delivers self-sufficiency. Moreover, this will lead to indirect waste elimination instead of waste management.
3. Inclusion of indigenous cassava components as natural material reinforcements for bioderivatives
4. The SRRC is a novel improvement approach to downstream processing of novel bio-derived products
5. Other potential applications:
   a. By-product’s regulation for waste elimination, reduction in costs of waste management and recycling,
   b. Generally, in processes which require efficient use of energy resources, reduction in cost of production, and other integration of product process designs;
   c. Development of tailored materials for both food and non-food uses: i) packaging films and edible coatings; ii) biobased bags for plastics replacement;
   d. As ingredients in food industry and excipients in drug delivery;
6. Ultimately, this has initiated a process which may lead to a wider utilisation in broad product research development.
7. Finally, this research contributes to scientific knowledge in material science and engineering process design.

Keywords: Bitter cassava; Green processing; Waste-reduction; Biopolymer derivative;

Packaging film; Mass transfer; Quantitative; Mechanistic; Relative humidity; Temperature-dependence; Desirability optimization; Standardization; Optimal design; Process integration; Sustainable system; Modified-atmosphere packaging; Cherry tomato; Nutraceutical; Tablet excipient; Delivery system; Iron; Zinc; Coating; Thymol-encapsulation; Antifungal; Strawberries.

ACKNOWLEDGMENTS

The PhD Programme has been supported by National Agricultural Research Organisation (NARO-Uganda), within the World Bank-East African Agricultural Productivity Project (EAAPP) framework. The financial and material assistance rendered during the course of research is appreciatively recognised.

I am indebted to Dr. Maria de Sousa Gallagher for the consistent supervisory guidance. The resolute patience, encouragement, participatory orientation, unconditional and enduring support provided to me is by far unrivalled. The words of encouragement, such as, “do not run before you crawl”, “let us not re-invent the wheel”, and “see where we are coming from”, were exciting, but also of a good supervisor character. These and more yet to come, are bound to shape my present and future career.

I would like to applaud Dr. Jorge Oliveira, to who I first communicated for what has come to be a foundation for my PhD. His acceptance has seen me through this PhD programme. I had many university admissions choice options, and I do not regret for the choice I made. Further, I will not forget his supervisory role qualities offered to me, which will go along to shape my career and future.

The complete story of my thesis would not be possible without the unconditional academic guidance and provision of an enabling analytical atmosphere of Dr. Abina Crean. Her cordial welcome, willingness to provide the required information, and ease of access were awesome.

A very special attention is drawn to my family. It has tirelessly seen me through all the trying moments. My absence has been felt, and has had a significant impact on the way and how far they would be. Nonetheless, I take to them good news of encouragement that the best is yet to come.

My sincere thanks go to Dr. Denis Ring for his unconditional support in analytical work provided to me. I would like to note that it is a rare situation to receive such favours from a person who was not part of the supervisory team.

My thankfulness goes to the Process and Chemical Engineering technical team for their significant support offered along my research undertakings. The "JPT" initialism-John, Paul, Tim, has been synonymous with the day-to-day operation of my work. Such assistance will never be forgotten as I develop my career. In particular, Paul Conway has been inspirational and outstanding. If Paul is not providing the fastest service I have not witnessed in many years, his jokes are stimulating, removing stress and making your day. Paul, you deserve the best from the Department and School of Engineering. I will not forgetting the e-services of John Barrett. To be honest, you seldom get such a prompt service. John is always available, and without explaining much, you get to see him rising from the seat and rushing to attend to the computer issues. Such characters are occasional, but common in John.

Special recognition goes to Ms. Anne-Marie McSweeney. I cannot describe her fully or even overemphasise her unrivalled support. The fastest communication attention I have received from Anne-Marie are unmatched, and I say bravo for all her untiring efforts and assistance with visas, university, accommodation, laboratory and office aids, to mention but a few. Anne-Marie, I will not forget your ever warm and smile welcome whenever a service is sought. I know everyone who has received a service from you will attest to this acknowledgement.

I would like to appreciate NARL-Kawanda colleagues and community with the support offered in processing the experimental materials. The diligence and methodological details have shaped my PhD research. I owe you a committed service.

Special cheers go to my Postgraduate colleagues, Andresa Viana Ramos, Raghu Vamshi Peddapatla, Ashutoshi Tank and Rita Sousa. As the UCC motto goes, "Great minds do not think alike …", your independent thinking has contributed greatly to my success. In particular, my special appreciations go to Andresa and Raghu. Andresa has been such an exciting academic colleague, willing to assist as far as she could. I say, the future is bright for you. I must say that Raghu has been an outstanding academic colleague, and his exemplary character made a significant contribution to the success of my PhD. To you Raghu and Andresa, for every peer group, there is always one, who through absolute vision, ultimate professionalism and meritorious eccentric, stand head and shoulders above his/her peers.

To my Mexican colleagues, friends and academic mates, Dr. Julio Montanez, Dr. Lourdes Morales Oyervides, Dr. Evangelina Garcia Amenta and Ms. Alejandra Osorio Fierros. This is the moment to express my gratitude and say thank you very much for your academic assistance, but also the social support I have enjoyed has been scintillating. Bravo to “Mehiko” group.

Finally, to my mother, Edith Kashubiriro, late father Kashubiriro, late uncle, Tibesigwa, and my sister, Medrin Kyomuhangi for bringing me up, and providing the early and rare opportunity of education. From the centre of my heart, I sincerely thank you very much.

SECTION 1

GENERAL INTRODUCTION

Background

Global environmental impact challenges such as supply chain by-product waste streams, high waste management costs, finite natural material sources and competition for food supply, have drawn much interest to invest in sustainable systems. Previously, environmental waste disposal, accruing from linear and irreversible behavioural patterns defined by produce–consume and dispose models, have resulted in significant negative environmental impacts. Up until recently, the concept of integrated sustainable process system has not been conceived and comprehended in various process designs and developments. Holistic approaches to process design, which reflect interactions and associated synergisms, could form an essential component of sustainability. Evaluation of novel options, using efficient, inexpensive and green processes/techniques including waste utilisation through addition of value to by-products (recovery and modification into reusable materials and energy), may provide solutions to sustainable systems.

Cassava (*Manihot esculenta* Crantz) positions itself among crops with the most desired biomaterials for broad range of applications. It is inexpensive with high polysaccharide proportions of starch, holocellulose, hemicellulose, cellulose, lignin, monosaccharides and other secondary metabolites. Additionally, cassava is fully degradable, renewable resource and versatile. The conventional process of sweet cassava polysaccharide starch involves many stages of refinements that produce a number of by-products such as solid waste, wastewater and their metabolic derivatives. However, the impact of these wastes discharged from this process contributes significantly to hazardous wastes, industrial disasters and environmental and human risks globally. In addition to sweet cassava-based high waste volumes, the high total cyanogen bitter variety, and its associated conventional poor and unilateral processing methodologies, has often compromised product and human safety thereby indirectly contributing to more wastes. Throughout the past two decades, sweet cassava has been an integral component of biobased packaging material, notably its derivatives have contributed significantly to edible films and coatings. However, starch matrices have been the most challenging, causing difficulties in the development of uniform tailored materials and limiting industrial applications. Recently, much attention has been dedicated on external reinforcements

and modifications as solutions for counteracting starch deficits in order to improve material development and foster applications. In spite of copious scientific successes regarding package material improvements, their variability in properties and high production costs, limit cassava applications for industrial development of biomaterials.

Exploring possibilities for tapping advantages inherent in cassava root should be prioritised in order to address, synergistically, issues intrinsic to cassava, as well as environment-borne concerns. This may offset cassava drawbacks and contribute to sustainable approaches. Harnessing innovations in downstream processes and new biomaterials which are unexplored, underutilized or region-specific, can facilitate low-cost and energy-efficient material production, indirect waste management and lead to zero environmental footprints. Simultaneous release recovery cyanogenesis (SRRC) is hereby proposed as a novel downstream process improvement that can result in necessary modifications of cassava processing. SRRC is a highly efficient and low-cost modification process in terms of its provision of derivative-rich polysaccharides, delignification ability, detoxification capacity, and easy to handle in a single process. Unlike in the conventional process whereby polysaccharides are obtained individually in different process, SRRC makes it easy to isolate them in a single process using intrinsic processes in the intact root. This contributes to the utilisation of what would be wasted thereby making the whole process cost-effective, energy-efficient and time saving. Delignification aids in release of cellulose and holocellulose, and clarifies material colour. Detoxification is achieved by intrinsically hydrolysing linamarin with enzyme linamarase leading to release of highly toxic hydrogen cyanide in the process of cyanogenesis. Reduction in lignin and total cyanogens is crucial before the pulp is subjected to the reactions process. Conventionally, all the above was achieved in different processes, and in this study it is achieved by the application of SRRC process.

Together, integrating downstream market product development processes into the design of upstream processes, could eliminate barriers, and improve adoption and application of cassava biobased materials in industry. Engineering design of an integrated sustainable process system for cassava biobased materials requires thorough consideration of holistic approaches. These should incorporate inexpensive cassava biomaterials, improvement in the downstream processing, green and synergistic processes and adding value to wastes. Finally, with an understanding of the impact of

supply chain conditions on material development and performance can maximise cassava biobased materials.

Thesis statement, objectives and rationale

Sweet cassava has been extensively studied for packaging, mainly in edible and antimicrobial films for food and non-food applications. In spite of these stimulating studies, further consideration is needed to improve cassava biobased materials for diverse applications. An alternative approach is to consider a holistic development system. A holistic approach to the development of cassava biobased materials with suitability and broad-based application is a function of a whole process design and development, as an integrated, complementary, and synergistic system. Thus, consideration of cassava biopolymer derivatives, the process development methodology, optimisation of the process conditions and parameters, environment, and associated interactions, is vital to add value to materials. The whole system must take into account green, low-cost and energy-efficient engineering processes in order for it to be sustainable.

The fundamental work is premised on, and anchored by, the thesis statement that provided the basis for all studies in the thesis: "A Holistic approach to processing, incorporating standardisation and integration, result in development of sustainable cassava biobased systems"

The ultimate aim of this study was to propose an integrated sustainable process system for cassava biobased materials development, and demonstrate its potential broad application. Bitter cassava was used as a natural biomaterial model; nonetheless the process can be used with other natural biomaterials. This aim was achieved through:

1. Development and standardisation of a methodology for elimination of waste and production of widely applicable cassava-rich biopolymer derivatives material. This presents a novel downstream processing method for intrinsic modification of intact root via simultaneous release recovery cyanogenesis (SRRC);

2. Formulation of biopolymeric film prototypes and assessment of their properties for food application. Besides, an attempt was made to evaluate them for different applications, such as non-food uses;
3. Quantification of film mass transport behaviour simulating different relative humidity and temperatures during supply chain. The purpose was to gain an understanding of film performance and resilience when they are placed in the distribution chain environments;
4. Optimisation of film prototypes for desirable properties;
5. Development of an integrated process design for effective use of cassava wastes, and development of sustainable packaging materials; and
6. Demonstration of application of biopolymer:
    - 6.1 Flexible films for the development of desired atmosphere packaging to extend shelf life of products;
    - 6.2 Derivatives for the development of nutraceutical excipient micronutrient carrier tablet for fast delivery systems; and
    - 6.3 Coatings for antifungal active food packaging.

Contribution to scientific knowledge

The ongoing research on cassava biobased material focuses on reinforcing starch matrices with externally-sourced polysaccharides like cellulose in order to improve physical, chemical and functional properties. However, within the root a reasonable proportion of these polysaccharides are present, apparently wasted as by-products during starch production. These conventional processes lead to significant disposal of wastes in form of by-products, and the reinforcements require additional processes with cost implications. In this work, the focus is uniquely on the reinforcements within the root, with the objective of optimising the process, utilising the byproducts and reducing the waste at low-cost. This is achieved by use of SRRC processing of intact root, purposely to increase value and reduce or eliminate waste through research.

Biobased materials centred on sweet cassava have been used extensively in research and application. Sweet cassava seems to have rivalled demand both in food supply and as an industrial raw material. In a situation of global population explosion, sources of biomass

should not compete with the crops necessary to provide food. Exploring novel alternative sources of bitter cassava is not only an improvement on easing the current cost and competition of biomaterials but ensuring the safety of bitter cassava and producing unrivalled biomaterial. Utilisation of bitter cassava is an additional strategy of indirectly adding to reduction of by-product wastes.

Modelling of processes has been used extensively in the optimisation of many different types of systems and materials, including cassava biobased materials. However, in the conventional approaches, these processes have been optimised separately. Using a holistic approach to process design, which emphasises unified processes and considers interactions and synergisms between different processes is a novelty on conventional modelling and optimisation methodologies and processes for cassava biobased materials. By using SRRC that entails intrinsic modification, optimisations in release and recovery, and exploiting synergisms in reuse in reaction material, and integration of novel materials on different applications is innovative. This has not been performed in the development of sweet cassava biomaterials.

The outcomes of integrated process design have potential applications:

1. In proper by-product's regulation for waste elimination, reduction in costs of waste manage and recycling,
2. Generally, in processes which require efficient use of energy resources, reduction in cost of production, and other product integration process designs;
3. Development of tailored materials for both food and non-food uses such as:
    3.1 Edible and non-edible food packaging films and coatings;
    3.2 Biobased bags for waste management and replacement of food plastics in the market;
4. As ingredients in food industry and excipients in drug delivery, and
5. Ultimately, this has initiated a process which may lead to a wider utilisation in broad product research development.

Finally, the research contributes to scientific knowledge in material science and engineering process design.

Thesis structure

This thesis is structured in three different sections, comprising a total of 9 chapters. The first section consists of Chapter 1 and presents the literature review. The second section is broken down into 5 chapters, which describe the experimental fundamentals of the study (Chapter 2 to 6). The third section of this study is composed of three chapters (Chapter 7 to 9), highlighting the potential application of the materials obtained from intact bitter cassava.

Chapter 1 presents a critical review on the progress of cassava biobased material research applications in the last decade, current and emerging techniques and methodologies to address cassava wastes. Furthermore, cassava research challenges encountered in biobased material application as well as the potential of integrated sustainable engineering process design framework for material development system are described.

Chapter 2 describes the development of an improved SRRC downstream processing methodology with intact bitter cassava. Waste reduction and biopolymer derivatives production are also investigated.

Chapter 3 reports the results of the standardisation of the methodology to produce biopolymer derivatives. An attempt was made to produce films to support the validity of the standardised methodology.

Chapter 4 gives an account of the mass transport system of intact bitter cassava films under different storage conditions of temperature and relative humidity.

Chapter 5 reports the results of desirability optimisation of cassava packaging development.

Chapter 6 presents an integrated process design system for cassava as a tool to use cassava waste in a cost-effective and energy-efficient manner. It presents a holistic approach to develop cassava biobased systems.

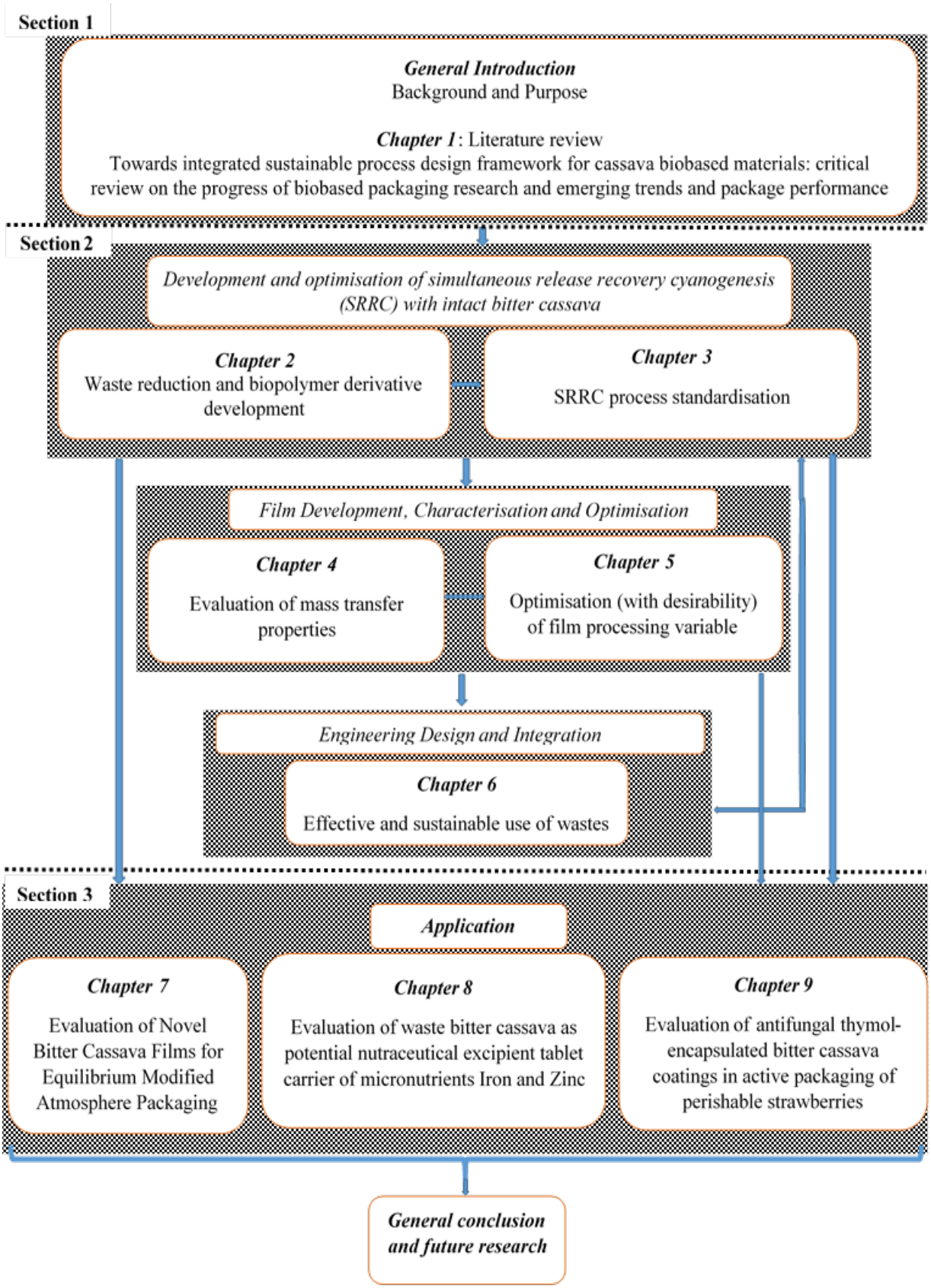
Chapter 7 provides an insight into application of cassava biobased films in modified atmosphere packaging of tomatoes.

Chapter 8 provides an insight into application of cassava biobased derivatives as an excipient tablet carrier of micronutrient Iron and zinc.

Chapter 9 provides an insight into application of cassava biobased derivatives as coatings in antifungal active packaging of strawberries,

Lastly, a general conclusion and future perspectives are presented.

The structural summary of this thesis, illustrating the linkage and interaction of different chapters is schematically presented hereunder.


Section 1
General Introduction
Background and Purpose
Chapter 1: Literature review
Towards integrated sustainable process design framework for cassava biobased materials: critical review on the progress of biobased packaging research and emerging trends and package performance
Section 2
Development and optimisation of simultaneous release recovery cyanogenesis (SRRC) with intact bitter cassava
Chapter 2
Waste reduction and biopolymer derivative development
Chapter 3
SRRC process standardisation
Film Development, Characterisation and Optimisation
Chapter 4
Evaluation of mass transfer properties
Chapter 5
Optimisation (with desirability) of film processing variable
Engineering Design and Integration
Chapter 6
Effective and sustainable use of wastes
Section 3
Application
Chapter 7
Evaluation of Novel Bitter Cassava Films for Equilibrium Modified Atmosphere Packaging
Chapter 8
Evaluation of waste bitter cassava as potential nutraceutical excipient tablet carrier of micronutrients Iron and Zinc
Chapter 9
Evaluation of antifungal thymol-encapsulated bitter cassava coatings in active packaging of perishable strawberries
General conclusion and future research

The information presented in the 9 chapters are partially, and in some instances, fully based on the published works listed hereunder:

Chapter 1: Tumwesigye, K.S., Oliveira, J.C., & Sousa-Gallagher, M.J. (2016). Integrated sustainable process design framework for cassava biobased packaging materials: critical review of current challenges, emerging trends and prospects, *Trends in Food Science & Technology*, 56, 103-114.

Chapter 2: Tumwesigye, K.S., Oliveira, J.C., & Sousa-Gallagher, M.J. (2016). New sustainable approach to reduce cassava borne environmental waste and develop biodegradable materials for food packaging applications. *Food Packaging and Shelf Life*, 7, 8–19.

Tumwesigye K.S., Oliveira J.C., & Sousa-Gallagher M.J. (2014). Intact bitter cassava processing can reduce waste and produce biopolymer packaging materials, Advances in Food processing-Challenges for the future, *In Programs & Abstracts,* O7.4, 5-8 Nov. 2014, Campinas, Brazil.

Tumwesigye K.S., Oliveira J.C., & Sousa-Gallagher M.J. (2014). Bioprocessing of bitter cassava solid waste for sustainable production of bio-based packaging materials, Eastern African Agricultural Productivity Program. April 2014, Entebbe Uganda.

Chapter 3: Tumwesigye, K.S., Peddapatla, R.V.G., Crean, A., Oliveira, J.C., & Sousa Gallagher, M.J. (2016). Integrated process standardisation as zerobased approach to bitter cassava waste elimination and widely-applicable industrial biomaterial derivatives, *Chemical Engineering and Processing*, 108, 139-150.

Chapter 4: Tumwesigye, K.S., Oliveira, J.C., & Sousa-Gallagher, M.J. Quantitative and mechanistic analysis of impact of novel cassava processing on fluid

transport phenomenon in humidity-temperature-stressed biobased films. (Prepared *Manuscript ready for submission*)

Leahy M.L., **Tumwesigye K.S**., Montanez J.C., Oliveira J.C., & Sousa-Gallagher M.J. (2015). Moisture sorption behaviour of intact bitter Cassava packaging films at different temperatures, 44th Annual Food Research Conference, 14th December 2015, Teagasc Food Research Centre, Moorepark, Fermoy, Co. Cork. *Conference Proceedings.*

McNulty R., **Tumwesigye K.S**., Montanez J.C., Oliveira J.C., & Sousa-Gallagher M.J. (2015). Effect of temperature and relative humidity on water vapour transmission rate of intact bitter Cassava packaging film, 44th Annual Food Research Conference, 14th December 2015, Teagasc Food Research Centre, Moorepark, Fermoy, Co. Cork. *Conference Proceedings.*

Chapter 5: Tumwesigye, K.S., Montañez, J.C., Oliveira, J.C., & Sousa-Gallagher, M.J. (2016). Novel Intact Bitter Cassava: Sustainable Development and Desirability Optimisation of Packaging Films. *Food and Bioprocess Technology,* 9(5), 801-812.

Tumwesigye K.S., Cummins T, Montanez J.C., Oliveira J.C., & Sousa-Gallagher M.J. Optimisation of processing conditions for improved film properties from intact bitter cassava using multi-response desirability, 44th Annual Food Research Conference, 14th December 2015, Teagasc Food Research Centre, Moorepark, Fermoy, Co. Cork. *Conference Proceedings.*

Chapter 6: Tumwesigye, K. S., Morales-Oyervides, L. Oliveira, J. C., & Sousa-Gallagher, M. J. (2016). Effective utilisation of cassava bio-wastes through integrated process design: A sustainable approach to indirect waste management. *Process Safety and Environmental Protection,* 102, 159–167.

Tumwesigye K.S., Morales-Oyervides L., Sousa R., Oliveira J.C., & Sousa-Gallagher M.J. (2016). Effective utilisation of cassava bio-wastes through integrated process design: A sustainable approach to waste, resource and environmental management in food processing, 18th IUFOST-World Congress of Food Science and Technology **"**Greening the global food supply chain through Innovation in Food Science and Technology", 21-25th August, 2016, Institute of Food Science and Technology, Dublin Ireland.

Chapter 7: Sousa, R., **Tumwesigye**, **K.S.,** Oliveira, J.C., Tank, A., & Sousa-Gallagher, M.J. Evaluation of Novel Bitter Cassava Films for Equilibrium Modified Atmosphere Packaging of Cherry Tomatoes. (Prepared *Manuscript ready for submission*).

Sousa R., **Tumwesigye K.S**., Tank A., Oliveira J.C., & Sousa-Gallagher M.J. (2016). Evaluation of Novel Bitter Cassava Films for Equilibrium Modified Atmosphere Packaging of Tomatoes, 18th IUFOST-World Congress of Food Science and Technology **"**Greening the global food supply chain through Innovation in Food Science and Technology", 21-25th August, 2016, Institute of Food Science and Technology, Dublin Ireland.

Chapter 8: Tumwesigye, K.S., O'Brien, E., Oliveira, J.C., Crean, A., & Sousa-Gallagher, M.J. Sustainable biomaterial retrieved from waste bitter cassava as a potential nutraceutical excipient tablet for fast delivery systems: Zinc and Iron evaluations. (Prepared *Manuscript ready for submission*).

Chapter 9: Tumwesigye, K.S., Peddapatla, R.V.G., Oliveira, J.C., & Sousa Gallagher, M.J. Bitter cassava polysaccharide-rich derivatives as thymol-encapsulated coatings in antifungal and antioxidant active packaging of perishable strawberries. (Prepared *Manuscript ready for submission*).

Table of Contents

DECLARATION ii
EXECUTIVE SUMMARY iv
ACKNOWLEDGMENTS xii
GENERAL INTRODUCTION xvi
Background xvi
Thesis statement, objectives and rationale xviii
Contribution to scientific knowledge xix
Chapter 1. Towards integrated sustainable process design framework for cassava biobased materials: critical review on the progress of biobased packaging research and emerging trends 1
1. Introduction 2
Cassava: A versatile crop resource of biomaterials 2
1.1 Cassava starch production and environmental impact 4
1.3 Overview of a decade of cassava bio-based packaging materials research application 5
1.4 Recent trends on cassava biobased material improvement and application 12
1.4.1 Tape casting technique (TCT) 13
1.4.2 Starch reinforcement techniques 13
1.4.3 Antimicrobial biobased materials intended for active packaging 14
1.4.4 Nutri-enrichment of biobased materials intended for active packaging 17
1.4.5 Utilisation of valuable derivatives and by-products in cassava wastes 18
1.5 Untapped conventional techniques suitable for cassava biobased system 19
1.5.1 Application of modified atmosphere (MAP) and active (AP) packaging systems: Desired package atmosphere 19
1.5.2 Mathematical models 21
1.5.3 Active packaging by fluid regulators 25
1.6 Emerging trends in integrated sustainable process design framework 27
1.6.1 The SRRC concept: exploiting intact (whole) cassava bitter cassava as a potential sustainable source of green biomaterials 27
1.6.2 Supercritical fluid technology (SFT) 29
1.63 Plasma surface activation and functionalisation 35
1.7 Process integration (PI) as a holistic approach for cassava biobased material development and consumption 36

1.7.1 Pinch analysis and mathematical optimisations as an integrated process design tool 38

1.7.2 Desirability optimisation package design and package performance 39

Chapter 2. New sustainable approach to reduce Cassava borne environmental 43

waste and develop biodegradable materials for food packaging applications 43

2.1 Introduction 44

2.2 Methodology 46

2.2.1 Source material 46

2.2.2 Cassava preparation 46

2.2.3 Waste solid analysis 47

2.2.4 Simultaneous release, recovery and cyanogenesis (SRRC) of biopolymer derivatives 47

2.2.4.1 Yield determination 49

2.2.4.2 Total cyanogens analysis 49

2.2.4.3 Amylose measurement 50

2.2.5 Film preparation 50

2.2.5.1 Optical properties 50

2.2.5.2 Solubility 51

2.2.6 Analysis of film Performance properties 51

2.2.6.1 Surface 51

2.2.6.2 Chemical 52

2.2.6.3 Barrier 52

2.2.6.4 Mechanical 53

2.2.6.5 Seal integrity 53

2.2.6.6 Thermal 54

2.2.7 Statistical analysis 54

2.3 Results and Discussion 55

2.3.1 Waste solids 55

2.3.2 Effect of SRRC on biopolymer derivative products 55

2.3.3 Biopolymer powder yields 58

2.3.4 Total cyanogen content 59

2.3.5 Amylose content 60

2.3.6 Film prototypes 60

2.3.6.4 Optical properties 61

2.3.6.5 Solubility of bitter Cassava films 63

2.3.7 Film performance properties 64
2.3.7.1 Surface 64
2.3.7.2 Chemical 65
2.3.7.3 Barrier 66
2.3.7.4 Mechanical properties 66
2.3.7.5 Seal integrity 67
2.3.7.6 Thermal 67
Chapter 3. Integrated process standardisation as zero-based approach to bitter cassava waste elimination and widely-applicable industrial biomaterial derivatives 71
3.1 Introduction 72
3.2 Materials and methods 74
3.2.1 Integrated process methodology for production of novel intact BC-BPD 74
3.2.1.1 Intact bitter cassava preparation 74
3.2.1.2 Integrated process methodology 74
3.2.2 Optimisation via desirability approach and statistical analysis 75
3.2.2.1 Factorial and Box-Behnken response surface experimental design 75
3.2.2.2 Simultaneous optimisation using desirability function 77
3.2.3 Standardisation of integrated process methodology by validation of optimal models 79
3.2.4 Impact of standardisation on Biopolymer derivatives and packaging film moisture barrier properties 79
3.2.4.1 Effect on total cyanide decontamination and BPD appearance 79
3.2.4.2 Microstructure and chemical 80
3.2.4.3 Thermal 80
3.2.4.4 Moisture adsorption 81
3.2.4.5 Film preparation 81
3.2.4.6 Film moisture barrier characterisation 81
3.2.4.7 Moisture barrier modelling 82
3.3 Results and discussion 83
3.3.1 Integrated process methodology for production of novel intact bitter cassava biopolymer derivatives (BC-BPD) 83
3.3.2 Optimisation of BPD production by Desirability 83
3.3.3 Standardisation of integrated process methodology by validation of optimal models' 87
3.3.3.1 Optimal model's validation 87
3.3.3.2 Standardisation of integrated process methodology 89

3.3.4 Impact of Standardisation on Biopolymer derivative properties and packaging film moisture barrier properties 89
3.3.4.1 Appearance 89
3.3.4.2 BPD dull colour and total cyanogen decontamination 90
3.3.4.3 Microstructure and chemical 91
3.3.4.4 Thermal 93
3.3.4.5 BPD moisture adsorption behaviour 94
3.3.4.6 Film moisture barrier properties 99
Chapter 4. Quantitative and mechanistic analysis of impact of novel cassava processing on fluid transport phenomenon in humidity-temperature-stressed biobased films 102
4.1 Introduction 103
4.2 Materials and methods 106
4.2.1 Materials 106
4.2.2 Mass transport characterisation 106
4.2.2.1 Moisture barrier (MB) 106
4.2.2.2 Gas barrier 107
4.2.2.3 Fluid barrier modelling 107
4.2.2.4 Film solubility (FS_{ol}) and swelling ratio (FS_{tm}) measurements 108
4.2.2.5 Statistics 109
4.3 Models and conceptual background 109
4.3.1 Analysis of film–solvent interaction 110
4.3.2 Film solvent permeation theory and mechanism 111
4.4 Film structural characterisation 112
4.5 Results and discussion 112
4.5.1 Moisture barrier 112
4.5.2 Permeation to oxygen 121
4.5.3 Mass transport characteristics of solvents through intact bitter cassava (IBC) films 123
4.5.4 Impact of solvent mass transfer on film structural changes 127
Chapter 5. Novel intact bitter cassava: Sustainable development and desirability optimisation of packaging films 130
5.1 Introduction 131
5.2 Methodology 132
5.2.1 Material source: Intact bitter cassava 132

5.2.2 Development of intact bitter cassava films 133
5.2.3 Characterisation of intact bitter cassava films 133
5.2.3.1 Thickness measurement 134
5.2.3.2 Moisture content 136
5.2.3.3 Optical properties 136
5.2.3.4 Solubility 137
5.2.3.5 Water vapour permeability 137
5.2.3.6 Thermal characterisation 137
5.2.3.7 Mechanical analysis 138
5.2.4 Model development and film optimization 139
5.3 Results and discussion 140
5.3.1 Example of transparent and homogeneous biobased films 140
5.3.2 Characterisation of intact bitter cassava biobased films 140
5.3.2.1 Thickness 140
5.3.2.2 Moisture content 143
5.3.2.3 Optical properties 143
5.3.2.4 Solubility 145
5.3.2.5 Water vapour permeability 145
5.3.2.6 Thermal properties 145
5.3.2.7 Mechanical properties 146
5.3.3 Modelling of film characteristics 146
5.3.4 Desirability optimisation of packaging films 147
Chapter 6. Effective utilisation of cassava bio-wastes through integrated design process: A sustainable approach to indirect waste management 153
6.1 Introduction 154
6.2 Experimental 155
6.2.1 Model development and optimisation studies 155
6.2.1.1 Waste derivatives yield 156
6.2.1.2 Total cyanogens and colour 157
6.2.2 Evaluation of integrated design process 157
6.2.2.1 Biopolymer derivatives drying rate studies 159
6.2.2.2 Biopolymer derivatives microstructure 159
6.2.3 Film formulation 159
6.2.3.1 Film thermal analysis 160
6.2.3.2 Film water vapour transmission rate 160

6.2.3.3 Film chemical characterisation 160
6.3 Results and discussion 160
6.3.1 Integrated design process description 160
6.3.1.1 A: Mechanical pulping 161
6.3.1.2 B: Reaction and release 162
6.3.1.3 C &D: Centrifugation and washing 166
6.3.1.4 E and F: Recovery 167
6.3.2 G: Film package development 168
Chapter 7. Evaluation of Suitability of Novel Bitter Cassava Films for Equilibrium Modified Atmosphere Packaging of Tomatoes 173
Abstract 173
7.1 Introduction 175
7.2 Methodology 177
7.2.1 Material preparation 177
7.2.2 Experimental set up and package performance analysis 177
7.2.3 In-package oxygen composition 178
7.2.4 Analysis of experimental data 179
7.3 Results and discussion 179
7.3.1 Influence of EMAP design parameters on gas composition for cherry tomatoes 179
Conclusion 188
Chapter 8. Sustainable biomaterials recovered from waste bitter cassava as potential nutraceutical excipient tablet carrier of micronutrients Iron and Zinc 189
Abstract 189
8.1 Introduction 190
8.2 Materials and methods 191
8.2.1 Materials 191
8.2.2 Polysaccharide-rich derivatives (PD) production 192
8.2.3 Characterisation of PD 192
8.2.3.1 Particle size and shape (PSS) 192
8.2.3.2 Bulk and tapped densities, Carr's Index and Heckel plots 192
8.2.4 Preparation and analysis of tablet excipient from PD 195
8.2.4.1 Preparation 195
8.2.4.2 Analysis of tablet properties 195
8.2.5 Preparation of Iron and zinc tablets 196
8.2.5.1 Wet granulation 196

8.2.5.2 Compression 197
8.2.6 Disintegration and dissolution 198
8.2.6.1 In vitro dissolution studies 198
8.2.6.2 Application of mathematical models for the description of Fe/Zn dissolution mechanism 198
8.2.7 Statistics 201
8.3 Results and discussion 201
8.3.1 Particle size and shape (PSS) 201
8.3.2 Bulking properties, Carr's Index and Heckel analysis 202
8.3.3 Impact of bitter cassava and SRRC on excipient tablet properties 205
8.3.4 Evaluation of Fe and Zn excipient tablets 207
8.3.5 Analysis of dissolution and release mechanisms 208
Conclusion 213
Chapter 9. Bitter Cassava Polysaccharide-rich Derivatives as Thymol-encapsulated Coatings in Antifungal Active packaging of Perishable Strawberries 214
9.1 Introduction 215
9.2 Materials and methods 217
9.2.1 Materials 217
9.2.2 Preparation of PD-thymol coating dispersions 218
9.2.3 Coating characterisation 218
9.2.3.1 Thymol loading and encapsulation capacity 218
9.2.3.2 Water vapour permeability 219
9.2.3.3 Coating surface free energy and wettability 219
9.2.4 Preparation of strawberry samples for coating, and antifungal analysis 220
9.2.4.1 Strawberry preparation and coating 220
9.2.4.2 Antifungal analysis 220
9.3 Results and discussion 221
9.3.1 Influence of bitter cassava and SRRC on thymol loading, encapsulation 221
efficiency and stability 221
9.3.2 Influence of PD-thymol coating on permeation to water vapour 222
9.3.3 Effect thymol loading on coating surface free energy and wettability 222
9.3.4 Impact of PD-thymol coating on mould growth inhibition in storage strawberries 223
General conclusion, outcomes and recommendations for future work 226
References 233

Chapter 1. Towards integrated sustainable process design framework for cassava biobased materials: critical review on the progress of biobased packaging research and emerging trends

Abstract

Cassava represents a reasonable share in biobased material development globally. The production of its biopolymer derivatives (BPD) using conventional techniques/methods is accompanied by huge wastes with potential negative environmental impact. Among the BPD, starch dominates as lone additive in cast matrices with packaging limitations, requiring other BPD, and/or external-source modifiers for matrix improvement. Exploiting integrated sustainable engineering process design of all BPD, is a novel approach in designing efficient system of cassava biobased materials for food and non-food applications.

A critical review on the progress of cassava biobased packaging research applications in the last decade is provided. The current and emerging techniques and methodologies to address cassava wastes and challenges of cassava research for application on biobased packaging are highlighted, and possible revisions suggested. The potential of integrated sustainable engineering process design framework for packaging system is discussed and emphasized together with the exploitation of novel cassava biomaterials and biowastes.

Research progress has been made in developing cassava biobased materials, mainly with improvements on structural and functional properties. Challenges were identified from the amount of waste generated during conventional processing and on the application process aiming at tailoring materials to industrial needs. These materials should be improved using a holistic approach reflecting the target products, variable environment, minimising production costs and energy. Use of novel material resources, eliminating waste, and employing a standardised methodology via desirability optimisation, present a promising process integration tool for development of sustainable cassava biobased systems.

Keywords: Cassava, wastes, green processing, packaging material, sustainable system

1. Introduction

The substantial global dependence on petrochemical based materials (BM) has given rise to packaging security concerns. These concerns, together with negative environmental impacts (Emmambux, Stading, & Taylor, 2004; Tokiwa, Calabia, Ugwu, & Aiba, 2009), increased population pressure on finite and dwindling natural resources and competition for food supply, have drawn the extensive research and development of sustainable alternatives (SA). The SA that are green, clean, post-use biodegradable, compostable, efficient and sustainable are desired (Coombs & Hall, 2000). The BMs, which have emerged as main alternatives to address the concerns, are obtained from renewable resources which is a component of a sustainable biobased industry. Cassava (*Manihot esculenta* Crantz) represents a sustainable resource of biobased products (Hood, Teoh, Devaiah, & Requesens, 2013).

Cassava: A versatile crop resource of biomaterials

Cassava is categorised into sweet or bitter, with sweet cassava (SC) being edible and safe for immediate use in fresh and processed forms, while the bitter ones are unsafe for immediate consumption. Cassava is consumed widely and highly valued as food security anchorage for tropical and sub-tropical countries. Mainly in Africa whereby more than half of the world's cassava or about 162.5 million t from over 15 million hectares, compared to more than 33 t (3.0 ha) and 92 t (5.0 ha) millions in Latin America and Asia, are cultivated (FAOSTAT, 2015).

Advancements in the biopolymer research triggered, in the last decade, the paradigm shift towards a fully industrial-applied SC (Adetunji, Isadare, Akinluwade, & Adewoye, 2015). Increasing awareness of the association between cassava biopolymer derivatives (BD) and cheap industrial biobased products might account for this trend. This popularity is due to its easily processed low cost biopolymer derivatives (Starch, cellulosic fibres, lignin, and hemicellulose) (Table 1.1). Of the BD, starch has been extensively studied, perhaps due to its high root proportionality, chemical and functionality (Blazek & Copeland, 2009) , and received a higher attention for biobased materials production (Paunonen, 2013). Starch molecular structures, with differentiated

amylose (20-30%) and amylopectin (70-80%) contents (Mufumbo et al., 2011), presents unique polymer functionality in wide range applications. The proportionality of amylose and amylopectin in extracted and applied starch can differ significantly depending on production methodology and amounts used to prepare products. Amylose is a nearly linear polymer of α-1, 4 anhydroglucose units that has excellent film-forming ability, rendering strong, isotropic, odourless, tasteless, and colourless film (Campos, Gerschenson, & Flores, 2011). Amylopectin is a highly branched polymer of short α-1, 4 chains linked by α-1, 6 glucosidic branching points occurring every 25–30 glucose units (Liu, 2005). Consequently, amylose and amylopectin provide materials of varying viscosities, crystalline quality and the energy required to melt the material (Mufumbo et al., 2011).

Table 1.1 Composition of sweet cassava root and different components

Component	**per 100 g (**On a fresh weight (dry matter) basis)	
Cassava root (Uchechukwu-Agua, Caleb, & Opara, 2015)		
Water, g	60	
Protein, g	1.4	
Fat, g	0.28	
Carbohydrate, g	38	
Fibre, g	1.8	
Sugar, g	1.7	
Minerals, g	0.46	
Vitamins, g	0.07	
Cassava peeled & unpeeled root (Ospina & Ceballos, 2002)		
	Peeled	unpeeled
Water, g	71.50	68.06
Carbohydrate, g	26.82	29.06
Crude fibre, g	0.12	0.99
Crude protein, g	0.74	0.87
Ash, g	0.13	0.17
Vitamins	0.69	0.85
Cassava waste solids (peel and edible fibre) polysaccharides (Salvador, Suganuma, Kitahara, Tanoue, & Ichiki, 2000)		
Others	1.8	
Pectin	17.8	
Hemicellulose	22.8	
Cellulose	48.2	

1.1 Cassava starch production and environmental impact

Due to SC starch ease of processing, low cost and potential high yields, conventional methods have been used for its extraction, purification and drying. Wet milling (WM) is the most common and simple conventional method, using at industrial level, simple equipment and heavy investment, depending on the desired final product (Lundy, Ostertag, & Best, 2002). Cassava starch can be obtained from fresh roots or its non-edible parts, stems, peels and leaves, primarily by WM and starch has also been produced from dry cassava chips. The complete step-wise process (using simple or large scale extraction) can be divided into four main stages: (i) preparation (peeling and washing); (ii) rasping/pulping/grating; (iii) recovery (starch sedimentation, washing, dewatering, drying); and (iv) finishing (milling and packaging).

Beyond starch extraction, cassava processing also generates large amounts of wastes as waste solids (WS) and wastewaters (WW) (Adeola, 2011). The United Nations Statistics Division, *Glossary of Environment Statistics* defines wastes as materials that are not prime products for which the initial user has no further use in terms of his/her own purposes of production, transformation or consumption, and of which he/she wants to dispose. Wastes can be generated during the extraction of raw materials, the processing of raw materials into intermediate and final products, the consumption of final products, and other human activities (UNSD, 1997). According to FAO (FAO, 2013), starch roots, mainly cassava contributes over 700 MT wastes in the global upstream food wastes, requiring conversion into valuable products and energy in an environmentally friendly manner. Besides, an active starch plant can generate up to 47% total fresh disposable cassava by-products (Heuzé, Tran, D Archimède, Lebas, & Regnier, 2013). When disposed for a given period in the environment, these could be typically associated with emission of strong unpleasant smells, carbon-dioxide and total cyanogens (TC). Cassava wastes (CW)-rich TC can contaminate surface water, groundwater, soil, and air which causes more problems for humans, other species, and ecosystems (Simonetto & Borenstein, 2007). In addition, CW can also be a source for rodents and insects, which can harbour gastrointestinal parasites, yellow fever, worms, the plague and other conditions for humans. Moreover, the increasing nature of non-beneficial sweet cassava competition might exacerbate waste disposal problems arising from more use of bitter cassava. During the traditional processing, huge WS and WW

are generated from bitter varieties in order to avoid total cyanogens contained in the peels (Cardoso et al., 2005; Tumwesigye, Oliveira, & Sousa-Gallagher, 2016a). With insufficient prioritization of packaging source reduction, recyclability, compostability, recycled content and recycling policies (MacKerron & Hoover, 2015), wastes are likely to increase in the years ahead.

Thus, this review provides a brief progress in cassava research application in bio-based materials in the last decade. The current technologies and methodologies used to address cassava wastes, and challenges of research to apply cassava biobased materials in food industry are highlighted. The potential of integrated green engineering process design framework for sustainable packaging system development is discussed and emphasized together with the exploitation of novel cassava biomaterials and biowastes.

1.3 Overview of a decade of cassava bio-based packaging materials research application

A decade of global utilisation of SC in the development of biobased packaging materials (BPM) is summarised in Figure 1.1. Among the SC biopolymer derivatives, the most versatile and valuable for BPM has been starch, while cellulose had the smallest use. Edible films dominated cassava research, with the remainder going to other products. Research developments in active packaging films showed continuous but unsteady increases up to the past 3 years, while film development targeting food packaging was minimal and currently show unstable decrease. Overall, the film development trend seems to continuously decrease in the past three years, and this is consistent with decreases in starch use and edible, active packaging and tailored food film development. Conversely, cellulosic fibre application seems to continuously increase in the past two years. The observed decrease trends might be due to limited and declining SC sources and competition for food supply (Tumwesigye, Montañez, Oliveira, & Sousa-Gallagher, 2016b). The increasing use of cellulosic fibres could be due to increase in awareness on alternative benefits of non-food plant derivatives.

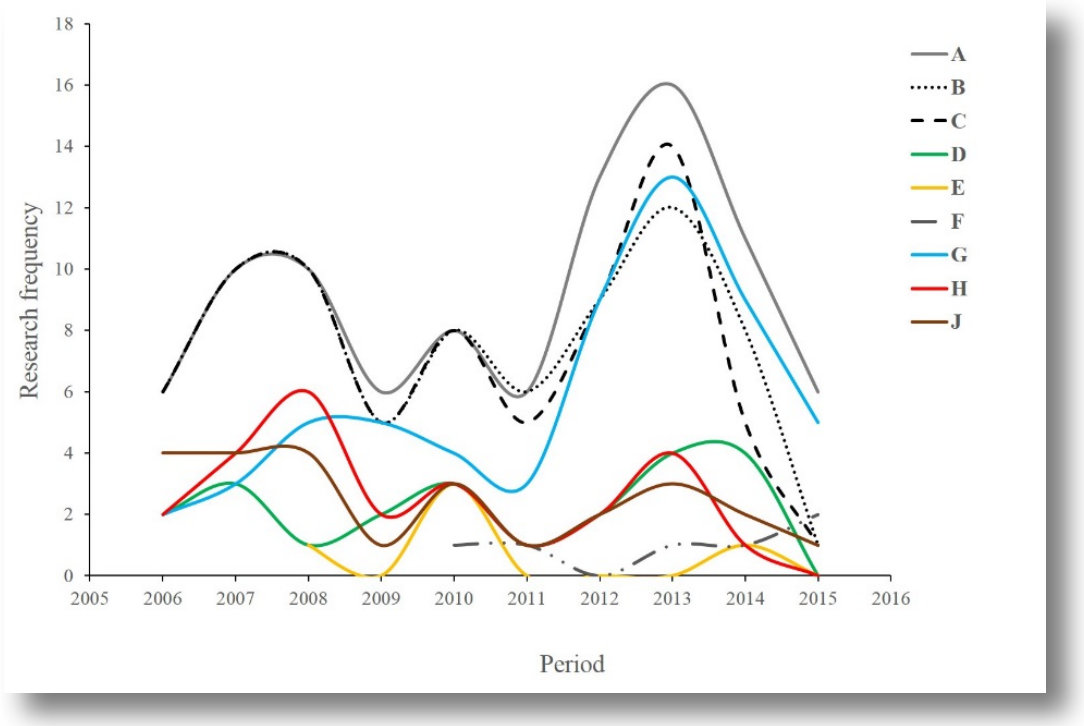


Fig. 1.1 Summary of a ten-year research application of sweet cassava in the development of biobased packaging materials: overall trend (A); edible films (B); starch use (C); active packaging (D); cellulose use (E); recommended for use in food packaging (F); physical modification (G); chemical modification (H); and non-modification (J).

A number of conventional methods/techniques for the development of BPM have been reported in literature, and they include: extrusion (sheet/film, reactive), baking, injection moulding, blow moulding, compression moulding, vacuum foaming, casting, spraying, lamination, calendaring and thermoforming (Imam, Glenn, Chiou, Shey, Narayan, & Orts, 2008). Casting has been the commonest technique used for producing edible and biodegradable starch films (Table 1.2), and was adequately described by Jiménez, Fabra, Talens, & Chiralt, (2012). Regardless of the technique used, the production and characterisation of BPM is a four-stage process: (i) pre-heating homogenisation of additives; (ii) heating of polymeric solution; (ii) drying; and structural and functional characterisation. Heating and drying are vital steps in the production of desired BPM because they can alter the structure and affect the functional application (Tumwesigye et al., 2016b). The most common convention characterisation techniques for cassava reported are: (i) thickness measurements (Micrometer); (ii) optical (colour-chroma; transmission-spectrophotometry); (iii) structure and morphology (scanning electron

microscopy); (iv) surface energy-sessile drop technique (optical tensiometer); (v) chemical and functional-flourier transform infrared (UV/Vis spectrophotometer); (vi) barrier- gravimetric measurement for water vapour permeability (with acrylic permeation cell), oxygen and carbon-dioxide transmission rate (Presens/Dansensor); (vii) mechanical-Texture analyser; (viii) thermal techniques (differential scanning calorimetry, thermogravimetric analysis, x-ray diffraction, Crystallinity).

Table 1.2 Summary of cassava biobased material mechanical and barrier properties

Materials	Method	Thickness, mm	Property				Reference
			Tensile strength, MPa	Elongation, %	Water vapour permeability	Oxygen permeability	
Starch*, glycerol	casting	0.08	4.0–49.0	3.0–46.0	4.02-8.33***u***	33	Mali et al. 2006
Starch*, Chitosan flake, Acetic acid (glacial)	casting	0.10-0.12	0.38-21.02	3.16–39.86	2.30–3.15**	-	Bangyekan et al. 2006
Starch*, amylose, glycerol	casting	0.10	2.2–52.8	4.5–263.1	0.24–0.49***u***	-	Alves et al. 2007
Starch*, glycerol, potassium sorbate	casting	-	0.16–2.35	1.30–29.0	6.10–16.1***u***	-	Flores et al. 2007
Modified starch		0.06–0.12	-	-	0.12–0.21**n**	-	Henrique et al. 2007
Starch*, montmorillonite, chitosan, glycerol, acetic acid	casting	0.071	21.2–24.64	1.1–4.5	1,082–2,000**	-	Kampeerapappun et al. 2007
Starch*, agar, glycerol, Polyethylene glycol200	casting	0.014–0.048	1.39–42.11	-	10.3–137.0***u***	-	The et al. 2008
Starch*, chitosan, gelatin, glycerol	casting	0.083–0.117	13.63–49.40	4.51–110.7	5.78–10.17***u***	0.64–2.58 ***p***	Zhong&Xia, 2008
Starch*, chitosan, glycerol, oregano oil	Extruder	-	1.43–2.54	21.95–48.40	0.62–1.39***u***	-	Pelissari et al. 2009
Starch*, PBAT, tween80, polyoxyethylene sorbitan	casting	0.15–1.21	0.5–14.5	12.5–32.5	0.0009–0.0115 ***u***	-	Brandelero et al. 2010

monooleate							
Starch*, xanthan gum, potassium sorbate	Extruder	-	Negligible	19.0–85.0	3.70–6.70***u***	-	Flores et al. 2010
Starch*, sucrose, inverted sugar, spinach	casting	0.084–0.116	1.81–7.75	65.0–217.0	12.3–99.9***u***	-	Veiga-Santos et al. 2010

* Commercial, native; ** Water vapour transmission rate, g / (m^2.day); ***u***, x 10^{-10} $gm^{-1}s^{-1}Pa^{-1}$; ***n***, g.mm m^{-2}. h^{-1}.kPa^{-1}; ***p***, x 10^{-8} $cm^3m^{-1}s^{-1}Pa^{-1}$

Materials	**Method**	**Thickness, mm**	**Property**				**Reference**
			Tensile strength, MPa	**Elongation, %**	**Water vapour permeability**	**Oxygen permeability**	
Starch*, carboxymethyl cellulose, glycerol	casting	-	2.0–30.0	4.0–86.0	-	-	Tongdeesoontorn et al. 2011
Starch*, cornstarch, glycerin, stearic acid, Sugarcane bagasse	casting	-	2.20-3.80	10.4–57.2	-	-	Vallejos et al. 2011
Starch*, glycerol, carnauba wax type 1, stearic acid	casting	0.128 - 0.132	0.25–2.14	19.30–51.06	32.75–54.74***R***	-	Chiumarelli& Hubinger 2012
Starch*, chitosan, glycerol	extruder	0.19–0.23	085-2.71	21.95-74.04	1.00–2.22***u***	-	Pelissari et al. 2012
Starch*, natural sodium montmorillonite, ethanol,	casting	0.077-0.092	1.85–6.06	89.9–213.4	3.36–7.08**n**	36,979.2-366,163.2***p***	Souza et al. 2012

glycerol, liquid inverted sugar, sucrose							
Starch*, wood fibre, glycerol	casting	0.101–0.138	1.50–21.32	12.9–201.5	negligible	-	Romera et al. 2012
Starch*, xanthan gum, potassium sorbate, glycerol	casting	0. 18–0.26	0.38–2.00	71.6-280.6	0.17–0.23***u***	-	Arismendi et al. 2013
Starch*, glycerol, β-zeolite nano-crystal /Na-beidellite	casting	0.148–0.210	1.40–2.70	25.0–110.0	2.3–3.5***u***	-	Belibi et al. 2013
Starch*, glycerol, agar, span80	casting	0.027-0.046	–	–	0.33–0.56***u***	402.0-496.0***p***	Maran et al. 2013
Flour, Glycerol, Sorbitol, Polyethylene glycol	casting	0.096–0.099	5.29–28.65	4.13–28.24	31.20–36.68**	48.67-55.33***T***	Suppakul et al. 2013
Starch*, cashew tree gum, carnauba wax, tween80, span80, glycerol	Extruder	0.15	0.76-1.48	76.5–136.3	3.70–6.70***uv***	-	Rodrigues et al. 2014

* Commercial, native; ** Water vapour transmission rate, g / (m^2.day); ***u***, x 10^{-10} g $m^{-1}s^{-1}Pa^{-1}$; ***uv,*** g $mmkPa^{-1}h^{-1}m^{-2}$; ***n***, g.mm m^{-2}. d^{-1}.kPa^{-1}; ***p***, x 10^{-8} $cm^3m^{-1}s^{-1}Pa^{-1}$; ***R,*** water vapour resistance (scm^{-1}); ***T***, oxygen transmission rate ($cm^3m^{-2}d^{-1}atm$)

The greatest practical challenges with cassava BPM developments using conventional approaches are associated with starch based matrices limitations in industrial application of food packaging materials. In the last decade, there has been intensified research on cassava material physicochemical and functional properties (mechanical, barrier and thermal) (Table 1.2) and antimicrobial (Table 1.3) in order to attain functional properties closer to the traditional plastic packages. Unfortunately, the approach has been a piecemeal development, associated with uncontrolled variability in material properties (Tables 1.2). This is due to native cassava starch inherent polar and hydrophilic nature, brittleness, resultant inferior functional properties and vulnerability to degradation. In order to improve starch properties, its matrices have to be modified to enhance process stability, performance and biocompatibility (see section 5). While improvers have shown to yield better properties, structure and general appearance of BPM (see section 5), they have the disadvantage of imparting unnecessary colours to the starch films leading to variations in opaqueness (Tumwesigye et al., 2016b). Additionally, various starch reinforcements tend to distort film morphology and introduce surface heterogeneity (de Moraes, Muller, & Laurindo, 2012). Although it has sufficed to extrinsically modify the starches and cellulose derivatives prior to or during matrix formulations to make them more highly functional, it has rendered the process lengthier and this could perhaps explain the high production costs, perhaps due to non-cost effectiveness and energy inefficiency of feedstocks.

In any case, the trend to focus on property improvements without considerations of the holistic approach, which considers useful validation information on package-product compatibility and behaviour during realistic distribution could account for food packaging application limitations. For example, by saying a given property reduced, improved, increased, etc. without testing/validating the research outputs' performance with target products could be the major cause for low end use adoption of these materials. Most developed films did not include validation pathways in situ that represent the real conditions while considering envisaged applications. To put it right, most techniques applied in situ tend to differ from ones developed by research in vitro. Generally, wide material property variations, which are not optimised and directed, had made it difficult for food industry to compare results and make objective application decisions.

Limitations still lie in optimisations, modelling or simulations to bring out the optimum performance of films and coatings. According to Van Boekel, (2008), a dynamic modelling approach permits advancement of an application scheme specific to a product and to select the most suitable regimes without the necessity for extensive testing of the product and indicator. Limited reports have focused on simulation for mechanical and barrier properties of starch-based composite matrix (Arismendi et al., 2013; Suppakul, Chalernsook, Ratisuthawat, Prapasitthi, & Munchukangwan, 2013). In spite of these advantages, few of these packaging systems are commercialized because of high cost, strict safety and hygiene regulations or limited consumer acceptance. Therefore more research is needed to develop cheaper, more easily applicable and effective packaging systems for various foods.

Careful manipulations in the perforation's density, pore localisations, dimensions, micropore structure, and the technique of microperforation can effectively permit desired in-package environment envisaged for a named product. However, the current concept of developing biobased materials to cater for different properties and functions could influence a particular product' in-package atmosphere, thereby making it difficult to match product and package properties. Besides, the constant use of perforations could make the process inefficient, damage the package or introduce contaminants particularly in dust-prone areas with differentiated pressures.

1.4 Recent trends on cassava biobased material improvement and application

Recently, some research has been concentrated on design techniques to improve the casting technique and starch biobased materials towards prescribing a uniform and standard system. In addition, work has also been intensified in reinforcing starch matrices in order to improve the properties by which tailored materials would be developed. Industries have demanded efficient and economy biobased materials, which has resulted into new innovations, with robust and cheap production processes.

8.2.1.1 1.4.1 Tape casting technique (TCT)

Until recently solution casting has been the widely used technique for laboratory-scale production of biobased materials. However, with the shortfalls of this technique to produce uniform materials, handle thicker gels or adjust when varying production volumes, alternative techniques have been investigated. Among the techniques, tape casting, successful in paper, plastic, ceramics and paint industries (Mistler & Twiname, 2000), has been investigated for large-scale material production that delivers a continuous process with success. TCT is a promising tool for production of multi-layered (Tanimoto, Hayakawa, Sakae, & Nemoto, 2006), thick, strong, uniform, varying size biocomposites films at industrial scale (de Moraes, Scheibe, Augusto, Carciofi, & Laurindo, 2015; de Moraes, Scheibe, Sereno, & Laurindo, 2013). Typically, TCT consists of micrometric screw-adjusted blade that helps spread the cast solution on batch or continuous carrier-tapes, ensuring uniform thickness (0.2-1mm) of films (Larotonda, 2007). The nature of cast solution in terms of rheological behaviour were previously well-described (de Moraes et al., 2013).

Even though materials produced by tape casting are reported to be homogeneous, reproducible and showing quick drying (60^0C, 2.3h) (de Moraes et al., 2015), their stability under high temperatures such roll-to-roll processing (Zucca et al., 2015) remains to be empirically proven.

8.2.1.2 1.4.2 Starch reinforcement techniques

Reinforcing starch-based materials helps to overcome weaknesses inherent in starch matrices (mentioned previously) in order to improve their mechanical, water resistance, and generally functional properties. Starch reinforcements have been mainly studied for improving mechanical (Scheibe, De Moraes, & Laurindo, 2014; Versino & García, 2014; Zainuddin, Ahmad, Kargarzadeh, Abdullah, & Dufresne, 2013), improving water resistance (Rodrigues et al., 2014) or barrier to moisture and gas (Argüello-García et al., 2014; Cardoso et al., 2005; De Pauli, Quast, Demiate, & Sakanaka, 2011).

While reinforcements improve starch material properties, they have the disadvantage of exhibiting non-cost effectiveness and energy inefficiency and their processing at source since in all the starch reinforcements, fillers and reinforcers are externally sourced. This

entails many individual stand-alone processes executed independently of each other. The extra energy and costs implied in stand-alone developments could be avoided if the individual processes were integrated.

8.2.1.3 1.4.3 Antimicrobial biobased materials intended for active packaging

The rapid development of cassava biobased materials, in particular the edible types, their compatibility to packaging material development, and successful research into extraction of bioactive functional natural compounds, has led to functional food packaging material development (de Souza, Dias, Sousa, & Tadini, 2014; Flores, Famá, Rojas, Goyanes, & Gerschenson, 2007; Kechichian, Ditchfield, Veiga-Santos, & Tadini, 2010). Different antimicrobial substances were added to cassava biobased materials in different ways intended to deliver various functions (Table 1.3). However, research information on the influence of antimicrobial packaging materials on in-package atmospheres and corresponding packed products' quality and safety is scanty, and this presents challenges to their full potential use in modified atmospheric packaging.

Table 1.3. Summary of cassava biobased material antimicrobial properties

Source of antimicrobials	**Active substance**	**Incorporation style in starch based matrix**	**Intended study/function**	**Reference**
Fruit and vegetable pomace extracts	anthocyanin, flavonoids & chlorophyll	direct addition	antioxidant properties (general)	Hyashi et al. 2006
Commercial	Potassium sorbate	direct addition	Antimicrobial release model and kinetics (general)	Flores et al. 2007
Commercial	chitosan	direct addition	Fungistatic activity (general)	Zhong & Xia, 2008
Commercial	chitosan	direct addition	antimicrobial performance on global quality of salmon muscle	Vásconez et al. 2009
Commercial	Chitosan & oregano essential oil	direct addition	antimicrobial against Bacillus cereus ATCC 25923, E. coli ATCC 25922, S. aureus FRI196e, and S. enteritidis,	Pelissari et al. 2009
Commercial	clove powder, volatile oils, cinnamon powder, red pepper powder, honey propolis, coffee powder & orange essential oil	direct addition	antimicrobial against yeast & mold counts of white pan bread slices	Kechichian et al. 2010
Mango & acerola pulps	carotenoid, polyphenol, & vitamin C	direct addition	antioxidants to preserve palm oil	Souza et al 2011
Commercial	nisin & potassium sorbate	direct addition	antimicrobial effectiveness against Listeria innocua & Zygosaccharomyces bailii	Basch et al. 2012

Commercial	natamycin	direct addition	antimicrobial effectiveness against Saccharomyces cerevisiae	Ollé Resa et al 2013
Commercial cinnamon & clove essential oils	cinnamaldehyde & eugenol	direct addition	inhibitory against Penicillium commune & Eurotium amstelodami	Souza et al. 2013
Commercial	potassium sorbate	direct addition	effective antimicrobial barrier against ygosaccharomyces bailii	Arismendi et al. 2013
Commercial	cin-namaldehyde	supercritical fluid technology	Antimicrobial inhibition of proliferation of Penicillium commune & Eurotium amstelodami fungi in bread products	de Souza et al. 2014
Green tea and palm oil carotenoids extracts	peroxides, total carotenoids, and total polyphenol	direct addition	inhibit oxidation & as a scavenger of oxygen radicals; oxidative protection in packaged butter	Perazzo et al. 2014
Red propolis & licuri leaves	Propolis & cellulose nanocrystals extracts	direct addition	coagulase-positive staphylococci in cheese curds & antioxidant against butter	Costa et al. 2014
oregano & clove essential oils	carvacrol (2-methyl-5-[1-methylethyl]phenol) and thymol (5-methyl-2-[1-methylethyl)phenol])	direct addition & surface coating	antimicrobial against molds, yeasts, & Gram-positive and Gram-negative bacteria	Debiagi et al. 2014

Hayashi & Veiga-santos, (2006) observed a significant antioxidant effect on the packed soybean oil with grape pomace (1.69 and 8.16% total solids) while (Flores et al., (2007) found that high amorphous film matrix relaxation greatly contributes to sorbate release kinetics. The cassava-chitosan fungistatic activities inhibited growth of phytopathogen on mango fruit surfaces (Q. P. Zhong & Xia, 2008) and reduced Zygosaccharomyces bailii external spoilage in a semisolid product but were not effective against Lactobacillus spp. (Vásconez, Flores, Campos, Alvarado, & Gerschenson, 2009), while those with oregano essential oil had a higher inhibition on *B. cereus* than *S. enteritidis* (Franciele M Pelissari et al., 2009). Films containing mango and acerola pulps with carotenoids and total polyphenols presented antioxidant effectiveness while acerola pulp vitamin C was a pro-oxidant agent (de Souza et al., 2014). Ollé Resa, Gerschenson, & Jagus, (2013) reported antimicrobial effectiveness against bacterial or yeast culture with nisin and potassium sorbate in starch films, while Souza, Goto, Mainardi, Coelho, & Tadini, (2013) reported fungicidal action against *Saccharomyces cerevisiae* with starch matrix containing natamycin. Similar results were observed on effective antimicrobial activity against *P. commune* and *E. amstelodami* bread product fungi by cinnamon and clove essential (Souza et al., 2013) and effective antimicrobial barrier against *Zygosaccharomyces bailii* external contamination (Arismendi et al., 2013). de Souza et al., (2014) reported success in supercritical impregnation of cinnamaldehyde (2.49 ± 0.30 mgCN/gfilm, 250 bar). Films with green tea extract and oil palm colorant exhibited oxidative protection in packaged butter, by decrease peroxide index (Perazzo et al., 2014), while those with cellulose nanocrystals (0–1%) and activated with alcoholic extracts of red propolis were effective on coagulase-positive staphylococci in cheese curds and reduced the oxidation of butter during storage (Costa, Druzian, Machado, De Souza, & Guimaraes, 2014).

8.2.1.4 1.4.4 Nutri-enrichment of biobased materials intended for active packaging

Among the few studies in active packaging is the nutrient enhancement of cassava biobased materials. Within the last 5 years, the potential to use gluconate iron in cassava-based edible films has been demonstrated by Castro de Cruz, (2012). The study evaluated the ability and efficiency of cassava-glycerol matrix to bind nutraceuticals and the impact of gluconate iron on its properties. The author reported that

incorporating nutraceutical into starch films (3% cassava, 30% glycerol and 97% water) resulted in: (i) change of homogeneous, smooth and film colour from transparent to yellowish translucent films, and (ii) an increase in properties (tensile strength, elongation at break and viscosity). Nonetheless, little is still known about turning cassava biobased materials as efficient and self-sustaining excipients for administering essential nutrient supplements to the malnourished population.

8.2.1.5 1.4.5 Utilisation of valuable derivatives and by-products in cassava wastes

As mentioned earlier, most studies have evaluated potential of extrinsic fillers and reinforcements for starch modification without considering intrinsic modifiers inherent in cassava parts. Daud, Kassim, Aripin, Awang, & Hatta, (2013) characterised the chemical composition of cassava waste peel (% w/w) as: holocellulose (cellulose + hemicellulose) (66.0), cellulose (37.9), hemicellulose (23.9), lignin (7.5), hot water solubility (7.6), 1% NaOH solubility (27.5), ash (4.5) and moisture (14.0).

However, within the last 5 years research into use of cassava waste as reinforcement fillers and source of bioactive extracts has been intensified. Wicaksono, Syamsu, Yuliasih, & Nasir, (2013) studied cassava bagasse-based cellulose nanofiber (5-8 nm) for application on tapioca-film. The authors reported good stability of cellulose nanofiber suspensions, successful removal of hemicelluloses and lignin from the fibre structure and improved films tensile strength and decreased elongation at break by 69%. Other studies include use of: (i) cassava roots peel and bagasse as natural fillers of thermoplastic materials using cassava bagasse (1.5%) to increased elastic modulus (by 260%) and maximum tensile stress (by 128%) of TPS composites (Versino, López, & García, 2015); (ii) fibrous residue of cassava starch extraction to achieve UV-barrier capacity and water vapour barrier properties (14.6 ± 0.7 10−11g/m s Pa), tensile strength (18.01 ± 0.19 MPa), mechanical resistance increase (>900%) with 1.5% residue, eco-compatible heat-sealed materials (Versino & García, 2014); (iii) cassava bagasse to develop biodegradable trays with effective antimicrobial activity against moulds, yeasts, and Gram-positive and Gram-negative bacteria, less resistant and more flexible trays, with a decrease in the water absorption and adsorption capacities (Debiagi, Kobayashi, Nakazato, Panagio, & Mali, 2014).

While the above studies show good progress in waste minimisation, they are limited in use by the lack of an integrated process design which would otherwise reduce the energy and costs implied in individual processes. To overcome this scenario, an improved process SRRC, which includes components of integrated process was studied (discussed in subsection 1.6.1).

1.5 Untapped conventional techniques suitable for cassava biobased system

8.2.1.6 1.5.1 Application of modified atmosphere (MAP) and active (AP) packaging systems: Desired package atmosphere

The desired atmosphere (DA) packaging demands manipulation of the environment inside the package as a function of both inside and outside package forces. Currently, this has been realised, for perishable products by mass balances between respiration rates and fluid (air, moisture) transfer through the packaging materials using modified atmosphere packaging, passive (MAP) and active (AP) techniques. In MAP, the DA develops naturally as a function of product respiration and fluid diffusion through the package, whereas AP occurs as a result of conditioning atmosphere either by gas replacement, package manipulation or scavengers/absorbers introduction.

Different products require different DA packaging, thus the package environment is developed for specified products which also depend on the type of packaging material, storage temperature, storage relative humidity and their specific respiration rates. Since the external environment has influence on the internal environment, the permeability properties of the package, gases (O_2, CO_2), liquid (water vapour) and temperature need to be matched to the product respiration rate in order to attain equilibrium modified atmosphere (EMA). The EMA packaging can ensure extended shelf-life of products. For EMA package design purposes, tolerance limits for O_2, CO_2, temperature and respiratory quotient of fresh have been suggested as 1-3%, 10-20%, 0-15^{0}C and 0.7-1.3 respectively depending on the product (Yam & Lee, 1995). Yam & Lee (1995) reported that keeping the O_2 concentration and temperature above, and CO_2 concentration below tolerance limits can ensure aerobic and anaerobic trade-offs. Other studies have suggested 3-6% O_2 and 2-10% CO_2 to achieve microbial control and extend shelf-life of

various fresh produce (reviewed by Oliveira et al., 2015). In other studies, Islam et al. (2011) reported 16-18% O_2 and 3-4% CO_2 in 'Madison' tomato packages, showing proper levels for MA storage in 20,000cc breathable film at 5^0C. Guan et al. (2008) reported that the optimal conditions to keep high quality tomato were obtained by MAP during storage at 0^0C for 29 days, independently of the film thickness, in which the adequate gas composition was 14.3%-14.5% O_2 and 4.2-5.6% CO_2.

To date no effective EMA packaging system has been developed. This could be due to the many factors influencing the environment of the package that have not been considered in the design. Factors that are related to existence of additional gases with different functional uses in the package like N_2 for maintaining the shape of the package, and nitrous oxide as an antimicrobial (Meng et al., 2012). Other factors include: (i) inadequate models for accurate prediction of every constraint of the MAP system (Yam & Lee, 1995); (ii) water, energy and heat generated by product respiration; (iii) limited adaptations of biobased materials to MAP designs resulting in limited knowledge of package permeability (P) and activation energies (AE) that match product P and AE. The P, AE and CO_2/O_2 permselectivity (Al-ati & Hotchkiss, 2003) of most widely packaging films for fresh fruits and vegetables that can be used as reference to develop biobased materials have been reviewed (Yam & Lee, 1995); (iv) only unsteady states have been used to design MAP systems, and has not been solved for long storage products which require the dynamic equilibrium state. MAP dynamic equilibrium state describes the steady state in which CO_2 evolution and O_2 consumption rates balance with CO_2 efflux and O_2 influx through the package (Yam & Lee, 1995); (v) limited models that describe respiration change with time for long storage products; (vi) the influence of external air velocity on in-package atmosphere; and (vii) interactions between scavengers or absorbers and in-package environment and its effect on the EMA has not been conclusively studied for different foods and materials.

Another big challenge to the design of MAP is related to the many cassava starch biobased materials that have been developed in the last 5-10 years. These materials have been prepared differently from the ones used commercially, particularly those intended for active packaging with different antimicrobial bioactives. The bioactives can alter the package environment and affect the shelf-life of packed products. Despite use of safe antimicrobial compounds to ensure product safety during migration, no research is

found in literature that includes cassava biobased materials in MAP design. It is important to validate the performance of the package. Unfortunately this has not been done for most developed biobased materials.

Most of the conventional studies to address: (i) MAP have been focused on mathematical models for improving non-perforated packages and perforated packages by optimising respiration rate, storage temperature, gas compositions, mass transport through the package (Yam & Lee, 1995; Pandey et al., 2012;); and (ii) AP use of absorbers and scavengers (Rodriguez-Aguilera & Oliveira, 2009; Lee et al., 2015).

8.2.1.7 1.5.2 Mathematical models

Modelling respiration rate

Most of the conventional studies to address MAP have been focused on: (i) mathematical models for improving non-perforated packages and perforated packages by modelling respiration rate as a function of storage temperature and gas compositions; (ii) mass transport through the package (Yam & Lee, 1995; Pandey et al., 2012;); and (iii) active MAP (Rodriguez-Aguilera & Oliveira, 2009; Lee et al., 2015).

The RR for closed system involves two major chemical reactions occurring in the package, aerobic (Eqn. 1.1) and anaerobic (Eqn. 1.2). Aerobic and anaerobic respirations are expressed as:

$$C_6H_{12}O_6 + 6O_2 \xrightarrow{\text{enzymes}} 6CO_2 + H_2O + HEAT \qquad 1.1$$

$$C_6H_{12}O_6 \xrightarrow{\text{enzymes}} 2CO_2 + 2C_2H_5O + H_2O + HEAT \qquad 1.2$$

The model approaches to respiration rates can be achieved either by empirical models or kinetic models that exploit Arrhenius equations.

Temperature is the most important factor that highly influences respiration rate (RR) including components that determine RR. Thus, the Arrhenius equation (Eqn. 1.3) has been used to measure temperature dependence of respiration rate (Bhande et al 2008).

$$R_r = R^r_{ref} \times e^{\left[-\frac{E_a}{C}\left(\frac{1}{T}-\frac{1}{T_{ref}}\right)\right]} \quad 1.3$$

Thus, the corresponding O_2 rate consumption and CO_2 rate consumption are derived and shown in Eqns. 1.4 and 1.5.

$$R_{O_2} = R^o_{ref} \times e^{\left[-\frac{E_o}{C}\left(\frac{1}{T}-\frac{1}{T_{ref}}\right)\right]} \quad 1.4$$

$$R_{CO_2} = R^{co}_{ref} \times e^{\left[-\frac{E_{co}}{C}\left(\frac{1}{T}-\frac{1}{T_{ref}}\right)\right]} \quad 1.5$$

where, Rr, respiration rate; R_{ref}, respiration rate at reference temperature (T_{ref}); Ea, activation energy; C, universal gas constant; T, temperature (K).

An alternative approach to determine the respiration rate as a function of temperature is to use the Q_{10} influence, corresponding to 10^0C rise in temperature (Eq. 1.6) (Rodriguez-Aguilera & Oliveira, 2009).

$$Q_{10} = \left[\frac{R_n}{R_1}\right]^{\frac{10}{T_n - T_1}} \quad 1.6$$

where, R_n, respiration rate at temperature T_n; and R_1, respiration rate at temperature T_1. Q_{10} represents values from 1 to n depending on the product. The Q_{10} range values for horticultural products at different temperatures have been reviewed by Yam & Lee, (1995) as: 2.5-4.0 (0-10^{0}C); 2.0-2.5 (10-20^{0}C); 1.5-2.0 (20-30^{0}C); 1.5-2.0 (30-40^{0}C).

The closed system of measuring respiration rates has been reported as the most efficient among the three methods for measuring the gas dependence of respiration rates, and have been computed and derived using Eqns. 1.7, 1.8 (Yam & Lee, 1995) in order to fit to empirical data with Eqns. 1.9 and 1.10.

$$R_{O_2} = \frac{d[O_2]}{dt} \times \frac{M_{O_2}\, PV}{100\, WRT} \quad 1.7$$

$$R_{CO_2} = \frac{d[CO_2]}{dt} \times \frac{M_{CO_2}\, PV}{100\, WRT} \quad 1.8$$

$$[O_2] = 21 - \frac{\alpha t}{(a_1 + b_1)^{C_1}} \quad 1.9$$

$$[CO_2] = 21 - \frac{\alpha t}{(a_2 + b_2)^{C_2}} \quad 1.10$$

Modelling mass transport through the packaging materials for MAP

Packaging materials are other important aspect, which highly influences MAP, and their admittance and expulsion of fluids and regulation of external and internal pressure deserve attention.

Conventionally, MAP has been determined for non-perforated and perforated films. As a barrier to the whole transfer process, the permeation of substances across it constitutes three major phases (Rodriguez-Aguilera & Oliveira); (i) adsorption on the outside package surface; (ii) transmission through the package; and desorption on the inside package surface to the headspace. To understand the transfer process, the term "permeability coefficient" (PC) has been used, which can be defined as, 'the volume flow rate of an incompressible fluid through a unit cube porous substance at a unit pressure difference'. Thus, two terms have been used to define the PC, as the product of a solubility coefficient, the thermodynamic parameter (amount of permeant molecules a packaging material can take up), and diffusion coefficient/diffusivity, the kinetic parameter (permeant mobility).

Based on the above theory, several models have been fitted, modified and new ones developed depending on the intended product. The recent investigated phenomenologically based mathematical model (Pandey & Goswami, 2012) example describes the modified atmosphere composition evolution in capsicum perforated package to predict performance under dynamic conditions. Since it is perforated it

considers gas transpiration in parallel to the packaging material and Fick's law of diffusion (Eqns. 1.11 & 1.12)

$$Q_g = q_{ff} + q_{pf} \quad 1.11$$

$$q_{ff} = \frac{A\delta}{l}\left(C_g^{out} - C_g^{in}\right) \quad 1.12$$

where, Q_g, total gas (g) flow; q_{ff}, gas (g) flow across package; q_{pf}, gas (g flow through the pore; A, film cross-sectional area (m^2); δ, film permeability; and l, film thickness (m).

Based on Geankoplis (2003), the O_2 and CO_2 mean free path, λ, (m) at 1 atmosphere and T = 283.2 K are 0.0673 and 0.0762 l μm;

$$\lambda = \frac{3.2\,\mu}{P}\sqrt{\frac{RT}{2\pi W}} \quad 1.13$$

where, μ, viscosity (PaS); P, pressure (N/m^2); T, temperature (K); W, molecular weight; and R, universal gas constant.

Using Fick's equation (Eqn. 1.12) and Knudsen number (Kn = λ/2r) and when r ≤ 1/100, where r, mean perforation diameter, diffusion flux can be expressed as:

$$q_{pf} = \frac{D_g A_p\left(C_g^{out} - C_g^{in}\right)}{l_p} \quad 1.14$$

where, D_g, diffusion flux of gs (g) through pore (P); A_p, pore area; l_p, effective path length.

Substituting $Ug = D_g A_p / l_p$ (the overall mass transfer coefficient in terms of effective permeability) in Eqn. 1.14, then:

$$q_{pf} = U_g\left(C_g^{out} - C_g^{in}\right) \quad 1.15$$

For n perforations,

$$q_{pf} = nU_g\left(C_g^{out} - C_g^{in}\right) \quad 1.16$$

Combining Eqns. 1.15-1.16, and applying mass balance for the O_2 and CO_2 gas exchange in a p perforation package, the O_2 and CO_2 gas volumetric change in-package MAP with respiring produce are expressed as Eqns.1.17 and 1.18:

$$\frac{dC_{o_2}}{dt} = \frac{nU_{o_2}}{V}\left(C_{0_2}^{out} - C_{o_2}^{in}\right) + \frac{P_{o_2}}{lV}\left(C_{0_2}^{out} - C_{o_2}^{in}\right) - \frac{R_{o_2}M}{V} \quad 1.17$$

$$\frac{dC_{co_2}}{dt} = \frac{nU_{co_2}}{V}\left(C_{c0_2}^{out} - C_{co_2}^{in}\right) + \frac{P_{co_2}}{lV}\left(C_{c0_2}^{out} - C_{co_2}^{in}\right) - \frac{R_{co_2}M}{V} \quad 1.18$$

where, $C_{o_2}^{in}$ and $C_{co_2}^{in}$, $C_{0_2}^{out}$ and $C_{c0_2}^{out}$, volumetric fraction of O_2 and CO_2 gases (v/v) in the container and at ambient conditions at time t (h) respectively; U_{o_2} and nU_{co_2}, O_2 and CO_2 effective permeability through perforations ($cm^3\ h^{-1}$); P_{o_2} and P_{co_2}, permeability of film to O_2 and CO_2 gases (ml m m^{-2} h^{-1} atm^{-1}); R_{o_2} and R_{co_2}, O_2 and CO_2 consumption and production rates of the packed product (ml kg^{-1} h^{-1}); M, product mass in the package (kg); and V, package free volume (ml).

8.2.1.8 1.5.3 Active packaging by fluid regulators

Fluid regulators (FR) can be thought of as a third generation strategy to try and design efficient MAP for extending the storage life of products. In previous studies, much efforts were focused on modified in-package atmosphere by manipulating gases, however, the impact of moisture and residual O_2 posed on MAP has resulted in use of FR. This is a downstream packaging development stage that aims to use additives inside the package in order to modify the current in-package environment and obtain the desired environment at a future date. In theory, the product, the package and the environment should associate in positive manner to maintain product quality. However, this is not the case because some additives can be influenced by many factors such type of package material and highly variable environments. The current FR used include: (i) oxygen, ethylene and carbon-dioxide scavengers; (ii) carbon-dioxide emitters; and

moisture absorbers (Santiago-Silva et al., 2009). This section reviews the application of these FR to modify in-package environment.

For gas scavengers, the reactive compounds are enclosed in sachets or stickers associated to the packaging material or directly incorporated into the packaging material (Charles et al., 2006). The common oxygen scavengers iron powder, ascorbic acid, photosensitive polymers and enzymes reduce oxygen in oxidation-reduction manner. Levels of oxygen reduction to 0.01% and (0.3-3%) in the conventional systems of modified atmosphere, vacuum or substitution of internal atmosphere for inert gas have been reported (Cruz et al., 2007). The list of commercial oxygen scavengers have been extensively reviewed (Rodriguez-Aguilera & Oliveira, 2009). Cruz et al. (2007) reported increase in oxygen absorption by the sachet when the relative humidity increase irrespective of temperature. They reported that the oxygen - absorbing sachets were most active under 25 ± 2 ºC and 85 % relative humidity. At ambient condition (25 ± 2 ºC/75 % RH) the rate of oxygen absorbed was 50 ml/day and 18.5 ml/day for 10 ± 2ºC.

Carbon-dioxide (CO_2) is sometimes applied as antimicrobial gas, and its balance in packages can contribute to the regulation of respiration. Conversely, high CO_2 levels can lead to anoxia conditions, and the use of CO_2 absorbers becomes necessary. They are reportedly applied in products where package volume and appearance are critical, i.e. peanuts or potato-crisps (Rodriguez-Aguilera & Oliveira, 2009).

Similarly, in dry packed products, condensation can occur resulting in loss of product quality. Silica gel is a common moisture absorber. Different types of moisture absorbers have been reported (Ozdemir et al., 2005): (i) drip-absorbent sheets containing a super-absorbent polymer in between two layers; (ii) inclusion of humectants which are placed between two of plastic film layers. They are highly permeable to water vapour; and (iii) moisture absorbent sachets, commonly used in dry foods.

Although fluid regulators are important in complementing the in-package atmosphere, they have not been extensively investigated in cassava biobased materials. Use of

absorbers, emitters and scavengers could face the following challenges: (i) the differences in material permeability; (ii) the addition of different bioactives with different physical and chemical properties; and (iii) the cost implication in designing different shapes, different amounts in-sachet contents to cater for fluctuations in package environment.

1.6 Emerging trends in integrated sustainable process design framework

Despite recent developments, in the last 5 years, to improve the biobased material production technologies, processes and functional properties, the proactive and robust holistic approach system is still non-existent. The application of integrated approaches to the development of materials hinged on cost-effectiveness, energy efficiency and zero environmental impact can be a promise for developing sustainable biobased materials tailored for broad applications. Among the green technologies, very few cassava biobased material development studies have been reported in literature, and include: (i) simultaneous release recovery cyanogenesis (SRRC) (Tumwesigye et al., 2016a); and (ii) supercritical fluid technology (de Souza et al., 2014).

8.2.1.9 1.6.1 The SRRC concept: exploiting intact (whole) cassava bitter cassava as a potential sustainable source of green biomaterials

The demand for low-cost material resources has led to emergency in research of unexploited plants-derived feedstock (UF) (Tumwesigye et al., 2016a). Bitter cassava (BC) is an example of UF which has not been conventionally utilised in biobased material development. The BC has many similarities with sweet cassava, with the two differing in the amount of total cyanogen (TC). The BC contains 900-2000 ppm TC (Cardoso et al., 2005; Tumwesigye et al., 2016a), whereas sweet cassava has lower TC ($0 \geq TC \leq 100$ ppm (Tumwesigye, Baguma, Kyamuhangire, & Mpango, 2006). The properties and benefits that make bitter cassava a sustainable feedstock source for biobased materials have been reported (Tumwesigye et al., 2006): (i) adaptation to diverse climatic conditions; (ii) high tolerance to drought, low soil fertility and low soil structure; (iii) high yield in energy per unit area per unit labour; (iv) planting and harvesting time allow for a greater flexibility; (v) the economically viable parts (FAO,

2007); (vi) gluten-free; and (vii) the high yield and bright colours of the biopolymers including the resistance to pests, rodents and swine (Tumwesigye et al., 2006). Latest findings by Tumwesigye et al., (2016a) had explored another benefit of BC as an effective biomaterial for production of food and non-food packages, and with significantly better properties than sweet cassava films.

However, during traditional processing, huge amount of waste is generated, in which 16 -30% are waste solids (peels, fibres, rejects) and wastewaters with unspecified total cyanogens (Heuzé et al., 2013). To transform BC into a green biomaterial required new approaches.

Simultaneous release recovery cyanogenesis (SRRC)

Improved novel alternative methodologies have gained interest in most processing research, and in addition to the principle of green process, more attention is likely. Simultaneous release recovery cyanogenesis (SRRC) can be defined as an improved downstream process that is capable of exploiting intrinsic system's nature, under predetermined conditions, to cause chemical and physical transformations in the products (Figure 1.2).

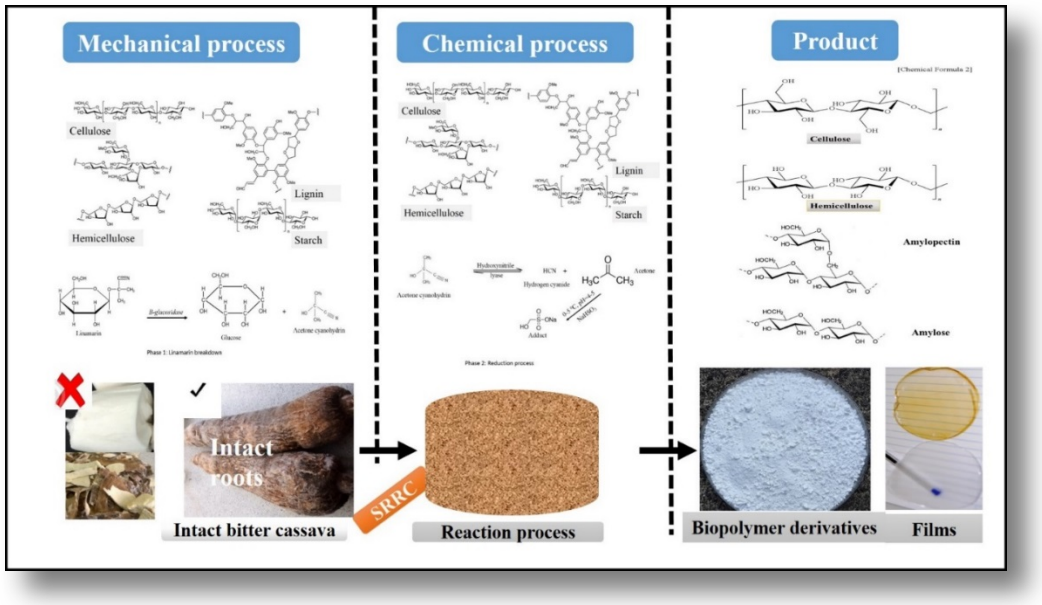


Fig. 1.2 Overview of simultaneous release recovery cyanogenesis (SRRC) concept using intact (whole) cassava for sustainable waste minimisation, recovery of valuable biopolymer derivatives, and food packaging development.

Recently, SRRC technique was applied to investigate the potential of using intact bitter cassava to minimise wastes and produce acceptable biopolymer derivatives capable of developing food packaging materials (Tumwesigye et al., 2016a). The authors reported significantly ($p < 0.05$) higher biopolymer derivative yields and 16% waste decrease. Furthermore, the method effectively reduced total cyanogen content from > 1,000 ppm to < 3 ppm, which is within acceptable limits for use of these poisonous cassava derivatives in food processing. More transparent, homogeneous and strong packaging materials were developed and found to be suitable for packaging application like current commercial packages which are on the market. An added advantage of SRRC is the development of transparent films as a requirement for food packaging. Most cellulose and other starch reinforced biocomposites produce coloured films suitable for only foods that undergo oxidation. The significance of the SRRC outcome implies that peeling cassava can be avoided (Tumwesigye et al., 2016a). When this happens, then there is limited chance of wastes accumulation into the environment. This could also have a possibility of reducing amount of water, energy and costs implications in: (i) extrinsic processing and modification of starch using reinforcements; and (ii) waste management. Moreover, the wastes are converted into useful added value products, human safety ensured, environmental impact reduced, and social-economic welfare of society improved.

The SRRC concept can be an initial step for the regenerative design models for the future to create sustainable systems, which integrate materials needs, society socio-economic requirements and environmental integrity.

8.2.1.10 1.6.2 Supercritical fluid technology (SFT)

As noted previously, interest in successful active packaging research in cassava biobased materials has grown tremendously. One of the potential technologies that can improve multiple properties of cassava biobased materials, which the conventional casting method failed to attain, is supercritical fluids. This might solve their slow adoption and lead to accelerated and widened application. The most SFT used technique is supercritical solvent impregnation (SSI) method due to the various individual SFT unique properties (Cooper, 2003). SSI has been successfully applied in the development

of biomedical materials intended for improved sustained drug delivery devices (Dias et al., 2011) and improved scaffold properties for tissue engineering applications (Reverchon & Cardea, 2012). The SSI application in active packaging research in cassava is limited (Souza et al., 2013).

SFT antimicrobial active package development

Among the major roadblocks in active packaging of cassava biobased material research has been to find a near best technique to help in controlled loading and unloading of antimicrobial compounds, and in particular those that are hydrophobic in nature such as organic lipids. Today, only a single study using SSI (Souza et al., 2013) is found in literature. The effect of impregnating antimicrobial compound cinnamaldehyde (CA) in cassava starch-nanoclay biocomposite films via supercritical carbon-dioxide ($SCCO_2$) was studied by (Souza et al., 2013), reporting successful incorporation, with highest conditions, CA loading (2.49 ± 0.30 mgCA/gfilm), pressure (250 bar), time (15 h) and at depressurization rate (10 bar min−1). They further reported that all impregnated CA contents, irrespective of the amounts, were able to deter *P. commune* growth and increased film surface hydrophobicity. They found that CA-treated films had reduced water vapour permeability (WVP) (4.09 ± 0.84) g mm $m^{-2}day^{-1}kPa^{-1}$ than WVP 10.09 ± 0.35) g mm $m^{-2}day^{-1}kPa^{-1}$) of untreated films. They concluded that: (i) the solubility of CA in $SCCO_2$ dictated the impregnation process; and it is possible to produce better cassava films for packaging with supercritical fluid technology.

Elsewhere, Torres, Romero, Macan, Guarda, & Galotto, (2014) investigated the development of a new technique for preparation of active polymers for food packaging using near critical and supercritical impregnation of thymol in linear low-density polyethylene (LLDPE) films. Using a $SCCO_2$ pressure (7–12 MPa) and temperature (313K), films with thymol concentrations (between 5100 and 13,200 ppm) were developed. They reported a higher affinity of fatty food simulant for thymol. Using a phenomenological mass transfer model thymol diffusion coefficient of $7.5 \times 10^{-1}3$ to $3.0 \times 10^{-12} m^2\ s^{-1}$ for the LLDPE films was achieved.

The supercritical fluid technology is encouraging and provide avenues and advantages for investigating the behaviour of cassava biobased materials particularly when cassava is a lone component in the development of active food packages. This would allow comparisons among cassava materials without or with different additives, and between cassava and non-biodegradable films. Besides, this would guide in the optimisation of incorporation and release of the active compounds in the packaging materials.

Nano- and Micro-porous material development

There is no doubt that modifying the inside package atmosphere through proper control of mass balances is vital to extending the shelf life of the fresh produce. It is also widely accepted that the package barrier properties which regulate water and gas permeation through the package define the success of the modified atmosphere packaging (MAP). However balancing the package properties and the required mass balances has eluded research for quite some time.

Cellulose reinforced cassava starch studies have so far been conducted to regulate the material barrier properties (de Moraes et al., 2012; Teixeira et al., 2009; Versino et al., 2015) and improve on MAP. While these efforts provide exciting results, it has not overall helped to develop effective films tailored to specific MAP of products due to non-validation of these materials. Besides, reinforcements distort material colour and heterogeneity unsuitable for packaging foods in which clear view of the inside packed products is a requirement. Recently, research has been intensified in investigating the effect of micro perforations in order to find alternatives solutions to effective MAP (Abdellatief et al., 2015; Hussein, Caleb, Jacobs, Manley, & Opara, 2015; Pandey & Goswami, 2012). However, constant use of perforations could make the process inefficient, damage the package or introduce contaminants particularly in dust-prone areas with differentiated pressures. Although the recent development of bio-based polymers provides feasibility of MAP for new applications, the research is far from real. To address the dilemma, a new alternative approach of developing nano- and micro-porous biobased materials using green SFT might be a potential solution to developing cassava materials that ensure effective MAP. The advantages of this method can be summarised as: (i) avoidance of pore collapse that characterises materials developed

with conventional liquid solvents (Cooper, 2003); (ii) works well where there are strict limits on number of pores, their distribution and sizes that cannot be regulated by conventional reinforcement methods; (iii) the ability of surficial carbon-dioxide as versatile wetting agent for surface modification (Cooper, 2003) and (iv) use of SCF does not block pores nor condense on them during surface modification of nanoporous materials due to its low viscosity as compared to high viscous organic liquids (Cooper, 2003). Nanoporous polyolefin films have been prepared in supercritical carbon-dioxide by the delocalized crazing mechanism (4–5 MPa and higher; 35°C), with creation of pore diameters of several nanometres (3–7 nm) (Trofimchuk et al., 2014). This can be used in the development of cassava biobased breathable materials with controlled pores for MAP development.

SCF impregnation of functional chemicals

Like in impregnation of active compounds into polymeric materials, SCF can be used to incorporate other functional chemicals into materials. SCF impregnation has been used to dye textile materials (Liu et al., 2006; Ngo, Liotta, Eckert, & Kazarian, 2003) studied supercritical fluid impregnation of azo-dyes with varying functional groups into poly (methyl methacrylate) (PMMA) films using UV/Vis spectroscopy in situ. The authors showed that the high partition coefficients (104-105) between PMMA and $SCCO_2$ phase allow incorporation of about 1% of azo-dyes into PMMA matrix. Although, in this study, reduction of polymer matrix-dye was reduced, similar studies can be initiated for cassava biobased reinforced materials to interact with bleachers and enhance functional efficiency. This can be possible since most chemicals dissolve in supercritical carbon-dioxide, and bleachers like sodium bisulphite has similarities in chemical structure with dyes. Food grade sodium bisulphite improved the colour of intact bitter biopolymer derivatives (Tumwesigye et al., 2016a), with residual quantities requiring a number of water washings to eliminate them. Use of SCF impregnation can be used to clean residues and produce materials with zero chemicals and reduced costs of using dialysis methods.

SCF polymer drying

There is increasing research attention for development of homogeneous polymeric materials such as packaging films. However, using drying ovens to remove water from cast solutions, has always posed challenges of non-uniformity in materials with multiple heterogeneous surfaces and various thicknesses. Its suffices to note that different drying methods for biopolymer derivatives, polymeric materials, powders and foods have been conducted using different techniques and environments such as convectional and non-convectional heat ovens, ambient conditions with different airflows and at different temperatures. Drying materials within heterogeneous environments makes them to lose water vapour at dissimilar velocities that affects their surface tension to act differently, and this can lead to cracked and deformed surfaces.

Some techniques have been tested to ensure uniform thickness, homogeneity and smoothness of biobased material surfaces. Tumwesigye et al. (2016b) reported a uniform thickness of 0.025 ± 0.005 mm for all packaging films tested. Earlier, de Moraes et al., (2015) studied the influence of the thickness of the spread suspension and the support temperature on the conductive drying rate and the properties of films prepared by tape casting technique. Even though the authors obtained better drying time (2.3 h) for 3-mm starch-fibre suspension thickness, the drying temperature (60^0C) could be unsuitable for drying delicate solutions with dissimilar or no reinforcements. The disadvantages of heating at high temperatures were summarised (Benali & Boumghar, 2015) as fast dehydration rates result in cracked and shrink suspensions, and loss of suspension transparency

The green SCF drying method can be used to correct anomalies in cast solution drying to produce desired smooth and homogeneous materials. SCF drying has been used to dry delicate materials during their processing and synthesis (reviewed by (X. Zhang, Heinonen, & Levänen, 2014). In principle, SCF technology controls evaporative drying of materials without necessarily deforming them. Supercritical extraction of water from gels during drying have been reported to produce high porosity gels, with dual roles of increasing drying rates and influencing microstructure (Benali & Boumghar, 2015), key in creation of micro-pores in materials.

(Brown, Fryer, Norton, & Bridson, 2010) studied the use of supercritical carbon-dioxide ($SCCO_2$) for the removal of water from agar gels and compared to air and freeze drying.

Using gel formulation (with and without sucrose) and drying conditions (with and without ethanol as a co-solvent, flow rate and depressurisation rate) and dried with $SCCO_2$, they demonstrated increase in voidage air drying (4% voidage) < supercritical drying with pure CO_2 (48%) < supercritical drying with ethanol-modified CO_2 (68%) < freeze drying (76%).

Certainly, the different routes discussed above can also be utilized in processing cassava biopolymer derivatives, films and coatings, as proposed in Figure 1.3.

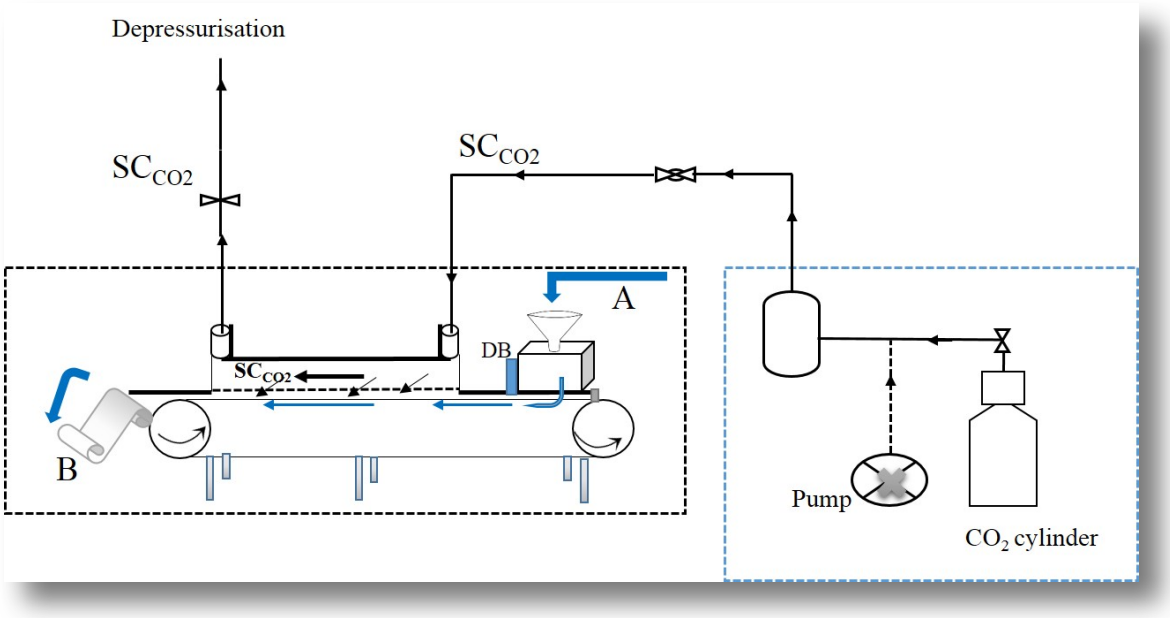


Fig. 1.3 Schematic view of integration of tape casting technique and super critical carbon-dioxide ($SCCO_2$) for cassava biobased material drying and pore formation, as reported in literature (sections 5 & 6). C_P, critical pressure; C, critical point; C_T, critical temperature; A, polymer solution; B, dried film using a parallel current flow drying.

SCF deposition of functional materials

SCF have become popular as smart way of depositing functional bioactive compounds onto surfaces. Specifically, supercritical carbon-dioxide ($SCCO_2$) has been widely studied for coating devices for medical and food application where traditional dip or spray interfered with performances such as unnecessary loss of spray or sustained release profile problems of thick dips (Leroux, Allémann, De Jaeghere, Doelker, &

Gurny, 1996). $SCCO_2$ is preferred to other liquid coating systems due to (Hussain, Wu, Ampaw, & Grant, 2007): (i) to its variable density similar to that of the supercritical stage at a low pressure and independent of temperature at ambient conditions is important for controlled coatings; and (ii) surface tension and viscosity of liquid carbon dioxide are much lower than those of the conventional liquids, with better mass transport and penetration into porous materials.

Among the $SCCO_2$–mediated coating processes studied, can be applied in cassava biobased materials, in production of films with 0.5-1.5 μm thick (X. Zhang et al., 2014). Nonetheless, these methods have not been applied in coating cassava biopolymer derivatives for food packaging. There is a continuing need for efficient methods to produce active packaging materials for food packaging; particularly thin flexible films made from cassava materials. Han, (2005) reported inclusion of iron-based oxygen scavengering sachets inside the packages as the most successful approach. Additionally, desiccant materials (moisture scavengers) were included in the package in the form of a sachet to control the interior humidity, in addition to antimicrobial packages (Han, 2005).

While these sachets have shown potential to deliver the functions they are intended for, their functioning is moisture level dependent and can sometimes lead to non-activation, and potential hazard of being consumed. Besides, the extra material load can impose unnecessary costs.

An alternate approach to metal-based oxygen-scavenging films is to use unique polymers to absorb headspace oxygen in packages. This can be achieved by applying $SCCO_2$ based coatings.

8.2.1.11 1.63 Plasma surface activation and functionalisation

The recent rapid development of cold atmospheric plasma (CAP) for food applications, particularly as an effective non-thermal antimicrobial inactivation technique on surfaces of foods (Misra et al., 2014; Niemira, 2012; Segat, Misra, Cullen, & Innocente, 2016), calls for a push in surface modification of packages, the immediate contact membranes. Polymer materials surfaces can be modified by physical, chemical, optical and biomedical based techniques. Current green methods that can deliver surface modification efficiency include supercritical fluid technology (discussed earlier).

The CAP technique can be of particular interest, when applied together with the supercritical fluid-assisted coating technique, for effective surface modification and total microbial inhibition. The application of CAP in food packaging was reviewed by (Pankaj, Bueno-Ferrer, Misra, Milosavljević, et al., 2014a), and found to influence crystallinity and surface properties (roughness and contact angle) of polyethylene films (LDPE, HDPE) (Ataeefard, Moradian, Mirabedini, Ebrahimi, & Asiaban, 2009). Recently, effects of CAP on dielectric barrier discharge of zein (Pankaj, Bueno-Ferrer, Misra, Bourke, & Cullen, 2014b), sodium caseinate (Pankaj, Bueno-Ferrer, Misra, O'Neill, et al., 2014c), high amylose corn starch (HACS) (Pankaj et al., 2015a) and bovine gelatin (Pankaj et al., 2015a) films were studied. The authors observed that CAP increased zein surface roughness and equilibrium moisture content, and protein conformational change. The major effects observed were increased hydrophilicity and decreased water vapour transmission and oxygen transmission rates in sodium caseinate and bovine gelatin films.

While CAP has shown potential with the films aforementioned, there is need to validate the results and its effectiveness, particular when it is tested on packages with packed foods. The fact that different foods behave differently in packages, a lot of research is still needed before it can be qualified. Similarly, testing the compatibility of cassava biobased materials and other many starch-reinforced packaging films is required to target different applications.

1.7 Process integration (PI) as a holistic approach for cassava biobased material development and consumption

Until very recently, most cassava biobased materials were developed following stand-alone approaches intended for mono-functional applications. The current growth in PI has put pressing challenges to biobased material development. Currently, little is known about integrated process designs which give insights into different cassava biobased material property interactions and their synergistic effects on the performance, economy and quality of materials and products. The PI designs ensure an output material has multifunctional applications. This is achieved by evaluating and optimising individual processes, followed by integrating their impacts and synergies/ interrelationships to

obtain an efficient and sustainable system. The PI for cassava biobased material development can be achieved by integrating one or more green processes (discussed above) with pinch analysis and mathematical optimisations, active (AP) and modified atmosphere (MAP) packaging, desirable package optimisation, and package performance simulating real conditions (Figure 1.4). Integrating SRRC-assisted waste minimisation and package production as well as desirable MAP optimisation and validation can improve energy efficiency, reduce costs and lead to sustainable cassava biobased systems.

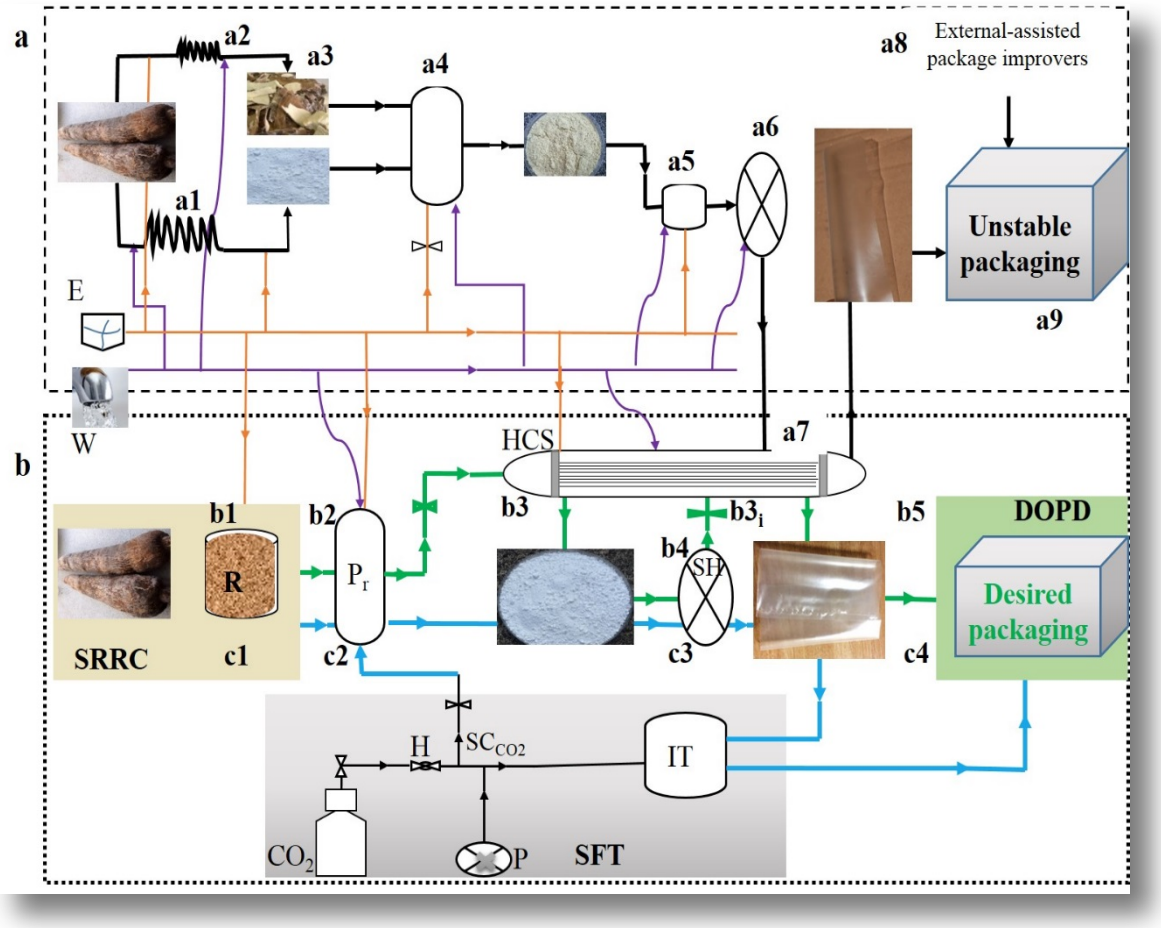


Fig. 1.4 Flowsheet of cassava biobased materials using conventional process (a) **(a1-a9)** and proposed process considering integrated process design (b) by combining either: simultaneous release recovery cyanogenesis (SRRC) & desirability optimisation packaging design (DOPD) **(b1-b5)** or SRRC, superfluid technology (SFT) & desirability optimisation packaging design (DOPD) **(c1-c4)** to reduce cost and energy for every process.

E, energy source; W, water source; HCS, heating & cooling system; Pr, recovery; SH, solution heating; H, filter; P, pump; IT, CO_2 impregnation tank; a1 & a2, series of steps for starch production & waste peel preparations; a3, bagasse refinement; a4, reaction tank; a5, biocomposite refinement, a6, solution preparation and casting; a7, drying & cooling; b1, pulp tank; b2, reaction tank; b3 & b3i, heating & cooling; b4, solution preparation and casting; c1, pulp tank; c2, reaction tank; c3, solution preparation and casting.

8.2.1.12 1.7.1 Pinch analysis and mathematical optimisations as an integrated process design tool

Many production processes consist of individual processes (IP) comprising several unit operations, which may include material production, product generation and waste management. The IP have to be carried in a manner that the final output product is economic with minimal socio-economic and environmental impact. The integration processes which emphasize process optimisations, component synergisms and mathematical models are highly regarded as sustainable systems.

Among the optimization techniques, pinch analysis and mathematical optimisations (PAMO) have been well-studied and employed in understanding many processes. The PAMO has an advantage of making complicated conventional mathematical models more comprehensible for many processes. PAMO is used synonymously with process integration, and is based on computing feasible low energy and low-cost process targets by optimising integrated process network elements, all underpinned by better process understanding (Kemp, 2007).

PAMO has been studied for various processes, and its application depends on conditions which define individual processes. Waste management, energy consumption, water, hydrogen and carbon-dioxide emission consumptions are the most studied areas using PAMO.

More recently, Ho, Tan, Hashim, Lim, & Lee, (2015) studied a new application of pinch analysis in solid waste management planning and reported that PA predicted 20% carbon emission and 70% landfill paper reductions, and 20%, 85% carbon emission, landfill food waste reductions. Beninca, Trierweiler, & Secchi, (2011) studied heat integration of an existing olefins plant by decomposing it into simpler processes, and

using PAMO to minimise the difficulty of the optimization problem and increase the possibility of finding an optimal solution. They reported that segregating the unit into two allowed generating feasible modification which gave better results.

Based on this scenario, it can be concluded that PAMO can be tailored to processing units with different processing magnitudes.

Grip, Larsson, Harvey, & Nilsson, (2013) demonstrated application of different tools (in-house simulation models, mathematical programming, exergy analysis and Pinch analysis) on an integrated steelmaking site. The in-house simulation models uses Supercalc 4 spreadsheet consisting of three main blocks: the Physical model, the Economic model and the Fluctuation model. The mathematical programming uses MILP (Mixed Integer Linear Programming) to find an optimal process configuration within a certain solution space. The exergy analysis uses the total entropy of system and surroundings. The authors reported that exergy analysis tool is suitable for problems involving different types of energy and transformations between them, and Pinch analysis is the simplest and probably the best tool for problems involving sources and streams of processes with interface between them.

The principles of pinch analysis, which were well-described by Kemp, (2007) is an important tool that can be applied in both large, medium and small scale processes. However, among the case studies in literature there is none showing using PAMO in cassava biobased processes.

8.2.1.13 1.7.2 Desirability optimisation package design and package performance

Desirability optimisation package design (DOPD) is a non-conventional method in atmosphere packaging. DOPD uses multi-response optimisation based on desirability function (Derringer, 1980), and use process targets and response deviations to represent a single objective. To achieve the desired products with highest productivity, some processing inputs and outcome measures must be assigned weights so as to keep them small or large. Both inputs and outputs are transformed from multiple objectives to sole objective by transforming: (i) individual performance measures into individual desirability (D) function; and (ii) multiple individual D functions into one objective function, the overall (global) desirability function (GD).

Limited use of DOPD in the development of cassava biopolymer derivatives and packaging films has been reported in literature (Tumwesigye et al., 2016b) and, it has also been widely reported for development of other materials (Aggarwal, Singh, Kumar, & Singh, 2009; Olivato, Grossmann, Bilck, Yamashita, & Oliveira, 2013; Pizarro, González-Sáiz, & Pérez-del-Notario, 2006). Unfortunately, there is no information in literature showing use of DOPD in MAP designs. Since the package environment is influenced by many factors, and only a few have been used in the MAP designs and development, it is necessary that DOPD is applied, the models developed thereof validated and package performance is done with real conditions. The scale-up of this design could help obtain an efficient MAP with wide applications.

Conclusion

The use of cassava in developing and improving biobased packaging materials, particularly edible films, has been extensively studied for over a decade.

The high starch demand and its production using conventional methods is associated with environmental wastes.

Various approaches have been employed for developing biobased materials, with a growing trend in the materials structural and functional improvements using reinforcements such as fillers, bioactive compounds and chemical modification. Although, their superior properties are better than those of starch matrices, they have the potential disadvantage of increasing the costs and energy associated with material production. The materials are limited to the development stage but fall short of evaluations with intended application conditions. Their interaction with in-package environment under real conditions is non-existent, and their influence and performance is not known. Thus, the exploration of these materials in commercial use, mainly food packaging, is challenging.

Holistic studies, integrating cost-effective, energy-efficient, green processes, using standard methodology, optimising conditions and properties and validation with specific products and environments, can be a sustainable strategy for increased commercial use, primarily food packaging. Understanding the performance of cassava biobased materials in target foods and environment is crucial to their accelerated adoption.

These findings however reflect a great potential of cassava biobased materials, as packages, in wide-range applications.

SECTION 2

Chapter 2. New sustainable approach to reduce Cassava borne environmental waste and develop biodegradable materials for food packaging applications

Abstract

Transforming waste Cassava into a sustainable resource requires a new approach and redesign of the current processing methodologies. Bitter Cassava cultivars have been employed mainly as an emergency famine food, but could also be used as a value added material for packaging. Processing of intact bitter cassava can minimise waste, and produce low-cost added value biopolymer packaging films for targeted applications. This study developed an improved simultaneous release, recovery and cyanogenesis (SRRC) downstream processing methodology for sustainable reduction of waste and development of film packaging material using intact bitter Cassava.

SRRC approach produced peeled (BP) and intact (BI) bitter Cassava biopolymer derivatives. BI showed significantly higher yields ensuring 16% waste decrease with no environmental impact caused by discard residues. SRRC was very effective in reducing the total cyanogen content to within Codex minimum safety limits, demonstrating that the peeling of bitter Cassava process can be avoided. Transparent films were produced using the casting method from both BP and BI derivatives. BI films were more transparent and homogeneous, less soluble, less permeable to moisture, less hydrophilic, more permeable to oxygen and carbon-dioxide, sealable, lower cost, than the BP.

Hence, intact bitter Cassava and SRRC can be used as sustainable, safe, integrative process solution for high value-added product (e.g., packaging film) production from low-cost biobased materials.

Key words: bitter Cassava, downstream processing, film development, waste-reduction, sustainability

2.1 Introduction

The environmental problems caused by food supply chain waste and by-product streams have triggered increased demand for research into biobased value added products and efficient sustainable renewable resources. Thus far, there is a growing realisation of the requirement to increase value products that are made out of secondary raw materials. Among these, waste is considered a valuable resource to provide sustainable feedstock and concurrently contribute to circular-based approach of energy recovery (Essel & Carus, 2014).

Cassava (*Manihot esculenta* Crantz) crop is considered among the highest generators of huge amount of wastes in the form of peel, pulp, wastewater and leaves during postharvest processing (FAO, 2013). With increased population, production and consumption of Cassava has increased consistently and thus waste disposal in the environment has increased tremendously due to a linear and irreversible behavioural pattern that follows a produce-consume and dispose model. According to (FAO, 2013), starch roots, mainly Cassava contributes over 700 MT wastes in the global upstream food wastes, requiring conversion into valuable products and energy in an environmentally friendly manner.

Apart from direct food wastes, other sectors such as foods, beverages and consumer goods packaging generate more non-eco-friendly plastic wastes and this has resulted into huge impact on the environment. With insufficient prioritisation of packaging source reduction, recyclability, compostability, recycled content and recycling policies (MacKerron & Hoover, 2015), wastes are likely to increase in the years ahead. It is estimated that less than 14% of plastic packaging materials are recyclable (MacKerron & Hoover, 2015), and as plastic commands the greatest proportion of food packaging industry, the need to design biobased material is a priority.

With increased devotion to research into packaging sustainability, it is highly likely that non-commercial and non-food plants-derived feedstock will anchor packaging industry. Besides, the finite and dwindling natural material sources and competition for food supply amidst population growth, justify the need to invest into efficient utilisation of

unexploited resources. Thus, addressing waste minimisation and developing packaging materials, in tandem, could result into a more competitive resource efficient economy.

An alternative strategy is to use a circular utilisation model whereby Cassava waste could be transformed into resource for development of value-added flexible packaging materials resulting in waste minimisation due to the biodegradable nature of the materials. If used efficiently, Cassava borne environmental wastes have the potential commercial viability in better eco-designing of materials for food and non-food applications. Semi-commercial crops such as bitter Cassava (BC) have the potential to sustain the growth of food plastic packaging industry. Like sweet Cassava, BC-based films have potential biodegradability and could form excellent film forming properties. However, their demands for processing prior to use due the high total cyanogens (TC) (containing 900-2,000 ppm) (Cardoso et al., 2005), has limited their commercial potential. Essentially, when bitter Cassava is used as food, the peels are extensively removed resulting in huge contribution to waste generation and even a negative environmental impact. Traditionally, processing is achieved by peel removal, generating great amounts of waste. Nonetheless, elimination of the peelings does not guarantee its safety, reasonable lethal amounts of TC still remain and the roots have to be further processed. Traditional soaking and heaping fermentation methods produce high levels of unspecified total cyanogens combined in waste waters and peels, and deliberate burning of peel wastes contributes to carbon dioxide emission and strong offensive smells to the environment (Heuzé et al., 2013). Using bitter Cassava for waste minimisation and package development could be done in an efficient manner, which is compatible with increased income and improved safety of Cassava dependants and reduced environmental impact, while providing a sustainable feedstock for packaging applications.

Transforming waste Cassava into a sustainable resource requires a new approach and redesign of the current processing methodologies. Simultaneous release, recovery and cyanogenesis (SRRC) could be a sustainable approach in processing and has been explored and piloted with success to ease downstream extraction of biopolymers from whole root Cassava (Tumwesigye *et al*., 2014). Safe and clear biopolymer derivatives have been produced, with success, from the whole root of Cassava for potential food and non-food industrial use. The SRRC processing methodology, utilising semi-

commercial intact bitter Cassava, could be explored in production of flexible food packaging film materials with improved properties. Moreover, for production of low-cost packages but also by obtaining sustainable feedstock because bitter Cassava has no competition with food supply since sweet Cassava has normally been utilised as food and non-food materials. Additionally, SRRC is an intrinsic processing methodology which re-enforces starch with compounds from the peel and other waste solids, and there is no generation of wastes and waste streams. This could reduce the cost of film package production and ensure process economy.

The objective of this study was to i) use intact bitter Cassava to reduce waste, ii) apply an improved systematic downstream processing approach to improve biopolymer derivatives physico-chemical properties, and iii) development of film packaging material. If biopolymer derivatives and films produced out of intact bitter Cassava presented comparable or better properties than those made from peeled equivalent, then it would be possible to eliminate the peeling, and its environmental impact, with additional production of flexible packaging material as added value product.

2.2 Methodology

2.2.1 Source material

Decisions to source for a sustainable raw material was based on many factors taking into account the renewable resources, no competition with food supply, minimising waste and environmental impact, and cost-effective option. Accordingly, bitter Cassava (Tongolo) was the preferred material used for package development.

2.2.2 Cassava preparation

Bitter cassava roots (Tongolo) at 12-18 months were picked from farmers' fields (Northern Uganda) according to recommended harvesting practices (CODEX, 2013). The roots were separated from soil debris, placed in ice boxes, transported to the laboratory and kept at -20°C for further treatment. Fresh bitter cassava was assessed for total cyanogen content immediately after harvesting and prior to pulp preparation. The cyanide kit A from Australian National University (Canberra) was used for

determination of hydrogen cyanide in fresh cassava as described (Meredith G. Bradbury, Egan, & Bradbury, 1999).

2.2.3 Waste solid analysis

Bitter Cassava was used intact (I) or peeled (control), washed thoroughly, rinsed 3 times with deionised water and kept at -20°C between sample extractions.
Waste solids quantification was done by randomly selecting 12 intact roots from the bulk bitter cassava. The wastes (peel, cambium, phloem, central xylem fibre) were carefully removed from the parenchyma, and both peel and peeled root portions were separately weighed. Each measurement was taken from 100g intact roots that were correspondingly assigned to 9 different treatments during subsequent tests. The weight of the waste solid was calculated by dividing the weight of waste by the weight of intact root and expressed as a percentage.

2.2.4 Simultaneous release, recovery and cyanogenesis (SRRC) of biopolymer derivatives

The downstream processing procedure is schematically presented in Fig. 2.1. Both intact and peeled roots were processed in two-stages, the mechanical tissue rupture and the biopolymer release, in order to obtain biopolymer powders. In elucidating the function of simultaneous release, recovery and cyanogenesis (SRRC) in downstream processing, intact (I) (periderm-free) roots were scrubbed, while in the peeled (P) (cortex-free) roots, the peel was manually and carefully detached from the edible portion (parenchyma). Intact and peeled bitter cassava roots were fed into an automated grating machine and the resulting pulp mass obtained after mechanical tissue rupture and cell disruption. The machine was equipped with a feeding hopper, a constant speed rotating perforated spiked drum and an inclined delivery channel. This initial action serves the dual purpose of activating cyanogens hydrolysis into release of volatile hydrogen cyanide and bringing together different polymer components for possible modification.

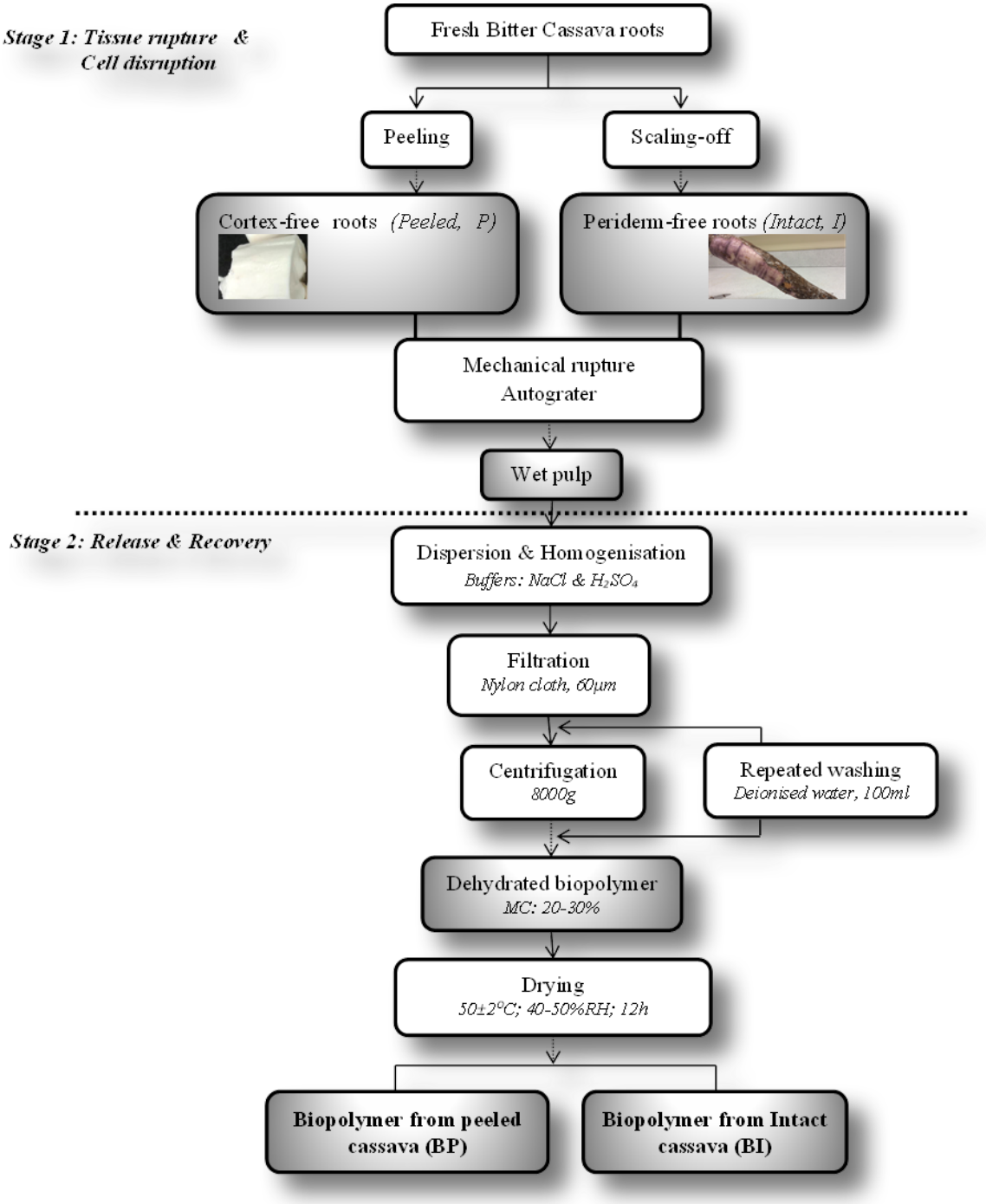


Fig. 2.1. Schematic flow of downstream processing for peeled (P) and intact (I) bitter Cassava and derived biopolymer products from peeled (BP) and intact (BI) roots.

Biopolymers' release and recovery was performed by adding 100 g of pulp mass into 100 ml of extraction buffers in a commercial blender (500 W Breville IHB086 Hand Blender). Full factorial design of 9 different solutions, i.e., 2 extraction buffers at 3 levels, NaCl (0, 1.5, 3.0 M) and H_2SO_4 (0, 25, 50 mM) were used. A total of 18 different

samples (9 Intact and 9 peeled cassava roots) were then homogenised for 4 min, filtered, centrifuged and washed in deionised water (Fig 2.1). The chemicals used in release and recovery, i.e., sodium chloride (≥99% AR), conc. sulphuric acid (99.9%), food grade sodium bisulphite (ACS 58.5% SO_2), and glycerol (99.5%) were analytical grade from Sigma Aldrich (Ireland).

The recovery was achieved by drying semi-dehydrated coarse pulp in an air-circulating oven at uniform conditions, temperature (50±5°C) and relative humidity (30-40%) until constant weights were obtained. The dried samples were milled to a fine powder using an Analytical Grinder (IKA Yellowline-R A 10, Germany) and kept refrigerated (4 - 7^0C) between tests and further use.

Release, recovery and drying of the biopolymer derivatives were performed at NARO-Kawanda laboratory (Uganda), and samples properly packed in air-tight bags and shipped to the labs in Process & Chemical Engineering, School of Engineering, University College Cork, Ireland for further experimental analysis.

2.2.4.1 Yield determination

8.2.1.14

Yield was defined as the percentage of constant weight dried powder recovered from initial mass of 100 g roots, and determined in triplicate for the 18 derivative products, totalling 54 samples per analysis. Considering the average moisture content of intact cassava root as 60 g per 100g root, then the total dry matter content was 40 g per 100 g.

2.2.4.2 Total cyanogens analysis

The total cyanogens (TC) content were quantified by the cyanide kit from Australian National University (Canberra). The quantification entailed grounding samples into 53µm particle size powders and their total cyanide contents (ppm) measured based on the colour chart and spectrophotometric-derived absorbance kit protocol B2 method as described by Bradbury et al., (1999).

2.2.4.3 Amylose measurement

Amylose contents of biopolymer derivatives and their corresponding proportions were determined by the assay kit from Megazyme International, Ireland. The determination involved grounding samples into 53μm particle size powders and their amylose contents assayed in a 25±0.1 mg sample as described in the kit (Megazyme International Ireland, 2011).

2.2.5 Film preparation

The films were manufactured using the casting method, either with peeled (BP) or intact (BI) bitter Cassava derivatives (3 w/v %) and glycerol (30 w/w %). The solution was placed in agitating water bath at 70°C, heated to 65°C with constant stirring until a viscous transparent gel was observed; and held for 20 minutes. Casting was done by pouring film-forming solution (30ml) onto a previously lubricant sprayed 14cm diameter flat glass plate using a dropper. The film solution was measured to ensure production of uniform thickness films (30±5 μm) for different samples, and the dry PTFE spray was used to ease peeling of films after drying. The plates were left at 25±1°C for 3 hours to allow stabilisation and bleeding of trapped bubbles, and then dried in a ventilated oven 40±1°C for 4 h. The dried films were peeled off the plates and equilibrated (54% RH, 23±2°C, at least 48h) for further use.

2.2.5.1 Optical properties

Film optical properties were assessed using transparency and colour parameters. Film transparency was determined with film strips (3 x 2 cm) as described (Mu, Guo, Li, Lin, & Li, 2012) with slight changes. Films strips were carefully inserted into cuvettes and placed inside a spectrophotometer cell. Transmission was measured using a spectrophotometer (Biochrom Libra S22 UV/Vis) at 700 nm. Three replicates of each film were tested. The percent transparency was calculated as described (Mu et al., 2012). For each value, the lower T implies that more light passed through a film, thus described as transparent.

Colour difference (ΔE) was determined according to Ramirez-Navas & Rodriguez de Stouvenel, (2012) using CR-400 Chroma Meter, Konica Minolta Sensing Japan without

major changes. Measurements were taken on six different equal positions on a circular film piece for 3 samples of BP and BI each, and mean values used in CIELAB L*, a*, b* using the Eqn. 2.1 as described (Ghorpade, Hanna, & Weller, 1995; Sharma, Wu, & Dalal, 2005).

$$\Delta E = \sqrt{[\ (\Delta L^*)^2 + (\Delta a^*)^2 + (\Delta b^*)^2\ ]} \qquad 2.1$$

where √, square root symbol; ΔL*, Δa* and Δb* , differences between sample and standard (S) colour parameters. S is film background colour parameters.

2.2.5.2 Solubility

Film solubility (FS) in water was measured as described (Belibi et al., 2014) with minimal modifications. Previously oven-dried film strips (3 x 2 cm) were weighed on an aluminium foil, submerged in a beaker with 50 ml of distilled water and tightly covered with parafilm to minimise water loss and airborne contaminants. The contents were kept at 23°C for 24 h, intermittently agitated to allow dissolution, partially dehydrated (where necessary filtered) on filter paper and dried in an air-circulating oven at 70°C until the sample weight was constant. Total soluble matter of the sample was calculated as described (Belibi et al., 2014). Sample tests were performed in triplicate, and mean values were used for computing FS in water.

2.2.6 Analysis of film Performance properties

2.2.6.1 Surface

Film surface properties were analysed in terms of its morphology and energy.

To supplement optical properties and gain better understanding of the film homogeneity and microstructure, film was examined using Scanning Electron Microscope (SEM), JSM-5510 (Jeol Ltd., Tokyo, Japan). Small film strips were fixed on stubs using double-sided carbon tape and leaving a space on either side of the strip to allow clear observation of film surfaces and cross section. Prior to capturing SEM images, stub-fixed strips were coated with a thin layer of gold. The films were subjected to a focus magnifications as high as 20 000x and images capture between 200x and 30 000x magnification and intensity of 5 kV.

Gaining insight of surface energy properties (surface hydrophobicity, hydrophilicity and wettability) was through measurement of contact angle (CA) using the sessile drop (SD) method by Optical tensiometer (Theta, BiolinScientific Finland) at 20^0C. SD determines the contact angle between drop baseline and drop boundary tangent. The Theta was equipped with a liquid dispenser holder fitted with a 0.5 mm diameter precision microsyringe steel needle, and OneAttension software for drop shape analysis and live measurements. A rectangular film strip (2 cm x 2 cm) was mounted on a pre-cleaned glass slide covered with double-sided tape, then placed on a horizontal holder at 90^0C to enable clear observation of film surface and cross-section. The syringe was positioned vertically 10 mm from the film surface and 2 µL deionised water drop automatically dispensed (1.0 μLs^{-1}) on the film. The measurements lasted 180s and data was analysed for contact angle (ɵ). All films were conditioned (23±2^0C, 50 %RH, 48h) prior to measurements and five measurements were carried out. Drop wetting, spreading and beading/shrinking away gives CA of 0, 0-$90^0$and > 90^0 respectively.

2.2.6.2 Chemical

Film chemical properties were analysed using Fourier transform infrared spectroscopy (FTIR). The films were prepared into thin round discs while under the lamp heater and mounted directly on the sample holder. The spectra were recorded with an UV/Vis spectrum one FTIR spectrometer (Perkin Elmer Lambda 35, USA), frequency range of 4000–400 cm^{-1} and $4cm^{-1}$ resolution in the transmittance and absorbance modes for individual spectrum with 30 scans at room temperature.

2.2.6.3 Barrier

Film barrier properties were assessed by determining its water vapour transmission rate (WVTR) as well as oxygen transmission rate (OTR) and carbon dioxide transmission rate (CTR). WVTR was determined gravimetrically according to (ASTM, 2005), whereas OTR and CTR were determined using a method described by Abdellatief et al., (2015) with deviations from steady state to dynamic oxygen accumulation procedure. Films for WVTR, OTR and CTR were formulated and cast on 8.4 cm and 14.0 cm diameter dishes to maximize uniformity and permeation cell fitting specificity. For

WVTR, each previously conditioned (54 %RH, 23±2^{o}C, at least 48h) film was carefully positioned between acrylic permeation cells containing $CaCl_2$ (0 %RH) and enclosed in a humidity-controlled plastic containers partially filled with 1000 ml of salts solution, corresponding to relative humidity of 95 %. The containers were put in temperature controlled incubators at 38°C, and changes in weight of the cell were recorded every 2 hours for 10 hours and data obtained was used for WVTR calculation. This was intended to elucidate the differential flux gradient as a deviation from the normally applied conditions (38^{o}C, 90 %RH), and also have results comparable to previous research on films. Similar procedure for film preparation was followed for OTR and CTR, but changes to the method by (Abdellatief et al., 2015) were made in terms of i) flushing (0% O_2, 20 % CO_2 and 80% N_2) and measurement (23^{o}C, 50% RH) conditions, using a PBI Dansensor (CheckMate 9900, USA). It was assumed that O_2 / CO_2 / N_2 concentration gradient was maintained across the film throughout experimental period. All tests were conducted in triplicate and mean values were used for calculating WVTR, OTR and CTR, expressed as g/(m^2.day) and cm^3/(m^2.day), respectively.

2.2.6.4 Mechanical

Mechanical properties, i.e. tensile strength (TS), elongation at break (E) and elastic Modulus (EM) were tested using TA HD Plus Texture Analyzer (Stable Microsystems, UK), fitted with a 50 kg load cell, according to (ASTM, 2009). Ten previously conditioned (23±2^{o}C, 54 % RH, at least 48 h) films were cut into 25 x 100 mm strips and their thickness measured with an absolute digital Caliper (Digmatic, Mitutoyo UK Ltd) prior to the tests. Measurements were taken for all the strips and at least 5 close values were used in estimating the cross-sectional area (thickness x initial grip distance). The initial grip separation (50 mm) and cross head speed (1 mm/s) were used. TS (MPa) was calculated by ratio of the force necessary to break a sample to the cross-sectional area, E (%) as a change in the sample original length between grips at break, and EM (MPa) by ratio of TS to the extensional strain. All 10 strips were tested and at least 5 with closest values were used in calculations of TS, E and EM.

2.2.6.5 Seal integrity

Seal integrity (SI) is used as an indicator of seal quality (F. ASTM, 2016) The film SI was determined by measuring its seal strength (ST). A manual impulse sealer, UK with adjustable temperature control was used for optimal seal quality. Two film strips (100 x 150 mm) were placed on top of each other between two pads for dwell time of 1 second. The sealed strips were removed from the sealer and cooled at ambient temperature (23 ± 2^0C) for 10 minutes to allow stabilisation. The ST was determined using a TA HD Plus Texture Analyzer (Stable Microsystems, UK), fitted with a 50 kg load cell. The film non-heat sealed end was held perpendicular to the direction of the pull, with the distance between the clamps of 20 mm and a test speed of 1.0 mm/min. The maximum force breaking the seal and causing seal failure was recorded as the seal strength in Gram-force/ millimetre (g (f)/25mm). Ten pair film strips measured and the means of at least 5 strips were used in computing seal strength.

2.2.6.6 Thermal

Thermal testing, glass transition (Tg) and melting (Tm) temperatures, heat of fusion (ΔH) and crystallinity (C), was conducted using a differential scanning calorimeter (DSC 200 F3) equipped with a thermal analysis data station. A previously conditioned (54 %RH, 23±2°C, at least 48 h) hermetically sealed DSC pan with film, together with a reference empty pan were heated from 20 to 220°C at a rate of 10°C/min, cooled back rapidly to below its glass transitional temperature (25°C) and reheated at a rate of 5°C/min to 220°C to give them thermal history. T_g, T_m, ΔH and C were calculated using the built in software and determined by considering the heat capacity change observed on the second heating.

Thermogravimetric analysis was carried out to establish thermal stability of films using TG Analyser (Spectrum 500) and analysed by the Universal Analysis 2000, New Castle USA) between 25^0C and 300^0C, heating rate of 10^0C/min. Prior to analysis, each sample was corrected against a background scan.

All samples were evaluated in triplicate and mean measurements reported.

2.2.7 Statistical analysis

A factorial analysis of variance (ANOVA) was performed, pooling the 3rd level interaction with the error and testing all main effects and 2-way interactions for

significance at a 95 % confidence level. The main effects were further decomposed in a linear and a quadratic component, drawing P and R^2 to analyse statistical significance at a 95 % confidence level. Statistica 7.1 software (StatSoft Inc., Tulsa, USA) was used. Colour was recorded in the CIE L*a*b* system and analysed using Microsoft Excel, version 2010.

2.3 Results and Discussion

2.3.1 Waste solids

Intact bitter cassava produced an average 16 % waste decrease, due to incorporation of the waste solids, and no environmental impact caused by discard residues. It is clearly shown that the use of intact roots reduces the waste yield when compared to the peeled roots. Thus, it's possible to avoid 160 kg waste peel per 1 ton bitter cassava processed when the SRRC process is deployed by small-to-medium enterprises to develop added value products such as biobased films. It has been shown that a 100 ton cassava starch production unit releases up to 47 tons fresh waste and can have a huge impact on the environment (Aro, Aletor, Tewe, & Agbede, 2010; Heuzé et al., 2013). Moreover, it is well established that cassava processing wastes produces strong offensive smell and their decomposing or incinerated disposal heaps immensely emit carbon dioxide (Aro et al., 2010; Heuzé et al., 2013). Taken together, these findings and the current study suggest that incorporating waste solids through use of intact bitter Cassava can be a sustainable waste reduction process that involves cutting down costs of waste treatment and legislation.

2.3.2 Effect of SRRC on biopolymer derivative products

The biopolymer derivative powders were evaluated in terms of total cyanogen and amylose contents. The Analysis of Variance of 6 responses are summarised in Table 2.1, showing the portion of the effect estimates explained by each factor and 2-way interaction, as well as the *p*-values. Statistically significant effects are denoted by bold typeface, whereas the highly significant ones are denoted with an asterisk mark. For each response the effects are shown by a value, irrespective of its sign (positive or negative), to facilitate the analysis of which is more influential in the response.

Table 2.1. Analysis of the influence of peeling and extraction conditions on biopolymer derivative and film properties. Statistically significant effects are denoted in bold and shown by a higher value regardless of direction (positive or negative). Asterisk shows highly significant effect.

	Biopolymer derivatives						Polymeric films					
	Yield		Total cyanogens		Amylose		Transparency		Colour		Solubility	
Factor	Effect	p-value	Effect	p-value	Effect	p-value	Effect	p-value	Effect	p-value	Effect	p-value
Mean/Interc	**26.710***	0.000	**2.257***	0.000	**28.512***	0.000	**16.556***	0.000	**15.249***	0.000	**29.675***	0.000
(1)NacL(L)	**5.052***	0.000	**-2.891***	0.000	**-2.739**	0.006	2.642	0.509	**-0.717***	0.000	**6.672***	0.000
NacL(Q)	**-1.202***	0.000	**-0.389***	0.000	0.5007	0.527	-0.858	0.799	-0.070	0.476	0.667	0.541
(2)H_2SO_4(L)	0.605	0.090	0.068	0.208	-0.432	0.636	**-10.258**	0.048	-0.156	0.174	-0.081	0.949
H_2SO_4(Q)	-0.293	0.338	**0.241***	0.000	-0.4128	0.601	0.794	0.814	-0.034	0.724	0.141	0.897
(3)Peeling(L)	**1.086***	0.000	**-1.575***	0.000	**-12.2522***	0.000	**-26.945**	0.001	**-12.423***	0.000	**-22.184***	0.000
1L by 2L	0.036	0.933	**-0.211**	0.002	-0.7782	0.487	6.390	0.226	-0.175	0.210	0.058	0.970
1L by 2Q	-0.043	0.907	-0.059	0.299	0.4651	0.630	4.229	0.336	0.114	0.342	0.077	0.954
1Q by 2L	-0.184	0.621	-0.007	0.908	-0.3401	0.725	-1.771	0.671	-0.222	0.072	-0.110	0.934
1Q by 2Q	-0.148	0.646	-0.030	0.547	0.6205	0.460	-2.863	0.441	0.001	0.992	-0.081	0.944

2.3.3 Biopolymer powder yields

Sodium chloride (NaCl) showed the most statistically significant (p<0.05) effect on yield (Table 2.1). NaCl had a statistically significant linear (L) and quadratic (Q) effect (Table 2.1), with higher yields the greater its content (Fig. 2.2). Peeling also showed a statistically significant (p<0.05) linear effect (Table 2.1), and the yields of intact (BI) bitter Cassava (Fig. 2.2 a_1) were significantly higher than for the peeled (BP) (Fig. 2.2 a_2). This difference could be attributed to a differential water holding capacity (WHC) of intact versus peeled material, with the former having lower WHC probably due to their reduced hydration capacity (Sannino, Demitri, & Madaghiele, 2009) and strong chemical bonds. Furthermore, the increased BI yield was due to incorporation of the waste solids. Therefore, it can be concluded that using an optimised SRRC will be more relevant to increase the yields when using intact bitter Cassava.

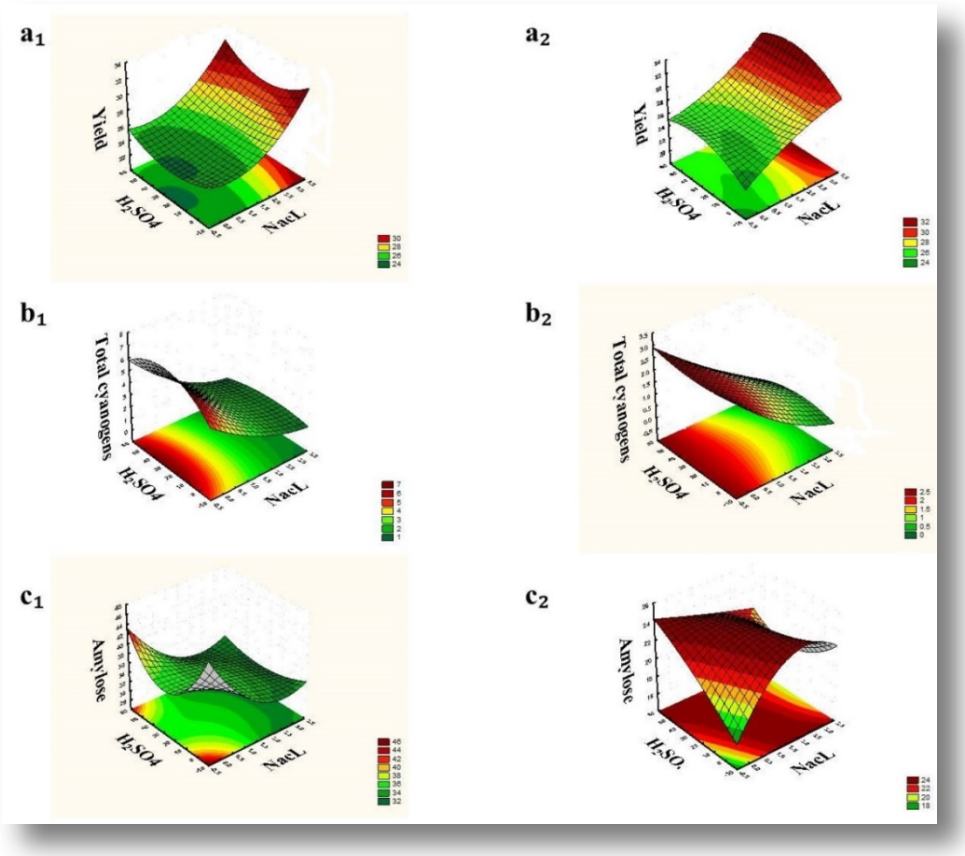


Fig. 2.2. Yield of BP (a_1) and BI (a_2), total cyanogens of BP (b_1) and BI (b_2) and amylose content of BP (c_1) and BI (c_2) bitter Cassava biopolymer derivatives as affected by extraction conditions (NaCl, H_2SO_4).

When the yield was determined in terms of the proportion of the maximum yield (%) (Table 2.2), intact bitter cassava produced higher yield (60.8 – 77.6 % wt dry basis) than peeled cassava (60.7 – 72.9 % wt dry basis). This was also ionic buffer concentration-dependent

Table. Yield of peeled and intact cassava as influenced by ionic buffers, and determined from maximum

NaCl, M	H_2SO_4 , mM	Peeled root (% of maximum yield)	Intact root (% of maximum yield)
0	0	60.7	60.8
0	25	59.7	62.7
0	50	61.6	63.3
1.5	0	63.4	66.1
1.5	25	63.1	64.8
1.5	50	64.5	66.7
3.0	0	72.4	74.3
3.0	25	70.4	77.0
3.0	50	72.9	77.6

2.3.4 Total cyanogen content

The total cyanogen (TC) content was significantly (p <0.05) reduced in all samples (Peeled, 1.1 – 4.8 ppm and Intact, 0.4 – 2.5 ppm) compared to TC content in fresh roots (400-900 ppm) or in defectively processed bitter cultivars (50-135 ppm). The Codex standards recommend 0.02 ppm TC per kg body weight in the daily diets of individuals, which is equivalent to less than 10 ppm in cassava product (CODEX, 2013).

The SRRC process had a greater degradation influence on TC; sodium chloride (NaCl), sulphuric acid (H_2SO_4) and peeling and their interaction showed highly significant (p <0.05) effects on total cyanogen loss (Table 2.1). NaCl had linear and quadratic reduction effects on TC (Table 2.1). Peeling also showed a significant linear effect on TC, both individually and combined with the linear and quadratic NaCl effect (Table 2.1). H_2SO_4 showed significant quadratic effect on TC, and combined linear effect with NaCl and combined effect with peeling (Table 2.1); these effects were less pronounced for the intact (BP) (Fig. 2.2b$_1$) than for the peeled (BI) (Fig. 2.2b$_2$) bitter Cassava.

SRRC processing was very effective in reducing the total cyanogen content well below the Codex minimum safety standard in all cassava samples, in comparison to fresh bitter cassava, demonstrating that there is no need for peeling bitter cassava.
SRRC processing was very effective in reducing the total cyanogen content well below the Codex minimum safety standard in all cassava samples, in comparison to fresh bitter cassava, demonstrating that there is no need for peeling bitter cassava.

2.3.5 Amylose content

Intact bitter Cassava showed lower amylose content (18 – 24 %) than peeled (31.4 – 39 %). The peeling showed the strongest significant (p<0.05) effect on the amylose content (Table 2.1). NaCl showed a significant effect individually and combined with peeling (Table 2.1). Peeled bitter Cassava showed slightly higher amylose content (Fig. 2.2c$_1$) than previously reported for sweet Cassava varieties (~15-30 % amylose content) (Alves, Mali, Beléia, & Grossmann, 2007; Nuwamanya, Baguma, Wembabazi, & Rubaihayo, 2013; A. C. Souza et al., 2012), whereas, amylose content (%) for intact bitter Cassava were within this range (Fig. 2.2c$_2$). The amylose content (%) reduction in intact bitter Cassava biopolymers could be explained due to the enzymatic hydrolysis during the SRRC process because of the presence of the waste solids. The lower amylose content (%) of the biopolymers produced with the intact roots can explain the more noticeable transparency of these types of films (see Fig. 2.3).

2.3.6 Film prototypes

The biopolymer packaging film prototypes from peeled (BP) and intact (BI) bitter Cassava powders are shown in Fig. 2.3. Eighteen formulations produced transparent and flexible films and further characterisation was performed in terms of Optical, solubility, barrier, mechanical, and thermal properties.

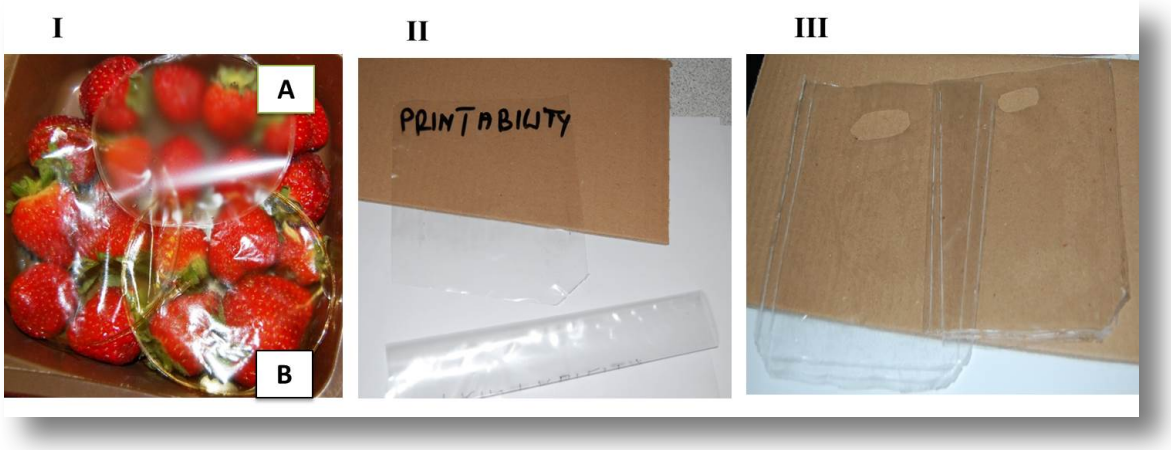


Fig. 2.3. Film visual images: Transparency of peeled (BP-A) and intact (BI-B) bitter Cassava films as affected by peeling and extraction conditions (NaCl, H_2SO_4) I, as potential printable material (II) and bag manufacturing capability (III).

2.3.6.4 Optical properties

Both peeled (BP) and intact (BI) bitter cassava films were transparent (Fig. 2.3). The BI films showed lower values of transparency (3.64 %) when compared to BP (11.94 %) equivalent, indicating that BI films were more transparent (lower Transparency %) than BP equivalents. When subjected to the same experimental testing methods and conditions, the BI Transparency % was found to be comparable to the commercial NVS (4.55 %) and PLA (3.39 %) but much more lower than OPP (13.55 %) films. Therefore, BI films were more transparent than OPP and with comparable transparency to other biobased films.

Analysis of the effect of peeling and extraction conditions (NaCl, H_2SO_4) on transparency is presented in Table 2.1 and Fig. 2.4 a_1 , $4a_2$, showing that peeling had a significant (p<0.05) effect on transparency. H_2SO_4 also showed a significant effect individually and combined with peeling (Table 2.1). The implication of this result is that more transparent films can be produced at low cost from intact bitter Cassava by applying an intrinsic modification during the SRRC process.

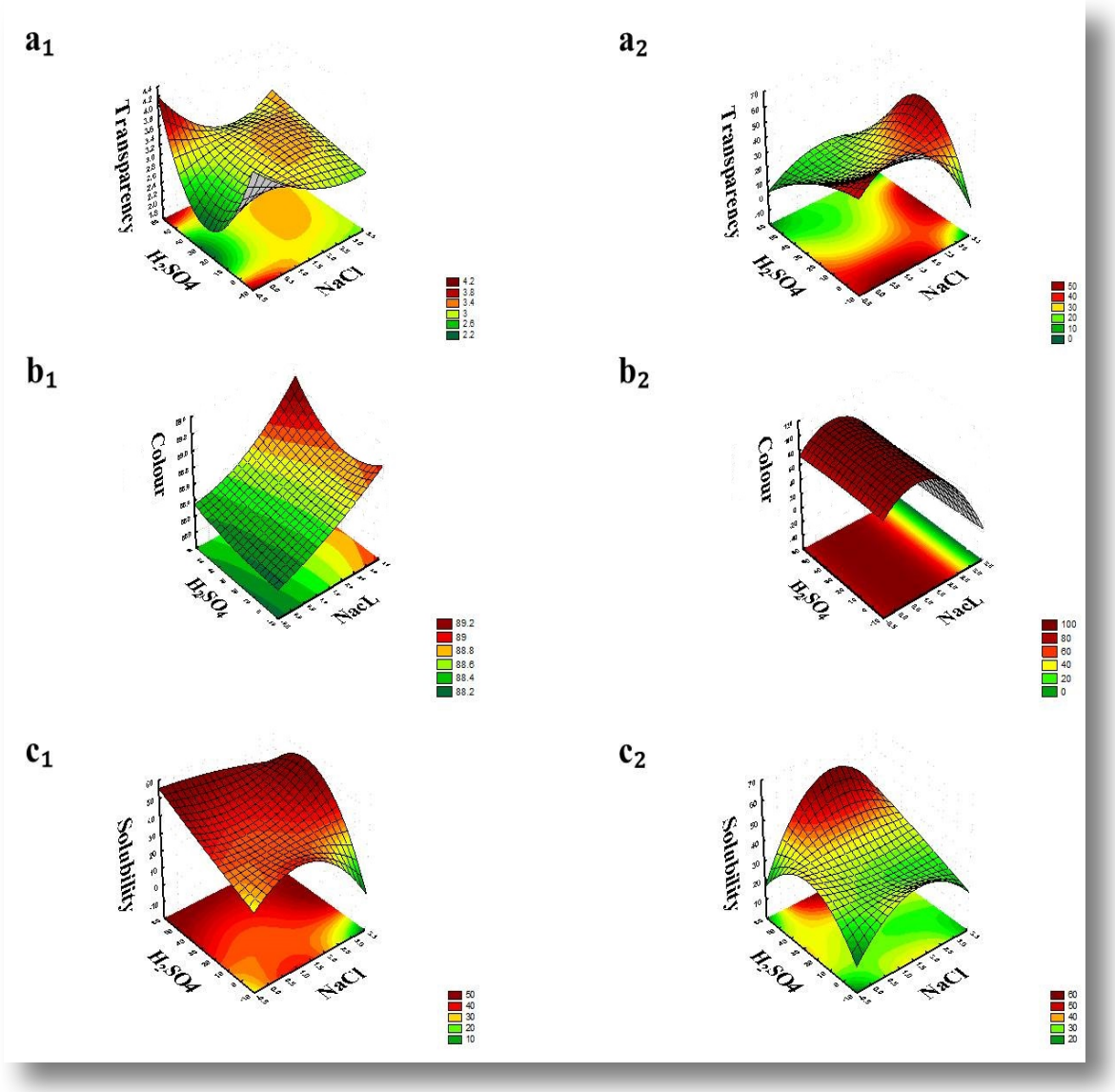


Fig. 2.4. Transparency of BP (a_1) and BI (a_2), Colour of BP (b_1) and BI (b_2) and solubility of BP (c_1) and BI (c_2) bitter Cassava biopolymer derivatives as affected by extraction conditions (NaCl, H_2SO_4).

To further corroborate the transparency results, film colour was determined and the analysis for the colour difference ($\Delta E_{a^*b^*}$) is shown in Table 2.1 while for their degree of lightness (L*) is presented in Fig. 4b. Unlike transparency, peeling and NaCl showed a higher significant (p<0.05) impact on film colour, thus confirming that BI (Fig 2.4b_2) films were more transparent than those of BP (Fig. 2.4b_1). The higher BI L* value is a manifest of better visual characters (minimum haze) of these films when compared to BP.

2.3.6.5 Solubility of bitter Cassava films

Water solubility, as a function of processing conditions (buffer and root type) is shown in Table 2.1 and Fig. 2.4c$_1$, 2.4c$_2$. Generally, films from the peeled (BP) bitter Cassava were more soluble compared to the intact (BI) equivalent as shown by a higher significant (p<0.05) effect of peeling on solubility (Table 2.1). This could be due to adding the waste solids that resulted in slightly higher water-resistant films. An increase in NaCl concentration increased film solubility in all treatment categories. Moreover, highly significant (p<0.05) effect was observed in BP films when NaCl was increased. Although the effect H_2SO_4 was not significant, as the H_2SO_4 concentrations increased, the BP and BI films were difficult to recover, maybe due to fast acidic cellulose depolymerisation forming hydrophilic oligomers that were easily lost in water. Nonetheless, the aforementioned solubility effect in the BI films could not match the higher effect in the BP categories, possibly due to water-resistance advantage induced in the film by the waste solids in BI films. The lower BI film solubility, at higher buffer concentrations (NaCl-3M: H_2SO_4-50mM), could be due to amorphised cellulose structure caused by enhanced high enzymatic digestibility at high acid concentrations (Ioelovich, 2012) leading to higher solvent mobility. Therefore, BP films produced with higher buffer concentrations (NaCl-3M: H_2SO_4-50 mM) cannot be used in their current form in an environment where a high water resistance is required, and would need further enhancement to reduce their solubility. In summary less soluble films can be produced with intact bitter (BI) Cassava, whereas BP films cannot be used on high humidity systems.

Knowledge of film properties is important in assessing package performance. Therefore assessment of BI films in comparison to commercial (OPP, PLA and NVS) films was done and is shown in Table 2.2, in terms of their barrier, mechanical and thermal properties.

2.3.7 Film performance properties

2.3.7.1 Surface

The scanning electron micrograph (SEM) of surface and cross-section is presented in Fig. 2.1. The film surface homogeneity is evident in Fig. 2.5a., suggesting that there was complete solubility of biopolymer derivatives in the polymer matrix but also this could have been a result of limited solvent migration at the interface. This result is also supported by the cross-section micrograph (Fig. 5b), suggesting a strong and uniform adhesion of material additives leading to homogenous mesh network structures in the film. Additionally, the result could explain the flexibility which was conspicuously evident in the films.

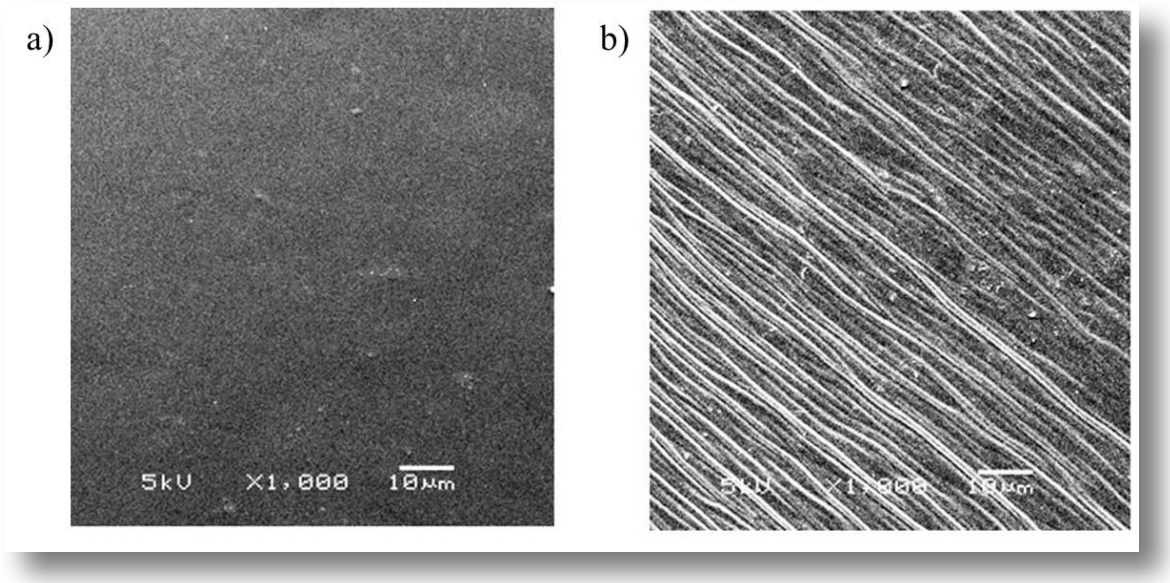


Fig. 2.5. Scanning electron micrographs of intact bitter Cassava film surface (a) and cross section (b) morphology.

Knowledge of surface energy is important in determining the printability and adhesion of flexible films. Intact bitter (BI) Cassava films presented contact angles (CA) of 72.7 – 87.6^0 between 0 and 180 seconds, suggesting the presence of polar functional groups in the film structure leading to less hydrophobicity. The polar functional groups were confirmed by FTIR analysis. Despite the low film hydrophobicity but less

hydrophilicity tendencies, films exhibited some degree of printability (Fig. 2.3). The BI Cassava films presented the CA within the range of sweet Cassava, 73.5-85.2^{o} (de Moraes et al., 2013), PLA, 73.4-81.0^{o} (Navarro et al., 2008) but lower than OPP, 111.0^{o} (Gourianova, Willenbacher, & Kutschera, 2005).

2.3.7.2 Chemical

The infrared (IR) spectra peak analysis of intact bitter Cassava films is shown in Fig. 2.7. It can be seen that there is peak absence at the 4000-3600 cm^{-1} position, indicating that there were no N-H stretching vibrations of amines or amides. The result meant that the film contained insignificant protein and total cyanogen contents. This is consistent with 0.4 -2.5 ppm total cyanogens of the powder derivative used in film formulation. The 3700-3000 cm^{-1} broad spectrum peak due to O-H stretching vibrations (Hinterstoisser & Salmén, 2000), the aromatic C-C peaks at 1600-1500 cm^{-1} could be an indication of cellulose, hemicellulose, pectin and lignin (Liang & Marchessault, 1959) in addition to starch incorporation in the film by solid wastes. This result agrees with the Cassava waste chemical composition obtained in earlier studies (Babayemi, Ifut, Inyang, & Isaac, 2010).

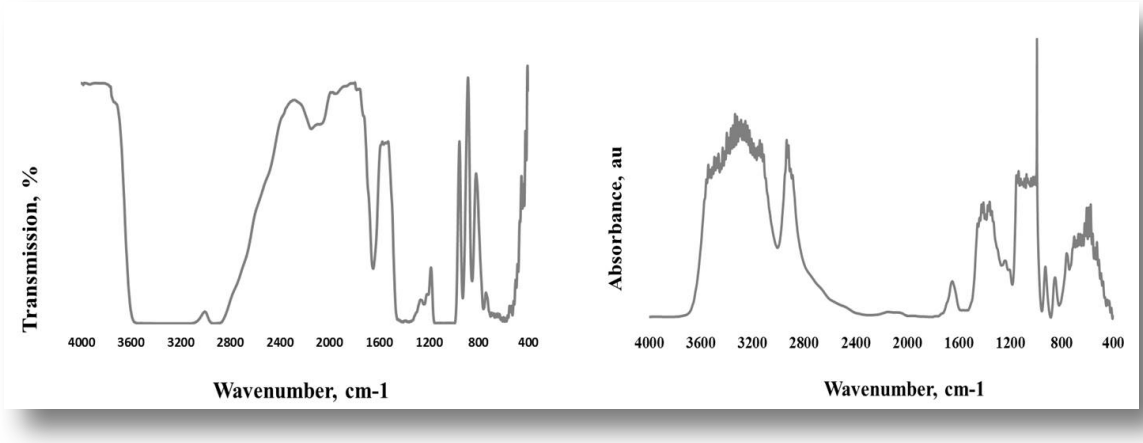


Fig. 2.6. FTIR spectra of intact bitter Cassava films prepared with derivative powder (3 w/v %) and glycerol (30 w/w %).

2.3.7.3 Barrier

Intact bitter (BI) Cassava films, produced from powders with NaCl: H_2SO_4, 1.5M: 25mM and Cassava: Glycerol: drying temperature, 3 w/v%: 30 w/w %: 50^0C conditions, exhibited different barrier behaviour in moisture and gas environments (Table 2.3). The permeability of BI Cassava films was within the range of commercial polylactic (PLA), Natureflex (NVS) and sweet Cassava, and less than that of commercial oriented polypropylene (OPP). Similarly, the BI oxygen transmission rate (OTR) was comparable to commercial PLA but higher than NVS and lower than OPP (Table 2.3). Conversely, the BI carbon-dioxide transmission rate (CTR) was reasonably lower than PLA, suggesting that the BI structure provided less solubility to carbon-dioxide than that of PLA. Comparably, bitter cassava produced films with lower OTR than commercially available OPP. These results could be an indication of highly amylopectin amorphous network structure of BI imparting less oxygen transfer in the films when compared to OPP and sweet Cassava. Regardless of CO_2 importance in modified atmosphere packaging, the noteworthy feature is that the CTR data on the Cassava films and its relations to the barrier properties is conspicuously lacking in literature.

2.3.7.4 Mechanical properties

Intact bitter (BI) Cassava film tensile strength (TS), elongation at break (E) and elastic modulus (EM) are shown in Table 2.3. As can be seen, TS of BI is comparable to commercial PLA, slightly lower than commercial NVS and OPP but higher than sweet Cassava. To gain further insight, the E and EM of BI were compared with PLA, NVS and OPP. It was found that BI films yielded lower E than for NVS, OPP and sweet Cassava but higher than the E of PLA. Conversely, the EM of BI was lower than that of PLA and NVS but higher than the EM of OPP and sweet Cassava.

Thus, it can be concluded that the comparative nature of BI films with commercial films could suggest that they have potential commercial application.

2.3.7.5 Seal integrity

Intact bitter (BI) Cassava films presented comparable seal strength with commercial Natureflex, NVS but lower strengths than PLA and OPP (Table 2.3). The BI films exhibited lasting seal strengths when left exposed to ambient conditions (15-20^{0}C; 50-60 %RH) for 12 hours beyond which the seals showed a gradual separation. However, in all the replicates tested, there was no evidence of instant separation, suggesting that they were less brittle and the film surfaces adhered adequately. The gradual loss of strength suggests that the films could be applied in moderately high temperatures and low humidity to form the internal lining of food bags.

2.3.7.6 Thermal

Like barrier and mechanical properties, glass transition (Tg) temperature, melting (Tm) temperatures, heat of fusion (ΔH) and crystallinity (C) of intact bitter (BI) Cassava were compared to commercial films. BI Cassava produced films with slightly lower Tg (54.3°C) than commercially available polylactic acid (PLA) (60.0°C), and comparable Tm (210.0°C) to PLA (170-230°C) (Curtzwiler et al., 2008). The BI film ΔH (67.0 J/g) was in a similar range with LLDPE (61.97 J/g), but higher than PLA (23.4 J/g), whereas, the C of BI (55.7%) exhibited higher values than those of PLA (12.9 %) and LLDPE (45.2 %) (Salamone, 1996). The comparable Tg and higher C could be due to the influence of SRCC on BI films, turning them into semi-crystalline state and falling into other semi-crystalline polymer category e.g. linear polyethylene, PE (Ehrenstein, 2001). Conversely, the higher Tm could be due to higher structural regularity of films imparted by incorporation of the waste solids. These findings suggest that intact bitter Cassava films can withstand thermal conditions similar to the other commercial films.

Table 2.3. Comparison of barrier and mechanical properties of intact bitter Cassava (BI), commercial (PLA, NVS, OPP) and sweet cassava films.

	Film type						
	Intact Cassava	Commercial				From previous studies	
Property	BI	PLA	NVS	OPP	Reference	sweet Cassava	Reference
Barrier							
Water vapour transmission rate g/(m^2 day)	438.6	375.0 [ii]	600.0 [ii]	20.0 [ii]	[ii] Innovia films	648.0	Polnaya *et al*., 2012
Oxygen transmission rate cc/(m^2 day)	812.9	524.9 [ii]	20.0 [ii]	1693.3 [ii]	[ii] Innovia films	21.5 x 10^{-9} *	Souza *et al*., 2013
Carbon-dioxide transmission rate cc/(m^2 day)	822.3	3080.0 [iii]	NIL	NIL	[iii] Curtzwiler *et al,* 2008	NIL	Belibi *et al*., 2014
Mechanical							
Tensile strength, MPa	41.1	48.8 [i]	70.0 [ii]	81.6 [i]	[i] ASTM D 638 [ii] Innovia films	1.2-2.4	Belibi *et al*., 2014
Elongation at break, %	17.4	9.2 [i]	70.0 [ii]	65.3 [i]	[i] ASTM D 638 [ii] Innovia films	26.8-49.4	Belibi *et al*., 2014
Elastic modulus, MPa	200.0	2020.2 [i]	> 1500 [ii]	13.2 [i]	[i] ASTM D 638 [ii] Innovia films	14.0-63.0	
Seal Strength, g(f)/25 mm	323.0	815 [iv]	200 [ii]	900 [v]	[iv] Hishinum, 2009 [v] Jindal films		

Note: * units given in cm^3/(m. day. Pa); NIL, not found in literature

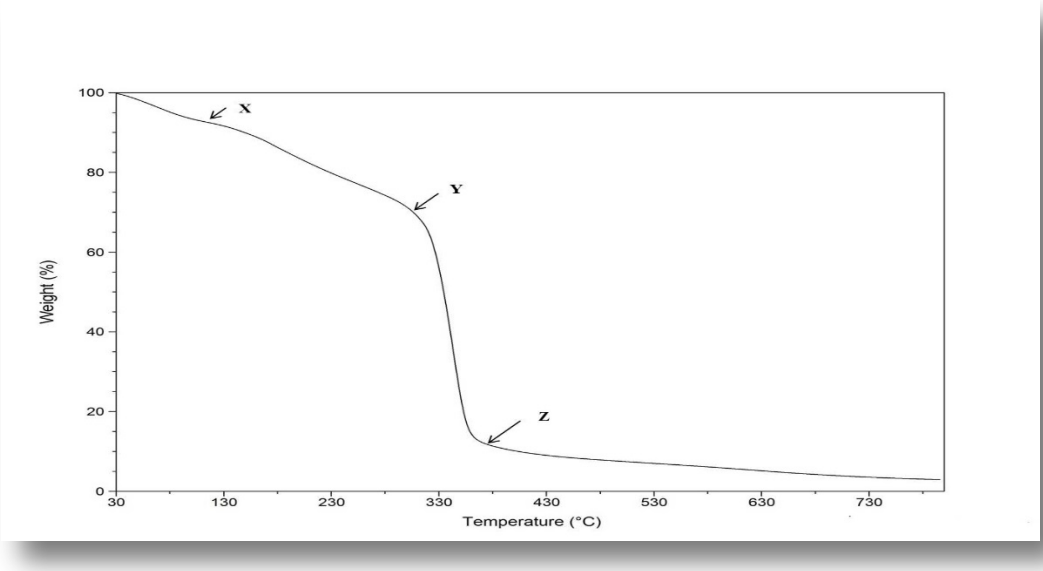


Fig. 2.7. Thermogravimetric analysis of intact bitter Cassava films prepared with derivative powder (3 w/v %) and glycerol (30 w/w %).

Thermogravimetric analysis (TGA) of intact bitter (BI) Cassava films is shown in Fig. 2.7. As shown at point X, the film weight loss of slightly less than 10% over 180^{o}C was due to bound water. This behaviour is similar to the one observed for most polymer networks (Gonsior, Mohr, & Ritter, 2012), although the loss is not much pronounced as shown by the linearity in the graph (Fig. 2.7). The uniform decomposition in film structure (region XY) could be attributed to other volatile compounds in film contributed by inclusion of the waste solids. However, BI Cassava films showed high thermal stability up to Z, corresponding to 373.06^{o}C, the onset of total degradation (OTD). Although BI Cassava film total weight loss (84.52 %) is slightly higher than values found for other polymers (>30%), the thermal stability loss to OTD point (373.06^{o}C) of BI Cassava films is higher than previously reported range (340-360^{o}C) for most polymer networks (Gonsior et al., 2012).

Conclusion

Intact bitter Cassava showed significantly (p<0.05) higher yields than peeled equivalent, and increasing with an increase on both extraction buffers. Intact bitter cassava produced an average 16 % waste decrease, showing higher yield due to incorporation of the waste solids, and no environmental impact caused by discard residues. The amylose content was significantly (p<0.05) lower for the intact bitter cassava than for the peeled equivalent. Simultaneous release recovery cyanogenesis (SRRC) processing of bitter Cassava was very effective in reducing the total cyanogen content well below the Codex minimum safety standard level in all cassava samples, in comparison to fresh bitter cassava. This outcome demonstrates that there is no need for peeling bitter cassava, and presents promising results for its application to food and non-food applications.

The films were produced using either peeled (BP) or intact (BI) bitter Cassava. BI films showed to be more transparent, homogeneous, exhibited lower solubility and hydrophilicity, higher WVTR, moderately OTR and CTR, with higher strength (higher TS, and EM) and thermal stability (higher Tm, sealable) than BP and commercial PLA, but with lower strength than NVS and OPP. The study showed that BI films can be produced at lower cost than the peeled (BP) equivalents.

Therefore, safe, high value-added biopolymers, with potential application for food packaging can be produced from intact bitter cassava, minimising waste and environmental impact, generating practical applicability and contributing to a sustainable system. Furthermore, it is noteworthy that although the goal of this study was a proof of concept to develop film prototypes from intact bitter cassava, the film production could be potentially scale up using tape casting as reported by (de Moraes et al., 2013).

Chapter 3. Integrated process standardisation as zero-based approach to bitter cassava waste elimination and widely-applicable industrial biomaterial derivatives

Abstract

An integrated standardised methodology for production of biopolymer derivatives (BPD) from novel intact bitter cassava was demonstrated by desirability optimisation of the simultaneous release, recovery and cyanogenesis (SRRC) process. BPD were evaluated for yield and colour by using buffer, 0, 2, 4 % v/v, cassava waste solids, 15, 23, 30 % w/w, and extraction time, 4, 7, 10 minutes. Using an Integrated process methodology, nearly all the intact root was transformed into BPD, resulting in higher yield, 41 % w.b. and colour difference, 1.3 in contrast to 26 % w.b. yield and 28 colour difference when cassava starch was extrinsically processed. Maximum global desirability, 1.0 predicted efficient material balance, buffer, 4.0 % w/v, cassava waste solids, 23 % w/w and extraction time, 10 minutes, for producing BPD with yield, 38.8 % w.b. Experimental validation, with buffer, 3.3 % w/v, cassava waste solids, 30 % w/w and extraction time, 10 minutes, produced BPD with 40.7 % w.b. yield. SEM, DSC, TGA, FTIR and moisture barrier analyses revealed a uniform microstructure and high thermal stability of BPD and film, thus demonstrating efficient performance of the standardised integrated methodology.

Hence, processing intact cassava root as a standardised integrated simple methodology, could be used to produce sustainable low cost BPD for a broad range of applications.

Methodologies designed around standard integrated procedures, matching zero-based approach to contamination elimination, are novel strategies, and if they are used effectively and widely can provide better avenues to eliminate cassava wastes and recover BPD resources as sustainable biomaterials.

Key words: bitter cassava, optimization, desirability, standardization, biopolymer derivative

3.1 Introduction

Environment-borne cassava wastes represent a potential economic source of biopolymer derivative cellulose, hemicellulose, pectin, lignin and starch (Babayemi et al., 2010; Hermiati, Mangunwidjaja, Sunarti, Suparno, & Prasetya, 2012). Cassava waste solids could support the sustainable production of low-cost industrial bioproducts such as food and non-food added value products. The global turnaround concept of regarding waste as a worthless material to the idea of a high demand secondary material resource has widened value-added waste research. Currently, research emphasis is focused more on waste minimisation than waste recycling (Ezejiofor, Enebaku, & Ogueke, 2014).

Among the cassava varieties, bitter cassava contributes a greater amount of disposed environmental waste, >16 % (Tumwesigye et al., 2016) as compared to sweet cassava, 0.5 % (Edama, Sulaiman, & Abd.Rahim, 2014). Unfortunately, bitter cassava (BC) waste minimisation, has not yet received much attention, therefore the environmental accumulation of BC wastes has been inevitable. Traditionally, there have been initiatives to transform BC into food and other low-value products such as fermented crude ethanol and flour (Tumwesigye, 2014), gari (Akinpelu, A.O. L. E.F. Amamgbo, A.O. Olojede, 2011). However, total cyanogens, inherent in these varieties and poor processing methodologies have impeded the efforts with negative environment impacts. Meanwhile, sweet cassava starch production, using reinforcements and modifications of biopolymer derivatives (SC-BPD) for various applications have also been studied (Raabe et al., 2015; Versino et al., 2015). Although, such procedures require high energy leading to higher production costs. Moreover, starch processing using added cellulose materials, have been limited by non-uniformity and less compatibility (Azwa, Yousif, Manalo, & Karunasena, 2013; Oliveira et al., 2015), requiring further additional chemical and physical modifications and costs. Recently, a novel methodology, using simultaneous release, recovery and cyanogenesis (SRRC), to transform intact BC wastes into safe (total cyanogens, <1.0 ppm) BPD with significant high yields, has been reported (Tumwesigye et al., 2016). Due to these findings, SRRC methodology could be successfully employed to produce safe intact BC-BPD.

Standardising methods of producing materials could ease the choice and cost of formulations, by defining the design space, processing parameters and material

functional properties, which could lead to the engineering design of tailored food and non-food added value products. Design of experiments (DOE) has been successful in simultaneous investigation of the effect of multiple variables, to determine the most efficient and economic matrix formulations needed for optimal formulations (Steele et al., 2012). Robust production processes provide methodologies for balancing desired material properties with processing parameters with marginal costs and maximum functionality. Desirability function approach is extensively employed in the optimization of multiple response processes, in which the operating parameters provide the "most desirable" responses. In order to broaden ways of modifying native polysaccharides and produce new materials for the utilisation of cassava in food packaging and other potential industries, customised methods that ensure combined release of BPD are necessary.

To the best of our knowledge SRRC, integrated process, optimisation of BC-BPD production, to minimise production costs, and standardisation of design methodology have not been studied. Thus, it was justifiable to develop a standardised integrated sustainable low-cost methodology to produce BPD from novel intact BC root.

The purpose of this study was to develop an integrated standardised process methodology for novel intact BC-BPD recovery, and evaluate its impact on BPD. The optimum processing parameters necessary to obtain maximum yield and colour as defined by maximum global desirability, and development of a standardised methodology by validation of optimal BPD were investigated. The potential of applying BC-BPD as food and non-food material was determined by assessing the effect of standardised methodology on BPD's quality (physical, chemical and safety), and film moisture barrier characteristics.

3.2 Materials and methods

3.2.1 Integrated process methodology for production of novel intact BC-BPD

3.2.1.1 Intact bitter cassava preparation

Bitter cassava, Tongolo, procured from farmers' fields, Northern Uganda was separated from soil debris, placed in ice boxes, transported to the laboratory and kept at -20°C for further use.

8.2.1.15 3.2.1.2 Integrated process methodology

Production of biopolymer derivatives followed the procedure developed earlier for peeled and intact roots via the simultaneous release, recovery and cyanogenesis (SRRC) process (Tumwesigye et al., 2016) with slight modifications. Mechanical tissue rupture and cell disruption of intact bitter cassava (BC) roots were performed using motorised method in a high-speed grating pulper (6,000 g).

SRRC was found to be crucial in the biopolymer derivatives (BPD) production as the process release stage and processing parameters influenced positively the yield and properties of BPD (Tumwesigye et al., 2016). Effects of various parameters at three levels, buffer, 0, 2, 4 % v/v, cassava waste solids, 15, 23, 30 % w/w, and extraction time, 4, 7, 10 minutes on biopolymers yield and colour were evaluated using a pre-designed experiment (subsection 2.3.1). During biopolymers' release stage, 100 g of pulp mass was mixed with 100 ml of various extraction buffers in a commercial blender (500 W Breville IHB086 Hand Blender), and the mixtures homogenised according to set time (Table 3.1) at ambient temperature (20 - 23ºC). The buffers used in release and recovery, i.e., sodium chloride (≥99 % AR) and conc. sulphuric acid (99.9 %) were analytical grade from Sigma Aldrich (Ireland).

Recovery was achieved by centrifuging the slurry at 8,000g, 5-7^{0}C for 10 minutes, washing in deionised water (3x) and drying semi-dehydrated coarse pulp in an air-circulating, temperature (30±5°C), relative humidity (30-40 % RH), and constant weights obtained after 9h. The dried samples were weighed, colour measured and milled to a fine powder using an analytical grinder (IKA Yellowline-RA 10, Germany) and kept refrigerated (4 -7^{0}C) between tests and further use.

3.2.2 Optimisation via desirability approach and statistical analysis

3.2.2.1 Factorial and Box-Behnken response surface experimental design

The BPD production was performed using a factorial and Box-Behnken response surface experimental design methodology. The individual factors and levels chosen for Box-Behnken design are shown in Table 3.1.

Table 3.1. Box-Behnken design matrix: Actual/coded variables of processing parameters and biopolymer derivatives (BPD) yield and colour.

Runs	**Actual/ coded independent variables**			Thermoplastic derivatives	
	Buffer concentration, w/v %*	Cassava waste solids, w/w %*	Extraction time, Min.	Yield, %	Colour change, ΔE
1	0.0 (-1)	23.0 (0)	4.0 (-1)	28.0±0.1 *a*	6.3±0.1 *a*
2	2.0 (0)	23.0 (0)	7.0 (0)	32.9±0.2 *b*	4.3±0.0 *b*
3	4.0 (1)	30.0 (1)	7.0 (0)	38.0±0.3 *c*	5.6±0.1 *c*
4	2.0 (0)	15.0 (-1)	10.0 (1)	27.9±0.3 *a*	4.8±0.0 *d,b*
5	4.0 (1)	23.0 (0)	4.0 (-1)	27.9±0.4 *a*	5.8±0.0 *a,c,e,g,l*
6	2.0 (0)	23.0 (0)	7.0 (0)	26.7±0.5 *a*	5.5±0.0 *e,c*
7	0.0 (-1)	23.0 (0)	10.0 (1)	27.0±0.4 *a*	5.2±0.1 *f,c,d,e*
8	2.0 (0)	30.0 (1)	10.0 (1)	27.9±0.4 *a,j*	6.3±0.1 *a*
9	0.0 (-1)	15.0 (-1)	7.0 (0)	27.8±0.4 *a,k*	6.1±0.0 *a,g*
10	2.0 (0)	23.0 (0)	7.00 (0)	33.8±0.2 *d,b*	5.7±0.0 *g,c,e,f*
11	2.0 (0)	15.0 (-1)	4.0 (-1)	37.1±0.3 *e,b,c*	5.1±0.0 *h,c,d,e,f*
12	4.0 (1)	15.0 (-1)	7.0 (0)	31.1±0.3 *f,d*	4.9±0.1 *i,d,h,f,j*
13	0.0 (-1)	30.0 (1)	7.0 (0)	23.0±0.4 *g*	4.7±0.1 *j,b,d,f,h*
14	4.0 (1)	23.0 (0)	10.0 (1)	38.8±0.1 *h,c.e*	4.1±0.0 *k,b*
15	2.0 (0)	30.0 (1)	4.0 (-1)	23.1±0.3 *i,g*	5.4±0.0 *l,f,g,h,j*

* w/v, weight (g) per 100 g solution; ** w/w, weight (g) per 100 g dry weight; and 100 g, maximum theoretical mass.

A factorial analysis was defined to determine the functional relationship between processing parameters and yield, colour responses, and their combined interaction effects.

Yield was defined as the percentage of constant weight dried powder recovered from initial mass of 100 g roots, and determined in triplicates.

Colour difference (ΔE) was determined according to Ramirez-Navas & Rodriguez de Stouvenel, (2012) using CR-400 Chroma Meter, Konica Minolta Sensing Japan without major changes. Measurements were taken, in triplicates, on derivative powders and BI each, and mean values used in CIELAB L*, a*, b* using the eqn. 3.1 as described (Sharma et al., 2005).

$$\Delta E = \sqrt{[(\Delta L'/k_L S_L)^2 + (\Delta C'/k_C S_C)^2 + (\Delta H'/k_H S_H)^2 + R_T (\Delta C'/k_C S_C)(\Delta H'/k_H S_H)]} \quad 3.1$$

where ΔE, differences between sample and standard (S) colour parameters; S, background colour reference parameters; √, square root symbol; k_L k_C k_H, parametric weighting factors; ΔL′ ΔC′ ΔH′, lightness, chroma and hue differences.

A statistical analysis and individual parameter empirical model equations for yield and colour were performed as reported (Vicente, Martínez, & Aracil, 2007) with slight modifications. The design matrix for both processing parameters (actual/coded independent variables) and responses (yield and colour), with a total of 15 experimental runs are presented in Table 3.1. Each run was an average of 3 replicates. Data was fitted to four models (linear, combined two factor interaction, quadratic) in order to describe the adequacy of the experimental linear models and determine the second order polynomial equations, their regression coefficients and R^2 values. The aliased cubic model was not considered for analysis. Analysis of variance (ANOVA) was used for regression coefficient determination, lack-of-fit test and significance of curvature effect. The model adequacy was determined by lack-of-fit test, residual analysis and coefficient of determination (R^2) and illustrated visually by contour plots. Following, processing parameters were harmonised with properties to determine significant effects for optimisation purposes.

3.2.2.2 Simultaneous optimisation using desirability function

Response surface methodology was applied to quantify factor-response associations in simultaneous determination of optimal processing parameters considering yield and colour by desirability function. Consideration of waste solids reinforced starch was important in order to gauge intact bitter cassava ability to produce biopolymer derivatives with desirable yield and colour (towards brighter colours). The lower and upper limits were set for buffer (2 and 4 % v/v), cassava-rich waste solids (15 and 30 % w/w) and extraction time (4 and 10 minutes).

The simultaneous optimisation (desired functional combination) of buffer concentration, waste solids, extraction time (material balance) and biopolymer derivatives yield and colour were achieved by a desirability (D) approach (eqn. 3.2) and suggested by Derringer, (1980). The method is reported widely in literature but also common for multiple responses optimisation in many industrial applications.

$$D = [d_y (Y) \times d_c (C)]^{1/n} \qquad 3.2$$

where, D, desirability; Y, yield (%); d_y (Y), yield desirability function, C, colour difference (ΔE); d_c (C), colour desirability function; n, responses (n=2); dy (Y) and d_c (C) = 0, perfectly undesirable; d_y (Y) and d_c (C) = 1, perfectly desirable.

In this study, for biopolymer yield, the desirability function demanded maximisation while colour difference minimisation. To achieve the preceding situation, the criteria set for material balance was: buffer, maximise concentration (range 0 – 4 % w/v); waste solids, in range content (15 – 30 % w/w); extraction time, maximise frequency (range 4 – 10 minutes).

Desirability concept:

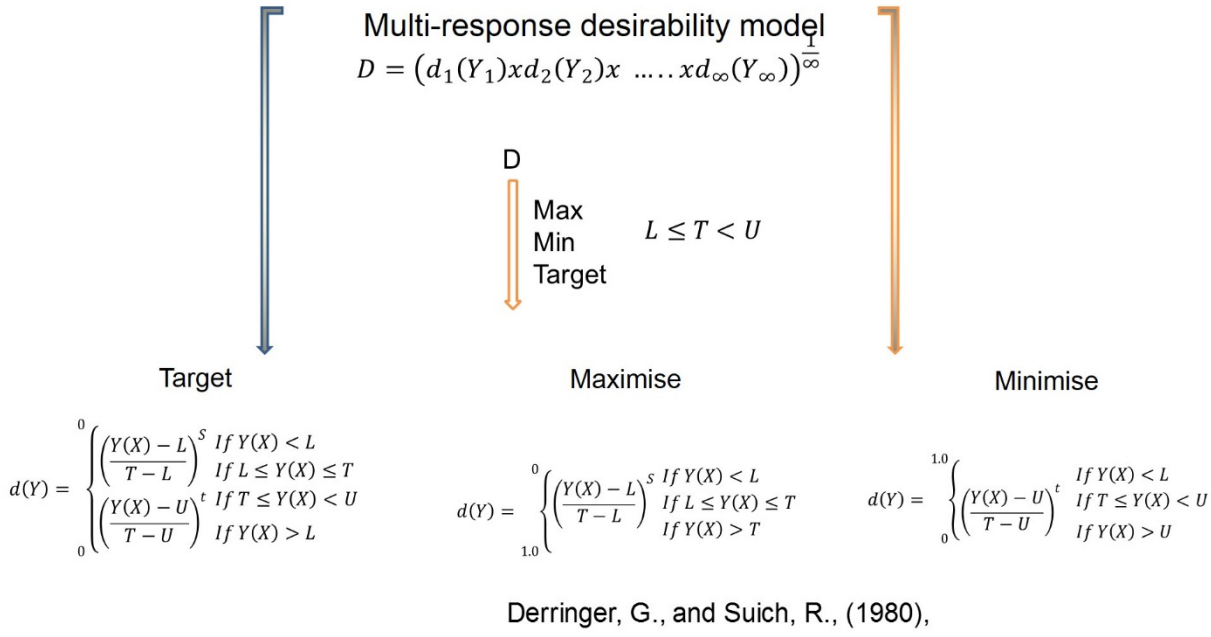
Desirability function methodology determines the working (active) parameters (independent variables), which provide the best desirable responses (dependent variables).

For a given dependent variable $\boldsymbol{Y_i(x)}$, a desirability (D) function $\boldsymbol{d_i(Yi)}$ assigns "0 to 1" numbers to possible values of Y_i, with $d_i(Yi) = 0$ (entirely undesirable Y_i value) and $d_i(Yi) = 1$ (absolutely desirable Y_i value). Individual desirabilities (Ds) by geometric mean give a global desirability (GD), such that,

$$GD = [d_1(Y_1) * d_2(Y_2) * d_3(Y_3) \dots\dots d_\propto(Y_\propto)]^{\frac{1}{\propto}} \qquad 3.3$$

where, α, number of dependent variables (responses). Practically, if any response is completely undesirable, i.e. $d_i(Yi) = 0$, then GD = 0. Thus, according to (Derringer, 1980), a response can be assigned a target, minimised or maximised (optimised).

The whole concept is illustrated in concept 3.1



Concept 3.1. Desirability function concept for using in multiple variable optimisations

Power (exponent), s and t, determine how essential it is to hit the target value. For **s = t = 1**, the desirability function increases linearly towards **Ti**; for **s < 1, t < 1**, the function is convex, and for **s > 1, t > 1**, the function is concave.

Generally, in multiple response optimisation, the independent and dependent variables can be optimised separately or simultaneously. Furthermore, it involves: implementing an experiment and fitting variable models for all α responses; defining D functions for each variable; and target, minimise or optimise the GD with respect to the controllable conditions.

Statistica 7.1 software (StatSoft Inc., Tulsa, USA) was used for experimental design, quadratic model buildings, response surfaces and charts generation, and numerical and graphical optimization.

3.2.3 Standardisation of integrated process methodology by validation of optimal models

Standardised methodology by validation of optimisation was accomplished by running experiments using optimal formulations. Results thereof were compared with optimal values in order to set standards for intact BC-BPD production.
Scenarios were developed based on set objectives i.e. 'minimise', 'in the range' and 'maximise', and using Design Expert (Version 9.0.4.1, State-Ease, Inc. 2015, Minneapolis, USA) and non-repetitive permutation approach, the most promising scenarios with the highest desirability (D) were found to better describe optimisation process.
In addition, a maximum global desirability (GD) was achieved for both parameters and responses, and predicted the optimal processing parameters from the material balance.

3.2.4 Impact of standardisation on Biopolymer derivatives and packaging film moisture barrier properties

8.2.1.16 3.2.4.1 Effect on total cyanide decontamination and BPD appearance

Biopolymer derivatives safety and appearance were determined by running two related experiments: i) testing the effect of ionic buffer (0, 2, 4 % w/v), waste solids (15, 23, 30 % w/v), and sodium bisulphite (1, 2, 3 % w/w of waste solids) on total cyanogens (TC) and colour difference (ΔE); and ii) sodium chloride (0, 1.5, 3 M), sulphuric acid (0, 25,

50 mM), and peeling (peeled, intact) on TC. The TC was determined using the cyanide kit developed by (Bradbury, Egan, & Bradbury, 1999) while ΔE was measured as described in section 2.3.1.

8.2.1.17 3.2.4.2 Microstructure and chemical

Biopolymer derivatives microstructural properties were examined using Scanning Electron Microscope (SEM), JSM-5510 (Jeol Ltd., Tokyo, Japan). A small amount of derivatives powder was placed on stubs using double-sided carbon tape to form a very thin layer and leaving a space on either side of the strip to allow clear observation of surfaces and cross section. Prior to capturing SEM images, powder stubs were spluttered with a thin layer of gold. Powder stubs were subjected to a focus magnifications as high as 20 000x and images capture between 200x and 30 000x magnification and intensity of 5 kV.

Biopolymer derivatives were analysed for their chemical composition and their possible interactions resulting from use of intact root and modification by SRRC using Fourier transform infrared spectroscopy (FTIR). A small sample of the derivative powder was mixed with potassium bromide in a mortar while under the lamp heater, converted into thin pellets using a timed pneumatic press for 20 seconds and placed in the sample holder. The spectra were recorded with an UV/Vis spectrum one FTIR spectrometer (Perkin Elmer Lambda 35, USA), frequency range of 4000–400 cm^{-1} and $4cm^{-1}$ resolution in the transmittance and absorbance modes for individual spectrum with 30 scans at room temperature.

8.2.1.18 3.2.4.3 Thermal

Biopolymer derivatives thermal analysis, glass transition (Tg) and melting (Tm) temperatures and crystallinity (C), was conducted using a differential scanning calorimeter (DSC 200 F3) equipped with a thermal analysis data station. A hermetically sealed DSC pan with fresh derivative powder (10 mg), together with a reference empty pan were heated from 20 to 250°C at a rate of 10°C/min, cooled back rapidly to 20°C and reheated at a rate of 5°C/min to 250°C to give them thermal history. T_g, T_m, ΔH and

C were calculated using the built in software and determined by considering the heat capacity change observed on the second heating.

Thermogravimetric analysis was carried out to establish thermal stability of derivatives using TG Analyser (Spectrum 500) and analysed by the Universal Analysis 2000, New Castle USA) between 30^0C and 500^0C, heating rate of 20^0C/min, nitrogen flow of 60 mm/min. Prior to analysis, each sample was corrected against a background scan. All samples were evaluated in triplicate and mean measurements reported.

8.2.1.19 3.2.4.4 Moisture adsorption

Thermoplastic derivative powder (100g) was dried (48 h) in a vacuum oven (60^0C) and cooled in a desiccator (2 h). Its moisture content was 8 % dry weight basis. The sample was placed in different relative humidity (10-90 % RH) using different saturated salt solutions (LiCl, CH_3COOK, $MgCl_2$, K_2CO_3, Mg $(NO_3)_2$, NaBr, NaCl, KCl, K_2SO_4) at 20^0C). Weight gains by the moisture-adsorbed powder, at regular interval (every 48 h), were obtained using an analytical balance (precision, 0.0001 g). Moisture adsorbed was reported as a percentage on dry weight basis. Three replicates were run.

3.2.4.5 Film preparation

Films were produced by solution casting using the procedure reported by Tumwesigye et al., (2016). Mixtures of BPD (3 % w/v) and glycerol (30 % w/w) were heated at 70^0C for 25 minutes. Prior to moisture barrier characterisation, films were conditioned at 23 ± 2 ^{0}C and 54 %RH. Thickness was measured in six different locations with using an absolute digital Calliper (Digmatic, Mitutoyo UK Ltd).

8.2.1.20 3.2.4.6 Film moisture barrier characterisation

Determination of moisture adsorption (MA) characteristics followed the method described for BPD in section 2.5.4 with slight modifications. Film strips (3 x 1.5 cm) were pre-dried until constant weight for 9 h at 90^0C.

Water vapour permeability (WVP) of the films was determined according to ASTM, (2005) method at 10, 20, 30, 40 °C and at a gradient from 0 to 75, 85 and 95% relative humidity. Results were expressed in gmm/m² s kPa).

8.2.1.21 3.2.4.7 Moisture barrier modelling

The MA and WVP data were fitted to different models (Table 3.4) in order to correlate equilibrium moisture content and water activity. Model parameters were estimated by the non-linear regression procedure using Excel (2010) solver and goodness of fit evaluated as mean relative percentage deviation in modulus, ρ, % (Eqn. 3.4) and regression variance, VR (Eqn. 3.5). Accurate mathematical description of isothermal was considered when $\rho \leq 5$ %, VR ≤ 5 and $R^2 \leq 0.97$.

$$\rho,\% = \frac{100}{n} \Sigma_{i=1}^{n} \frac{|\varepsilon_i|}{X_{i(o)}} \quad 3.4$$

$$VR = \Sigma_{i=1}^{n} \frac{|X_{i(p)} - X_{i(o)}|^2}{n-1} \quad 3.5$$

where, n, number of experimental points; ε_i, absolute value; (p) and (o), predicted and observed.

The effect of standardisation on the water uptake and diffusion characteristics of intact bitter cassava films was determined using eqn. 3.6 following the procedure described by Sultana & Khan, (2013).

$$\frac{M_t}{M_e} = 2\left(\frac{D_t}{\pi l^2}\right)^{\frac{1}{2}} \quad 3.6$$

Where, M_t, moisture weight uptake at time (t); M_e, moisture weight uptake at equilibrium (e); l, film thickness; and D, diffusion coefficient, which was calculated from the slope by plotting M_t / M_e against $t^{1/2}$.

To predict long-term behaviour of intact bitter cassava materials, the temperature-time dependence of WVP was determined by fitting experimental data to Arrhenius and time-temperature superposition of William-landel-Ferry (WLF) models.

3.3 Results and discussion

3.3.1 Integrated process methodology for production of novel intact bitter cassava biopolymer derivatives (BC-BPD)

Process integration methodologies are fundamental techniques for designing sustainable methodologies, processes and materials for broad range applications. In this study, a process integration methodology was developed, optimised, and standardised to provide important means of achieving environmental-resilient approaches for production of intact bitter cassava biopolymer derivatives suitable for both food and non-food applications.

The standardised methodology demonstrates an integrated process that uses cheap novel intact bitter cassava and SRRC approach for sustainable biopolymer derivatives production and cassava waste reduction.

3.3.2 Optimisation of BPD production by Desirability

Yield is an indicator of any process efficiency and economy (Mudgal et al., 2012). Biopolymer derivatives (BPD) yield is shown in Fig. 3.1 & Table 3.1, revealing that parameter main effects and their interactions had a significant (p<0.05) impact on yield. Except for buffer-waste solid and buffer-extraction time interactions with linear and quadratic negative impacts, all main effects and their sole interactions with time had linear positive effects on yield. The increased yield signalled the intact BC-SRRC process efficiency. Unlike sweet cassava (SC) which yielded 17-26 % w.b., intact BC-BPD presented higher yields (23-39 % w.b.) when SRRC was employed (Tumwesigye et al., 2016), signifying that BC could be the future sustainable source of BPD production for industrial applications.

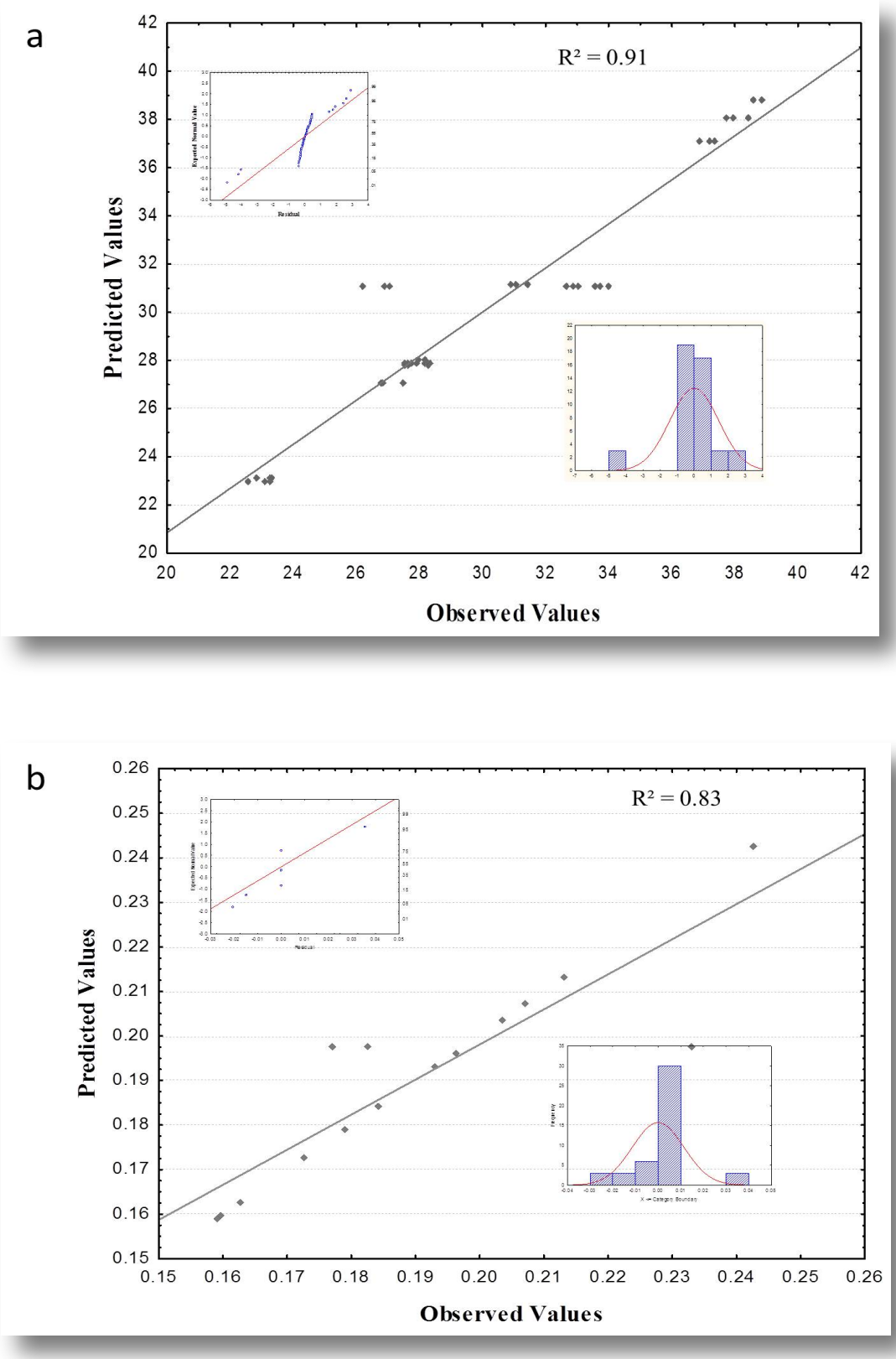


Figure 3.1. Model fitting, residual plots and normal distribution for effect of processing parameters on biopolymer derivatives (BPD) a) yield and b) colour change, ΔE.

Colour difference (ΔE) results are presented in Fig. 3.1 &Table 3.1. Extraction time had a highly significant positive linear effect as compared to linear buffer positive, buffer-extraction time positive and buffer-waste solid interaction negative effects on ΔE. In this study, major parameter interactions presented negative effects on ΔE. Similarly, it was shown that increasing extraction time reduced the BPD brightness, due to high positive effects. Conversely, negative parameter interactions (I) impacts on ΔE implied brighter colours. Thus, optimising the formulation was necessary to obtain trade-offs and produce industrial-appealing BPD.

Production of intact BC-BPD through integrated methodology showed, 0-1.3, 92, 3.6 for ΔE, luminosity parameter (L*) and chroma (C*), respectively. Production of SC-BPD from peels and bagasse (Versino et al., 2015), showed, ΔE, values ranged from 11-28, 10-22 and 78-90 for ΔE, L*, and C*, respectively. Comparably, previous work using intact SC root under similar SRRC processing conditions produced BPD with 1.1-4.6, 88-92 and 0.5-1.0 for ΔE, L*, and C*, respectively (Tumwesigye et al., 2016).

Therefore, an integrated process methodology and SRRC produced BPD higher yields and lower colour difference (ΔE) than previously reported, providing positive evidence for future production of sustainable low-cost BPD.

Variations in processing parameters led to significant changes in BPD yield and colour (Table 3.2). The ANOVA regression coefficients, p-values, R^2, significant curvature and lack of fit test (Table 3.2) showed that the quadratic models were highly significant ($p < 0.05$) for all responses while an aliased condition occurred for cubic models. Therefore, the second order polynomial model equations (Eqns. 3.7 & 3.8) adequately described the association between buffer concentration, waste solid content, extraction time and BPD yield and colour. Additionally, yield and colour R^2 of greater than 90 % and 82 % respectively suggested that data explained the adequacy and significance of the models.

$$\text{Yield, \%} = 31.110 + 2.901\,\mathbf{B} - 3.483\,\mathbf{W} - 1.123\,\mathbf{T} + 2.939\,\mathbf{BW} + 2.974\,\mathbf{BT} + 3.515\,\mathbf{WT} + 0.152\,\mathbf{B^2} - 1.276\,\mathbf{W^2} - 0.825\,\mathbf{T^2} + 1.696\,\mathbf{BW^2} + 3.991\,\mathbf{B^2W} + 3.590\,\mathbf{BT^2} \quad (R^2 = 0.91) \qquad 3.7$$

$$\text{Colour, } \Delta E, \% = 5.142 - 0.388\,\mathbf{B} + 0.442\,\mathbf{W} + 0.142\,\mathbf{T} + 0.534\,\mathbf{BW} - 0.140\,\mathbf{BT} + 0.276\,\mathbf{WT} + 0.068\,\mathbf{B^2} + 0.127\,\mathbf{W^2} + 0.136\,\mathbf{T^2} + 0.306\,\mathbf{BW^2} - 0.639\,\mathbf{B^2W} - 0.837\,\mathbf{BT^2} \quad (R^2=0.83) \qquad 3.8$$

where, B, buffer concentration (% w/v); W, waste solid (% w/w); T, extraction time.

Table 3.2. Analysis of variance of effects of a) processing conditions on total cyanogen and colour, and b) peeling on total cyanogen.

a)

Parameter	Sum of Squares (SS)	
	Total cyanogens	Colour difference, ΔE
(1)Buffer L+Q	0.0164**	0.9214^{ns}
(2)Waste L+Q	9.1808^{ns}	0.20632*
(3)Sodium bisulphite L+Q	16.8033*	4.22208*
1*2	23.0613*	6.42021*
1*3	68.5222*	4.62008*
2*3	4.2222*	0.9148*
Error	4.334	3.29029
Total SS	118.5975	18.9811
R^2	0.97	0.83

* Significant at 1% level; ** Significant at 5% level; ns, not significant

b)

Parameter	Sum of Squares (SS)
	Total cyanogens
(1)Sodium chloride L+Q	39.7139*
(2)Sulphuric acid L+Q	4.8668*
(3)Peeling L	74.8370*
1*2	4.2133*
1*3	7.1268*
2*3	5.5200*
Error	4.5923
Total SS	140.8700
R^2	0.97

* Significant at 1% level

Processing parameters had a higher influence on yield than colour difference (ΔE), as shown by results from Equations 3 and 4. However, based on the importance of both yield and colour of BPD, a trade-off was necessary in order to balance their production, leading to acquisition of an optimal formulation. Thus, the criteria were set to establish the maximum yield and minimum ΔE with the best desirability function (D). Accordingly, 21 scenarios were developed based on set objectives, and using Design Expert and non-repetitive permutation approach, 11 promising scenarios with the highest D were found to better describe optimisation process (Table 3.3a). In addition, a maximum global desirability (GD) of 1.0 was achieved for both parameters and responses, and predicted material balance of buffer concentration, 4.0 % w/v, cassava waste solids, 23 % w/w and extraction time of 10 minutes. Meanwhile, the processing parameter balance simultaneously predicted yield and colour difference of 38.8 % and 4.2 (reciprocal, 0.24) respectively.

3.3.3 Standardisation of integrated process methodology by validation of optimal models'

8.2.1.22 3.3.3.1 Optimal model's validation

The best formulations were predicted at the highest waste solid content (10 % w/w) and extraction time (10 minutes), as shown in Table 3.3a, and the best D did not predict highest yields and lowest ΔE. Thus, applying zero-based standardisation approach (Anderson, 2014) and sustainability (Essel & Carus, 2014), within the experimental scope, most important desirability values and corresponding parameters and responses were selected (Table 3.3a, asterisk).

Validation of the optimisation process in order to develop a standardised methodology, BPD were produced using the 4 optimal formulations (Table 3.3a, asterisk) including GD analysed for yield, and the results thereof compared with optimal values using mean relative deviation modulus (ρ) (Table 3.3b). Although there were significant colour differences in the 15 formulations, biopolymer derivatives did not show any differences visually. Applying the ASTM's E313 yellowness index measure, BPD whiteness did

not show much deviation from perfect white (100 % lightness). This, coupled with BDP similar visual appearance, colour was not considered in the validation process.

Table 3.3. Optimised intact bitter cassava biopolymer derivatives (BPD) a) individual response desirability using non-repetitive permutation approach, and b) validated optimal yield for global standardised methodology.

(a)

Permutation	Buffer, % w/v	Waste solids, w/w %	Extraction time, Min.	Yield, %	Colour change, ΔE	Desirability, D
A	3.6	30	10	43	4.8	0.87
B	3.7	30	10	43	4.8	0.89*
C	3.7	30	10	43	4.8	0.86
D	3.4	30	10	41	4.5	0.87
E	3.4	30	10	41	4.5	0.87
F	3.3	30	10	41	4.5	0.87*
G	3.2	30	10	40	4.5	0.87
H	2.9	30	10	39	4.5	0.92
I	2.9	30	10	39	4.5	0.94*
J	2.9	30	10	39	4.5	0.93
K	3.1	30	10	39	4.5	0.93*

(b)

Permutation	Buffer, % w/v	Waste solids, w/w %	Extraction time, Min.	Optimal yield, %	Experimental validated yield, %	Mean relative deviation modulus ρ, %
B	3.7	30.0	10	43.0	42.3	24.5
F	3.3	30.0	10	41.0	40.7	4.5
I	2.9	30.0	10	39.0	37.8	72.0
K	3.1	30.0	10	39.0	38.4	18.0
GD formulation	4.0	23.0	10	38.8	38.4	8.0

8.2.1.23 3.3.3.2 Standardisation of integrated process methodology

As shown in Table 3.3b, it was evident that ρ values less than 10 % illustrated a good agreement of optimal values with experimental validation values. Furthermore, the ρ value of less than 5 % showed a stronger association, indicating that parameter adjustment sufficiently responded to higher BPD yields. The BPD yield slightly above 40 %, corresponding to the dry solids range of cassava roots, showed the capability for the developed method to use most waste solids.

Thus, using an integral methodology, incorporating intact root with 23-30 % w/w waste solids, 4 % v/v ionic buffer concentration and 10 minutes extraction time, could be applied for sustainable production of BPD. This integral methodology is a systematic approach for the production of BPD from intact (whole) cassava root in three major steps. It intended to support production of high yield and bright coloured BPD in an integrated economic, relatively short time production process and to impart some level of modification necessary in their applications.

3.3.4 Impact of Standardisation on Biopolymer derivative properties and packaging film moisture barrier properties

8.2.1.24 3.3.4.1 Appearance

The produced BPD exhibited bright powders with uniformly distributed and semi-flowing particles (Fig. 3.2), demonstrating the potential of standardisation to turn wastes into value added bioproducts. Transparency is always a requirement in packaging foods in which their identities and visibilities are highly valued. Thus, BPD total cyanogen, colour, microstructure and chemical properties, thermal and adsorption behaviour were further investigated. Transparent films are generally used in food packaging when other properties such as barrier, mechanical or thermal are adequate. Therefore, BPD moisture barrier properties were determined together with the developed films in order to determined impact of standardisation on these vital properties. As pointed out earlier, the higher BC yield compared to the yield of analogue SC could point to the unique BC-

BPD. Thus, the impact of standardized methodology of optimal BC-BPD, i.e., GD was compared with SC-BPD.

a **b**

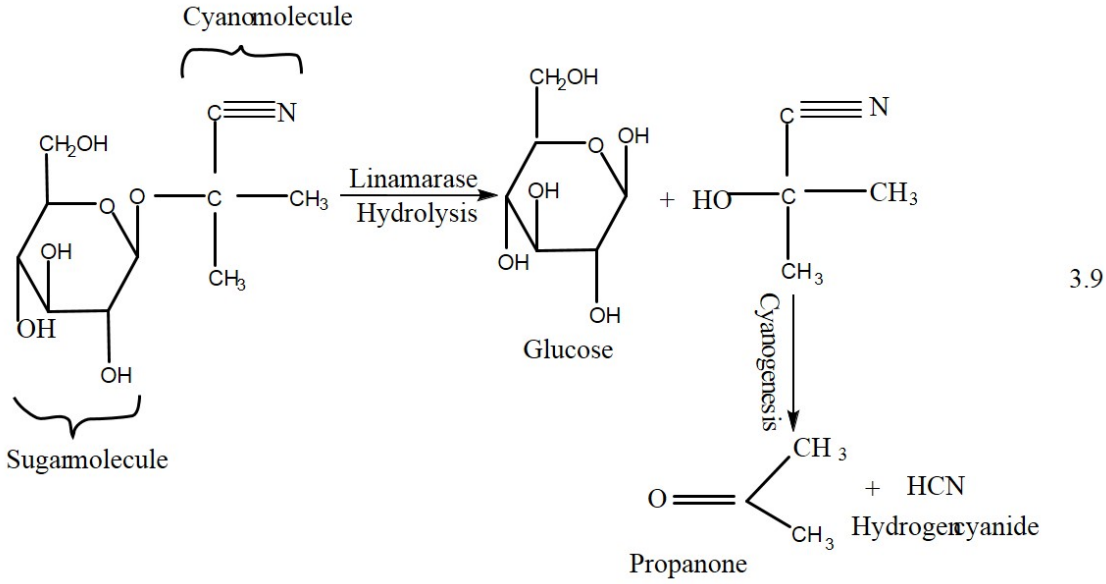


Figure 3.2. Illustration of a) intact bitter cassava root and b) biopolymer derivatives (BPD) example.

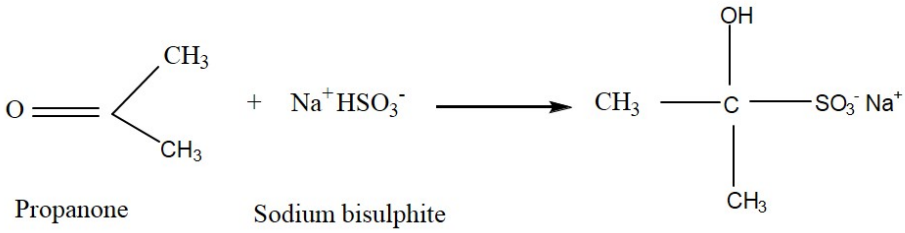
8.2.1.25 3.3.4.2 BPD dull colour and total cyanogen decontamination

Total cyanogens (TC) and colour were found to reduce and brighten, corresponding to increase in the biopolymer derivatives yield, when intact (whole) bitter cassava was processed following a previously developed SRRC methodology (Tumwesigye et al., 2016). TC and colour decontamination is achieved through functionalising bisulphite and acid reaction during SRRC. When compared with the conventional cassava processing methods, the SRRC produced biopolymer derivatives with far less TC (Tumwesigye et al., 2016). Therefore, to determine the impact of integrated process methodology on safety and appearance of derivatives, TC reduction and/or possible elimination, and colour brightening were established. The analysis of variance results are shown in Table 3.2a. As observed in Table 3.2a showing the sum of squares, the combined effects of ionic buffer and bisulphite, ionic buffer and wastes, and sole bisulphite presented the highest ($p < 0.01$) TC reduction potential. Similarly, their impact on colour difference (ΔE) did not deviate much from that of TC. These results

can be attributed to: i) the enhanced TC intrinsic hydrolysis by the intact root (Eqn. 3.9) during SRRC process; ii) reductive effect of the food grade sodium bisulphite (Eqn. 3.10); and iii) ionic buffers providing acid environment for hydrolysis.



3.9



3.10

The effect of peeling factor on TC, practiced in traditional processing, was also determined and results shown in Table 3.2b. The peeling factor showed a much higher ($p < 0.01$) TC reductive effect, that using whole root is more important in reducing cyanide from bitter cassava.

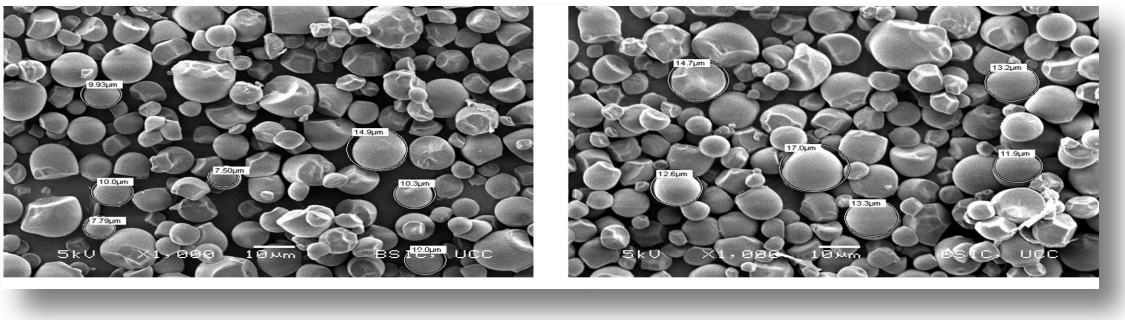
3.3.4.3 Microstructure and chemical

The scanning electron micrographs (SEM) of BPD are presented in Fig. 3.3a, showing heterogeneous particle sizes for SC (Fig. 3.3ai) and optimal GD (Fig. 3.3aii) with round and polygonal shapes (Doporto, Dini, Mugridge, Viña, & García, 2012). Although slightly bigger round granule size range occurred in GD (11.79-17.00 µm) than in SC (7.50-14.9 µm), over all particle size distribution did not differ, suggesting that the optimal GD formulation produced near similar BPDs. Unlike in the externally

reinforced starch biocomposites, whereby cellulosic and other fibrous materials were observed surrounding the starch granules (Versino & García, 2014; Versino et al., 2015), SRRC allowed a more homogenous mixture with minimal material surrounding starch granules (Fig. 3.3ai & ii).

Fourier transform infra-red (FTIR) spectroscopy applied to gain insight into structural alterations and possible physical and chemical interactions in SC and optimal -GD BPD as a function of optimisation are illustrated in Fig. 3.3b. Despite the SC and GD spectra looked similar, manifesting clear patterns, GD exhibited high absorption intensity than SC. The differential absorption intensities could be explained by the differences in chemical composition (Tumwesigye et al., 2016; Versino et al., 2015), and perhaps might suggest that SRRC seems to release more chemical components in BC than in the SC analogues. This result is supported by the higher BC yields attributed to more BPD compounds by SRRC. In addition, the peak band gap dissimilarities might be due to differences in the structure, with the broader band of GD revealing the more amorphous regions in BC-BPD.

ai **aii**



bi **bii**

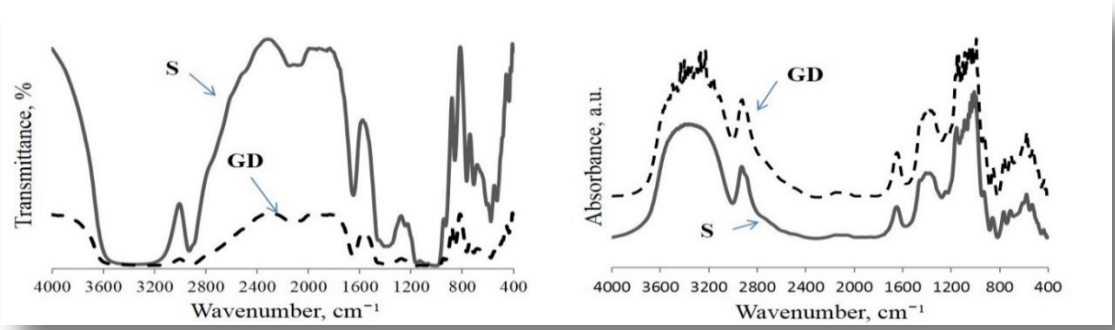


Figure 3.3. Scanning electron micrograph a) and Fourier transmission infra-red spectra, b) analysis of biopolymer derivatives at optimum conditions using sweet cassava (SC) (ai & bi) or intact bitter cassava global desirability (GD) (aii & bii).

Apparent interactions largely depended between hydrogen bonding of hydroxyl functional groups in starch, cellulose, hemicellulose, pectin and some polyphenols (tannin) (Bodirlau, Teaca, & Spiridon, 2013; Tumwesigye et al., 2016) due to an observed broad peak between 3000 and 3500 cm^{-1}, manifesting alcohol O-H, alkyne C-H stretching vibrations. Additionally, the peak at around 1700 cm^{-1} is an indication of associations between carbonyl groups among the compounds mentioned above. However, the interaction phenomenon was non-existent beyond 3500 cm^{-1} with absence of amine C-H stretching vibrations indicating that there were insignificant total cyanide and protein contents. The low protein content could be explained by the protein-tannin complexing in BPD.

8.2.1.26 3.3.4.4 Thermal

The differential scanning calorimetric (DSC) thermograms of BPD demonstrated that the processing history was similar for SC and GD (Fig. 3.4a) despite the higher GD melting (Tm) and glass transitional (Tg) temperatures and lower crystallinity (C) than SC. Both SC and GD presented sharp and narrower melting endotherms in temperature ranges, 150-205°C for SC and 180-205°C for GD, than earlier reported (A. P. Kumar & Singh, 2008). Additionally, SC and GD exhibited bimodal endotherms at about 70 and

110°C as reported by De Meuter, Amelrijckx, Rahier, & Van Mele, (1999). The differences in melting transitions between SC and GD could be due to more component hydrogen bond interactions in GD than SC caused by waste solids incorporation. Both SC and GD did not show any water crystallisation due to amylopectin since there were no visible endotherm changes between 50 and 120°C (A. P. Kumar & Singh, 2008) rather a shift to above 150°C Tm, possibly due to incorporation of waste solids.

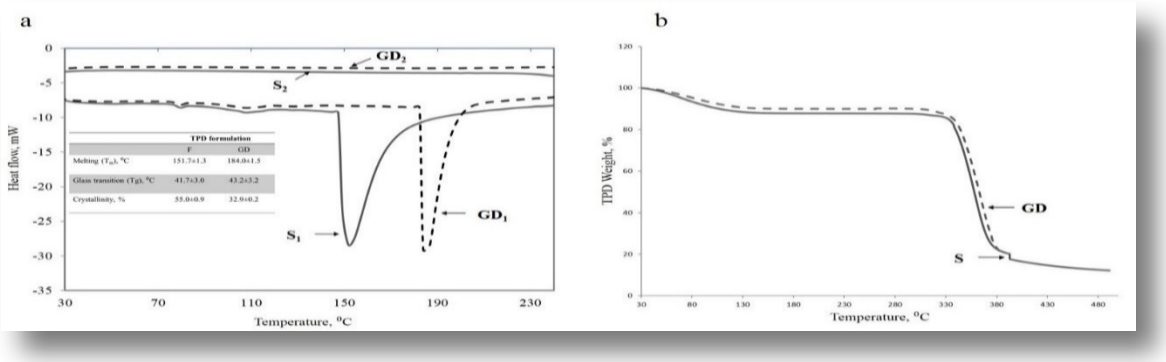


Figure 3.4. DSC (a) and TGA (b) analysis of intact bitter cassava (BC) and sweet cassava (SC) biopolymer derivatives (BPD). S_1 & S_2, DSC thermograms of SC BPD for first & second heating; S, TGA decomposition curve of SC BPD; GD_1 & GD_2 global desirability, DSC thermograms of BC BPD for first & second heating; and GD global desirability, TGA decomposition curve of BC BPD.

A similar pattern of SC and GD due to thermal effect is exhibited by thermogravimetric analysis (TGA) (Fig. 3.4b). TGA revealed that BPD thermal stability of SC and GD followed same pattern during the decomposition period (30-400^{0}C), with highest weight loss observed at 335-380°C. In both cases, the almost linear decomposition stability up to 300°C could be due to stability of BPD resisting fast decomposition as exemplified by DSC analysis (Fig. 3.4a).

8.2.1.27 3.3.4.5 BPD moisture adsorption behaviour

Isotherms of BPD powders require a lot more time than BPD films, and thus SC was not considered in the adsorption studies. Fitting of sorption models to experimental data of the equilibrium moisture contents of BPD is shown in Table 3.4. The three models followed type II isotherm (Green & Perry, 2008) and demonstrated an increase of

moisture content corresponding to increasing water activity. The models' estimated parameters for BPD and R^2, mean relative deviation modulus (ρ) and variance of regression (VR) constants are presented in Table 3.4. The higher R^2 and the lower ρ and VR signify the goodness of fit. While all the three models presented low ρ and VR, Peleg model provided the best fit when the BPD was subjected to the whole range of water activity and temperatures of 10, 20 and 30 ^{0}C. Monolayer moisture contents (mo) of BPD using GAB and BET models were similar and decreased with increase in temperature.

Table 3.4. Fitted sorption models and estimated parameters for intact bitter cassava BPD (a) and film diffusion coefficients (m^2s^{-1}) (b) at various temperatures and relative humidity.

(a)

Model name	Equation		Parameters at various temperatures (°C)		
			10	**20**	**30**
Modified BET, Brunauer, (1943)	$M_{eq} = \frac{M_0 C a_w}{\lvert(1-a_w)(1-C\,ln(1-a_w))\rvert}$	MMC, % d.b.	9.90-67.44	2.07-53.24	2.00-50.46
		M_O	17.98	16.18	15.46
		C	10.38	2.73	2.66
		Ṕ, %	4.08	4.29	3.42
		VR,%	1.13	0.41	0.28
		R^2	1.00	1.00	1.00
Oswin, Chen & Morey, 1989)	$MC_{eq} = k\left[\frac{a_w}{1-a_w}\right]^C$	MMC, % d.b.	7.98-65.59	3.81-54.55	3.57-51.95
		K	0.48	14.90	14.20
		C	22.88	0.59	0.59
		Ṕ, %	9.58	4.01	4.50
		VR,%	5.03	0.73	0.38
		R^2	0.99	1.00	1.00
Peleg, Peleg, (1993)	$MC_{eq} = A{a_w}^B + C{a_w}^D$	MMC, % d.b.	10.92-67.49	4.10-54.12	3.92-51.42
		A	28.04	29.32	27.35
		B	0.41	0.91	0.92

C	83.53	81.20	67.55
D	6.84	10.05	8.78
Ṕ, %	3.26	5.58	3.13
VR,%	0.59	0.53	0.12
R^2	1.00	1.00	1.00

Arrhenius, Arrhenius, (1874)	$P = P_0 \exp^{-E_P/RT}$	a_w	0.1	0.2	0.3	0.4	0.5	0.6	0.7	0.8	0.9
		E_p	43106.6	303887.7	22983.8	17893.7	14414	12472.6	11859.8	11462.9	9609.9
		P_0	1.03E-07	3.21E-05	9.1E-04	8.03E-29	0.05	8.22	0.12	0.32	1.11
		R^2	0.92	0.93	0.95	0.97	0.98	0.98	0.94	.92	0.99

P, mean relative deviation modulus; VR, standard error of estimate; R², coefficient of determination; M_{eq}, equilibrium moisture content; MMC, modelled moisture content; M_o, monolayer moisture content; d.b., dry basis; a_w, water activity; A, B, C, D, K, models' coefficients; P, water vapour permeability; P_0, pre-exponential factor; Ep, activation energy for permeation; R, gas constant (8.314 J/mol K); *T, temperature (expressed in .K)*

(b)

Temp, ^{o}C	Relative humidity, %		
	75	85	95
10	4.02051E-12	4.04668E-12	4.03098E-12
20	4.01528E-12	4.03883E-12	4.04798E-12
30	4.03621E-12	4.03752E-12	4.05322E-12
40	4.11994E-12	4.1448E-12	4.90538E-12

The low mo at high temperatures coincided with absence of visible mould at high relative humidity above 70 % RH within 6 weeks of storage.
Like any other food material, BPD moisture adsorption decreased with increasing temperature as shown by mo values (Table 3.4).

8.2.1.28 3.3.4.6 Film moisture barrier properties

The moisture barrier property of materials is essential to approximation and prediction of the product-package shelf-life, with a precise package system barrier requirement governed by the product characteristics and the targeted applications. Moisture regulation in packaging can cause negative changes in product quality and shelf-life, and change package material characteristics.
As shown in Table 3.4a, there was a decrease in activation energy (E_p) of permeation and an increase in pre-exponential factor (P_o), which proves a usual pattern of global (Arrhenius-type) model- dependency of temperature, and an activation energy independent of RH, with a pre-exponential factor varying exponentially. The diffusion coefficients (D) (Table 4b) showed insignificant increased trends with increases in both temperature (T) and relative humidity RH), which suggest that there were minimal physical and chemical changes in film matrix. The minimal structural changes might be due to the compact packing density in the structural matrix. As compared to previously tested materials for thin films and scaffolds (Sultana & Khan, 2013), intact bitter cassava film D for the entire RH are much smaller than polyhydroxy-butyrate-co-hydroxyvalerate (PHBV) (593E-12 m²/s), PHBV + polylactic acid (PLLA) (598E-12 m²/s) and PHBV + PLLA + hydroxyapatite (229E-12 m²/s) films. Therefore, the film provides interesting potential barrier properties that can be used in developing films, not only for food use but also there is a possibility of their wide application.

The temperature-time dependence of WVP as predicted by Arrhenius and William-landel-Ferry models is presented in Fig. 3.5, showing linearity of the plots and best fits. The linearity confirms that water uptake is regulated by the diffusion process (Sultana & Khan, 2013). It has been reported that WLF model allows for estimation of temperature shift factors by extrapolation, thereby being able to predict the life-span of products (Sullivan, 1990).

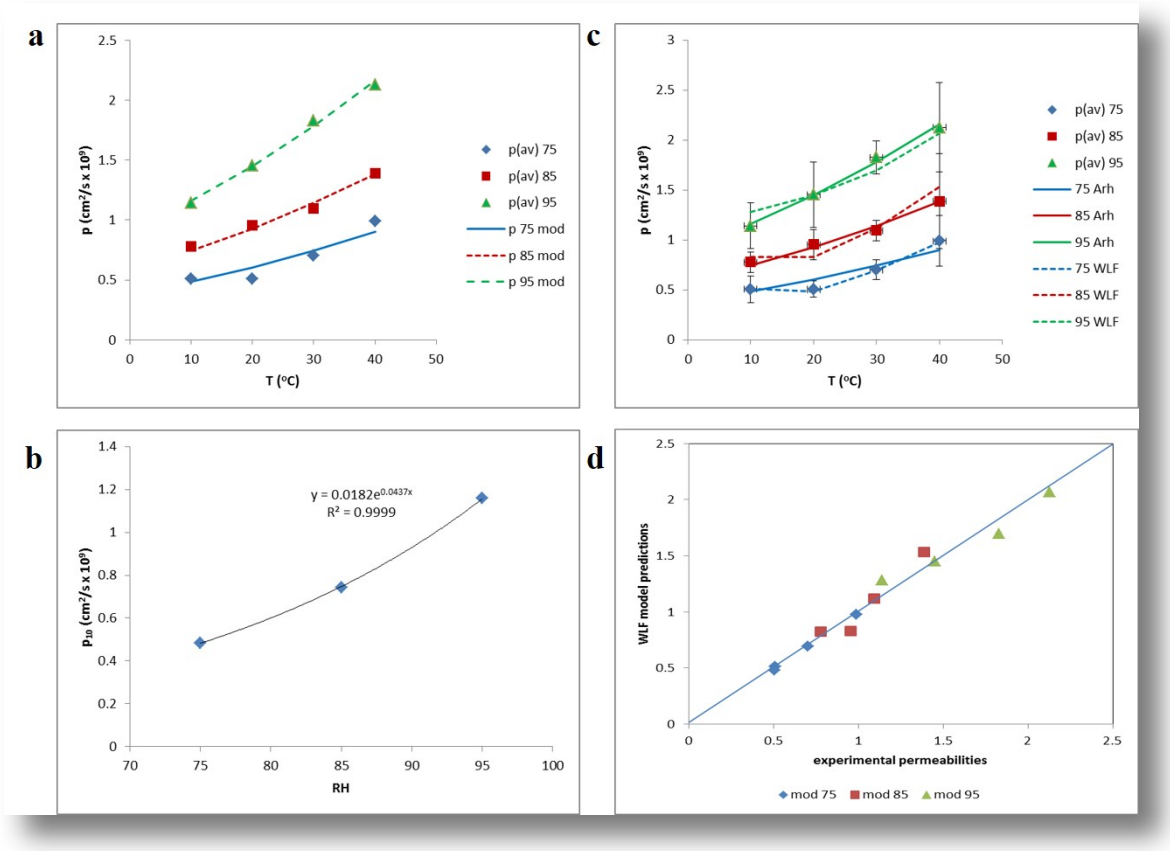


Figure 3.5. Standardisation effect on film moisture barrier properties as influenced by a) temperature, b) relative humidity, c) temperature-time dependence of WVP as predicted by Arrhenius and William-landel-Ferry (WLF) models, and d) time-temperature superposition of William-landel-Ferry (WLF) model.

Together with Arrhenius model, the shelf-life of materials with temperatures close to and above their glass transition (Tg) can be estimated. In this study, BPD and films with Tg of around 40^{o}C (Fig. 4a), corresponding to WVP test temperatures of 40^{o}C, were produced from intact bitter cassava, suggesting that the above models are applicable to this polymer.

Conclusion

A standardised simple, integrated methodology which allowed efficient and low-cost production of biopolymer derivatives (BPD) from novel intact BC was developed. Employing an integrated methodology, incorporating intact BC root with 23-30 % w/w waste solids, 4 % v/v ionic buffer and 10 minutes extraction time, allowed production of more BPD compared to a commercial method using SC.

The BPD yield of 41 % showed that it is possible to utilise the nearly the whole root during processing since the root dry matter contents of most cassava varieties lie between 40 and 45 %. It can be concluded that the standardised methodology is an efficient process and could be used as a simple, low cost and sustainable method in production of BPD. This has implications in eliminating the triple BPD preparation steps, production, reinforcements and modifications, as separate entities that increase energy in industrial production of materials.

SEM, DSC, TGA, FTIR and moisture barrier analyses revealed a uniform microstructure, high thermal stability of BPD, and promising good barrier properties, thus demonstrating efficient performance of the integrated standardised methodology.

Standardised integrated methodology for production of biopolymer derivatives (BPD) from novel intact bitter cassava was demonstrated by desirability optimisation, allowing sustainable low cost production of BPD for a broad range of applications.

Methodologies designed around standard integrated procedures, matching zero-based approach to contamination elimination, are novel strategies, and if they are used effectively and widely can provide better avenues to eliminate cassava wastes and recover BPD resources as sustainable biomaterials.

Chapter 4. Quantitative and mechanistic analysis of impact of novel cassava processing on fluid transport phenomenon in humidity-temperature-stressed biobased films

Abstract

Realistic performance and integrity of packages are mainly determined by their resilience in highly variable storage humidity and temperature. Package resilience is a function of its ability to timely respond to these variable conditions and manage its barrier to moisture and gases appropriately. Biobased materials have been proposed as alternatives to solve current poor barrier properties of packages. Nonetheless, the sensitivity of biobased materials to variable moisture and temperature has more often posed a challenge to balanced mass transfer in packages, and thus causing decreased in-package product shelf-life. Studies to quantify mass transport behaviour in biobased materials have been limited to representations, mainly of water vapour and gas transfers, which might be imperfect to understand fully mass transport phenomenon. This study reports the quantitative representations as well as underlying mechanisms that define mass transport phenomenon of fluid-phase solvents in cassava packaging films under highly variable relative humidity and temperature. Time dependent behaviour of BC films is analysed, and models accounting for the effect of Simultaneous Release Recovery Cyanogenesis and their predictive efficacy are studied. Intact bitter cassava films were tested for solvent solubility, swelling ratio, sorption and permeability to water vapour and oxygen at different temperature, 10-40 and relative humidity, 10-90% (adsorption) and 75, 85 95% (transfer rates). Film's structural alterations were characterised by their thermal and chemical properties. Results indicate that Modified-BET (R^2, 1.0; deviation, 3-4%) and Peleg (R^2, 1.0; deviation, 3-5%) models best described the sorption data. The temperature dependence of permeability for water vapour through films is best simulated by Arrhenius and WLF models (R^2, 0.999), while that of oxygen was influenced by crystalline and high RH.

The diffusion of non-organic and organic solvents through films follow case II non-diffusional and Fickian patterns, respectively. Solvents through films induce structural changes in IBC films with concentration-dependent diffusion.

The integrity of the cassava biobased films will depend on the host environment, and maximum care should be ensured to minimise environment effects in the distribution chain.

Key words: Quantitative, Mechanistic, Cassava film, Mass transfer, Fickian diffusion, Temperature-dependence

4.1 Introduction

Cassava biobased films (CBF) are widely produced to replace non-biodegradable plastics for broad range functional applications such as guarding food and non-food products against physical, chemical and microbiological hazards throughout the distribution chains. As industrial demand for CBF becomes a reality, it is expected that these materials will be applied at different temperatures and relative humidity (RH). Highly variable temperature and RH is the main physical threat, along the distribution chain, that enhance chemical and microbiological risk to products, and thus create challenges to the development of suitable packaging materials (El-Ramady et al., 2015). In particular, biobased materials are sensitive to moisture fluctuations (Mekonnen et al., 2013; Joffe et al., 2014). Thus, an understanding of the phyisco-chemical and microbiological resilience nature of the CBF will play a crucial role in developing sustainable packaging materials that ensure product integrity. This can be achieved by quantifying the transport phenomenon, through dissecting its mechanisms that underlie fluid (moisture and gas) transfer in CBF. Although research on fluid transport mechanisms through biobased materials remain inconclusive, it is widely known that fluid permeability through polymer membranes is largely a function of: (i) solubility and diffusivity (George & Thomas, 2001; Choudalakis & Gotsis, 2009); and (ii) material composition, structure and mechanical properties (Cheng et al., 2012; Dubreuil et al., 2003). Unlike in commercial materials utilizing liquid solvents, a unified approach to quantity and describe the complex mechanisms of mass transport in biobased packaging materials is still shaky. As the integrity issues of packages become more apparent in their applications, so are the requirements to develop novel materials and precise methods that ensure proper regulation of barrier properties across differentiated environmental conditions in the distribution chain.

The barrier properties of packages are commonly determined by applying existing fundamental empirical mathematical models. Several model references for describing effect of temperature and relative humidity on moisture adsorption and permeability to water

vapour and oxygen have been widely used in different films (Belibi et al., 2014; A. C. Souza et al., 2012; Y. Zhong & Li, 2011). Models for sorption isotherms include diffusion-adsorption equation that eliminates thickness effect in assessing adsorption of hydrophilic films (Yoshida, Antunes, Alvear, & Antunes, 2005). Other models related to sorption-diffusion and solubility are also described using Fickian theories (Bedane, Huang, Xiao, & Elc, 2012; Ni, 2011; Sultana & Khan, 2013). Sorption isotherms for cassava was evaluated using Peleg model in flour film (Suppakul et al., 2013); BET, GAB, Henderson and Oswin models for starch and soy protein concentrate edible films (Chinma, Ariahu, & Abu, 2013; Mali, Sakanaka, Yamashita, & Grossmann, 2005). The water vapour and oxygen/carbon dioxide transmission rates as function of relative humidity and temperature are often described by fitting the data to Arrhenius and Williams–Landel–Ferry (WLF) models (Lazaridou, Biliaderis, Bacandritsos, & Sabatini, 2004; Sopade et al., 2002). The models described above are only quantitative representations that use concentration-time and mass flux-time curves to describe mass transfer behaviour of solvents through film membranes (M. J. Chen et al., 2015; Cheng, Chen, Cheng, Lin, & Lai, 2012; Xu & Que Hee, 2008). Alternative mechanical assessment techniques that provide useful insights into underlying mechanisms of processes have been applied in understanding of the dissolution behaviour of crystals under the influence of ionization and micellar solubilisation (Cao, Amidon, Rodriguez-Hornedo, & Amidon, 2016), modelling mass balances, flux capacity, fluid permeation through compressible fibre beds (Zhu, Pelton, & Collver, 1995) and reaction directionality constraints to predict fluxes through metabolism (Cotten & Reed, 2013). Recently, the contribution of seals to the permeability of thermosealed packages has been quantified, showing approximately 25 % of the system total mass transfer (Reinas, Oliveira, Pereira, Mahajan, & Poças, 2016). Taken together, the quantitative and mechanistic approaches could be used to describe properly the mass transport phenomenon and provide avenues in CBF development.

Although quantitative assessment has been significantly used to understand the barrier properties of polymeric materials (PM), little has been done to assess fluid transport mechanisms through PM in stressed temperature and relative humidity environments. This may be partly due to the limited research validation of PM under realistic natural conditions. Furthermore, there are still scarce literature reports about the quantitative evaluation of effect of temperature and relative humidity on the barrier properties of CBF. Moreover, the

insignificant validation research under realistic conditions is largely shared by CBF. Starch, in combination with natural fibres, is often used to manufacture whole bio-based composites. While there are direct benefits to use natural fibres in composites, their performance is often very nonlinear, due to their highly sensitivity to moisture and temperature (Joffe, Rozite, & Pupurs, 2013).

Recently, a combination of a novel bitter cassava (BC) material and an improved simultaneous release recovery cyanogenesis (SRRC) processing methodology resulted into development of new low-cost biobased film, which demonstrated potential use in food packaging (Tumwesigye, Oliveira, et al., 2016). In order to develop sustainable materials with efficient barrier properties, an understanding of the association between structural characteristics of BC and underlying mechanisms that define fluid mass transport phenomenon as well as their quantification is necessary.

While poor barrier properties are often associated with hydrophilic nature of CBF, their limited validation in realistic conditions, as well as the quantitative analyses that disregard underlying mass transport mechanisms under highly variable relative humidity and temperature, influence package use. The objective of this study was to determine moisture sorption characteristics as well as permeability to water vapour and oxygen of intact bitter cassava films; and evaluate the relevance of the various models in predicting barrier performances in simulated realistic conditions of different relative humidity for specific storage temperature. Furthermore, to provide an understanding of the mechanism of mass transport phenomena of water vapour and oxygen through the film under similar storage conditions, relevant models which relate to solubility, diffusion and adsorption laws were applied. The models were then related to the film structural (chemical and thermal) characteristics, determined using Fourier Transform Infrared (FTIR) and Differential Scanning Calorimetry (DSC). This was done in order to assess the adequacy of the models to predict nature of mass transport, and the time-dependent behaviour, and impact, of novel BC and SRRC.

4.2 Materials and methods

4.2.1 Materials

Films were produced by solution casting using the procedure reported by Tumwesigye et al., (2016). Mixtures of BPD (3 % w/v) and glycerol (30 % w/w) were heated at 70^{0}C for 25 minutes. Prior to moisture barrier characterisation, films were conditioned at 23 ± 2^{0}C and 54 %RH. Thickness was measured in six different locations using an absolute digital Calliper (Digmatic, Mitutoyo UK Ltd).

4.2.2 Mass transport characterisation

8.2.1.29 4.2.2.1 Moisture barrier (MB)

The MB characteristics were determined in terms of moisture adsorption (MA) and water vapour permeability (WVP).

Determination of MA characteristics was done by creating an environment of specific relative humidity with glycerol solution (0 % to 100 % v/v). Various methods of creating specific relative humidity environments such as saturated salt solutions have been proposed (ASTM E104, 2012). However, glycerol was preferred due to its lone advantage and ease in making 0 – 100 % v/v solutions that are cheap, non-corrosive and do not vary with temperature changes.

Film strips (3 x 1.5 cm) were pre-dried until attaining constant weights, achieved at 90^{0}C for 9 h. Film MA was determined at 10, 20 and 30^{0}C, and 10-90 %RH in controlled chambers and the final moisture content (MC) calculated, on a dry basis, according to Eqn. 4.1.

$$\mathrm{MC,\%} = \left(\frac{M_{io} - M_{it}}{M_{it}}\right) 100 \qquad 4.1$$

where, M_{io}, initial mass (equilibrated for 48 h at predetermined constant pressure and relative humidity) and Mit, final mass at time, t (equilibrated films dried at 105^{o}C for 29 h).

The WVP was determined according to ASTM, (2005) method at 10, 20, 30, 40°C and at RH gradients across the film of 75, 85 and 95 % using Eqn. 4.2. The detailed procedure was followed based on Tumwesigye et al., (2016) without changes. Concisely, films strips (7.4 cm diameter) were mounted on acrylic cells and hermetically sealed around the open transfer zone. Calcium chloride and salt solution were used to create 0-75, 0-85, 0-90 %RH gradient between inside the cells and outside hermetically sealed chambers respectively. Weights were taken after every 2 h for 10 h. Results were expressed in gmm/m² s kPa).

$$m = m_0 + \frac{P_w}{\delta} * A * P_s \left(a_{w_1} - a_{w_2}\right)^t \quad 4.2$$

where, m, film weight at time t; m_o, initial film weight; P_w, permeability; δ, thickness; A, exposed film area; P_s, partial pressure of saturation at temperature considered; a_w, relative humidity of the environment with $a_{w1} = 1$ and $a_{w1} = 0$.

8.2.1.30 4.2.2.2 Gas barrier

The gas barrier characteristics were determined in terms of permeability to oxygen (PO_2). The PO_2 was measured following the method described by Abdellatief et al., (2015) and reported in Tumwesigye et al., (2016) without significant modifications using a PBI Dansensor (CheckMate 9900, USA). The PO_2 was determined at the temperature of 10, 20, 30 and 40^0C and RH gradient of 0-75, 0-85 and 0-95 %. The possible leakage within testing chambers was tested with an empty chamber and found to lie within minimum mean limits (1.5 x 10^{-3} cm^3 / (m^2 day). Triplicate tests were considered and mean values for calculating PO_2 expressed as cm^3 / (m^2 day).

8.2.1.31 4.2.2.3 Fluid barrier modelling

The MA and WVP data were fitted to different models (Table 4.1) in order to correlate equilibrium moisture content and water activity. Model parameters were estimated by the non-linear regression procedure using Excel (2010) solver and goodness of fit evaluated as mean relative percentage deviation in modulus, ρ, % (Eqn. 4.3) and regression variance, VR

(Eqn. 4.4). Accurate mathematical description of isothermal was considered when $\rho \leq 5$ %, VR ≤ 5 and $R^2 \leq 0.97$.

$$\rho,\% = \frac{100}{n} \sum_{i=1}^{n} \frac{|\varepsilon_i|}{X_{i(o)}} \quad 4.3$$

$$VR = \sum_{i=1}^{n} \frac{|X_{i(p)} - X_{i(o)}|^2}{n-1} \quad 4.4$$

where, n, number of experimental points; ε_i, absolute value; (p) and (o), predicted and observed.

The temperature-time dependence (TTD) of WVP was determined by fitting experimental data to Arrhenius and time-temperature superposition of William-landel-Ferry (WLF) models, whereas TTD of gas was obtained by fitting the data to Arrhenius equation.

8.2.1.32 4.2.2.4 Film solubility (FS_{ol}) and swelling ratio (FS_{tm}) measurements

The FS_{ol} and FS_{tm} measurements were conducted gravimetrically using an electronic balance (Sartorius, Cubis MSA, Germany) with a 0.1 mg resolution. Initially, a pre-weighed and laboratory fumehood-dried (1.0 % moisture content) films were immersed in 100 ml of water at 40^{o}C, 75 % & 95 % RH). The wet film was removed from water after every 10 min until 60 min, pre-dehydrated on filter paper and quickly weighed on the balance. The process of withdraw was maintained within 60 s to minimise any difference in weights of different film portions. Seven (7) similar film portions were used, each withdrawn from water sequentially at an accumulated time, weighed and discarded. This was done to avoid interruptions of water diffusion and film swelling processes during transfers between water and electronic balance. The similar experiment was replicated with toluene and paraffin oil. Organic solvents are encountered in the supply chain of the materials, and their evaluation could provide an understanding of how IBC materials will behave when subjected to water in addition to organic solvents. Triplicate measurements were considered for the purposes of reproducibility of the experimental results. The solvent weight gain was considered as weight loss (desorption) of solvent if the solvents were to lose what has been absorbed. Thus, a

weight loss-time plot was derived, and an instantaneous mass uptake was obtained by extrapolating the linear regression curve back to zero (M. J. Chen et al., 2015). The FS_{ol} and FS_{tm} were estimated as described in Chen et al., (2015) using Eqns. 4.5 and 4.6.

$$FS_{ol} = \frac{M_{eq} - M_d}{V_d} \quad 4.5$$

$$FS_{tm}, \% = \left(\frac{M_{tm} - M_d}{M_d}\right) 100 \quad 4.6$$

where, FS_{ol}, water solubility in the film; M_{eq}, total weight of wet film at equilibrium (eq); M_d & V_d, film weight and volume; FS_{tm} & M_{tm}, saturation swelling ratio and total weight of wet film at a given immersion time (tm). The FS_{tm}, V_d and film density (F_d) were determined as described in Chen et al., (2015). It is noted that film V_d was 1, and thus F_d was equal to its solubility. The FS_{ol} and FS_{tm} experiments were conducted at 25^{o}C.

8.2.1.33 4.2.2.5 Statistics

Data analysis was performed by Statistica 7.1 software (StatSoft Inc., Tulsa, USA) and Microsoft Excel, version 2013 to determine if RH and T has significant impacts on MB and GB, evaluate the goodness of fit of each model, the coefficient of determination and the mean relative percentage deviation modulus. Differences were considered to be significant when $p \leq 0.05$.

4.3 Models and conceptual background

The mass transport behaviour of fluids (moisture and gas) through polymeric films is preferably assessed by considering models that adequately fit the empirical data., e.g. rate of mass sorption (Ritger & Peppas, 1987), sorption-diffusion (Ochs, Lothenbach, Wanner, Sato, & Yui, 2001), film swelling and film-moisture interaction (Orwoll & Arnold, 2007), gas permeability, diffusivity and solubility (Fallis, 2013; Stannett, 1978), and temperature-sorption-permeation (Arrhenius, 1874). All the above plus adsorption models (Table 4.1) are used to assess the mass transport behaviour in this study.

4.3.1 Analysis of film–solvent interaction

Biobased films swell when they are exposed to solvents, and the degree of swelling is a function of the length of the network chain, temperature, type of solvent and strength of thermodynamic interaction between the film chains and solvent molecules (Marzocca, 2010). To assess the effect of SRRC and bitter cassava on the film molecular structure and possible modifications, which are pertinent factors that can influence barrier properties, the Flory-Huggins equation (Eqn. 4.7) (Finch, 1983; Flory, 1953) was applied. The thermodynamic parameters evaluated here include film volume fraction (ϕ_f), solvent volume fraction, film-solvent interaction (χ), and film mass between possible crosslinks (M_f).

$$\frac{1}{M_f} = \frac{\emptyset_f + \chi\emptyset_f^2 + \ln(1-\emptyset_f)}{\rho_f V_s\left(\emptyset_f^{\frac{1}{3}} - \frac{1}{2}\emptyset_f\right)} \quad 4.7$$

$$\emptyset_f = \frac{1}{1+q} \quad 4.8$$

where, M_f, molecular weight between cross-links [reciprocal of moles of cross-linked units per unit film weight (g)]; ϕ_f, swollen film volume/total film volume; χ, film-solvent interaction parameter; ρ_f, film density; and V_s, molar volume of solvent. Considering solvent soluble polymers (e.g. cassava film), q was further segregated into Eqn. 4.9.

$$q = \frac{W_s}{W_f} \quad 4.9$$

where, W_s, weight of solvent in film; and W_f, weight of film.

Furthermore, χ was calculated according to Bristow & Watson, (1958) Eqn. 4.10, and described in Barlkani & Hepburn, (1992).

$$\chi = \beta + \left(\frac{V_w}{RT}\right)\left(\partial_s - \partial_f\right)^2 \quad 4.10$$

where, β, lattice constant (0.34); V_s, solvent molar volume; R, universal gas constant; T, absolute temperature; δ_s & δ_f, solubility parameters of solvent and film respectively. The δ_f was derived by immersing film in water and quantifying the loss within 24 h, while δ_s were obtained from Burke, (1984).

4.3.2 Film solvent permeation theory and mechanism

For the gas flow, flowed through the film from outside of the test permeation chamber, whereas the diffusional movement of water vapour between the inner and outer surfaces was unidirectional, all across film thickness. Applying the assumptions: i) perpendicular diffusional flow; ii) insignificant pressure flux variation; iii) constant gas velocity; and iv) concentration gradient as driving force and constant diffusion coefficients, Ritger and Peppas empirical equation (4.11) (Ritger & Peppas, 1987) was used to express solvent transport behaviour in BC films. In addition, since the experiment was conducted in specific conditions of temperature and RH, isothermal conditions were assumed.

$$M = kt^n \qquad 4.11$$

where, M, mass of solvent sorption behaviour at a given time (t); k, kinetic constant, which is the mass sorption rate; and n, diffusional exponent (indicative of the solvent transport mechanism). For Fickian diffusion, n = 0.5, and non-Fickian diffusion, n > 0.5 (n = 1, case II diffusion & 0.5 < n < 1.0, anomalous diffusion) (Cheng et al., 2012), and this was determined from the total mass absorbed. According to Fickian and non-Fickian diffusional adsorption through a thin film (Eqn. 4.11), applies to only 60 % of the process, and this was used (in this study) to evaluate solvent diffusion in and out of the film in the permeation tests.

Since the thickness-to-radius ratio of films used (0.002) was < 0.2 (Crank, 1979), the neck-in (edge) effect (film thickness and width reduction) (Canning & Co, 2000) was neglected, and the one-dimensional diffusion of water vapour and O_2 through the film was assumed for the permeation tests. Using the mass balances, the concentration-time (c-t) curves were developed and used in the description mass transfer patterns.

4.4 Film structural characterisation

Thermal analysis of glass transition (Tg), melting (Tm) temperatures, crystallinity (CRY) and enthalpy change (ΔH), was conducted using a differential scanning calorimeter (DSC 200 F3) equipped with a thermal analysis data station. A hermetically sealed DSC pan with fresh derivative powder (10 mg), together with a reference empty pan were heated from 20 to 250°C at a rate of 10°C/min, cooled back rapidly to 20°C and reheated at a rate of 5°C/min to 250°C to give them thermal history. T_g, T_m, ΔH and C were calculated using the built in software and determined by considering the heat capacity change observed on the second heating.

Structural changes and modification due to mass transport phenomenon of solvents in films were characterised by using Fourier transform infrared spectroscopy (FTIR). This procedure was derived from (Tumwesigye, Oliveira, et al., 2016). A film strip was placed in the sample holder. The spectra were recorded with an UV/Vis spectrum one FTIR spectrometer (Perkin Elmer Lambda 35, USA), frequency range of 4000–400 cm^{-1} and 4cm^{-1} resolution in the transmittance and absorbance modes for individual spectrum with 30 scans at room temperature.

4.5 Results and discussion

4.5.1 Moisture barrier

The moisture adsorption isotherms at 10, 20, 30^{0}C for 10-90% RH are shown in Fig. 4.1. Accordingly, intact bitter cassava films (IBC) follow a Type II isotherm, regardless of the temperature in question, implying that these films possess wide pore size distributions leading to fluid pathways that are tortuous and highly variably (Fig 4.1a). Additionally, the equilibrium moisture content (EMC) increased corresponding to increases of RH at constant temperature, perhaps due to the exposure of these films to higher quantities of moisture. However, a relatively lower increase in EMC was observed when these films were exposed to higher temperatures, i.e. the EMC increased with decreasing temperature at constant RH.

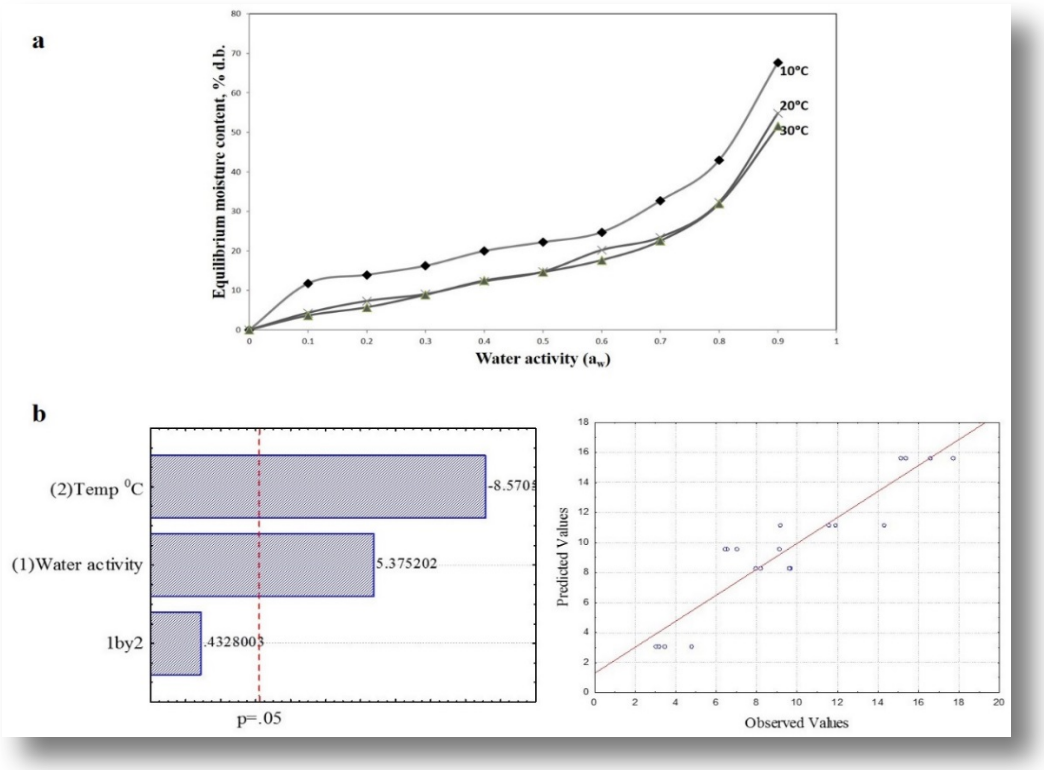


Fig 4.1. Moisture barrier properties shown by adsorption isotherms (a) and ANOVA Pareto showing statistical differences and fit (b)

Statistically, Fig 4.1b showed that temperature had more impact on film adsorption of moisture than RH. This phenomenon can be explained by the fact that at lower temperatures, films moisture affinity is high with higher capacity adsorption. It could be also due to the faster mobility of water molecules at higher temperatures causing a decrease in the intermolecular attractive forces. Chowdhury, Huda, Hossain, & Hassan, (2006) reported that, at higher temperatures, water molecules move to higher energy levels, become less stable and break away from the binding sites of the materials thus decreasing the monolayer moisture content. Similar temperature dependent adsorption isotherms trends in biobased materials were observed elsewhere (Chinma et al., 2013; Farahnaky, Ansari, & Majzoobi, 2009).

Adsorption isotherms are often applied in industry to select suitable adsorbents during separation processes but also to select the best storage conditions of products in various environments. A number of models and the corresponding parameter adequacy to describe the above phenomena are presented in Table 4.1. As shown, Peleg, modified BET, Oswin and Forran-Fontan models best described the relationship between EMC and water activity at

each temperature (10, 20, 30^{o}C) and under the conditions tested (10-90 % RH), with Peleg posting the most suitable model for IBC films.

The moisture barrier property of materials is essential to approximation and prediction of the product-package shelf-life, with a precise package system barrier requirement governed by the product characteristics and the targeted applications. Moisture regulation in packaging can cause negative changes in product quality and shelf-life, and change package material characteristics.

Table 4.1. Fitted Models, fitness evaluation parameters and constants for moisture adsorption of intact bitter Cassava films at three different temperatures.

a

Model name	**Equation**	**Parameters at various temperatures, °C**			
			10	**20**	**30**
Experimental		EMC, % d.b.	11.74-67.67	4.32-54.83	4.32-54.83
Ferro-Fontan	$MC_{eq} = \left\lvert \frac{\gamma}{ln\left(\frac{\bar{Q}}{a_w}\right)} \right\rvert^{\frac{1}{r}}$	MMC, % d.b.	9.89-67.37	4.32-54.83	3.62-51.60
		ɣ	74.07	14.98	14.26
		$\bar{Q}$	1.02	1.06	1.07
		ɾ	1.51	1.13	1.12
		Ṗ, %	5.99	5.84	9.12
		VR,%	1.71	1.10	0.86
		R^2	0.98	0.99	1.00
Predicted		MMC, % d.b.	8.61-77.49	5.16-54.41	4.97-51.43
GAB	$MC_{eq} = \frac{M_o C K a_w}{(1 - K a_w)(1 + (C - 1) K a_w)}$	M_o, % d.b.	7.74	5.94	5.64
		C	920.49	2467.95	2467.55
		K	2892.00	1359.37	1359.37
		Ṗ, %	24.53	17.51	23.47
		VR,%	42.15	11.05	11.72
		R^2	0.90	0.96	0.96
Halsey		MMC, % d.b.	10.34-67.97	6.60-59.42	6.27-56.42
		M_o, % d.b.	3245.42	2327.45	2288.58
		A	0.43	1.33	1.26

	$MC_{eq} = M_0 \left\lvert -\frac{A}{(RT\ ln a_w)} \right\rvert^{\frac{1}{n}}$	n	1.64	1.39	1.39
		Ṗ, %	4.81	8.27	13.63
		VR,%	1.14	1.28	1.75
		R²	0.98	0.99	0.99
Henderson	$M_{eq} = \left\lvert -\frac{ln(1-a_w)}{C} \right\rvert^{\frac{1}{n}}$	MMC, % d.b.	5.04-62.26	6.01-55.42	5.73-52.63
		C	0.01	0.05	0.05
		n	1.23	0.96	0.96
		Ṗ, %	18.64	16.76	15.48
		VR,%	19.65	5.79	3.76
		R²	0.95	0.98	0.99
Modified BET	$M_{eq} = \frac{M_0 C a_w}{\lvert(1-a_w)(1-C\ ln(1-a_w))\rvert}$	MMC, % d.b.	9.90-67.44	2.07-53.24	2.00-50.46
		M_O	17.98	16.18	15.46
		C	10.38	2.73	2.66
		Ṗ, %	4.08	4.29	3.42
		VR,%	1.13	0.41	0.28
		R²	1.00	1.00	1.00
Oswin	$MC_{eq} = k\left[\frac{a_w}{1-a_w}\right]^C$	MMC, % d.b.	7.98-65.59	3.81-54.55	3.57-51.95
		K	0.48	14.90	14.20
		C	22.88	0.59	0.59
		Ṗ, %	9.58	4.01	4.50
		VR,%	5.03	0.73	0.38
		R²	0.99	1.00	1.00
Peleg	$MC_{eq} = Aa_w{}^B + Ca_w{}^D$	MMC, % d.b.	10.92-67.49	4.10-54.12	3.92-51.42
		A	28.04	29.32	27.35
		B	0.41	0.91	0.92
		C	83.53	81.20	67.55
		D	6.84	10.05	8.78
		Ṗ, %	3.26	5.58	3.13
		VR,%	0.59	0.53	0.12
		R²	1.00	1.00	1.00
Smith	$MC_{eq} = A + B\ ln(1-a_w)$	MMC, % d.b.	7.68-63.63	3.57-54.78	3.30-51.62
		A	5.00	0.52	0.31
		B	-25.46	-21.83	-20.91
		Ṗ, %	13.28	12.65	11.59
		VR,%	10.36	5.82	3.88
		R²	0.97	0.98	0.99
Arrhenius	$P = P_0 exp^{\frac{-E_p}{RT}}$	a_w	0.1	0.2	0.3	0.4	0.5	0.6	0.7	0.8	0.9

E_p x 10^4	4.31	30.39	2.30	1.80	1.44	1.25	1.19	1.14	1.00
P_o	103	3.21	0.91	8.03e-4	0.05	8.22	0.12	0.32	1.11
R^2	0.92	0.93	0.95	0.97	0.98	0.98	0.94	0.92	0.99

P, mean relative deviation modulus, VR, standard error of estimate, R^2, coefficient of determination, EMC, equilibrium moisture content, MMC, modelled moisture content, M_o, monolayer moisture content, d.b., dry basis and A, B, C, D, F, G, H, ɣ, $\bar{Q}$, r, K, n, models' coefficients

b

Model	Parameters	Water activity, a_w								
		0.1	**0.2**	**0.3**	**0.4**	**0.5**	**0.6**	**0.7**	**0.8**	**0.9**
Ferro-Fontan	**Ea, J mol^{-1}**	-24748.1	-22053.4	-19954.8	-18073.3	-16267.3	25546.33	25546.75	29052.56	-9683.08
	A, s^{-1}	0.000243	0.000978	0.002907	0.007782	0.020224	1657797	1657797	5395091	1.073796
	S, J K^{-1} mol^{-1}	-1.00082	-0.83352	-0.70247	-0.58404	-0.46917	1.722411	1.722411	1.864331	0.008563
	R^2	0.81	0.81	0.81	0.82	0.82	0.83	0.98	0.99	0.91
Modified BET	**Ea, J mol^{-1}**	-36726	-28043.2	-22711.1	-19040.2	-16317.2	-14179.6	-12412.7	-10865.4	-9368.79
	A, s^{-1}	1.44E-06	8.48E-05	0.00101	0.005664	0.02102	0.06152	0.159024	0.403734	1.227157
	S, J K^{-1} mol^{-1}	-1.61801	-1.1276	-0.82961	-0.62224	-0.46453	-0.33537	-0.22114	-0.10909	0.02462
	R^2	0.81	0.82	0.83	0.84	0.85	0.86	0.87	0.88	0.9
Oswin	**Ea, J mol^{-1}**	-25573.8	-22465.8	-20399.7	-18706	-17152	-15597.2	-13903.5	-11837.4	-8729.4
	A, s^{-1}	0.000138	0.000774	0.002433	0.006223	0.014732	0.034874	0.089198	0.280467	1.571766
	S, J K^{-1} mol^{-1}	-1.06894	-0.86165	-0.72387	-0.61092	-0.50727	-0.40363	-0.29068	-0.1529	0.054387
	R^2	0.81	0.82	0.83	0.83	0.84	0.85	0.86	0.87	0.91
Peleg	**Ea, J mol^{-1}**	-43106.6	-30388.7	-22983.8	-17893.7	-14414	-12472.6	-11859.8	-11462.4	-9609.91
	A, s^{-1}	1.03E-07	3.21E-05	0.000911	8.03E-29	0.045831	8.222711	0.195853	0.321294	1.111044
	S, J K^{-1} mol^{-1}	-1.93505	-1.24445	-0.84202	-7.7806	-0.37077	0.2534	-0.19609	-0.13656	0.012665
	R^2	0.82	0.83	0.85	0.87	0.88	0.88	0.84	0.82	0.92

E_a, Activation energy, A, Pre-exponential factor and S, entropy

The temperature dependence of WVP is presented in Fig. 4.2, showing increases in RH and temperature increased the IBC film permeance to moisture (Fig. 4.2a), statistically demonstrating that high significant ($p \leq 0.05$) impact followed the order of RH, temperature and RH-temperature interaction (Fig 4.2b). As expected, the phenomenon is associated with molecular activation, causing film segment movement with formation of cavities that often facilitate movement of solvents through porous films (Weinkauf & Paul, 1990).

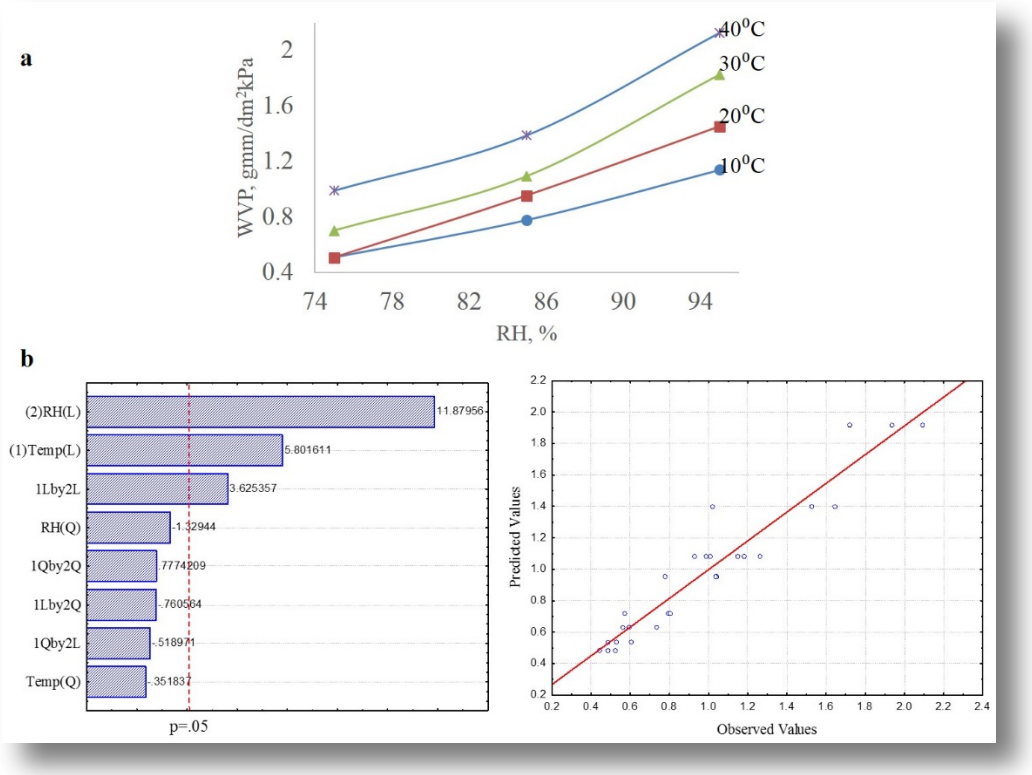


Fig 4.2 Temperature dependence of water vapour permeability, showing exponential increases with RH (a) and statistical differences and fit (b)

The temperature-dependence phenomenon is normally presented by an Arrhenius type association (Arrhenius, 1874). In this study, the combined Arrhenius and William-landel-Ferry model was used to predict behaviour of moisture permeation of IBC films (Fig 4.3 & Table 4.2).

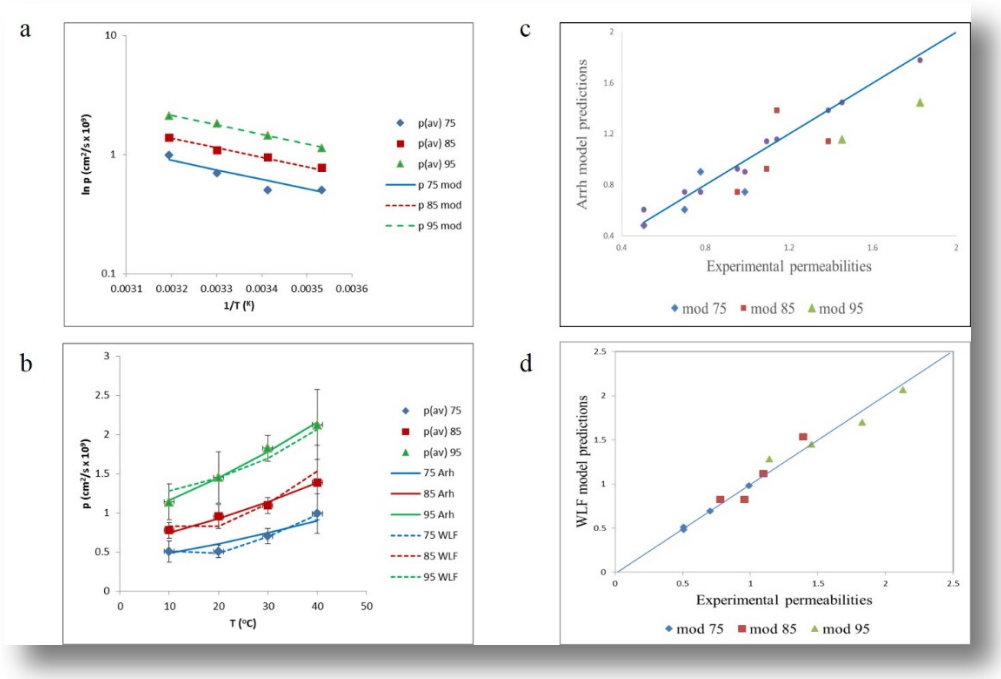


Fig 4.3 Permeability effect on film moisture barrier properties as influenced by a) temperature, b) temperature-time dependence of WVP as predicted by Arrhenius and William-landel-Ferry (WLF) models, and c & d) corresponding fit efficiency

A rise in temperature resulted in increases in permeation for all RH tested (Table 4.2a, b, c), which is also well-illustrated in Arrhenius-WLF model graphs by the linearity of the plots and best fits (Fig 4.3a, b, c, d). The linearity confirms that water uptake is regulated by the diffusion process (Sultana & Khan, 2013). It has been reported that WLF model allows for estimation of temperature shift factors by extrapolation, thereby being able to predict the lifespan of products (Sullivan, 1990). A decrease in activation energy (E_p) of permeation and an increase in pre-exponential factor (P_o), proved a usual pattern of global (Arrhenius-type) model- dependency of temperature, and an activation energy independent of RH, with a pre-exponential factor varying exponentially (Table 4.2a). The relatively low E_p at all RH (Table 4.2a) compared to wheat gluten coating of 14.20 Kcal/mol (59.41 KJ/mol) (M. N. Kumar & Yaakob, 2011), low density polyethylene and oriented polypropylene of 21.23 KJ/mol and 21.39 KJ/mol (Kulchan, Boonsupthip, & Suppakul, 2010), implies that IBC films can be performed in applications that require relatively higher temperatures. This is interestingly good for IBC films, and shows the advantage of SRRC over other conventional processing

methods. Together with Arrhenius-WLF model, the shelf-life of materials with temperatures close to and above their glass transition (Tg) can be estimated. In this study, films with Tg around 40^0C (Fig. 4.3a), corresponding to WVP test temperatures of 40^0C, were produced from intact bitter cassava, suggesting that the above models are applicable to IBC films.

Table 4.2. Permeability and parameters of Arrhenius (a), WLF model fit (b), and joint (c) model fits

a

	Expt WVP			Model WVP						
T, ^{0}C	**p(av) 75**	**p(av) 85**	**p(av) 95**	**p 75 mod**	**p 85 mod**	**p 95 mod**	**stdev**	**E_a (kJmol^{-1})**	**A**	**R^2**
10	0.51	0.78	1.14	0.48	0.74	1.16	0.1	11.9	244.6	0.99
20	0.51	0.95	1.45	0.60	0.93	1.45	0.1			
30	0.70	1.09	1.83	0.74	1.14	1.78	0.1	14.4	981.5	0.97
40	0.99	1.39	2.13	0.90	1.39	2.16	0.3	24.5	104088.8	0.99

b

	Expt WVP			Model WVP			
T, ^{0}C	**p(av) 75**	**p(av) 85**	**p(av) 95**	**p 75 mod**	**p 85 mod**	**p 95 mod**	**sq.res**
10	0.51	0.78	1.14	0.51	0.83	1.28	0.022
20	0.51	0.95	1.45	0.48	0.83	1.45	0.017
30	0.70	1.09	1.83	0.69	1.12	1.70	0.017
40	0.99	1.39	2.13	0.98	1.53	2.07	0.025

c

	Expt WVP			Model WVP					
T, ^{0}C	**p(av) 75**	**p(av) 85**	**p(av) 95**	**75 Arh**	**85 Arh**	**95 Arh**	**75 WLF**	**85 WLF**	**95 WLF**
10	0.51	0.78	1.14	0.48	0.74	1.16	0.51	0.83	1.28
20	0.51	0.95	1.45	0.60	0.93	1.45	0.48	0.83	1.45
30	0.70	1.09	1.83	0.74	1.14	1.78	0.69	1.12	1.70
40	0.99	1.39	2.13	0.90	1.39	2.16	0.98	1.53	2.07

4.5.2 Permeation to oxygen

The purpose of measuring oxygen transport through IBC films at three different temperatures and RH was meant to simulate their effect under supply chain conditions. The effect of temperature and RH on the permeability to oxygen (PO_2) is illustrated in Fig 4.4, showing that temperature had a highly significant ($p \leq 0.05$) positive impact, whereas RH had highly negative impact on PO_2. At any given temperature, an increase in RH caused a slight decrease in the permeation of the two gases, suggesting that moisture could be involved in antagonising diffusion perhaps due to reductions in the size of voids. In a purposive pre-test trial (PPT) with micro-perforated biobased films, to determine package performance, it was apparent that increase in RH reduced gas permeation. Although the effect was not so much pronounced with the type of film used, this could pose challenges to the development of biobased films, particularly for those destined for edible packaging. The PPTs are sometimes carried out in vitro to gauge the direction of an experiment/study.

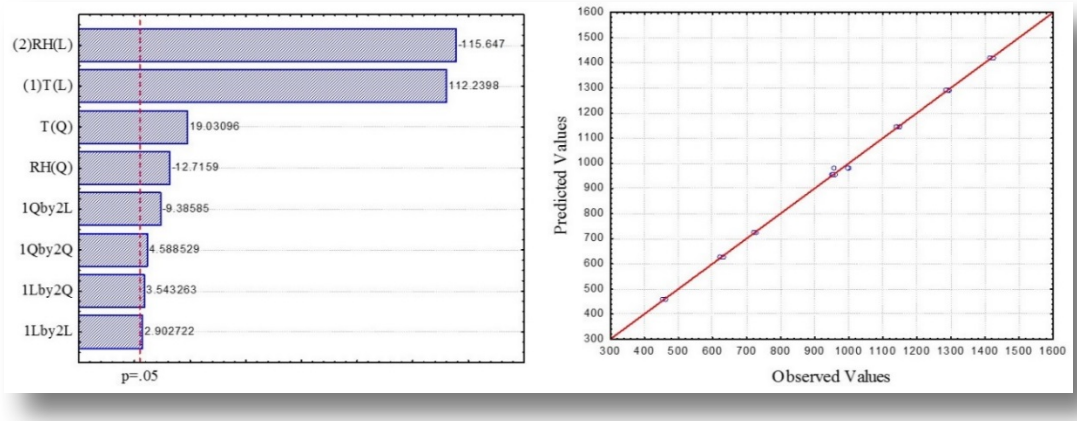


Fig 4.4. Effect of temperature and RH on the permeability to oxygen

Table 4.3 shows the temperature-dependence permeability coefficients (PC) of oxygen (O_2) at 75 and 95 % RH in IBC films. In the 10-40 ^{o}C, films stored at 95 % RH exhibited highest O_2 permeation compared to those kept at 75 % RH, while their pre-

exponential factors and activation energies were in the order of the PC: 75 % RH > 95 % RH. However, increase in temperature resulted in a decrease of oxygen (O_2) at 75 and 95 % RH. Furthermore, as the temperature increased in the lower RH (75 %), IBC glass transition temperature (Tg) and crystallinity (CRY) increased. By contrast, the increase in temperature at higher RH (95 %) caused a decrease in Tg, with Cry associated with temperature and RH increases.

Table 4.3 Permeation of oxygen in relation to thermal properties of intact bitter cassava films

Gas	T, ^{0}C	RH, %	Thermal properties		P, cm^3 cm / (cm^2.s.cmHg)	A_t; RH, ^{0}C, %	P_{ef}, cm^3 cm / (cm^2.s.cmHg)	E_p, Kj/mol
			Tg	Cry, %				
O_2	10	75	38.7	52.28	7.66 x 10^{-5}	10–40; 75	1470.00 x10^7	32.79
	40	75	40.2	60.63	2.016 x 10^{-5}			
	10	95	38.00	30.72	23.6 x 10^{-5}	10–40; 95	2.52 x10^7	20.45
	40	95	36.7	55.45	10.266 x 10^{-5}			

According to Table 4.3, the PO_2 obeyed Arrhenius rule as temperature increased from 10^{0}C to 40^{0}C regardless of RH. The observed change of PO_2 at Tg suggest that PO_2 is influenced by a change in chain mobility. The PO_2 seems to be significantly influenced by RH, with reductions in permeation (Table 4.3). This supports the explanation provided earlier on the influence of moisture on the shape and perhaps size of voids in IBC films. Additionally, it is observed that the increase in PO_2 at high RH is independent of increase in moisture. Generally, the information provided is important particularly for the choice of deploying IBC films in commercial applications in which most polymer materials are applied below or above transition conditions (Komatsuka & Nagai, 2009). Since IBC temperature dependence of PO_2 was not influenced by CRY at high RH is a good signal that IBC materials can be blended with other commercial polymers such polylactic acid (PLA) to deliver good quality materials under moisture-

stressed environments. The temperature dependence of gas permeability of PLA has been reportedly not affected by transition conditions (Komatsuka & Nagai, 2009).

4.5.3 Mass transport characteristics of solvents through intact bitter cassava (IBC) films

The pattern of solvent diffusion through IBC films is shown in Fig 4.5. It can be clearly noted that there was lower moisture absorption at 75 % RH than 95 % RH (Fig 4.5a); and similar differences were also apparent for toluene (Fig 4.5b) and paraffin oil (Fig 4.5c) diffusions in the IBC films at 30^{0}C, 50 % RH. The sigmoid nature of toluene and paraffin oil profiles might be due to the dilution effect (Cheng et al., 2012) and, perhaps, minimal interaction and effect of these solvents on IBC films. This is also supported by their low mass uptake as compared to moisture at 75 % RH and 95 % RH (Table 4.4). The patterns of toluene and paraffin oil are similar to those that have been reported for these solvents through polymer gloves (Chen et al., 2015), implying that the latter and IBC films behave similarly. However, as compared to polymer gloves, the diffusion of toluene and paraffin oil through IBC films is faster.

Table 4.4. Film transport properties in different solvents at 30^{0}C, for IBC (a) and comparison of IBC film-solvent interaction with polymer glove's rubber-toluene interaction.

a

Solvents	Inst. Mass uptake	Desorption rate, mg/min	FS_{ol}, mg/ml	FS_{tm}	R^2	n
Water 75, mg	0.2228	0.0047	0.4713	1.0765	0.90	1.002
Water 95, mg	2.5640	0.0272	3.9752	10.6156	0.81	0.997
*Toluene, µg	1.4832	0.3139	0.0390	0.0046	0.90	0.339
**Paraffin oil, µg	0.0032	0.0005	0.0813	0.0757	0.95	0.536

n, kinetic exponent associated with solvent transport characteristics; 75 & 95, water activities (0.75 & 0.95); stars (& **), values measure in micrograms (µg).*

b

Material	χ	Reference
IBC film -75RH	0.357	This study
IBC film - 95RH	0.369	This study
IBC film-Toluene	3.670	This study
IBC film-paraffin oil	0.342	This study
Butyl rubber-Toluene	0.540	(M. J. Chen et al., 2015)
Nitrile rubber-Toluene	0.690	(M. J. Chen et al., 2015)

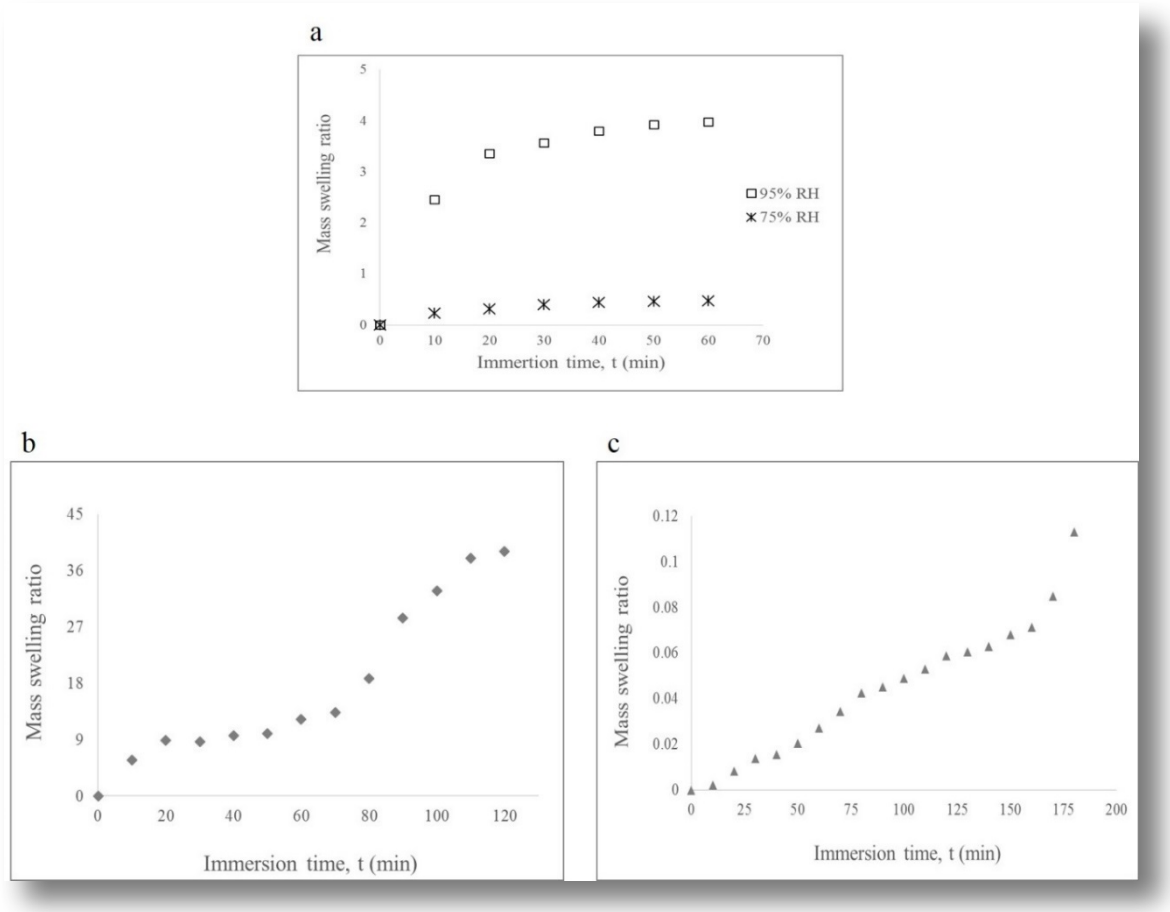


Fig 4.5 Comparison of the effect of solvents on swelling of IBC films. Water at 75 and 95 % RH (a), toluene (b) and paraffin oil (c)

The desorption rate patterns could be explained on the account of the viscous nature of the solvents. Although viscosity was not determined in this study during the experiment, paraffin oil showed high stickiness and low flow compared to toluene. In macromolecular network systems, fluid transport mechanisms through polymers are often described by diffusional kinetic exponents, which also describes Fickian and non-Fickian diffusional release from thin films (Ritger & Peppas, 1987). Thus, the water at 75 % RH and 95 % RH through IBC films followed case II non-Fickian compared to Fickian diffusion exhibited by toluene and paraffin oil when diffused through the film (Table 4.4a). The Fickian diffusion nature of IBC films is in agreement with what was observed with toluene penetration of rubbery polymers (Chen et al., 2015; Miller-Chou & Koenig, 2003).

Furthermore, the lower interaction factor of IBC films with water at 75 % RH and 95 % RH, and paraffin oil imply that these two solvents cause less swelling compared to toluene (Table 4.4b). In comparison with butyl and nitrile rubbers, toluene causes more swelling to IBC films than to the former.

The profiles of mass transfer of solvents are illustrated in Fig 4.6, showing that the adsorption and diffusion of water at 75 % RH and 95 % RH through the film is initially governed by case II non-Fickian diffusion (RP model) in the first 80 % (Fig 4.6a) and 75 % (Fig 4.6b) of adsorption. Conversely, the mass transfer behaviour of toluene (Fig 4.6c) and paraffin oil (Fig 4.6d) exhibited Fickian diffusion.

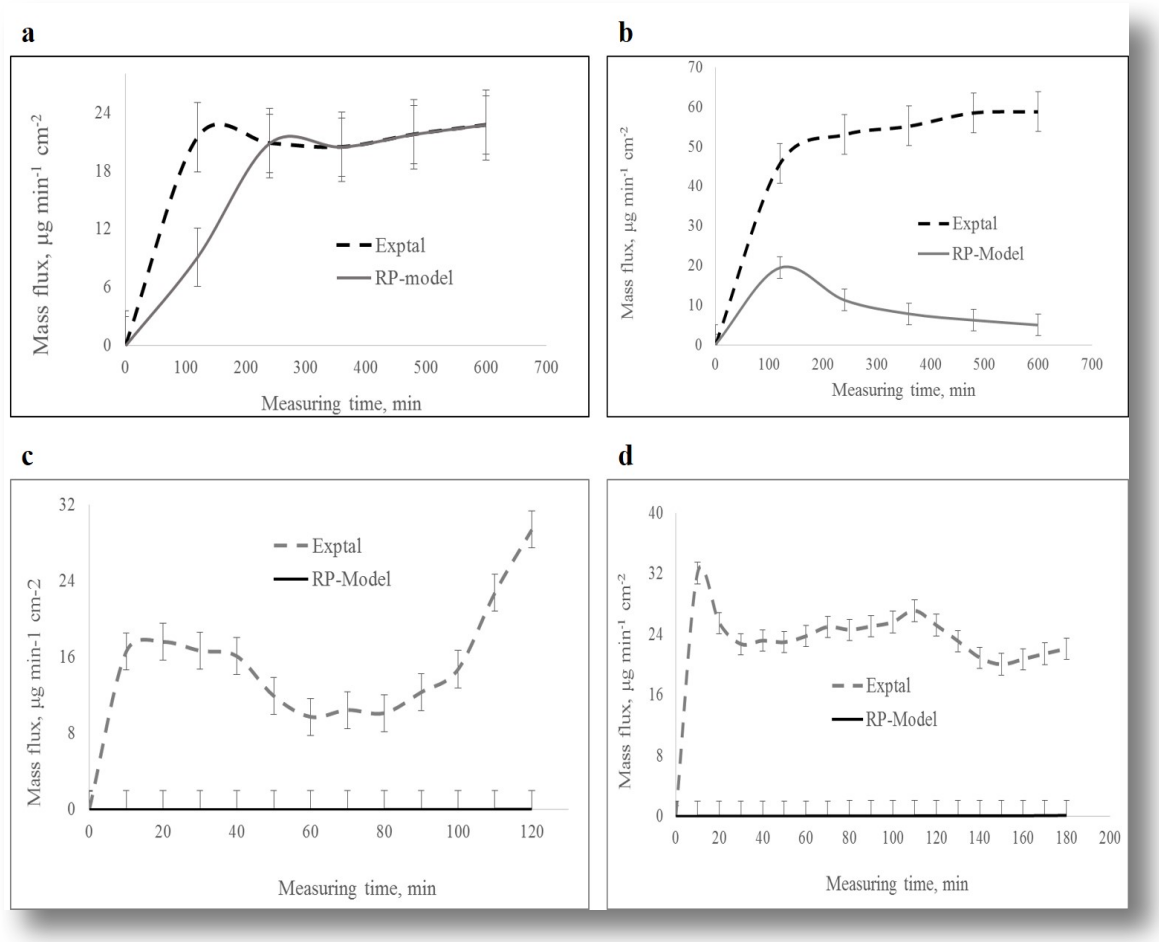


Fig 4.6 Typical concentration-time curves for water at 75 % RH (a), 95 % RH (b), toluene (c) and paraffin oil (c) transfer in IBC films showing profiles of rate of transfer (Exptal) and those modelled by power equation (RP) illustrating the type of diffusion (Fickian or non-Fickian)

These results imply that IBC films behave like glassy polymer under high moisture stress reflecting generally low cohesion and disorderly hole structures characteristic of case II diffusional deformation as result of structural swelling (Masaro & Zhu, 1999). The observed case II diffusion might also be due to thin membrane exhibited by the IBC films. The heterogeneity in these films confirm some level of modification imparted by SRRC. It has been reported that most commercial polymers are heterogeneous in nature (Cheng et al., 2012). By contrast, the diffusion of toluene and paraffin oil did not cause any deformation to IBC films. This is a good indication of the potential of these films to

be used in commercial products in contact with a range of organic solvents, e.g. oils, but with restricted water contact, such as dry products.

4.5.4 Impact of solvent mass transfer on film structural changes

An understanding of the association between solvent absorption and structural changes and modification of the film matrix is essential in order to ensure safe handling in the distribution chain. Structural changes is one of the approaches to assess the impact of permeants into the film material. As shown in Table 4.5, the broader transition from the glassy to the rubbery region caused by the 10^{o}C- 75 % RH solvent characterises IBC films having a wider distribution of crosslinking density and lower homogeneity of these networks (Petrovic, 2008). The films penetrated with 40^{o}C- 95 %RH and 10^{o}C- 95 % RH showed a slight decrease in glass transition, which might be attributed to higher solvent concentration (Table 4.4) due to increased plasticisation and more flexibility. In this study, it was observed that Toluene permeation caused films to become more brittle, consistent with low solubility and low swelling (Table 4.4) and higher Tg and Tm (Table 4.5).

Table 4.5 Effect of solvents diffusion on thermal properties of IBC films

Solvents	**Tg, ^{0}C**	**Tm, ^{0}C**	**CRY, %**	**Enthalpy change, J/(gK)**
10^{0}C-75% RH	38.7 (36.3-41.2)	200.5	52.3	0.121
10^{0}C-95% RH	38.0 (37.5-38.6)	197.9	30.72	0.003
40^{0}C-75% RH	40.2 (40.0-40.1)	179.0	60.63	0.006
40^{0}C-95% RH	36.7 (36.8-38.8)	197.2	55.45	0.074
Toluene	56.8 (55.1-56.2	203.3	40.72	0.007
Paraffin oil	36.6 (36.5-36.7)	164.8	79.21	0.003

Fourier transform infrared spectroscopy (FTIR) thermograms of film-solvent interaction during the transfer process are presented in Fig. 4.7.

The O-H stretches around 3000 cm^{-1} in Fig 4.7a and 4.7b, shown by broad bands, imply that moisture was involved in film-water interaction. However, it could also imply that glycerol was also involved. In this study glycerol was used to obtain solutions of relative humidity of 75 and 95 %RH. Furthermore, the C-H stretch peaks high than 3000 cm^{-1} in Fig 4.7c and 4.7d point to the presence of organic solvents, and thus involvement of toluene and paraffin oil interactions.

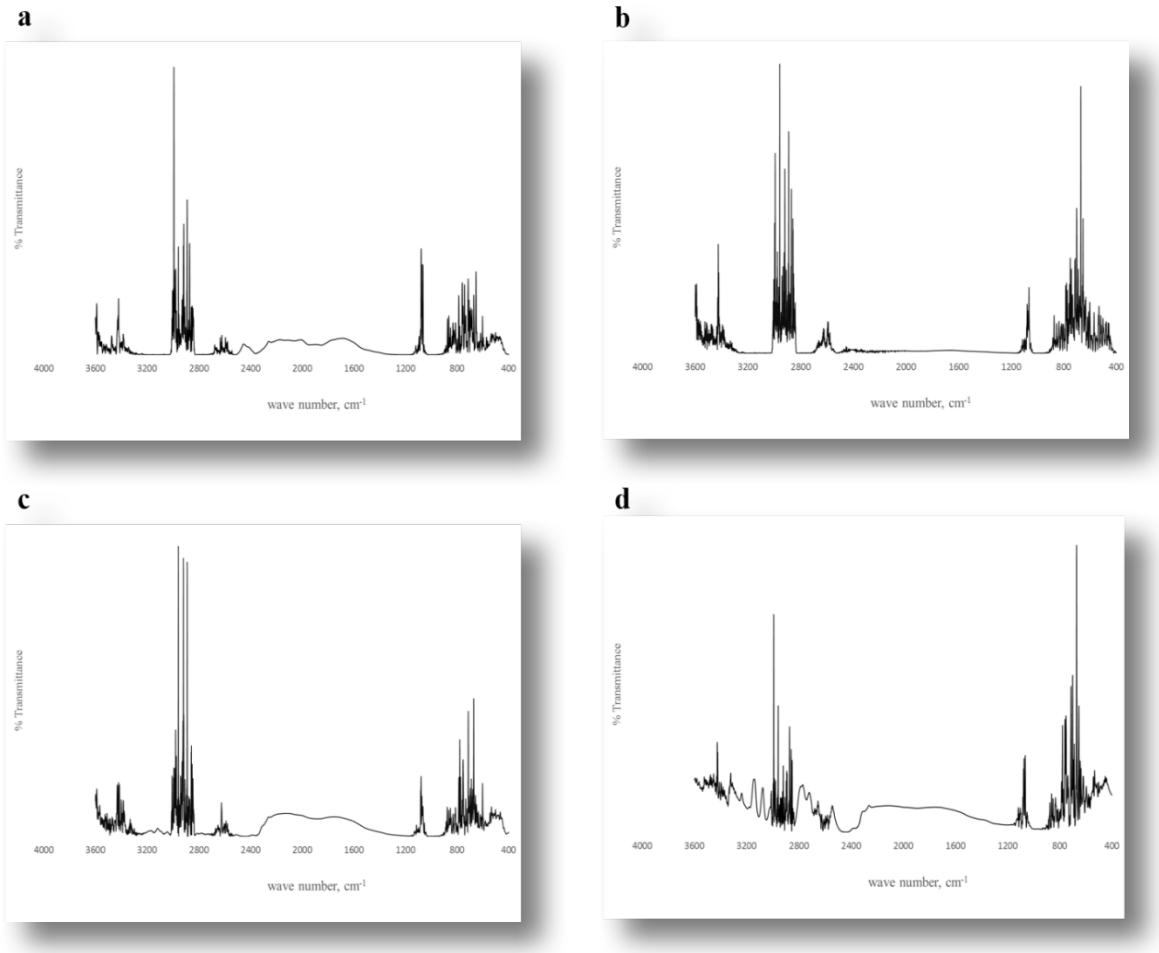


Fig 4.7 Effect of solvent diffusion on chemical properties of IBC films illustrated by FTIR thermograms of water at 75 % RH (a), water at 95 % RH (b), toluene (c) and paraffin oil (d).

Conclusion

The transport phenomenon of fluids and solvents in humidity- temperature-stressed intact bitter cassava films has been assessed by qualitative and mechanistic techniques, and related to the structural characteristics of interactions.

The intact bitter cassava (IBC) films follow a Type II isotherms, with wide pore size distributions leading to fluid pathways that are tortuous and highly variable. This suggests that these films might have wide variable permeability to fluids, which can be explored for packaging a broad spectrum of products. However, it also shows that care need to be taken to avoid exposure to high humidity.

Peleg, modified BET, Oswin and Forran-Fontan models best described the relationship between equilibrium moisture content and water activity at each temperature and under the conditions tested. Thus, these models could be used as promising tools, to describe sorption behaviour of future developed IBC films.

Temperature and humidity have shown to increase, exponentially, water vapour and oxygen permeation through IBC films. This was in agreement with temperature dependence of Arrhenius concept. Thus, validation of developed films in conditions for their targeted use should be taken as a priority during biobased film package development including IBC films.

The mass transfer mechanism of solvents through IBC films was found to vary widely with the time of solvent, with water at 75 RH and 95% RH obeying case II non-Fickian and toluene and paraffin oil following Fickian diffusion. It can be concluded that, like any other packaging films on the commercial markets, mass transfer in IBC films is governed by evaporation, diffusion, material solubility and interactions.

The DSC and FTIR tests disclosed that solvents induce structural changes in IBC films, which is solvent type-dependent. These results suggest that thermal and structural tests should be initiated along with tests of developed biobased materials during validation experiments.

In a nutshell, the integrity of the cassava biobased film packages will depend on the host environment, and maximum care should be ensured to minimise environment effects in the distribution chain.

Chapter 5. Novel intact bitter cassava: Sustainable development and desirability optimisation of packaging films

Abstract

Novel biomaterials and optimal processing conditions are fundamental in low-cost packaging material production. Recently, a novel biobased intact bitter cassava derivative was developed using an intrinsic, high-throughput downstream processing methodology (simultaneous release recovery cyanogenesis). Processing of intact bitter cassava can minimise waste, and produce low-cost added value biopolymer packaging films. The objective of this study was to i) develop and characterise intact bitter cassava biobased films, and ii) determine the optimal processing conditions, which define the most desirable film properties.

Films were developed following a Box-Behnken-design considering cassava (2, 3, 4 %w/v), glycerol (20, 30, 40 %w/w), and drying temperature (30, 40, 50°C) and optimised using multi-response desirability. Processing conditions produced films with highly significant ($p<0.05$) differences. Developed models predicted impact of processing conditions on film properties. Desirable film properties for food packaging were produced using the optimised processing conditions, 2 %w/v cassava, 40.0 %w/w glycerol, and 50°C drying temperature. These processing conditions produced films with 0.3%; transparency, 3.4%; solubility, 21.8%; water-vapour-permeability, 4.2 $gmm.M^{-2}.day^{-1}kPa^{-1}$; glass transition, 56°C; melting temperature, 212.6°C; tensile strength, 16.3 MPa; elongation, 133.3%; elastic modulus, 5.1 MPa; puncture resistance, 57.9 J, which are adequate for packaging applications. Therefore, intact bitter cassava is a viable material to produce packaging films that can be tailored for specific sustainable, low-cost applications.

Key words: Bitter cassava, biobased film, sustainability, optimization desirability.

5.1 Introduction

Natural bioresources have drawn packaging research interest due to rising environmental sustainability awareness and demand for economic food packages. This demand is due to growing negative impact of the fossil-based non-biodegradable plastic packaging materials on the environment (Souza, Monte, & Pinto, 2011) and perhaps concerns of escalating costs of package production. Among the natural materials, sweet cassava has been progressively used in film formulations due to abundance, biodegradability and low-cost of its polysaccharide derivatives, but this makes it unsustainable due to competition with food supply. Its derived polysaccharide starch is by far evaluated as a main component in the formulation of biobased films (Flores, Costa, Yamashita, Gerschenson, & Grossmann, 2010; Maran, Sivakumar, Sridhar, & Thirugnanasambandham, 2013; Phan The, Debeaufort, Voilley, & Luu, 2009; Souza et al., 2012). Biobased packaging films have been reported to maintain quality and improve shelf-life of fresh and processed foods especially when they exhibit good mechanical properties and selective barriers (Cerqueira et al., 2010). Sweet cassava has been successful in the development of biobased films with wide range of properties (Embuscado & Huber, 2009), but these films have not been used in many food packages possibly due to lack of standardisation and systematic approach. Bitter cassava cultivars, regarded traditionally as a famine-reserve crop (Burns, Gleadow, Cliff, Zacarias, & Cavagnaro, 2010; Chiwona-Karltun et al., 1998; Essers, 1988; Sayre et al., 2011; Thi & Vuong, 2012), are being transformed into resourceful commercial crops but many issues regarding their full value as industrial materials are yet to be resolved. Recently, a novel biobased intact bitter cassava derivative was developed using an intrinsic, high-throughput downstream processing methodology known as simultaneous release recovery cyanogenesis (SRRC) (Tumwesigye et al., 2016).

Novel materials and optimal processing conditions are fundamental in low-cost packaging material production.

Optimisation of formulations is dependent of material balance and processing conditions. Optimisation of formulations has been accomplished mainly for various compositional blends of starch/flour of any botanical crop, other additives and different

plasticisers. Examples that have been reported include optimisation of amaranth flour/glycerol matrix (Tapia-Blácido, do Amaral Sobral, & Menegalli, 2011), optimisation of starch/polyester film properties (Olivato et al., 2013), optimisation of xanthan gum/tapioca starch/ potassium sorbate edible matrices (Arismendi et al., 2013). Few studies have used banana flour to determine the optimal processing conditions of films (Franciele Maria Pelissari, Andrade-Mahecha, Sobral, & Menegalli, 2013). These studies allude to the fact that better films can be produced when initial material additives and plasticisers are balanced. Optimisation of a good film requires precise control of the processing conditions and careful examinations of the fluctuations that occur in film properties. However, no systematic optimisation study, integrating biobased film production by combining material balance, processing conditions and low-cost processing has been performed for intact bitter cassava. Nowadays, experimental design methodology tools have been employed to determine the most efficient and economic matrix formulations needed for optimal formulations (Steele et al., 2012). Robust packaging design provides approaches for fine-tuning processing conditions to the desired possible package properties with marginal costs and maximum functional presentation. For each property-condition match, there is need to tailor the formulation that best suites a specific product. Desirable properties could be achieved by process robustness incorporating low-cost base materials and formulations. Unfortunately, the common current approach is characterised by piecemeal evaluations whereby there is a tendency to improve the properties of films by evaluating parameters on individual basis.

The objective of this study was to i) develop and characterise intact bitter cassava biobased films, ii) define the parameters and conditions, which relate formulation to film development properties, and iii) optimise processing conditions and properties in order to obtain films with desirable characteristics for tailor food packaging.

5.2 Methodology

5.2.1 Material source: Intact bitter cassava

Intact (whole) bitter cassava (Tongolo), with total cyanogen content between 900 and 2000 ppm, were processed using an intrinsic extraction procedure known as

simultaneous release recovery cyanogenesis (SRRC) into biopolymer derivative with a total cyanogen around 0.5 ppm according to the method described by Tumwesigye et al., (2016). The biobased intact bitter cassava derivative was used for film formulation.

5.2.2 Development of intact bitter cassava films

The development and production of semi-commercial intact bitter cassava biobased films was performed based on Box-Behnken design. The design matrix for both processing conditions (actual/coded independent variables) and responses (film properties), with a total of 15 experimental runs are presented in Table 5.1. Each run was an average of 3 replicates. The criteria for selection of processing conditions that have a significant impact on the film development was set considering previously reported range values of cassava starch/flour and their reinforced films (de Moraes et al., 2013; Tumwesigye et al., 2016).

Biobased intact bitter cassava derivative (2, 3, 4 % w/v) and glycerol (20, 30, 40 % w/w) were mixed in 100 mL deionized water, and homogenised using a magnetic stirrer (100 rpm, 20°C, 5 min). The mixture was transferred to a bath (Huber Ministat 240 Heating Recirculating Unit, UK) and heated (70°C, 2°C/min., during 5 min) until a viscous transparent gel was observed, and held for 20 minutes.

Film casting was done by pouring solution (30 mL) onto a previously lubricant sprayed 14 cm diameter flat glass plate using a dropper. The film solution was measured to ensure production of uniform thickness films (30±5 μm) for different samples, and the dry film release spray (Ambersil Formula 5 non-silicone, UK) was used to ease peeling of films after drying. The plate was left at 25±1°C for 3 hours to allow stabilisation and bleeding of trapped bubbles, and then dried in a ventilated oven (30, 40, and 50) ±1°C for 4-8 h. The dried film was peeled off the plate and equilibrated at 23±2^{O}C, 54 % relative humidity for at least 48 h prior to experimental analysis.

5.2.3 Characterisation of intact bitter cassava films

5.2.3.1 Thickness measurement

For each experiment (Table 1), film thickness (mm) was measured using an absolute digital Calliper (Digmatic, Mitutoyo UK Ltd). Measurements were taken at 6 different random sites and the average values were calculated for film surface area that was intended only for use in each test. The purpose of measurement was to ensure that films' thickness was maintained within the same range during characterisation.

Table 5.1. Box-Behnken design matrix: Actual/coded variables of processing conditions and film properties.

Runs	Actual/ coded independent variables			Film properties									
	Cassava % w/v	Glycerol % w/w	Temp °C	Moisture content %	Optical (%)	Solubility (%)	Water Vapour Permeability gmm / (m².day.kPa	Glass transition °C	Melting temperature °C	Tensile Strength MPa	Elongation at break %	Elastic modulus MPa	Puncture resistance J
1	4 (1)	30 (0)	30 (-1)	0.6±^{a}0.0	8.4^{a}±0.2	19.6^{a}±0.1	6.5^{a}±0.0	44.4^{ab}±0.0	190.7^{a}±1.2	23.0^{a}±0.1	45.1^{a}±0.5	9.4^{a}±0.0	56.3^{a}±0.5
2	2 (-1)	30 (0)	30 (-1)	0.2±^{b}0.0	10.0^{b}±0.0	17.1^{b}±0.5	5.2^{b}±0.0	41.7^{cd}±0.1	203.8^{b}±1.0	20.0^{ba}±0.4	5.2^{b}±0.4	5.7^{b}±0.0	2.1^{b}±0.0
3	3 (0)	20 (-1)	30 (-1)	0.2±^{c}0.0	7.1±^{c}0.1	18.3^{c}±0.0	4.1^{c}±0.0	42.9^{d}±0.0	188.0^{ca}±1.0	21.2^{ba}±1.7	3.0^{b}±0.5	10.6^{c}±0.0	2.5^{b}±0.5
4	3 (0)	40 (1)	30 (-1)	0.7±^{d}0.0	10.9^{d}±0.1	23.1^{d}±0.4	7.7^{d}±0.1	39.7^{aec}±0.1	185.0^{gc}±1.0	4.7^{cd}±1.1	74.6^{c}±13.4	0.7^{d}±0.0	63.9^{c}±0.8
5	2 (-1)	20 (-1)	40 (0)	0.2±^{e}0.0	5.6±^{e}0.2	18.1^{e}±0.3	3.4^{e}±0.0	49.5^{fg}±0.1	202.7^{db}±2.1	11.1^{e}±0.7	2.8^{b}±0.6	5.9^{b}±0.0	1.7^{b}±0.1
6	4 (1)	20 (-1)	40 (0)	0.2±^{f}0.0	9.9±f0.2	21.9^{f}±0.4	4.4^{f}±0.0	50.7^{gh}±0.1	196.7^{e}±1.2	37.6^{f}±3.0	4.1^{b}±0.8	9.7^{e}±0.0	29.0^{d}±1.5
7	2 (-1)	40 (1)	40 (0)	0.3±^{g}0.0	3.5±^{g}0.5	20.1^{g}±0.3	4.8^{g}±0.0	46.8^{gi}±0.0	208.0^{f}±0.0	1.9^{c}±0.1	189.3^{d}±9.5	0.1^{f}±0.0	51.6^{e}±0.1
8	4 (1)	40 (1)	40 (0)	0.5±^{h}0.0	5.3±^{h}0.5	30.5^{h}±0.1	4.5^{h}±0.0	44.1^{ab}±0.1	191.5^{a}±1.5	3.7^{c}±0.1	181.3^{d}±14.3	0.1^{f}±0.0	73.2^{f}±0.7
9	4 (1)	30 (0)	50 (1)	0.3±^{i}0.0	3.6±^{i}0.4	36.4^{i}±0.1	3.5^{i}±0.0	54.3^{e}±0.0	186.7^{g}±1.5	39.8^{gb}±0.2	43.9^{b}±0.4	14.2^{g}±0.0	37.0^{bg}±0.7
10	2 (-1)	30 (0)	50 (1)	0.2±^{j}0.0	5.6±^{j}0.2	33.2^{j}±0.2	6.4^{j}±0.0	46.1^{b}±0.1	208.3^{gc}±1.2	16.4eh±0.4	4.5^{b}±0.3	7.6^{h}±0.0	2.7^{g}±0.1
11	3 (0)	20 (-1)	50 (1)	0.2±^{k}0.0	3.7±^{k}0.1	40.9^{k}±0.4	4.6^{k}±0.0	51.7^{e}±0.1	199.7^{gc}±0.0	33.6^{e}±1.0	6.4^{b}±0.2	13.8^{i}±0.1	2.6^{bg}±0.3
12	3 (0)	40 (1)	50 (1)	0.5±^{l}0.0	7.0±^{l}0.4	39.1^{l}±0.2	4.9^{l}±0.0	47.6^{j}±0.1	199.0^{gc}±1.5	7.5^{f}±0.2	33.1^{a}±0.6	1.5^{j}±0.0	52.5^{h}±0.3
13	3 (0)	30 (0)	40 (0)	0.5±^{m}0.0	4.7±^{m}0.4	36.1^{m}±0.2	3.4^{m}±0.0	38.3^{bi}±1.9	183.7^{f}±1.5	17.8^{hg}±1.9	4.2^{a}±0.8	5.2^{k}±0.2	3.5^{bg}±0.3
14	3 (0)	30 (0)	40 (0)	0.5±^{n}0.0	4.1±^{n}0.1	36.2^{n}±0.3	5.4^{n}±0.0	37.9^{h}±1.6	185.3^{ed}±0.6	13.7^{i}±1.1	4.2^{b}±0.0	4.4^{l}±0.0	4.5^{bg}±0.6
15	3 (0)	30 (0)	40 (0)	0.5±^{p}0.0	4.2^{p}±0.1	35.7^{p}±0.2	5.4^{p}±0.0	39.0^{fi}±0.6	186.0^{e}±1.0	12.6^{d}±0.7	14.4^{a}±3.7	7.1^{m}±0.0	3.3^{e}±0.1

Marked differences (subscripts) are significant at $p < 0.05$

5.2.3.2 Moisture content

Film moisture determination was performed in two stages: i) initial weight loss (WL) and ii) moisture content (MC). The initial WL allowed films to lose free moisture and transformed them into films which could be subsequently applied. Herewith, 15 films (8.4 cm diameter each), formulated according to the experimental design (Table 5.1), were dried at three different temperatures (30, 40, 50°C) and their WL monitored every 30 minutes until constant readings were obtained. These films were designated WLF. To evaluate the effect of processing conditions on the MC, triplicate samples from each batch of freshly dried WLF was determined gravimetrically. WLF was dried in a hot air circulation oven at 105°C for 9 hours until when the WLFs had constant weights. MC was calculated as the ratio of the mass of water lost to the total WLF weight and expressed in percentage, wet basis. Three replicates of each WLF were tested.

5.2.3.3 Optical properties

Film optical property (transparency level) was determined as described (Mu et al., 2012) with slight changes. Film strip of each formulation was carefully inserted into cuvettes and placed inside a spectrophotometer cell. Spectrum intensity of an empty cuvette (I_0) (as a baseline) was run concurrently with the sample film. Transmission was measured using a spectrophotometer (Biochrom Libra S22 UV/Vis, Cambridge CB4 0FJ UK) at wavelength 700 nm. Transparency (T %) was calculated using Eqn. 5.1. For each of the values, the higher T implies that less light passed through a film, thus described as opaque. Three replicates of each film were tested.

$$T = \log I_0/(It)100 \quad 5.1$$

where, t, film thickness (mm).

5.2.3.4 Solubility

Film solubility (FS) in water was measured as described in Belibi et al., (2014) with minimal modifications. Previously oven-dried film strips (3 x 2 cm) were weighed on an aluminium foil, submerged in a beaker with 50 mL of distilled water and tightly covered with parafilm to minimise water loss and airborne contaminants. The contents were kept at 23°C for 30 days, intermittently agitated every 24 h to allow dissolution, partially dehydrated (where necessary filtered) on filter paper and dried in an air-circulating oven at 70°C until constant weight. Total soluble matter of the sample was calculated as described (Belibi et al., 2014). Sample tests were performed in triplicate, and mean values were used for computing FS in water.

5.2.3.5 Water vapour permeability

Film water vapour permeability (WVP) was determined gravimetrically at 38°C, 95% RH according to ASTM, (2005) method. Films for WVP were formulated based on experimental design (Table 5.1), cast on 8.4 cm diameter dishes to maximize uniformity and permeation cell fitting specificity. Each previously conditioned (54% RH, 23±2°C, at least 48h) film was carefully positioned between acrylic permeation cell containing $CaCl_2$ (0% RH) and enclosed in a humidity-controlled plastic container partially filled with 1000 mL of salt solution, corresponding to a relative humidity of 95%. The container was stored in temperature controlled incubator at 38°C, and cell weight gain was recorded every 2 hours for 10 hours and used for WVP calculations. WVP was calculated using Eqn. 5.2.

$$WVP = (\acute{m}\delta)/[AP(r_{95} - r_o)] \quad 5.2$$

where ḿ, mass flow rate (g/day); δ, thickness (mm); A, cross-sectional area (m^2); P, saturation partial pressure at 38°C (kPa); and r_{95}- r_o, relative humidity of outside environment (95 %) and cell (0 %). All tests were conducted in triplicate and mean values were used for calculating WVP.

5.2.3.6 Thermal characterisation

Thermal characteristics, namely glass transition (T_g) and melting temperatures (T_m), of bitter cassava films were evaluated using a differential scanning calorimeter (DSC 200 F3, Germany) equipped with a thermal analysis data station.

Films were prepared based on experimental design (Table 5.1) and each film (10 mg) was placed into a pre-weighed DSC pan. The pan was hermetically sealed, heated from 20 to 220ºC at a rate of 10ºC/min, cooled back rapidly in liquid nitrogen for 10 seconds, and reheated at 5ºC/min to 220ºC. The purpose of rapid cooling and second heating was to give film samples thermal history, key in understanding the effect of previous processing on thermal characteristics of films. The T_g and T_m were calculated using the built in software (NETZSCH Proteus® 6.0, Germany) and determined by considering the midpoint of the heat capacity change observed on the second heating. All samples were evaluated in triplicate and mean measurements reported. An empty pan was used as a reference.

5.2.3.7 Mechanical analysis

Mechanical properties, tensile strength (TS), elongation at break (E), elastic Modulus (EM) and puncture resistance (PR) were evaluated by a TA HD Plus Texture Analyser (Stable Microsystems, UK) equipped with a 50 kg load cell, according to ASTM, (2009) method.

For TS, E and EM measurements, an initial grip separation (50 mm) and cross head speed (1.0 mm/s) were used. Measurements were taken for at least 5 close values to obtain cross-sectional area (thickness x initial grip distance). Ten film strips (25 x 100 mm) were cut from each formulation according to the experimental design (Table 5.1). TS (MPa) was calculated by ratio of the force necessary to break a sample to the cross-sectional area., E (%) as a change in the sample original length between grips at break, and EM (MPa) by ratio of TS to the extensional strain.

For PR, a circular opening (10mm), probe diameter (3mm) and a speed (1.0 mm/s) were used, and 7 mm diameter film discs from each formulation according to the experimental design (Table 5.1). PR was calculated as a maximum penetration force at the tear.

5.2.4 Model development and film optimization

The response polynomial models were developed using factorial and Box-Behnken response surface design by varying parameters namely cassava derivatives (2, 3, 4 % w/v), glycerol (2, 3, 4 % w/w), and drying temperature (30, 40, 50 minutes) based on experimental design (Table 5.1) described in section 2.2. Appropriately, four models (linear, combined two factor interaction, quadratic) were fitted to the data in order to obtain the second order polynomial equations, their regression coefficients and R^2 values. The aliased cubic model was not considered for analysis.

Analysis of variance (ANOVA) was used for regression coefficient determination and significance of examination. The model adequacy was determined by coefficient of determination (R^2) and illustrated by the mean square pure error (MSPE). Processing conditions were matched with properties to determine significant effects for optimisation purposes.

The optimisation of conditions (parameter balance) and film properties (desired functional combination) were achieved by a desirability methodology after fitting polynomial models to the data as suggested by (Derringer, 1980) (Eqn. 5.3) and reported widely.

$$D = [d_y\ (Y)^{1/n}\ ] \qquad 5.3$$

where, D, over all desirability; Y, responses; dy (Y), response desirability function, n, number of responses. (n=1); dy (Y) = 0, perfectly undesirable; dy (Y) = 1, perfectly desirable. Validation of optimisation was accomplished by comparing experimental results and predicted values obtained from fitted model equations.
Statistica 7.1 software (StatSoft Inc., Tulsa, USA) was used to perform the above tasks.

5.3 Results and discussion

5.3.1 Example of transparent and homogeneous biobased films

An example of biobased films produced using intact bitter cassava is shown in Fig 5.1. Notwithstanding film individual unique properties, all formulations produced homogeneous, flexible, transparent films, demonstrating the potential of this novel sustainable material to reduce cassava borne environmental waste and develop biodegradable materials for food packaging applications.



Figure 5.1. Example of films produced from intact bitter Cassava as illustrated by their visual image when formulated with Cassava, 4 w/v %, glycerol, 30 w/w %, drying temperature, 30^0C.

5.3.2 Characterisation of intact bitter cassava biobased films

Both formulation and optimisation experiments demonstrated that variations in processing conditions strongly associate with intact bitter cassava film properties. Moreover, processing conditions showed highly significant ($p<0.05$) difference in film pattern properties (Table 5.1 & 5.2), suggesting that individual and compounded effects are important in matching parameters with ultimate properties.

5.3.2.1 Thickness

The potential influence of thickness on film properties has been widely reported with examples from (Prakash Maran, Sivakumar, Thirugnanasambandham, & Sridhar, 2013) and

(de Moraes et al., 2013). In this study extreme care was taken to minimise variations in film thickness to an average of 0.025 ± 0.005 mm for all experiments. Therefore, there were no significant differences ($p > 0.05$) due to influence of processing conditions on the thickness. Nevertheless, insignificant deviation was expected to be caused by combined differences in processing parameters, with formulations falling below centre points (such as cassava: glycerol, 2:20 %) producing films close to 0.02 mm due high loss of water during heating and drying stages. (Jaqueline Oliveira de Moraes et al., 2013; Maran et al., 2013). (2013) reported film thickness of 0.027-0.046 and 0.070 -0.299 mm when using cassava starch, 1-3 % w/v, glycerol, 0.5 – 1.0 mL, agar, 0.5 – 1.0 g and span80, 0.1 - 0.5 L; 85 – 99 % with starch, 3 - 5 % w/v, glycerol, 20 w/w% and cellulose fibre, 0.3g respectively.

Table 5.2. Regression coefficients and analysis of variance for film properties. Mean (β0), cassava content (β1), glycerol content (β2), drying temperature (β3), their corresponding interactions (β12, β13, β23), and mean square residual error (MSPE.

Coefficients	Moisture content %	Optical %	Solubility %	Water Vapour Permeability g.mm/(m².day.kPa)	Glass transition ^{0}C	Melting temperature ^{0}C	Tensile strength MPa	Elongation at break %	Elastic modulus MPa	Puncture resistance J
β_0	1.713*	90.548*	-203.520*	-19.467***	274.725*	440.500*	92.103**	-1402.20*	13.314	623.252*
Linear										
β_1	-1.344*	-54.204*	66.155*	5.599	-83.098*	-155.833*	-25.362	1007.93*	31.785*	-252.896*
β_2	-0.177*	1.001*	8.665*	1.315*	-8.301*	3.800**	5.245*	1.58	-0.114	-29.588*
β_3	0.045*	-2.000*	0.822*	0.021*	-2.840*	-6.792*	-6.171*	30.24*	-1.902*	-4549*
Quadratic										
β_{11}	0.139*	12.840*	-8.524*	0.778	9.214*	31.875*	5.743	-195.016*	-7.309*	35.027*
β_{22}	0.002*	-0.061*	-0.112*	-0.021	0.134*	-0.041**	-0.060*	1.09*	0.027*	0.502*
β_{33}	-0.000*	0.019*	-0.009*	0.008*	0.030*	0.028*	0.066*	-0.24*	0.032*	0.062*
Interactions										
β_{12}	0.107*	0.572*	-2.258*	-0.061	2.070*	-2.688*	-0.832	-27.16*	-0.163	8.358*
β_{122}	0.001*	0.024*	0.021*	0.006**	-0.031*	0.031*	0.005	-0.21*	-0.016*	-0.099*
B_{112}	-0.009*	-0.344*	0.191*	-0.055**	-0.050***	0.096***	-0.011	6.61*	0.173*	-0.427*
β_{13}	-0.010*	0.261*	0.878*	-0.214***	0.051**	3.563*	0.800***	-5.76*	-0.315**	0.637*
B_{113}	0.001*	-0.045*	-0.144*	0.018	-0.062**	-0.629*	-0.048	0.95*	0.065**	-0.189*
β_{23}	-0.001*	-0.0014	-0.017*	-0.009*	-0.002	0.006	-0.024*	-0.11*	-0.006*	-0.029*
R^2	0.999	0.987	0.999	0.877	0.987	0.984	0.986	0.993	0.987	1.000
MSPE	0.000	0.108	0.079	0.244	0.485	1.646	2.714	37.338	0.355	0.470

* Significant at 1% level; ** Significant 5% level; *** Significant at 10% level

5.3.2.2 Moisture content

Film moisture content (MC) was highly influenced by the processing conditions (Table 5.1 & 5.2). Glycerol and cassava had a significantly high effect on MC than temperature in the linear and quadratic ranges respectively. Film MC determined following constant weight drying was in the range of 0.22–0.71 % (w/w, wet basis), which was very low suggesting that, in general, drying impacted on MC. It can be thought that increasing the content of cassava biopolymer derivatives in the matrix would reduce the amount of water needed. However, this was not observed in the present work, since derivatives worked associatively with glycerol to increase the moisture content of the films. This could be explained by: i) the high hygroscopic nature of glycerol which held water molecules into the film matrix by creating more hydrophilic hydroxyl groups as active sites with high affinity for water molecules, ii) characteristics of the derivatives of intact bitter cassava such as bigger granule size that absorbed more water in order to swell, and iii) pre-formed gel or post thermal gelation during drying such that these strong gels were able to hold water firmly within the matrices.

5.3.2.3 Optical properties

Intact bitter cassava film optical properties demonstrated highly significant associations with processing conditions. Drying temperature showed a highly significant ($p<0.05$) impact on film optical properties (low transparency values), with films becoming more transparent as temperature increases linearly and non-linearly, as shown in Table 5.1 & 5.2, Fig. 5.2 a_1 & a_2. Cassava and glycerol had a significant negative effect on film transparency, with films becoming more opaque when the cassava quadratic and glycerol linear combination effects became more apparent. However, films demonstrated more transparency when the former and latter combined effects were transposed. Also, notable is the individual processing conditions contribution on film transparency, with glycerol quadratic and linear, and cassava quadratic effects showing positive influences while cassava linear effect exhibited a negative impact. Results showed that increasing cassava content improves film transparency. This is inconsistent with what is known (Moraes et al., 2013) whereby increase in cassava starch caused translucency or opaqueness in films, thus suggesting that intact root processing might be associated with modification of starch and general increase in film transparency.

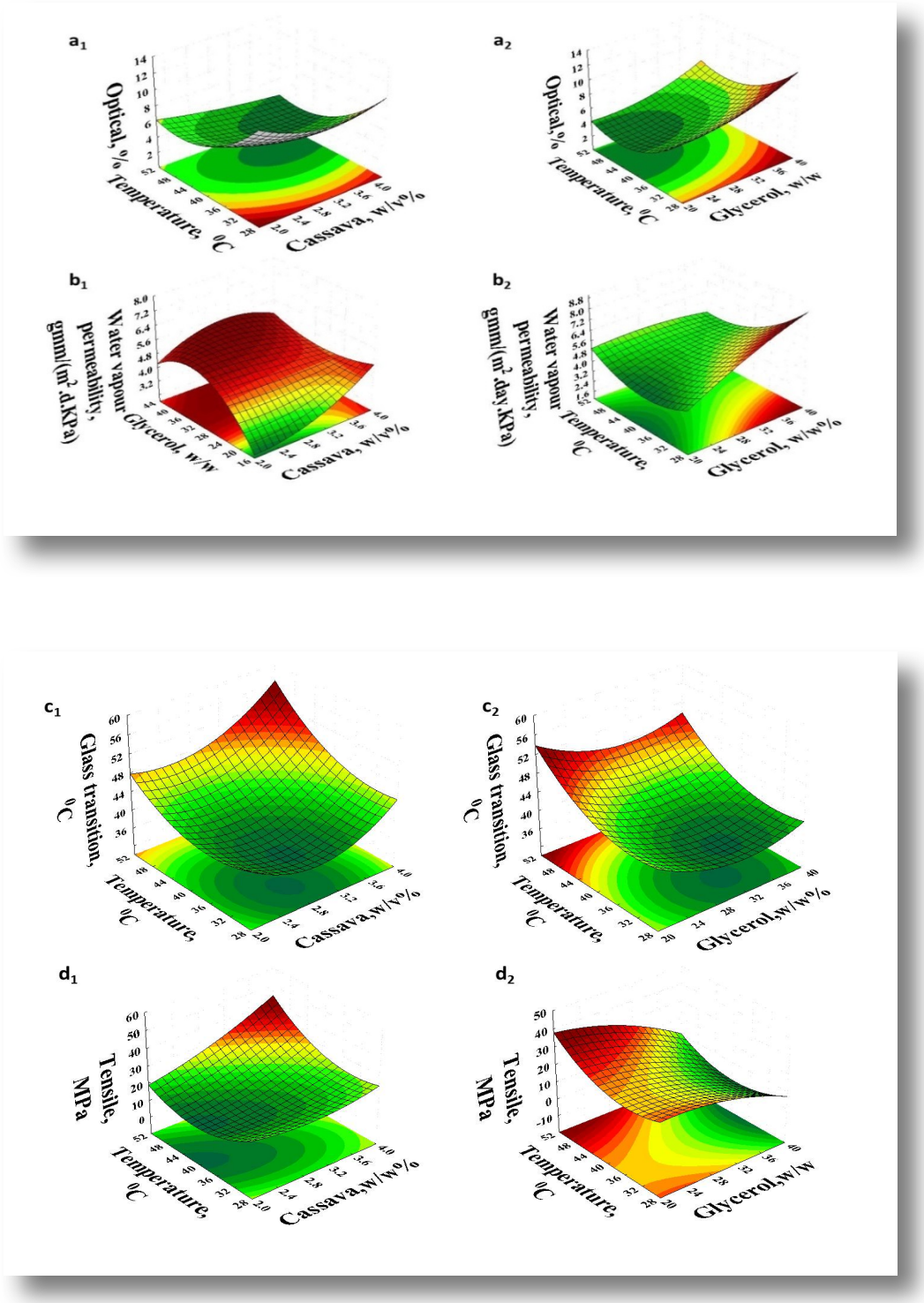


Figure 5.2. Fitted response surfaces for (a) optical properties (MPa), (b) water vapour permeability (gmm/(m^2.day.KPa), (c) tensile strength (MPa), and (d) glass transition (°C) as a function of different levels of cassava (w/v%), glycerol (w/w%) and drying temperature (°C).

5.3.2.4 Solubility

The film solubility as a function of processing conditions is presented in Table 5.1 & 5.2. Similar to optical properties, drying temperature caused the highest film solubility in water, increasing linearly when drying temperature increased. Additionally, the main (cassava and glycerol) effects, interaction between cassava and glycerol, and between cassava and drying, linearly and quadratic, were significant (p<0.05). Regardless of the high solubility-enhancing drying temperature, causing film structural disruptions and high water mobility, low solubility of 16 – 40 % was obtained after 30 days. Film solubility (16 – 40 %) was considered to be low compared to 11-41 % obtained when solubility was measured within 24 hours (Belibi et al., 2014). Low values might be explained by relatively stable network components in the film structure imparted by intact root and other processing properties. The stability of solubility values after 30 days could also be explained by decreased swelling ability in glycerol plasticized films and their ability to resist degradation.

5.3.2.5 Water vapour permeability

Water vapour permeability (WVP) significantly (p<0.05) decreased, linearly and quadratically, with increase in drying temperature and linearly with combined interaction effects of cassava-drying temperature (DT) and glycerol-DT (Table 5.1 & 5.2; Fig. 5.2 b_1 & b_2). Conversely, glycerol alone, and when combined with cassava, caused a positive impact on WVP, increasing linearly and quadratically as the concentrations increased. The patterns observed can be explained by the effectiveness of glycerol in lowering intermolecular forces between polymer chains leading raised WVP and perhaps the disruption of these forces at high temperatures leading to their strength.

5.3.2.6 Thermal properties

The impact of processing conditions on thermal properties of intact bitter cassava, associated with glass transition (Tg) and melting (Tm) temperatures, are shown in Table 5.1 & 5.2. The cassava content had the most significant (p<0.05) effect on Tg followed by the glycerol content, both having the expected impact. However, the drying temperature showed a very highly significant effect, which is higher the higher the concentration of cassava (Fig 5.2c1). This is likely due to the glass transition temperature of the dried film being in the range of temperatures of the drying process itself. Therefore, the extent of vitrification of the structure during drying depends on this processing variable. In the case of Tm the effect of drying temperature is even more important than that of glycerol content (Table 5.2). Altogether, the observed extensive variations in effects of processing conditions on Tg and Tm point to the need to find a balance so as to produce films with desired Tg and Tm.

5.3.2.7 Mechanical properties

Film formulations produced wide variations in mechanical behaviour (Table 5.1 & 5.2), with statistical significance (p<0.05) among tensile strength (TS) (Fig d_1 & d_2), elongation at break (E), elastic modulus (EM) and puncture resistance (PR). Glycerol presented the highest negative linear impact on TS and EM and highest linear positive effects on E and PR, statistically shown in Table 5.2. Additionally, interaction between cassava and glycerol, cassava and drying temperature, were significant, imparting a negative linear effect on all mechanical properties. Altogether, these results showed the extent of plasticising and effects of glycerol on mechanical properties.

5.3.3 Modelling of film characteristics

Tables 5.2 shows the regression coefficients, and highlights significant terms for response surface quadratic models fittings and choice. Thus, the quadratic models were highly significant for all responses (p< 0.05) whereas there was an aliased condition for cubic models. Accordingly, the quadratic model and corresponding linear and combined two factor interactions was used in determining the association between processing conditions and film properties. Generally, all formulations, except for WVP, for the quadratic model used presented significant influence (p<0.05), with R^2 > 0.90 and their differences < 0.2

respectively, alluding that the model amply projected the tangible association between the processing conditions and film properties. Moreover, obtained R^2 suggested that over 90% of conditions and responses data explained the adequacy and significance of the models.

5.3.4 Desirability optimisation of packaging films

The optimal individual values for film properties as a function of optimal processing conditions using a desirability function (DF) is shown in Table 5.3. DF falls between 0 and 1, with 0 as minimum and 1 maximum. As values, tend to 1, the more optimised the process is achieved; the more desirable properties are provided by optimal processing conditions. With the exception of optical properties, the higher individual desirability values show that most optimised parameters were highly desired.

In order to elucidate a universal optimal formulation of processing conditions that would concurrently deliver the most desirable film properties, a global desirability (GD) of 0.7 was determined for all parameters (Fig 5.3). The overall desirability considers the combined magnitudes of individual desirability (Table 3), expressed as a mean and achieved using Statistica software.

Table 5.3. Optimal values of intact bitter cassava films as determined by individual response desirability function.

Parameter			Objective	Experimental		Optimal	Desirability
Property	Condition	PC	FP	Lower limit	Upper limit		
Moisture			Minimize	0.22	0.71	0.19	1.00
content	c	Minimize		2	4	4.00	
	g	Minimize		20	40	20.00	
	dt	Minimize		30	50	50.00	
Optical			Minimize	3.06	11.07	3.43	0.85
properties	c			2	4	2.00	
	g			20	40	40.00	
	dt			30	50	40.00	
Solubility			Minimize	16.58	41.34	15.52	1.00
	c			2	4	2.00	
	g			20	40	20.00	
	dt			30	50	35.00	
Water			Minimize	3.28	7.72	3.19	1.00
Vapour	c			2	4	2.00	
permeability	g			20	40	20.00	
	dt			30	50	35.00	
Glass			Maximise	36.10	54.30	56.25	1.00
transition	c			2	4	4.00	
	g			20	40	25.00	
	dt			30	50	50.00	
Melting			Maximise	182.00	220.00	213.63	1.00
temperature	c			2	4	2.00	
	g			20	40	40.00	
	dt			30	50	50.00	
Tensile			Maximise	1.80	41.05	48.44	1.00
strength	c			2	4	4.00	
	g			20	40	25.00	
	dt			30	50	50.00	
Elongation			Maximise	2.38	200	187.27	0.95
at break	c			2	4	2.00	
	g			20	40	40.00	
	dt			30	50	40.000	
Elastic			Maximise	0.10	14.20	15.95	1.00
modulus	c			2	4	4.00	
	g			20	40	25.00	
	dt			30	50	50.00	
Puncture			Maximise	1.54	74.07	81.02	1.00
resistance	c			2	4	4.00	
	g			20	40	40.00	
	dt			30	50	35.00	

c, cassava derivative (% w/v); g, glycerol (% w/w); dt, drying temperature (^{0}C); PC, processing condition; FP, Film property

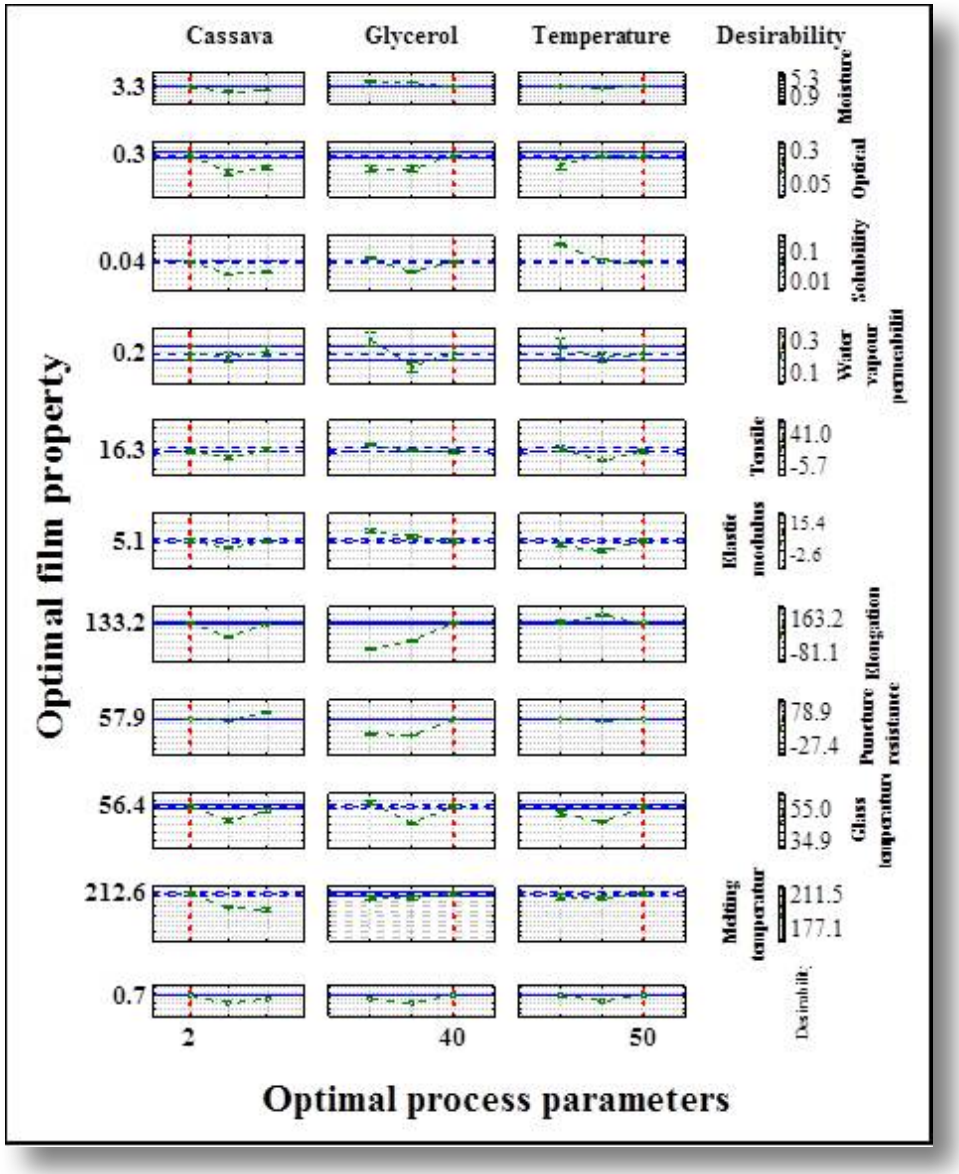


Figure 5.3. Predicted response variables and desirability values used in multiple response optimisation of process conditions and properties during development of intact bitter Cassava films.

The multiple criteria optimisation was validated by comparing values relative to an absolute optimal process (Fig 5.4) in order to check the relative deviation from the optimal and determine desired properties.

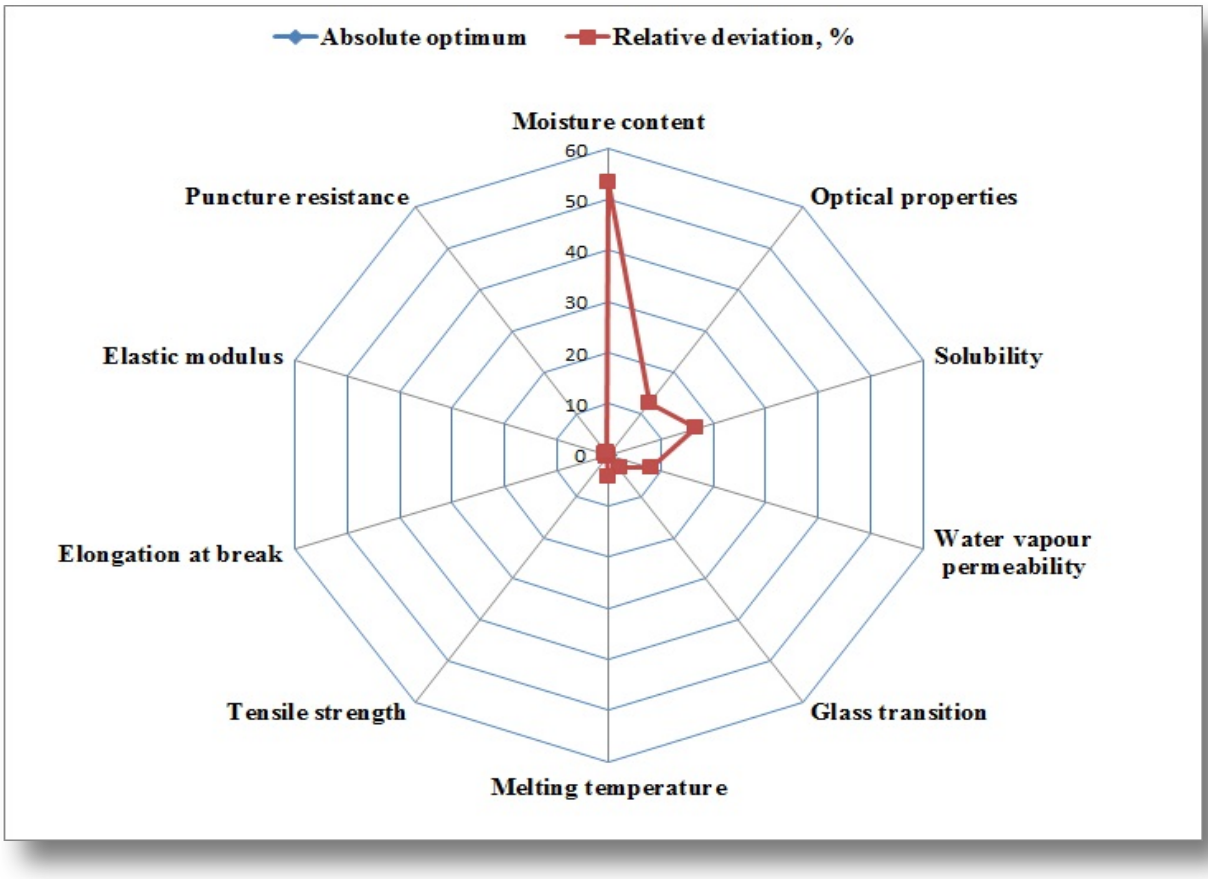


Figure 5.4. Multiple criteria optimization technique for the validation of optimal values deviating from the set absolute optimal point (♦). The relative deviation considers how a response value disperses from the theorectical optimum.

Except for moisture content (53.2 %), solubility (16.7 %) and optical properties (12.4 %), parameters had a relatively low deviation (< 10 %), indicating that the optimal values of processing parameters and conditions produced optimal properties with less effect on each other. Thus, to achieve the maximum possible match properties with low cost and maximum film functional performance, optimal parameters, within the experimental scope, were found to be: cassava powder, 2.0 %w/v; glycerol, 40.0 %w/w; drying temperature, 50.0°C; moisture content, 0.3 %; transparency, 3.4 %; solubility, 21.8 % ; water vapour permeability, 4.2 $gmm.m^{-2}.day^{-1}kPa^{-1}$; glass transition, 56°C; melting temperature, 212.6°C; tensile strength, 16.3 MPa; elongation at break, 133.3 %; elastic modulus, 5.1 MPa and puncture resistance, 57.9 J. Suffice to mention that individual optimal properties (Table 5.3) are slightly different from those obtained with a global optimal formulation, possibly due to the need to match all properties to a single formulation of processing conditions. Therefore, it can be possible to

use individual or a combination of optimal parameters to produce films. Nonetheless, with demand of robust design procedures at low cost production, the global procedure would suffice.

To validate the simultaneous optimisation design, a comparison between the experimental and predicted responses was determined after a confirmatory controlled step was performed with all parameters at optimal conditions. Table 5.4 presents analogous divergence (ϱ), delineated as the percentage of the differences between experimental and predicted values for individual properties.

Table 5.4. Validation of the effectiveness and adequacy of the optimization process for development of intact Cassava films.

Response property	**Observed (optimal) value***	**Predicted value**	**Difference (ϱ), %**
Moisture Content, %	0.19	0.45	58 (↓)
Optical, %	3.43	5.29	34 (↓)
Solubility, %	15.52	30.54	50 (↓)
Water Vapour Permeability, gmm/(m^2.day.kPa)	3.19	4.50	29 (↓)
Glass Transition Temp, °C	56.23	44.05	22
Melting Temp, °C	213.63	193.57	9
Tensile Strength, MPa	48.44	3.71	92
Elongation at break, %	187.03	181.33	3
Elastic Modulus, MPa	15.95	0.11	99
Puncture Resistance, J	81.02	25.57	68

* Values achieved with optimal processing conditions: Cassava derivative, 2 % w/v; glycerol, 40 % w/w; drying temperature, 30^0C;

↓, relative deviations tending to minimum (computed following the object of minimising the parameter to obtain the desired values.

With ϱ > 0 and GD of 0.7, it implies that the optimisation process was ideal and represented the best association between the processing conditions and film properties over the scope of

the parameters studied. In addition, calculated coefficient of determination (R^2), 0.996 and mean relative percent deviation modulus ($\dot{P}$) > 50% further confirm the adequacy of optimisation. Since, in practice, fitted properties' values were used instead of observed values in desirability optimisation, a $\dot{P}$ of 56 % implied that better (above/set criteria) values were achieved experimentally which, correspond to better quality films.

Conclusion

Packaging films with desirable properties were produced from intact bitter cassava, demonstrating the potential of this novel sustainable material to reduce cassava borne environmental waste, and develop biodegradable materials for food packaging applications.
Desirable film properties were produced using optimised processing conditions, i.e., 2 %w/v cassava derivative, 40.0 %w/w glycerol, and 50°C drying temperature. With these processing conditions the film properties obtained were: 0.3%; transparency, 3.4%; solubility, 21.8%; water-vapour-permeability, 4.2 $gmm.M^{-2}.day^{-1}kPa^{-1}$; glass transition, 56°C; melting temperature, 212.6°C; tensile strength, 16.3 MPa; elongation, 133.3%; elastic modulus, 5.1 MPa; puncture resistance, 57.9 J. The use of drying temperature in the range of values of the glass transition temperatures of the dried film provided significant effects to modulate the properties of the films with the processing variables. A set of empirical equations was developed relating the properties to the processing conditions for tailoring to specific packaging applications.

Chapter 6. Effective utilisation of cassava bio-wastes through integrated design process: A sustainable approach to indirect waste management

Abstract

An integrated design process, which can be applied in small-to-medium batch processing, was proposed. The process is based on the exploitation of intact (whole) cassava root, through optimisation of simultaneous release recovery cyanogenesis downstream processing for sustainable wastes minimisation and packaging material development.

An integrative seven unit process model flow was considered in the design process modelling. Using the release process models, it was possible to predict the maximum yield (45.8%) and the minimum total cyanogens (0.6 ppm) and colour difference (4.0) needed to avoid wastes and unsafe biopolymer derivatives. The design process allowed saving on the energy and water due to its ability to reuse wastewaters in the reactions and release processes. Drying rates, Scanning electron micrograph, Differential scanning calorimetry, Water vapour transmission rate and Fourier transmission infrared spectroscopy analyses have demonstrated the practical advantage of laminar flow hood air systems over oven-drying heat for integrated design process.

Thus, the integrated design process could be used as a green tool in production of cassava products with near zero environmental waste disposal.

Keywords: Cassava, process integration, optimal design, waste management, sustainability.

6. Introduction

The continued demand for waste-free environments coupled with the unregulated and high costs of proper waste management, requires customised, robust, and inexpensive solutions to ensure sustainable waste minimisation. Currently, cassava by-products are increasingly contributing to the global hazardous wastes, industrial disasters and environmental health risks (Adeola, 2011; Kolawole, 2014). The poisonous nature inherent in most bitter cassava cultivars (Tumwesigye et al., 2016) contribute to some extent to environmental health risks, and this has been exacerbated by the decline of suitable disposal sites. Previous research focus has been on minimising the environmental cassava wastes by developing them into valuable products (Ezejiofor et al., 2014; Raabe et al., 2015; Tumwesigye et al., 2016; Versino et al., 2015). However, with increasing population and small-to-medium processing (SMP) facilities of cassava, into starch and other products, for food, feed, and non-food applications, waste streams such as waste solids (WS) and wastewaters (WW) will be serious hazards. Additionally, the above interventions are unilateral processes that are not integrated leading to increase waste costs. The WS and WW are usually characterised by acidification due to the hydrolysis of total cyanogens producing hydrogen cyanide which is toxic to household animals, fisheries and other organisms (Kolawole, 2014). Furthermore, serious environmental pollution such as foul odour and pathogen-suspended solid carriers are other components of WS and WW leading to surface and underground water and soil contaminants (Ubalua, 2007). Moreover, the greater numbers of SMP units, their poor and more time-consuming processing methodologies, and limited disposal routes, override WS and WW management capacities.

The inherent traditional processing nature of SMPs does not support process integration for the minimisation of waste solids (WS) and wastewaters (WW). Some approaches have been employed to minimise environmental accumulation of cassava WS and WW. Examples of the strategies used currently include cultivar selection for minimisation of residue generation and water consumption in the industrial processes (Maieves, Oliveira, Frescura, & Amante, 2011), bagasse for bioprocessing of organic acids, ethanol, aroma (John, 2009) and root peel production of biocomposites (Versino et al., 2015). Unfortunately, the underlying high processing costs, energy and time of the above and other strategies complicates further WS and WW minimisation. These strategies do not incorporate holistic approaches

to process design, adding further constrain to sustainable WS and WW minimisation management. A sustainable cassava WS and WW minimisation solution can be approached by optimal design models of individual processes, as drivers that give best interface leverages. Examples of such leverages could be achieved by applying cassava wastes in packaging materials production using an integrated design process.

The integrated methodologies which emphasise process optimisations and consider production component synergisms and mathematical models are highly regarded as sustainable solutions for waste minimisation. The process design methods previously employed had been reported as graphical-based techniques such as water pinch' analysis and mathematical optimisation (Majozi & Gouws, 2009). While these techniques offer a striking approach for waste minimization in large scale processing systems, there is need to develop simple attractive substitute process design that address environmental WS and WW of dominant cassava SMPs from a sustainable technological point of view.

The key aim of the study was to develop and optimise an integrated design process (IDP) for effective use of cassava wastes, and development of sustainable packaging materials. Specifically, the study investigated an optimal structure of simultaneous release recovery cyanogenesis (SRRC) using individual processes and process models. The purpose was to gain insight into important individual processes and models that would facilitate SRRC integration in order to maximize WS and WW utilisation while minimising water solvent usage. It was anticipated that such models would exploit individual process interfaces, bringing in synergies and lead to sustainable processes.

The study comprised process integration applicable to small-to-medium-scale batch processing of bitter cassava that contributes in part to accumulated environmental wastes. A case study for the development of packaging films demonstrating IDP improvement and application potential was undertaken.

6.1 Experimental

6.1.1 Model development and optimisation studies

6.1.1.1 Waste derivatives yield

The objective was to develop an all-embracing optimised waste yield model and provide a foundation from which other process models could be optimised, and support integration into holistic design. Waste derivatives were processed using the root biomass of intact bitter cassava following the method described by Tumwesigye et al., (2016a) without modifications. The yield model was developed using a Box-Behnken-design by varying parameters namely buffer (0, 2, 4 % w/v), cassava waste solids (15, 23, 30 % w/w), and extraction time (4, 7, 10 minutes) based on experimental design (Table 1a). Data analysis was performed as describe in Tumwesigye et al., (2016b) using Statistica 7.1 software (StatSoft Inc., Tulsa, USA) The resulting process model was optimised with multi-response desirability model (Eqn. 6.1) (Derringer, 1980).

$$D = [d_y (Y)]^{1/n} \quad 6.1$$

where, D, over all desirability; Y, yield (%); d_y (Y), yield desirability function, n, responses (n=1); dy (Y) = 0, perfectly undesirable; d_y (Y) = 1, perfectly desirable.

Table 6.1. Box-Behnken experimental design processing parameters used in biopolymer derivatives production. Biopolymer yield (a), total cyanogens and colour (b).

(a)

Variables	**Coded levels**		
	x₁ (-1)	***x₂ (0)***	***x₃ (+1)***
Buffer (w/v %)	0	2	4
Waste derivative (w/w %)	15	23	30
Extraction time (minutes)	4	7	10

(b)

Variables	**Coded levels**		
	x₁ (-1)	***x₂ (0)***	***x₃ (+1)***
Buffer (w/v %)	0	2	4
Waste derivative (w/w %)	20	30	40
Sodium bisulphite (%)	1	2	3

6.1.1.2 Total cyanogens and colour

Total cyanogens (TC) was analysed using the kit developed by Bradbury et al., (1999), and colour estimated by the colour difference (ΔE) using CR-400 Chroma Meter, Konica Minolta Sensing Japan. The TC and ΔE models were developed using a Box-Behnken-design with buffer (0, 2, 4 % w/v), cassava waste solids (15, 23, 30 % w/w), and sodium bisulphite (1, 2, 3 %) based on experimental design (Table 6.1b). Their process models were optimised using multi-response desirability model (Eqn. 6.2) (Derringer, 1980).

$$D = [d_{TC}\,(TC) \times d_{\Delta E}\,(\Delta E)]^{1/n} \qquad 6.2$$

where, D, over all desirability; TC, total cyanogens (ppm); d_{TC} (TC), total cyanogens desirability function, ΔE, colour change; $d_{\Delta E}$ (ΔE), colour desirability function; n, responses (n=2); d_{TC} (TC) and $d_{\Delta E}$ (ΔE) = 0, perfectly undesirable; d_{TC} (TC) and $d_{\Delta E}$ (ΔE) = 1, perfectly desirable.

6.1.2 Evaluation of integrated design process

Integrated design process for cassava waste solids (WS) and wastewater (WW) minimisation and packaging film development was studied using a conceptualised process model flow depicted in Fig. 6.1.

Processes inherent within the root SRRC and those externally sourced, were defined, described, analysed and used in the design of integrated downstream processing model. The criterion for selection and analysis was based on the added value each process would contribute to utilisation of wastes and greatly facilitated WS and WW minimisation at low cost, energy and time. In particular, special attention was paid to reaction processes in the release and recovery through wastes recovery, total cyanogens reduction and colour improvement after pulping.

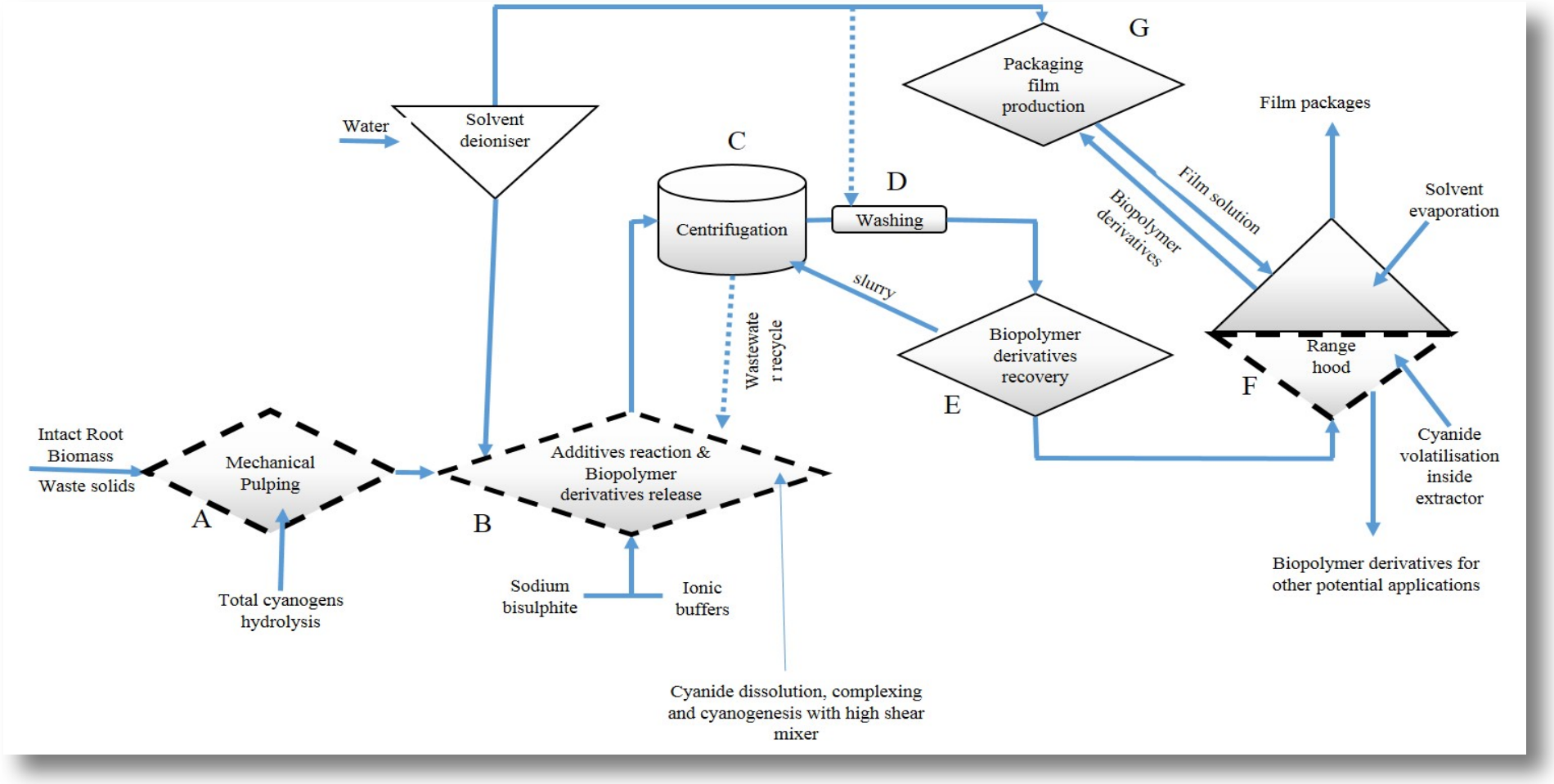


Fig. 6.1 Generalised integrated design process model. A, B, C, D, E, F, G represent unit operations.

The doted lines process units show where water, energy and implied costs were minimised

6.1.2.1 Biopolymer derivatives drying rate studies

The drying rates of the biopolymer derivatives, were performed by using either a conventional oven- drying (Memmert Universal Oven U, Model 600, Germany), or a laminar flow hood air system (Rangehood) (Kottermann High Performance Lab Hood Cupboards, UK. The loss in weight of the derivatives was measured every 30 minutes until a constant weight was reached. The air flow velocity, temperature and relative humidity (RH) of the rangehood was 0.62 m/s, at 20-22ºC, and 50-60 %RH, respectively, while those of the oven was 0.2 m/s, 25ºC and 50-60 %RH. The airflow velocity was monitored using an environmental monitor (Solomat 510e, UK). All the measurements were taken in triplicate and the drying rates comparisons were considered using the constant rate period.

6.1.2.2 Biopolymer derivatives microstructure

Biopolymer derivatives microstructure (DM) characteristics were examined using Scanning Electron Microscope (SEM), JSM-5510 **(**Joel Ltd., Tokyo, Japan). A derivatives powder sample was placed on stubs using double-sided carbon tape to form a very thin layer and leaving a space on either side of the strip to allow clear observation of surfaces and cross section. Prior to capturing SEM images, powder stubs were spluttered with a thin layer of gold. Powder stubs were subjected to a focus magnifications as high as 20 000x and images capture between 200x and 30 000x magnification and intensity of 5 kV.

6.1.3 Film formulation

Intact bitter cassava films were formulated and optimised as described by Tumwesigye et al., (2016). Biopolymer derivatives (3g) and glycerol (30%) were dissolved into deionised water to make 100% solution, mixed by magnetic stirrer (5 min) and heated to 70ºC until a clear solution was obtained. The cycle lasted 25 minutes. The solution was cast onto circular dishes (d=14 cm) and dried in a rangehood (airflow velocity, 0.62 m/s). The dried films were easily peeled off and kept for further use.

6.1.3.1 Film thermal analysis

Differential scanning calorimeter (DSC 200 F3) was performed by weighing a derivative sample (10 mg) into aluminium pan, sealing and treating it to heating-cooling cycle from 20ºC to 250ºC at 10ºC/minute. Experiments were performed in triplicate.
Thermogravimetric analysis (TG Analyser, Spectrum 500) was performed by heating a derivative sample between 30^0C and 500^0C, at 20^0C/min using nitrogen at 60 mm/min. Experiments were performed in triplicate.

6.1.3.2 Film water vapour transmission rate

Water vapour transmission rate (WVTR) was measured gravimetric using ASTM, (2005). A sample was mounted between acrylic permeation cells, containing previously dried (105ºC, 9h) 4g $CaCl_2$ (0% RH), enclosed in a humidity-controlled (95%RH) container placed in an incubator (38°C). The changes in weight of the cell were recorded every 2 hours for 10 hours and data obtained was used for WVTR calculation. Experiments were performed in triplicate.

6.1.3.3 Film chemical characterisation

Fourier transform infrared spectroscopy (FTIR) was performed by using UV/Vis spectrum one spectrometer (Perkin Elmer Lambda 35, USA). The changes in spectra intensities were measured between 4000–400 cm^{-1} at $4cm^{-1}$ resolution in the transmittance mode with 30 scans at room temperature. The averages of three samples were used plotting the spectra.

6.2 Results and discussion

6.2.1 Integrated design process description

The cassava simultaneous release recovery cyanogenesis (SRRC) downstream processing for waste solids (WS) and wastewater (WW) minimisation integrated with packaging film development comprised seven operation units (Fig. 6.1). The concept was intended to

minimise wastes by directly processing fresh intact bitter cassava root biomass and avoid underlying costs, energy, time, intended and unintended disposal efforts, of additional alternative processes for waste management. Process modelling and optimisation was intended to determine the most economic SRRC design process for sustainable use of bitter cassava into value added products and minimise wastes. Particular focus of modelling and optimisation was on early stages of the design (pulping and reactions/release) because it holds most important processes to enhance modifications and release of wastes and associated compounds.

6.2.1.1 A: Mechanical pulping

In order to attain sufficient total cyanogens hydrolysis and finer fibrous waste solids for production of good quality and non-toxic pulp, an efficient mechanical pulping was required. This was achieved by ensuring that the pulping efficiency of ≥ 90% was applied in pulping process using time-dependent model (Eqn. 6.3).

$$\text{Pulping time, s} = 36144.36 + 33.11\text{v} - 845.74\eta_g - 0.39v\eta_g + 0.01v^2 + 4.97\eta_g^2 \quad (R^2 = 0.95) \qquad 6.3$$

where, v, pulper drum velocity; and η_g, pulping efficiency.

In pulping process, the breakdown of cells activates hydrogen cyanide release from cyanoglucoside linamarin, a precursor of cyanide related compounds (Fig. 6.2a).

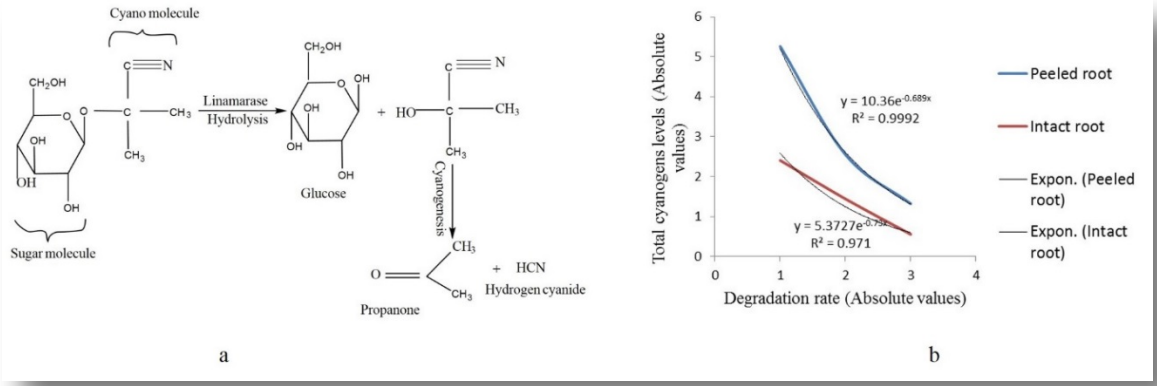


Fig. 6.2 Total cyanogen behaviour during pulping stage. Hydrolytic pathway (a) and comparison of degradation rate between intact and peeled cassava root (b).

The hydrolysis of linamarin into cyanohydrins and hydrogen under the influence of linamarase enzyme (Fig 6.2a) has been widely reported as important factor in cyanogenesis process (Cereda & Mattos, 1996; Crowe & Bradshaw, 2014). Cyanogenesis (loss of total cyanogens) was examined between intact and peeled during pulping process, and was found to vary greatly when pulping efficiency was increased. As shown (Fig. 6.2b), intact roots demonstrated higher total cyanogens loss than the peeled roots, further confirming the intrinsic hydrolysis by the intact root as previously reported (Tumwesigye et al., 2016).

6.2.1.2 B: Reaction and release

The goal of the reaction and release was to improve extraction and yield of biopolymer derivatives. Addition of ionic buffers (sodium chloride and dilute sulphuric acid) helped to release the biopolymers. Nearly all the root biomass was converted into the derivatives when the model and optimised yield was applied in the extraction (Eqn. 6.4, Table 6.2, Fig. 6.3).

$$Yield, \% = 27.55 + 21.81b + 1.21w - 2.27t - 1.10bw - 0.62bt + 0.16wt$$
$$-4.95b^2 - 0.06w^2 - 0.11t^2 + 0.017bw^2 + 0.13b^2w + 3.59b^2t \quad (R^2 = 0.91) \qquad 6.4$$

Table 6.2. Global desirability analysis of yield showing optimal results as influenced by optimal processing conditions

Parameters	Experiment Levels			Optimal derived parameter values	Properties		
					Yield, %		Desirability
					Optimum	Range	
Buffer, % v/v	0.0	2.0	4.0	4.0	45.8	15.0 – 55.0	1.0
Waste, % w/w	15.0	23.0	30.0	30.0			
Extraction time, minutes	4.0	7.0	10.0	10.0			

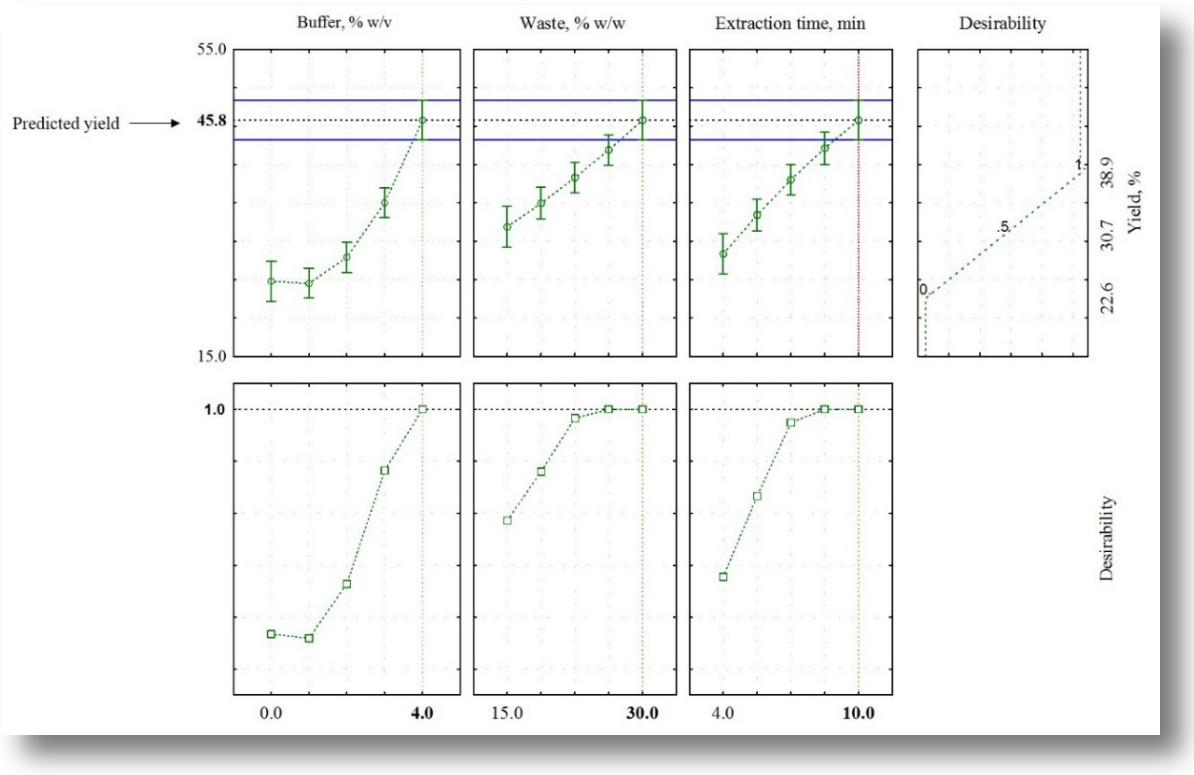
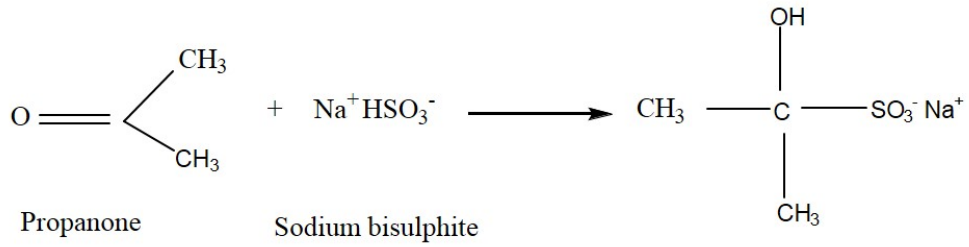


Fig. 6.3 Global desirability analysis of yield

Furthermore, the purification of biopolymers from impurities of special interest, total cyanogens (TC) and colour, were accomplished by reaction additives. Reactions between TC

(from the pulping stage) and sodium salts of bisulphite and chloride further ensured that more derivatives were freed from total cyanogens, as shown by the reaction Eqns. 6.5 and 6.6. Another important impurity of concern is the colour, which is the liberated colour of peel biomass after derivative extraction. This was handled by employing food grade sodium bisulphite (SB), in addition to ionic buffers, which has been widely used to bleach coloured products such as paper pulp (Guo, Zhou, & Lv, 2013) and food. The SB, under acidic conditions, acts as a reducing agent and in the process is oxidised (Eqn. 6.3) (Guo et al., 2013).

Bisulphite (HSO_3^-) → HSO_4^- 6.5



6.6

In order to improve the release and reaction, TC and colour were modelled and optimised as shown (Eqns. 6.7 & 6.8, Table 6.3, Fig. 6.4. The individual and global desirability showed that the solution for TC and colour reduction in biopolymers could be feasible by obtaining 0.6 ppm and 4.0 when applying buffer (4.0 % v/v), waste solids (18.8 % w/w) and sodium bisulphite (3.0 %) respectively at the release stage.

$$Total\ cyanogens, ppm = -9.65 - 0.65b + 1.59w - 0.52sb - 0.50bw + 1.07bsb - 0.03wsb + 0.93b^2 - 0.03w^2 + 0.04sb^2 + 0.01bw^2 + 0.05b^2w - 0.28b^2sb \quad (R^2 = 0.96) \qquad 6.7$$

$$Colour\ change, \Delta E = 10.08 - 0.26b + 3.31w - 0.07sb - 0.02bw + 1.00bsb - 0.00wsb + 0.71b^2 - 0.01w^2 + 0.24sb^2 + 0.00bw^2 + 0.02b^2w - 0.02b^2sb \quad (R^2 = 0.96) \qquad 6.8$$

Table 6.3. Global desirability analysis of total cyanogens and showing optimal results as influenced by optimal processing conditions

Parameter	Experimental Level			Optimal derived parameter value	Properties					
					Total cyanogens, TC		D	Colour difference, ΔE		D
					Optimum	Range		Optimum	Range	
Buffer, % v/v	0	2	4	4.0 (TC) 4.0 (ΔE)						
Waste, % w/w	15	23	30	18.8 (TC) 22.5 (ΔE)	2.0	-0.5-3.5	0.8	0.24	0.12-0.3	1.0
Sodium bisulphite, % w/w	1	2	3	3.0 (TC) 3.0 (ΔE)						

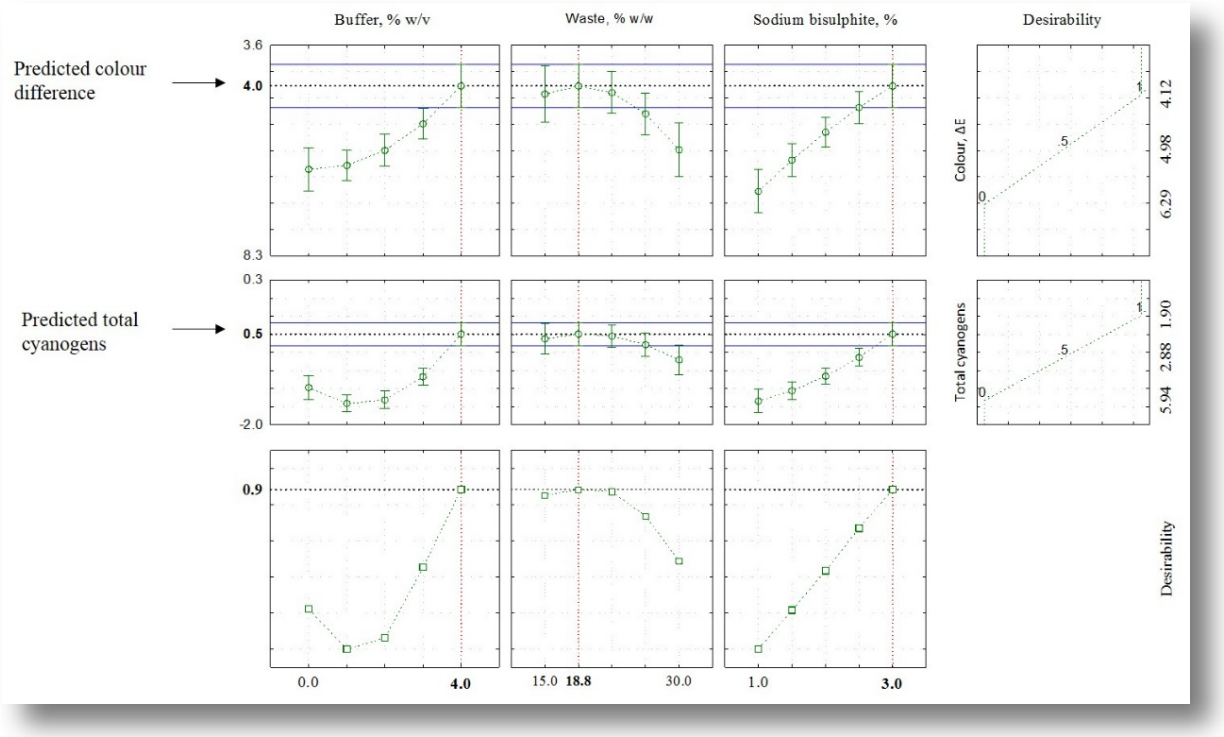


Fig. 6.4 Global desirability analysis of total cyanogens and colour difference

6.2.1.3 C &D: Centrifugation and washing

Centrifugation and washing design stages were aimed at refining the biopolymer derivatives, separation of wastewater (WW) and dilutions of hydrogen cyanide and bisulphite compounds. For the purpose of saving energy on deionising water and maximize resource utilisation, WW was recycled between centrifugation, washing and release stages. The WW was concurrently used to further aid the reaction stage and refine the biopolymers. This is because WW still contained bisulphites and ionic salts, which were sent back to reaction and release stage as a reaction solution for efficient TC and colour removal. Frequent washing and filtration eliminated a bigger proportion of cyanide-bisulphite complexes since the latter ionise in water to form soluble complexes.

In order to quantify the volume of solvent recycled in release-centrifugation-washing-recovery cycle, the supernatant retained after the slurry was separated and measured. Cumulative volumes were measured from the frequency of the cycle. The supernatant-rich dissolved ions of cyanide and bisulphite reused at every cycle is shown in Table 6.4.

Table 6.4. Water involved in release-recovery cycle during processing of biopolymer derivative production

Release-Recovery cycle	Volume of water/100 g pulp, ml	Supernatant reuse, ml	Solvent recovery, %
1	100	85.5 (85-90)	87.5
2	100	90.0 (88-92)	90.0
3	100	92.5 (91-94)	92.5

As shown in Table 4, the volume of solvent required included 100, 12.5 (range 10-15) and 7.5 (range 6-9) ml for initial, second and third cycle, respectively. Therefore, the integrated reuse would save about 60 % of extraction solvent by the fourth cycle, in comparison to the traditional process.

6.2.1.4 E and F: Recovery

The recovery stage was aimed at eliminating the solvent-rich residues of remaining cyanide and bisulphite in a safe and economic way using a rangehood. Similarly, film solvent was evaporated using the rangehood. This was done in order to avoid energy costs of using a separate drying method. The disposal pathway gave optimal results by consuming wastes from derivative processes and film production with zero direct emission of wastes into the environment. To minimise the energy costs associated with conventional heat drying of the biopolymers during the recovery stage, a comparative study using laminar flow hood air system and oven-heating was conducted. The comparative results between oven-drying rates and microstructural characteristics and those of laminar flow hood air system are presented in Fig 6.5.

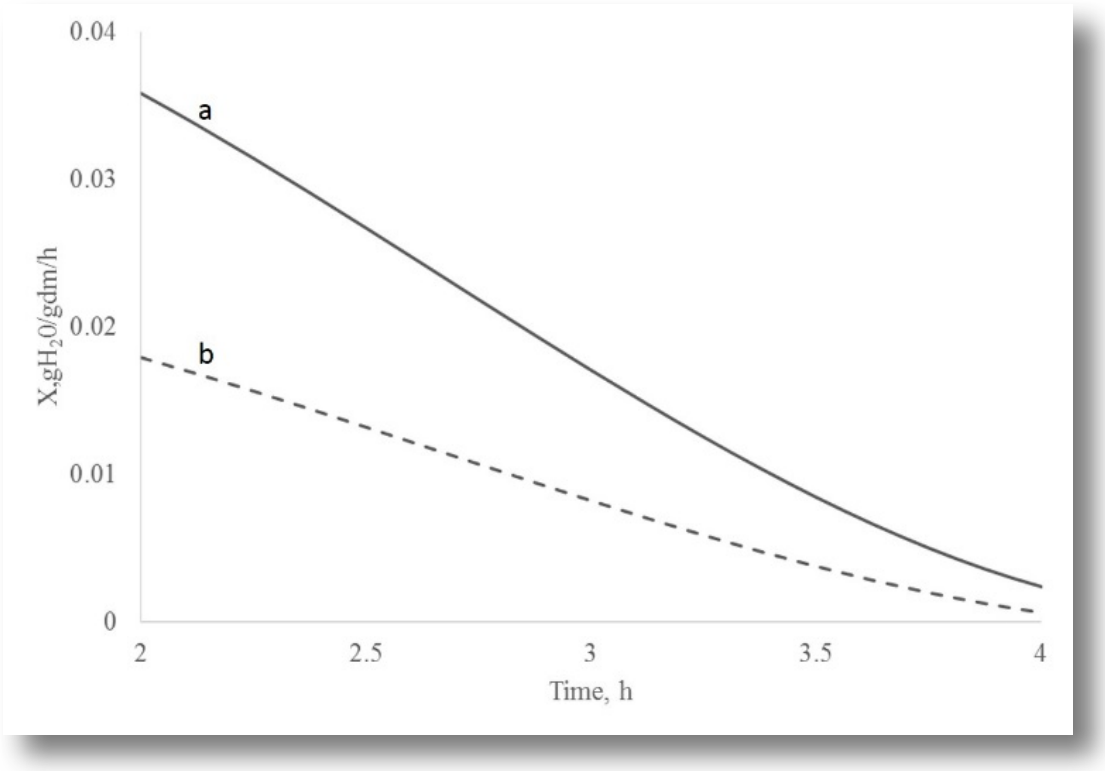


Fig. 6.5. Drying rate curves of biopolymer derivatives associated with rangehood (a) and oven-drying (b).

Fig 6.5 shows the differences in drying rates exhibited by the two drying systems, but with similar linear decreasing curves. However, the drying rate of rangehood (curve a) is slightly faster than of oven-drying (curve b). Thus, the slightly faster drying rate of the rangehood could be an option in low-cost design processes.

The scanning electron micrographs (SEM) wastes derivatives (WD) are illustrated in Fig. 6.6, showing a more compact structure for a rangehood dried WD (a) and heterogeneous loose structure for oven-dried WD (b). These results imply that drying in the rangehood did not cause much alteration in the structure in contrast to the oven-drying impact, which could suggest that less physico-chemical changes occurred in the rangehood dried WD. Thus, the rangehood could be integrated in the WD design production process as a potential tool for green waste disposal.

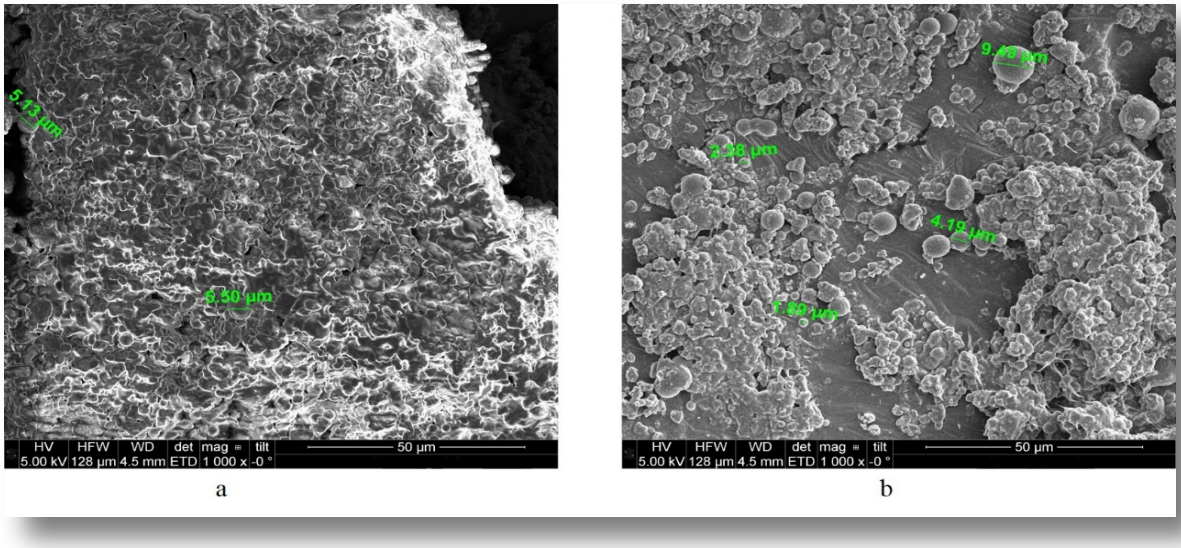


Fig. 6.6 SEM microstructural characteristics of biopolymer derivatives dried using rangehood (a) and oven-drying (b).

6.2.2 G: Film package development

The purpose of integrating package development into the design was to exploit available waste derivatives, the same solvent source and a rangehood drying process. In this way, wastes to the environment are minimised and energy for solvent purification and materials

drying are minimised. As a result of successful production of derivatives, flexible and transparent films with potential packaging applications were produced. The prototype films developed from the wastes and dried with the rangehood are shown in Fig. 6.7.



Fig. 6.7 Film prototypes dried using a rangehood, as a roll (a) and bag (b).

The thermal performance of the films shown by the comparisons between rangehood and oven-drying conditions is shown in Fig. 6.8. The thermal degradation of rangehood (a) was slightly lower than for oven-drying (b), which suggested the slow loss of volatiles. However, the degradation equalled later for both treatments. Similar behavioural patterns were observed with differential scanning calorimetric (DSC) thermograms of a and b but with lower melting temperature and sharper peak in a than b. As can be seen from the inset table, the melting (Tm) and glass transitional (Tg) temperatures were in the same range, in contrast to the lower crystallinity (C) of the rangehood. The high C in films dried by ovens could be due to heating that disrupted the microstructure (Denry, Holloway, & Gupta, 2012).

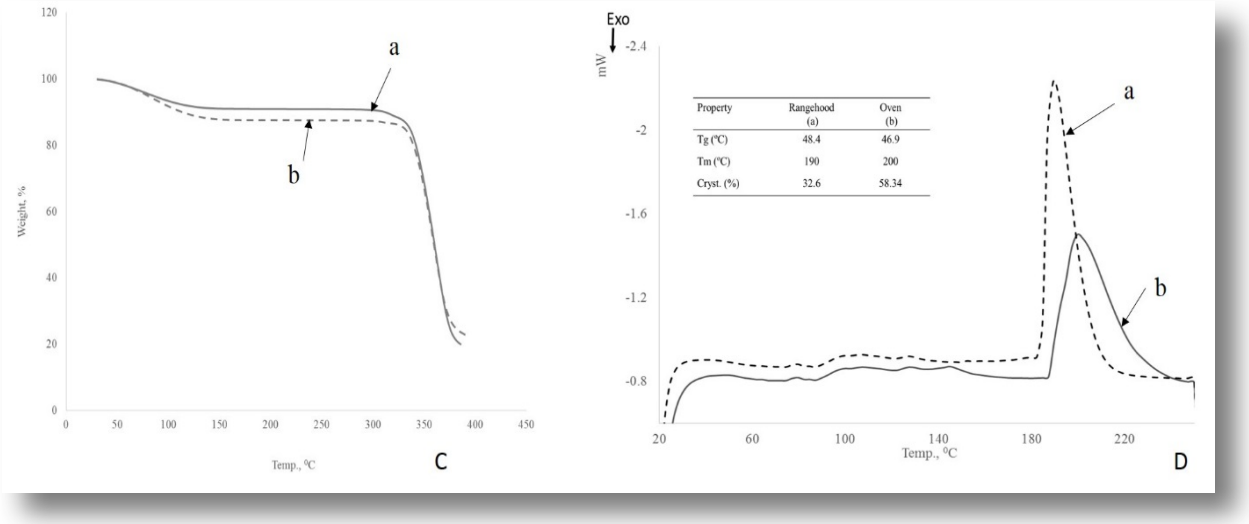


Fig. 6.8 TGA degradation (C) and DSC thermograms (D) of rangehood (a) and heat oven (b) dried films

The water vapour transmission rate (WVTR) is an important parameter for package performance and could be used to compare technologies. The film WVTR using the rangehood (707.4 g/m² day) was slightly higher than for oven-drying (685.7 g/m² day). The results show that non-heat drying process can be integrated with heat dryers to reduce energy. This could be due to a weak surface resistance of films at higher airflow velocity. Conversely, the observed value in oven dry films could be related to saturated vapour pressure of water at lower velocity.

Physical and chemical changes can be affected by many production processes including drying. Fourier transform infra-red (FTIR) spectroscopy was aimed at understanding the possible structural and physico-chemical alteration differences among the rangehood and oven-dried films. As shown in Fig. 6.9, the rangehood (a) and oven-dried (b) films spectra were similar, suggesting that the two drying methods did not post any differences in films chemical composition (Tumwesigye et al., 2016). These findings give light on the improvement of the rangehood, through optimisation of the conditions, as an alternative for integration in the design process.

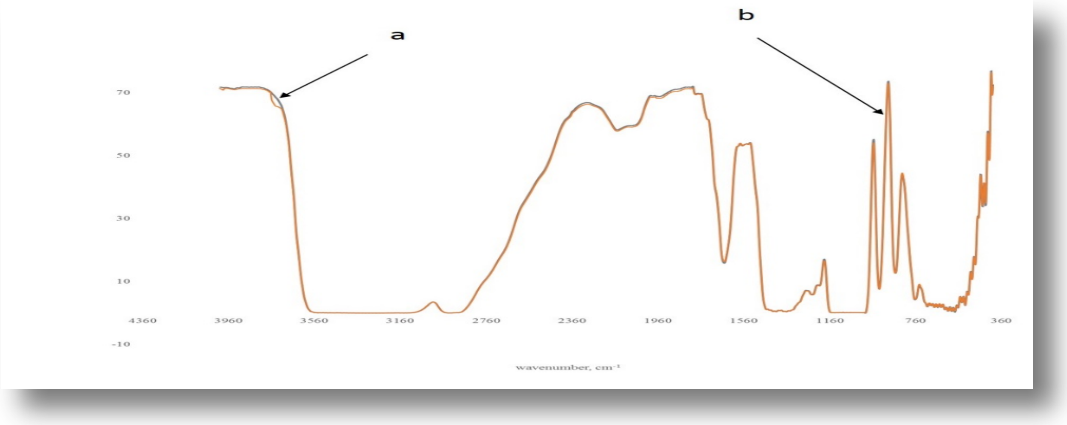


Fig. 6.9 FTIR spectra of rangehood (a) and heat oven (b) dried films

Conclusion

This work proposed a new sustainable approach for potential utilisation of cassava waste and reduction of their environment impact using an integrated seven unit process design. The design approach is founded on the exploitation of: (i) intact (whole) cassava root; and (ii) optimised SRRC as an effective way to avoid environmental wastes accumulation, and also to reduce the energy and costs of designing additional processes for starch production, waste management and package production.

The optimised model results showed that using intact root and SRRC in biopolymer derivatives production, could be an effective tool for green cassava production processes. If ionic buffer (4% w/v), wastes (30/w/v), and extraction time (10 minutes) is applied in the process, the optimum yield could reach 45.8 % which approximates the weight of the intact root. Furthermore, the integrated design process has the advantage of saving on the energy of water deionisation/distillation due its ability to reuse wastewaters in the reactions and release processes. The analyses of drying rates and SEM for derivatives, and DSC, WVTR and FTIR for films have shown that it could be possible to substitute oven-drying with laminar flow hood air systems in the integrated design process.

Thus, the integrated design process could be used as a green tool in production of cassava products with near zero environmental waste disposal.

SECTION 3

Chapter 7. Evaluation of Suitability of Novel Bitter Cassava Films for Equilibrium Modified Atmosphere Packaging of Tomatoes

Abstract

Equilibrium modified atmosphere packaging (EMAP) of fresh produce relies on modification of atmosphere inside the package, achieved by the natural interplay between product respiration and transfer of gases through the package. While designing an EMAP system is important to consider product respiration rate, packaging permeability, supply chain (temperature and relative humidity, RH), and potential need for perforations to achieve the recommended product-specific gas composition. EMAP films are usually non-bio-based (oriented polypropylene, OPP), but interest has been shown in sustainable bio-based materials. A novel packaging material film was recently developed from intact bitter cassava (IBC) and preliminary trials showed potential for EMAP of tomatoes. The objectives of this work were to i) assess effect of EMAP design parameters on gas composition for cherry tomatoes, and ii) compare performance of bio-based IBCF with non-bio-based film (OPP) for EMAP. Cherry tomatoes (125g) were packed considering an experimental design with 4 factors and 2 levels (bio-based, non-bio-based films; 0, 1 perforation; 10, 20°C; 75, 95 % RH). Package oxygen composition was analysed in duplicate using a non-invasive optical oxygen sensor until the equilibrium was reached.

The results show that intact bitter cassava film (IBCF) in-package O_2 composition reached an equilibrium at 2 % and 3 %, after 180 h (over 7 days) at 10°C, with 0 or 1 perforation, for 75% and 95% RH respectively. This ensured that the mould growth on cherry tomato surface was inhibited until 15-19 days of storage at 10^0C. The similarities in the equilibrium O_2 composition of 2% between perforated and non-perforated suggest that there would not be need to perforate IBCF. Besides, there is need to establish the possible structural changes likely to occur in IBCF at high RH. Factorial analysis on package performance showed that film type, perforations, temperature, relative humidity, and their interaction had varying significant ($p \leq 0.05$) effects on O_2 composition. Temperature and RH influenced IBCF significantly, whereas perforations, temperature and their interaction impacted on OPP significantly. Desirable O_2 composition of 3.73 % for IBCF EMAP of cherry tomatoes was achieved with optimised design parameters, 13.8°C, 82 % RH, 0.135 mm, while one of OPP

(8.6 %) did not fall within the recommended 2-5 % O_2 composition; hence, IBCF can be an alternative film for EMAP.

Demonstration of the potential application of IBC film for EMAP was shown. However, further studies on the impact of external environments on EMAP of IBC film, in view of tailored application, are necessary.

Keywords: Bitter cassava, Modified atmosphere, Oxygen, Relative humidity, Temperature, Cherry tomato

7.1 Introduction

Increased consumers' interest and demand for more natural and minimally-processed fresh fruits and vegetables has increased in the last 20 years. Consumer's lifestyles towards convenience, nutritious and ready-to-use fruits, and the awareness of disease-reducing capacity of quality fruits and vegetables, have led into innovative technologies in food processing. Modified atmosphere packaging (MAP) is a widely-demonstrated technology, which is increasingly used for the preservation of natural quality of fruits and vegetables in addition to extending the storage life (Horev et al., 2012). MAP storage is one of the most successful preservation techniques suitable for wide varieties of agricultural and food products. In particular, there is increased awareness of value chain actors on advantages of MAP due to stringent regulations on the use of chemical preservation methods.

The equilibrium atmosphere packaging (EMAP) concept for fresh produce is all about adaptation of the in-package atmosphere, realised by the natural interplay between the product respiration and the mass transfer of gases and water vapour through the packaging material. The modification results into in-package environment superior in CO_2 and inferior in O_2, with the objective of extending the shelf life of perishable food and concurrently maintaining the product integrity. EMAP can be used to preserve the quality of tomatoes by reducing the respiratory rate, inhibiting the colour changes and the growth of microbial populations that lead to rotting. It is widely established that the oxygen concentration reduction results in a decrease of respiration rate causing a slowdown of various biochemical processes and reduction in tomato quality degeneration.

For EMAP of tomatoes, mostly commercial non-biodegradable films, applying perforations (micro and macro), with some change in package gas composition (O_2 and CO_2), are among popular technical solutions. However, the environmental issues of non-biodegradable films, effect of highly variable supply chain conditions (humidity, temperature) on in-package gas composition, have inevitable consequences in tomato EMAP quality. Although, in vitro EMAP experiments to modulate in-package gas composition have shown promise, non-biodegradability of film packages, anomalies in perforations and absence of in situ evaluations to take care of supply chain conditions, would limit their applications in tomato

packaging intended to extend their shelf life. Besides, these approaches have not provided satisfactory responses to the challenges of EMAP of tomato. Currently, there is no universal agreement on desirable EMAP of tomatoes, and this can impact significantly on tomato supply chain.

Tomato storage, trade and consumption are repeatedly challenged by fungal rot contamination, prompted by a plethora of factors; the major ones include poor handling and suitable conditions for microbial growth such as in-package oxygen, temperature and moisture. Tomato decay can be caused by many fungal organisms (yeasts or moulds), and fungal elimination has been always difficult to control than their counterpart bacterial due to their much larger cells and environmentally-resilient high spore numbers (Bartz, Sargent, & Scott, 2012). Substantial devotion has been put in tomato fungal rot control measures using various approaches (Chapin, Wang, Lutton, & Gardener, 2006; Gil, Selma, López-Gálvez, & Allende, 2009; Matthews, Sapers, & Gerba, 2014). Among the approaches, the most commonly used packaging films for fresh tomatoes are based on non-biodegradable materials such as polyethylene terephthalate (PET), polyvinylchloride (PVC), polyethylene (PE), orientated polypropylene (OPP) and polystyrene (PS). While these are readily available with good physico-chemical properties (Siracusa, Rocculi, Romani, & Rosa, 2008), their non-biodegradability can lead to adverse effects on the environment, and thus triggering risk to human health or ecosystems (Mahalik & Nambiar, 2010). Recently, there have been increased efforts to use natural and renewable biobased sources such as starch, cellulose, polylactic acid (PLA) and polyhydroxyalkanoate (PHA) for food packaging purposes. However, they have not yet found wide use in food packaging application perhaps due to the high development costs, low performance and difficult processing (Mensitieri *et al.*, 2011). Thus, sourcing for an inexpensive dependable alternative biobased material for EMAP is crucial.

Intact bitter cassava (IBC) flexible films are fully biodegradable and their potential for food packaging (Tumwesigye, Oliveira, & Sousa-Gallagher, 2016) can provide promising alternatives for EMAP. The non-competitive bitter cassava bioresource and the possibility of producing it in one step by using simultaneous release recovery cyanogenesis makes it particularly suitable for industrial scale up and development of EMAP at cheaper cost. Owing to their sensitivity to moisture, IBC film evaluations for package performance across

conditions under the supply chain is vital. Thus, an understanding of the environmental impact on, and performance of, IBC films in EMAP of tomatoes is fundamental to their recommended use in packaging of fresh produce. IBC can be of great value to minimize the cost of package development and improve package performance, enhance storage efficiency and extend the shelf-life of tomatoes, and provide sustainable convenience in EMAP development. The objective of this study was to assess effect of EMAP design parameters on gas composition for cherry tomatoes, and ii) compare performance of bio-based IBC film with non-bio-based oriented polypropylene (OPP) film for EMAP. The results would help in determining the IBC film performance and design EMAP for fresh produce.

7.2 Methodology

7.2.1 Material preparation

Flexible packaging films for EMAP designs were prepared from intact bitter cassava (IBC) derivatives as described in Tumwesigye et al., (2016) without further modifications. Prior to in-package oxygen evaluations, the films were conditioned at 54 %RH, for 48 h, at 23±2°C, followed by equilibration conditions of 75 or 95 % RH, at 10 or 20°C, for 48 h. The equilibrated films were used within 2 days. A commercial reference packaging film, oriented polypropylene (OPP) (Infania Group GmbH, Germany) was also prepared together with IBCF and used for comparison.

Freshly-delivered cherry tomatoes (*Solanum lycopersicum*) were purchased from a local supermarket (Tesco, Cork, Ireland), cleaned of any dirt with distilled water, dried on clean adsorbent papers, and kept under refrigeration (4 - 7°C) until further use. To ensure that the qualitative analysis yielded convincing results, red tomatoes with smooth, shiny and reasonably hard skin, with no visible mould (Fig 7.4) were sampled for the study.

7.2.2 Experimental set up and package performance analysis

EMAP performance of IBC film was evaluated and compared to OPP film based on the experimental design (Table 7.1). The parameters and conditions were chosen based on the average recommended temperature (10°C), for handling of tomatoes, and abuse conditions (20°C) encountered in the supply chain. It is widely accepted that package behaviour and

performance of any packaging material are by far influenced by the environmental conditions (temperature and relative humidity) and the in-packaged product characteristics. Thus, further to the quantitative measurement, a qualitative parameter (mould growth) was factored in the performance evaluation.

Table 7.1. Equilibrium Modified Atmosphere Packaging (EMAP) design evaluation parameters

Factor	**Level**	
	x_1	x_2
Packaging film	OPP	IBC
Perforation	0	1
Temperature (°C)	10	20
Relative humidity (% RH)	75	95

7.2.3 In-package oxygen composition

Cherry tomatoes (125 g) were placed into polypropylene trays (11.1 cm x 15.5 cm x 3.4 cm), a film (IBC or OPP), with a thickness of 0.03 ± 0.002 mm and breathable area of 0.013 m², laid on top and hermetically sealed. For a film requiring perforation, a needle of diameter 0.27 mm was used to pierce the film perpendicularly, careful enough not to impart unnecessary tear to the micro pore. It was assumed that the pore area corresponded to that of the needle. Both perforated and unperforated films were stored in relative humidity controlled boxes (75 and 95%) and in temperature incubators (10°C and 20°C) for 15-19 days. The required RH was achieved by using pre-determined quantity of water and glycerol as per Forney and Brandl (1992).

Changes in package oxygen composition were measured directly by placing the optical fibre cable on the headspace side, containing the sensor, (PreSens Precision Sensing, Germany). The measurements were performed in duplicate packages, and the means used in computing headspace oxygen composition at regular intervals. When equilibrium was reached O_2 and CO_2 measurement was determined using PBI Dansensor, Check-mate 9900 Rønnedevej 18).

7.2.4 Analysis of experimental data

A full factorial analysis of variance was used to determine the significant ($p < 0.05$) impact of 4 factors at 2 levels on the headspace oxygen amounts. A Statistica software (release 7, Statsoft, USA) was used to fit polynomial models to O_2 and effect of estimates necessary for evaluating the closeness of the experimental data to fit values.

7.3 Results and discussion

7.3.1 Influence of EMAP design parameters on gas composition for cherry tomatoes

An example of the effect of design parameters (Table 7.1) on the dynamics of headspace oxygen composition for cherry tomatoes stored using IBC film is shown in Fig 7.1. The O_2 concentration of cherry tomato in-package gas composition reached equilibrium at 2 % and 3 %, after 180 h (over 7 days) at 10°C, with 0 and 1 perforation, for 75 % and 95 %RH respectively. Thereafter, the O_2 concentration remained stable for the rest of the test period, suggesting that equilibrium was attained.

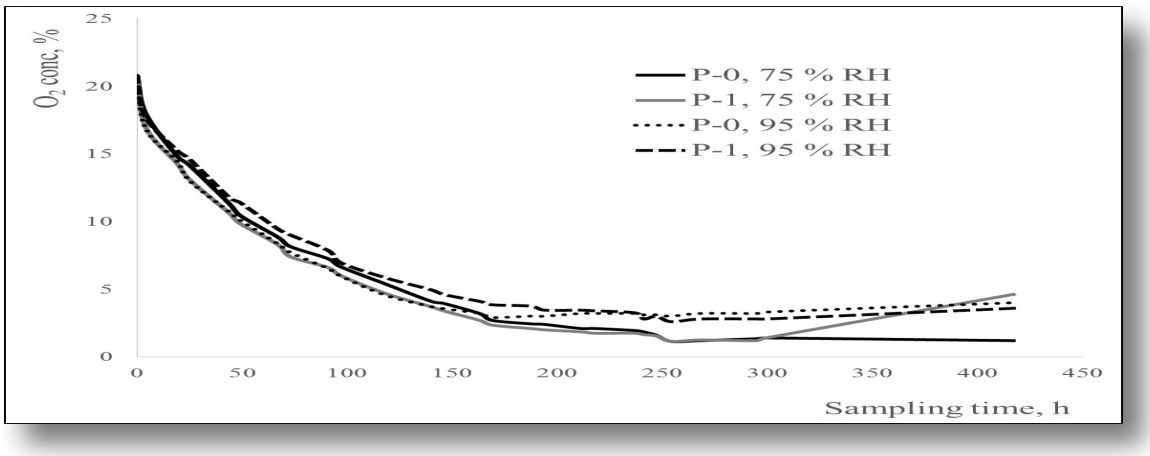
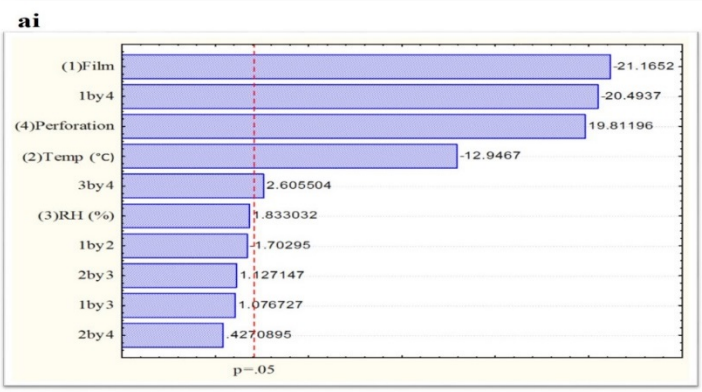


Fig 7.1. Evolution of the dynamics of in-package headspace oxygen concentration of stored cherry tomato using intact bitter Cassava (IBC) film, at 10°C, with 0 and 1 perforations at 75 or 95 % Relative humidity (RH).

These results imply that there would not be the requisite for perforating the IBC film since a minimum of 2 % O_2 concentration in respiring tomato packages is acceptable. However, due to the relative humidity and temperature dependence of product respiration, and O_2 permeability of IBC packaging films, this could enhance significant fluctuations of the O_2 concentration of EMA in-packaged fresh tomato. Thus, to gain insight into the influence of the impact of individual or combined EMAP design parameters on headspace O_2 behaviour, this was further analysed, and the results are presented in Fig. 7.2.

ai

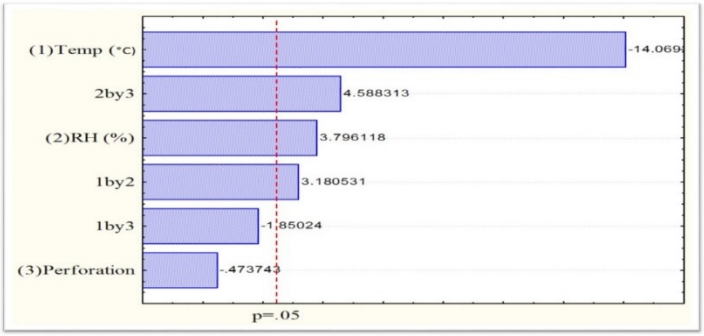


aii

Parameter	Coefficient (SE)
Mean/Intercept	**.933** (0.124)**
Film	**-2.624** (0.124)**
Temperature (T)	**-1.605** (0.124)**
Relative humidity (RH)	0.227 (0.124)
Perforation (P)	**2.338** (0.118)**
F x T	0.211 (0.124)
F x RH	0.133 (0.124)
F x P	**-2.418** (0.118)**
T x RH	0.140 (0.124)
T x P	0.050 (0.118)
RH x P	**0.307** (0.118)*
R^2	0.989

Significant: *, p < 0.05; **, p < 0.01

bi



bii

Parameter	Coefficient (SE)
Mean/Intercept	**3.411** (0.122)**
Temperature (T)	**-1.714** (0.122)**
Relative humidity (RH)	**0.463** (0.122)**
Perforation (P)	0.052 (0.109)
T x RH	**0.389** (0.122)*
T x P	-0.202 (0.109)
RH x P	**0.500** (0.109)**
R^2	0.990

Significant: *, p < 0.05; **, p < 0.01

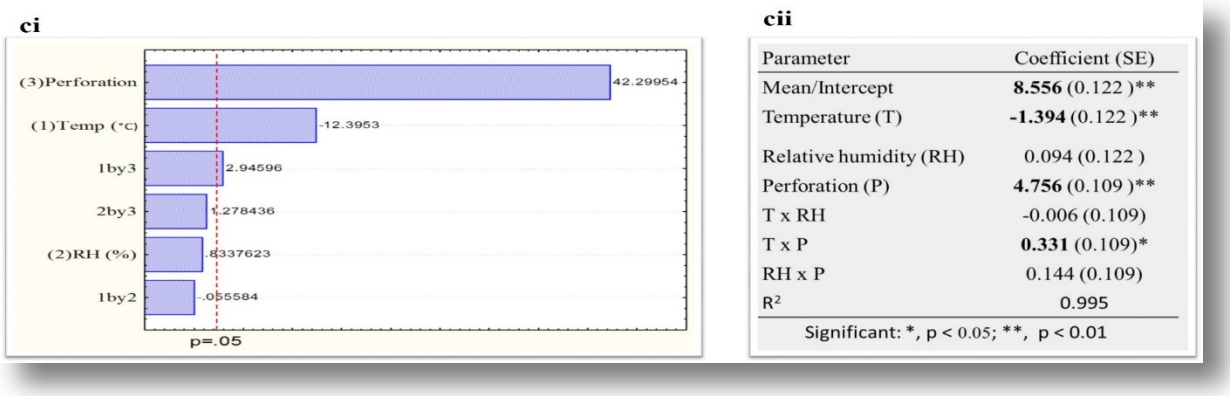


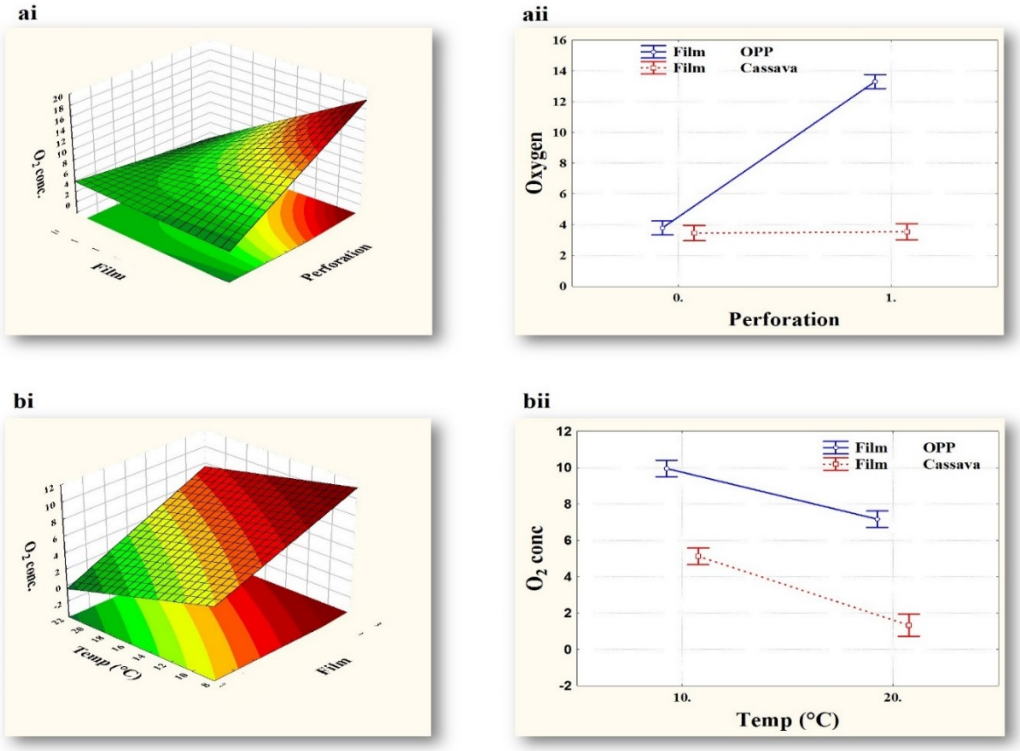
Fig 7.2. Individual or combined influence of EMAP design parameters on equilibrium headspace O_2 concentration, as shown by Pareto analysis of ai) combined IBCF and OPP; bi) IBCF, ci) OPP; and ANOVA of aii) combined IBCF and OPP; bii) IBCF; and cii) OPP.

Pareto analysis showed that individual and combined EMAP design parameters had influence on equilibrium headspace O_2 concentration (Fig. 7.2). The type of film, film-perforation interaction and temperature had highly significant ($p < 0.01$) negative effects, while perforating a film caused a significant positive impact on O_2 concentration (Fig. 7.2ai). Further analysis of these results showed that the influence of the type of film and its perforation had a more pronounced influence than the effect of temperature (Fig. 7.2aii). The results seem to imply that perforating a film results in high initial headspace O_2 concentration in-package (positive value), whereas non-perforated film lead to low initial O_2 concentration (negative values).

To determine which individual film parameters had more influence, the data for IBCF and OPP were analysed separately, and the results are shown in Fig 7.2b and Fig 7.2c. It is shown that temperature had negative (Fig 7.2bi) and highly positive (Fig 7.2ci) significant ($p < 0.05$) effect on oxygen dynamics in the IBCF and OPP package respectively. Temperature and its interaction with perforation also showed less significant negative and positive effect on OPP in-package O_2 concentration. On the other hand, RH-perforation interaction, RH, and temperature-RH interaction influenced positively the IBCF in-package O_2 concentration. Taken together, the results showed that perforations caused more pronounced impact in OPP in-package (average, 8.556) (Fig 7.2cii) than did the combined influence of temperature and RH in IBCF (average, 3.411) (Fig 7.2bii) in-package headspace O_2 concentration. The results

mean that temperature provided a higher concentration gradient in-package and caused more loss of O_2 than the combined O_2-raising effects of RH-perforation, RH and temperature-RH. Perhaps, this could explain the almost same equilibrium O_2 stability of perforated and non-perforated IBCF (Fig. 7.1). Conversely, the perforated OPP tended to offset the temperature and gradient effects, thereby allowing more O_2 in-package. In other words, OPP showed a contrasting effect of providing a higher equilibrium O_2 concentration than IBCF, as shown by the positive value (Fig. 7.2cii).

Generally, when all the EMAP design parameters were compared, it was revealed that perforations had a higher influential behaviour on oxygen dynamics in the OPP in-package than when temperature and RH were considered individually or combined (Figs. 7.3a, b, c, and d). This could be due to definitive relevance and stability of OPP perforations to allow more permeation of O_2 regardless of temperature and relative humidity.



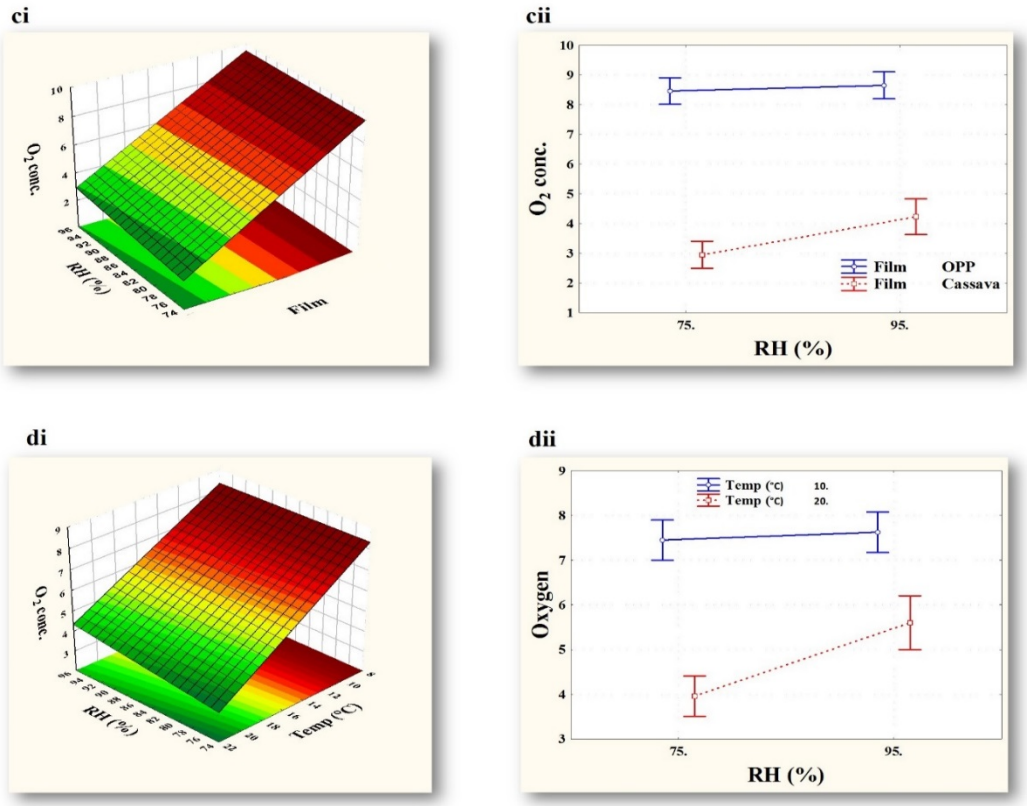


Fig 7.3. Influence of a) film type-perforations; b) film type-temperature; c) film type-RH; and temperature-RH, and their respective plots of marginal means on the dynamics of cherry tomato in-package headspace oxygen concentration using IBC (Cassava) and oriented polypropylene (OPP) films.

It is shown that perforating IBC films did not have any influence on equilibrium headspace O_2 concentration, while using a single perforation in OPP had a significant influence on equilibrium headspace O_2 concentration (Fig. 7.3ai and aii). Temperature had more marked effect on OPP than IBCF in-package modulation of O_2 concentration (Fig. 7.3bi), with IBCF managing its O_2 concentration to lower levels than OPP (Fig 3bii). Similarly, it is shown that RH had an influence on IBCF than OPP (Fig. 7.3ci). The result showed that OPP packages the headspace O_2 concentrations independent of RH (Fig. 7.3cii). Overall, increase in RH at 10°C did not influence O_2 concentration, whereas, when temperature was raised to 20°C, the increase in RH became important.

The disparity in the impact of perforated and non-perforated IBC in-package O_2 composition might be due to either the presence of sufficient IBC film micro pores to allow for proper permeability or the antagonistic effect on pores that occur at high RH leading to non-

functional voids. If the former holds true, then it can be postulated that the IBC film permeability for O_2 gas varies with temperature in the same way as tomato respiration rate, thereby preventing anoxia conditions inside the package, for the conditions studied. However, this hypothesis requires validation with more experiments at different temperatures and relative humidity closely related to the supply chain ones. By contrast, the antagonistic effects at higher relative humidity that cause structural changes in the IBC film could be averted by modifications in the film formulation for desired permeability. Unfortunately, matching the package properties with desired in-package atmosphere is not a simple task. This requires models that can consider the kinetics of respiration of in packaged tomatoes and the prediction of IBC film mass transfer properties in order to develop tailored film packages. Similarly, a variety of EMAP influential parameters, such as those intrinsic to the tomatoes and from environment, can be optimise to obtain optimum O_2 gas composition, and leads to desirable optimised EMAP.

A critical analysis (Figs. 7.3d and 7.3e) reveals that a single perforation (used in this study) was more important to cause high changes in the headspace O_2 composition than the combined effects of RH and temperature. On the other hand, the result showed that OPP was not significantly influenced by changes in RH and temperature, for the conditions studied. However, changes in environmental conditions could cause high variations in headspace O_2 composition which could compromise attaining the desirable headspace gas concentrations. Perhaps, a better meaningful perforation system would be attained when the size of the perforation is downsized below the current 270-300 microns.

Another approach to evaluate the effective performance of packaging films is to quantify the quality parameters of the packed product. However, in the absence of quantitative assessments, in-package product can be evaluated qualitatively. In this study, the qualitative evaluations were conducted by observing mould growth on tomatoes as a function of changes in the IBC and OPP in-package atmospheres, and an example of these results are presented in Fig 7.4.

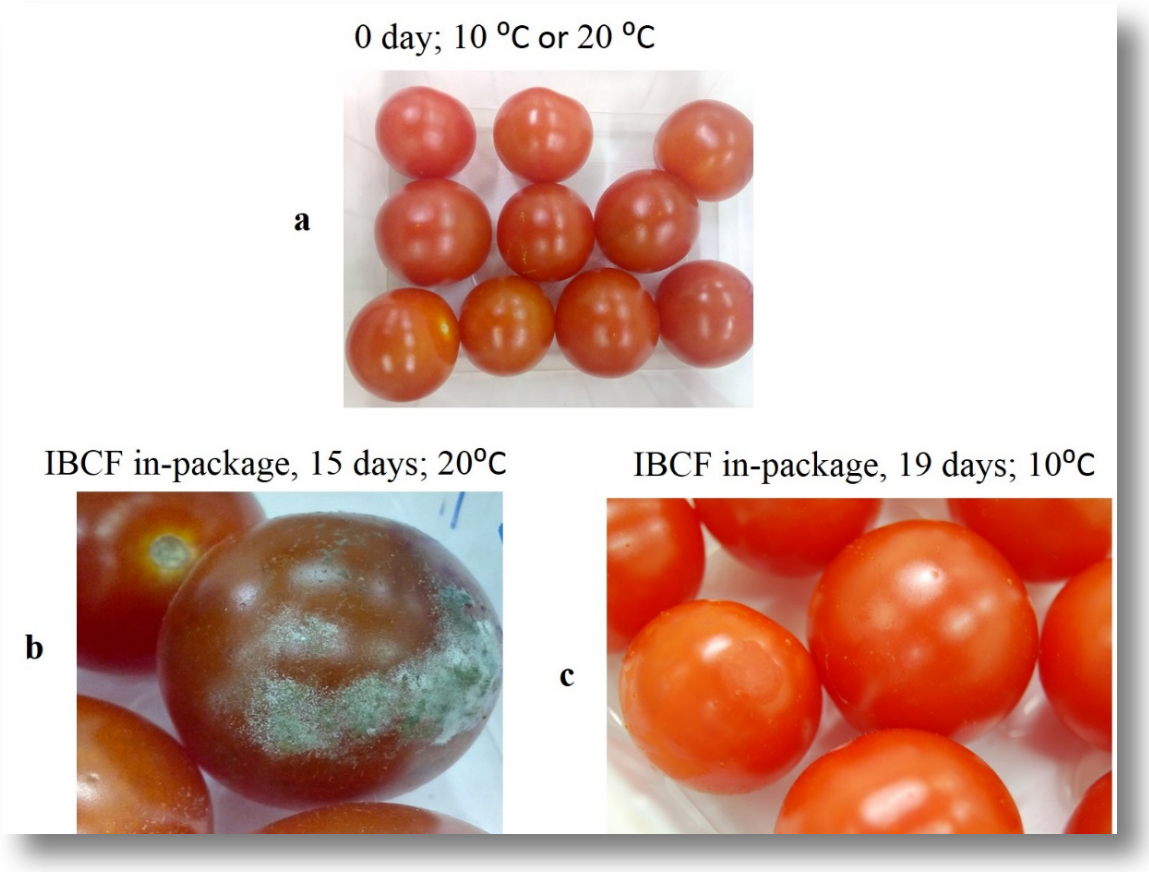


Fig 7.4. Example of cherry tomatoes in-package using IBC film at (a) 10°C or 20°C at 0 day, 95 % RH (b), 20°C, 95 % RH after 15 days and (c) 10°C, 95 % RH after 19 days of storage.

The mould growth on tomato surface was seen on the OPP packages of tomatoes within 10 days, whereas in IBCF packages mould only appeared after 15 days (Fig 7.4b) at 20°C, 95 % RH, and after 19 days of storage at 10°C, 95 % RH (Fig 7.4c). The mould growth delay observed with IBC film-packages (Fig 7.4b), might be due to optimum equilibrium headspace concentration (O_2 and CO_2 3-5%).

An attempt was made to optimise the parameters, and determine if they could provide a desirable level of O_2 concentration for EMAP design, and the results are presented in Fig 7.5 and Fig. 7.6.

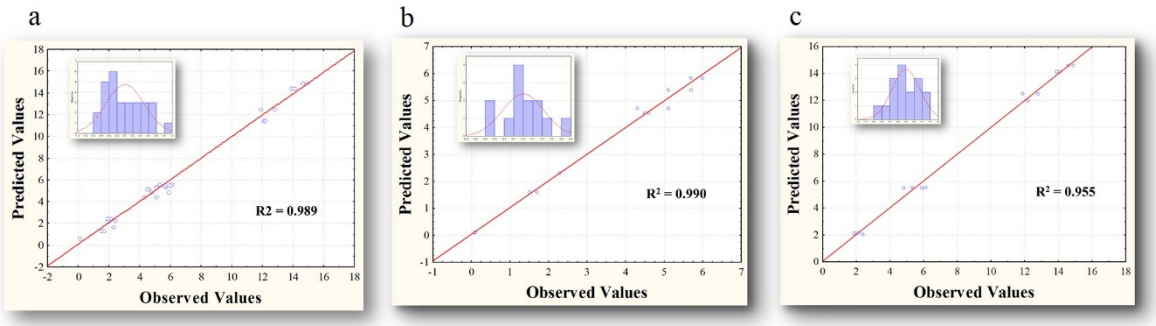


Fig 7.5. Fittings used to determine the adequacy of main effect and two-way interaction models to predict O_2 concentration for EMAP with a) combined IBCF and OPP; b) IBCF; c) OPP.

The significant terms for main and interaction effects model fittings and choice, is shown in Fig. 7.5. Consequently, the main effects and combined two factor interactions was used in determining the relationship between design parameters and equilibrium headspace O_2 concentration. As shown, the model sufficiently predicted the correlation between design parameters O_2 concentration, as best fit plots of combined parameters (Fig. 7.5a), IBC (Fig. 7.5b), and OPP (Fig. 7.5c). Besides, over 98 % of parameters and O_2 concentration data explained the suitability and significance of the models ($R^2 > 98$).

The results show that the desirable 3.11 % O_2 (Fig. 7.6ai) and 4.73 % CO_2 (Fig. 7.6aii) concentration was achieved for IBC, whereas for OPP was 7.65 % O_2 (Fig. 7.6bi) and 11.39 % CO_2 (Fig. 7.6bii), with temperature (10°C), RH (75 %), zero perforation. Thus, it can be concluded that, within short-term storage under the conditions defined, IBCF can maintain EMAP in contrast to OPP. However, validation of these results is important to determine the integrity of IBCF at high temperatures and RH as well as prolonged storage.

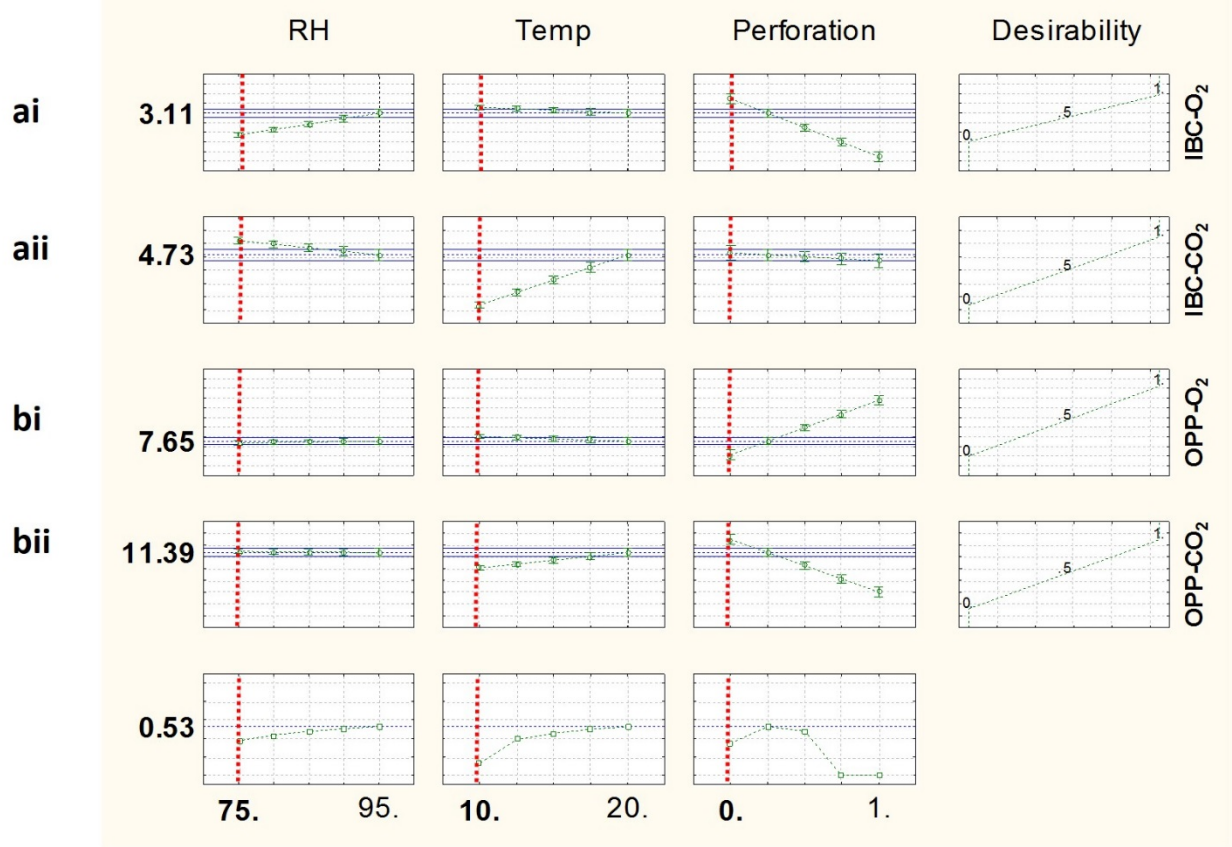


Fig 7.6 Predicted optimal parameters, desired O_2 and CO_2 concentrations and desirable values used in optimization of EMAP as shown by profiles for predicted values and desirability of: ai and aii) and bi and bii) OPP at ai) at ai) at optimum (75 % RH, 10 ºC, zero perforation).

Conclusion

This work evaluated the suitability of intact bitter cassava (IBC) films for the design of equilibrium atmosphere packaging of cherry tomatoes. Both perforated and non-perforated films produced similar equilibrium headspace O_2 composition, implying that perforating the IBC film might not be necessary. Temperature and RH were significantly ($p< 0.05$) associated with shifts in equilibrium headspace O_2 composition, suggesting that care must be exercised when IBCF packages are placed under real conditions during the distribution chain. The optional requirement of perforations for IBC than OPP films is an advantage of these films to be deployed as alternative film packages for fresh produce. Nonetheless, care should be taken while using IBCF as these film are highly influenced by variable environmental conditions. The delayed mould growth on tomatoes packaged in IBCF packages could be attributed to optimum equilibrium headspace O_2 /CO_2 concentration, showing potential for application of IBC film in EMAP designs of fresh produce. The targeted desirability value of 3.11% O_2 and 4.73 % CO_2 headspace concentration of intact bitter cassava films is a good promise for these films to be used for EMAP. However, more research is needed to validate the desirable value under stress conditions of the supply chain.

Chapter 8. Sustainable biomaterials recovered from waste bitter cassava as potential nutraceutical excipient tablet carrier of micronutrients Iron and Zinc

Abstract

The drive of this study was to explore the possibility of using polysaccharide-rich derivatives, recovered from intact bitter cassava using simultaneous release recovery cyanogenesis (SRRC), as an apt to find alternative materials for micronutrient carrier table excipients. Explicitly, the study aimed to determine the properties of SRRC-processed intact bitter cassava suitable for making tablet excipients, formulate tablets with iron and zinc and determine disintegration time rate and simulate in-vitro dissolution rate. The tablets were prepared from peeled and intact bitter cassava powders, based on a preliminary screening designed to select the powder derivative, and with best tableting properties, capable of formulating nutraceutical excipients for fast Iron (Fe) and zinc (Zn) delivery. Microcrystalline cellulose was used as a reference material with known properties for developing drug excipients. Both peeled and intact bitter cassava derivatives (PD) were characterised for properties suitable for making tablets. Tablet formulation was prepared with Fe and Zn, and by wet granulation of PD. Disintegration and in-vitro release were performed in deionized water, pH 1.2 and pH 6.8 media, at 37^{o}C. Kinetic models were used for describing matrix dissolution and Fe/Zn release mechanisms.

Intact bitter cassava PD allowed formulation of tablets, showing better properties than peeled cassava PD, to which the tablets were selected for in vitro dissolution studies. Tablet excipient matrices demonstrated faster dissolution and Fe/Zn release within 30 to 45 min, across all tablet weights, with dissolution rates of about 90%. All the kinetic models described the release mechanism, with best fits ($R^2 > 0.85$).

The study highlights potential of intact bitter cassava polysaccharide-rich derivatives as an excipient that can enhance fast releases of Iron and zinc. The recovered biomaterial from waste cassava may provide broader applications as potential alternative nutraceutical excipients.

Keywords: Waste, cassava, Nutraceutical, Tablet excipient, delivery system, Iron, Zinc

8.1 Introduction

The popularity of the concept of waste valorisation (WV) and research on green materials from natural sources have attracted great attention in a number of applications such as packaging, pharmaceutical, nutraceutical, agro-chemical, polymer and biofuel manufacturing among other industries. The WV is the idea of adding value to the waste stream in an economically viable manner (Lin et al., 2013). Among the waste biomass is cassava by-product streams, which can be categorised as food and industrial grade wastes. Cassava by-products have the potential to provide sources of economically polysaccharide-rich derivatives that might be used in the development of high value functional products for different manufacturing industries. Ongoing research on valorisation of cassava by-products includes the simultaneous release recovery cyanogenesis (SRRC) of biopolymer derivative-rich polymers such as cellulose, holocellulose, lignin and other monosaccharides (Tumwesigye, Morales-Oyervides, Oliveira, & Gallagher, 2016a).

Conventional drug carrier system involves intravenous administrations (IA) to enhance fast deliveries and bioavailability. However, the IA may be distressing and can cause local reactions to the recipients. Furthermore, although the oral administration route meant to ensure recipient satisfaction and compliance, has gained steadily, some orals may exhibit poor gastrointestinal instability and poor solubility as well as cost. Thus, pursuing a carrier and delivery process that is inexpensive and user-friendly is crucial to ensure a sustainable delivery system.

One common method in drug delivery is the development of excipients which have the potential to enhance the bioavailability, stability and cost-effectiveness. Although, most tablet excipients have been used to deliver pharmaceutical drugs, the trend of their use in nutraceutical is growing fast globally. Current nutraceutical table excipients' market growth trends are driven by changes in the consumer diet trends, influenced by high malnutrition incidences such as lack of micronutrients (Iron, zinc), and escalation of non-communicable diseases such as coronary heart diseases, obesity and diabetes. According to World Health Organization, (2014), cardiovascular diseases caused death to 1.5 million people in 2012. Thus, increasing availability of nutraceutical excipients might be a solution to both iron deficiencies and non-communicable diseases. It is estimated that men iron requirement is on

average 8.7 mg/ day, women who are menstruating need iron around 14.8 mg/day, and extremely iron-deficient groups may need up to 200 mg a day.

Currently, polymeric excipients constitute the largest share in the delivery system, as tablet binder, lubricant, anti-adhesives, tablet disintegrator, filling agent, coating agent, solubilising agent, stabiliser, emulsifying and gelling agents among other properties (Karolewicz, 2015). Among the polymers, cassava could be a potential low-cost tablet carrier and binder of nutraceuticals. At present, the by-products produced from cassava processing, and in particular bitter cassava, are considered as waste products. In our previous research, waste biomass derivatives from intact bitter cassava provided polysaccharide-rich derivatives which might deliver useful excipient tablet properties. Thus, there is a need to assess the potential applications of these waste by-products.

The purpose of this study was to: i) determine the properties of polysaccharide-rich derivatives, recovered from intact bitter cassava using SRRC, suitable for making tablet excipients; (ii) formulate tablets with iron and zinc, and (iii) determine disintegration time rate and simulate in-vitro dissolution rate.

The study was conducted into two stages. In the first part, the experiment was intended to determine the sole effect of SRRC and intact bitter cassava on PD properties that have potential in the development of new oral tablet excipients for enhancement of bioavailability and stability of nutraceuticals. Specifically, establish whether the novel PD can be endowed with properties for the development of an ideal (self-sustaining) excipient with two or more functionalities such as good flowability and compressibility. Here, two samples, subjected to different process conditions (Tumwesigye, Oliveira, & Sousa-Gallagher, 2016b), were tested for direct tablet compression. For the second part, the flowability and compression properties were optimised, based on the results obtained in the first stage, using granulation, and tablets were formulated with Iron and zinc.

8.3 Materials and methods

8.3.1 Materials

Bitter cassava roots were obtained from producers' fields in northern Uganda.

Iron (II) sulphate heptahydrate (ACS reagent, ≥ 99%); and Zinc acetate (ACS reagent, ≥ 99%) were purchased from Sigma Aldrich Ireland. All the chemicals were used as they were without further modification or treatment, and in the form they are available and absorbed in the body.

8.3.2 Polysaccharide-rich derivatives (PD) production

Bitter cassava PD were recovered from the root biomass according to Tumwesigye, Oliveira, & Sousa-Gallagher, (2016b) without modifications. Using this method, two different samples, a test sample (named PD_I) and a control (named PD_P) were prepared. The PD_I was obtained from intact root (without peeling) and PD_P was extracted from the peeled root using SRRC. The traditional methods of obtaining biomaterials includes peeling, and in this study, PD_P was used as a control to determine the potential of using intact root, while exploring SRRC, on developing self-sustaining excipients. The PD powder used for subsequent tests was kept below 10 % RH using a desiccator.

8.3.3 Characterisation of PD

8.3.3.1 Particle size and shape (PSS)

The PSS analysis was carried out by using woven wire test sieves in the 35 μm to 1 mm pore size range (Endecotts, UK), and by a CAMSIZER XT with 1 μm - 3 mm pore size measuring range (Retsch Technology, Germany).

The sieves were stacked top-down according to sieve aperture in the 1.4, 90 and 710 μm range, a 50 g PD powder placed on the top sieve, and the sieving performed with auto-vibration for a fixed time of 10 minutes.

To ensure a uniform particle size, shape and distribution, the samples were further analysed using the CAMSIZER, and the results analysed by Quad Core PC software.

8.3.3.2 Bulk and tapped densities, Carr's Index and Heckel plots

The determination of the bulk density (B_d) and tapped density (T_d) followed a method described in USP (2012). The PD samples (10 g) were transferred into a pre-weighed

graduated cylinder (25 ml, 0.5 ml markings, 14.3 mm diameter). The bulk volume was recorded after manually tapping the cylinder 10 times on a flat table top surface. The tapped volume was recorded with the Electrolab ETD-1020 Tap Density Tester (Globe-Pharma, Toronto) after tapping in increments of 500 and 1250 taps with 250 drops per minute. Triplicate tests were conducted for B_d and T_d.

The bulk density (B_d) was calculated as the fractional bulk weight (B_w) of the bulk volume (B_v) according to Eqn. 8.1.

$$B_d = \frac{B_w}{B_v} \quad 8.1$$

The B_w is the initial weight of the particles in the cylinder, and B_v is the initial volume before tapping (T).

The tapped density (T_d) was computed as the fractional bulk weight of the tapped density, expressed in Eqn. 8.2.

$$T_d = \frac{B_w}{B_v} \quad 8.2$$

where, T_d, the tapping density.

The Carr's compressibility/compatibility index (CCI) provides insight into the flow properties of powder substances. The CCI was calculate from the B_d and T_d using Eqn. 8.3, and the Hausner ratio (HR) Eqn. 8.4.

$$CCI = (T_d - B_d)\frac{100}{T_d} \quad 8.3$$

$$HR = \frac{T_d}{B_d} \quad 8.4$$

The Heckel equation (HE) determines the reduction mechanism under the compressional/compaction force, and in this study was determined following the compaction

method described in Heckel, (1961) with modifications. According to Heckel, the product bulk densification is a proportionality between the change in density with pressure and the pore fraction (porosity) (Eqn. 8.5):

$$\frac{\partial \rho_r}{\partial P} = \alpha(1 - \rho_r) \quad 8.5$$

where, ρ_r, the relative density (ratio of the density of the compaction pressure to the density of the compaction at zero void); P, the compaction pressure, 1- ρ_r, pore fraction (porosity); and α, constant associated with proportionality.

Similarly, Porosity (1- ρ_r) can be stated as Eqn 8.6:

$$1 - \rho_r = \frac{V_P - V}{V_P} \quad 8.6$$

where, VP & V, volume at any applied load and volume at theoretical zero porosity, respectively.

Rearranging Eqn. 8.5 and integrating Eqn. 8.7

$$\frac{\partial \rho_r}{(1-\rho_r)} = \alpha \, \partial P \quad 8.7$$

$$\int_{\rho_{ro}}^{\rho_r} \frac{\partial \rho_r}{(1-\rho_r)} = \alpha \int_{P_0}^{P} \partial P \quad 8.8$$

where, ρ_{ro}, relative density of uncompact PD powder at zero pressure (P_o).

The Eqn. 8.9 can be linearized as:

$$\ln\left(\frac{1}{1-\rho_r}\right) = \alpha P + \ln\left(\frac{1}{1-\rho_{r0}}\right) \quad 8.9$$

It is known (Heckel, 1961) that, often, the data do not lie on a straight line when ln (1/1- ρ_r) vs P plot is obtained due to the impact of rearrangement processes in the PD powder and, the general behaviour of the PD as discrete particles rather than a coherent mass at low pressures. Thus, Eqn. 8.9 was transformed into Eqn. 8.10 by substituting [ln (1/1- ρ_r)] with a constant (A). Eqn. 8.10 gives a quantitative validity which disregards lowest pressures.

$$\ln\left(\frac{1}{1-\rho_r}\right) = \alpha P + A \qquad 8.10$$

where, A (intercept), is the degree of packing achieved at low pressures, and α (slope of the linear region), a measure of the ability of the compact to density by plastic deformation (Heckel, 1961).

8.3.4 Preparation and analysis of tablet excipient from PD

8.3.4.1 Preparation

A hydraulic hand press (Specac P/N 15011/25011, UK), set at predetermined low (2 MPa), medium (5 MPa) and high (7 MPa) pressures was used to press PD into 100, 250 and 500 g tablets. Precisely weighed PD samples were introduced into the press and compressed using stainless steel flat-circular punches (9.3 mm in diameter) with a constant force for pre-determined pressures. The resulting tablets were inspected for possible visual defects such as flecks, cracks, shape and size.

To determine the effectiveness of intact bitter PD to make quality excipients, a comparative study of known polymer material, microcrystalline cellulose, was run concurrently using the same procedure and test conditions.

8.3.4.2 Analysis of tablet properties

The uniformity of weight of the tablets was determined by weighing, individually, a set of 20 tablets using a digital analytical balance (AX 105 Delta Range ± 0.0001 g, Mettler-Toledo, Greifensee, Switzerland), and their weights averaged. The percentage deviation of the individual tablets from the mean was determined according to Eqn. 8.11. No more than 2 of

the individual masses should deviate from the average mass by more than the percentage deviation applicable for the tablet and, no individual mass should deviate by more than twice that percentage.

$$D, \% = \left(\frac{\varpi - w}{\varpi}\right) 100 \quad 8.11$$

where, D, deviation;ϖ, mean weight; and w, weight of individual tablets.

Tablet thickness and diameter were measured by a Mitutoyo micrometer (Absolute Digimatic ID-S Série 543–790B ± 0.003 mm, Codima Roboflux, Décines, France) immediately after compression as permitted by the European Pharmacopeia methods (European Pharmacopoeia, 2015) and reported in Juban, Nouguier-Lehon, Briancon, Hoc, & Puel, (2015).

Tablet tensile strength was determined 2 days following their formulation at 20-25 ^{o}C by an ElectroPuls^{TM} E10000 Linear-Torsion All-Electric test instrument (Norwood, MA 02062, USA). For each compression load (50 MPa, 100 MPa and 200 MPa), a minimum of three tablets per composition were tested, and the tensile strength (TS in MPa) was calculated according to Fell & Newton, (1970) using Eqn. 8.12.

$$TS = \frac{2f}{\pi dl} \quad 8.12$$

where, f, fracture fore; d, diameter; and l, overall thickness.

8.3.5 Preparation of Iron and zinc tablets

8.3.5.1 Wet granulation

Tablet formulation was prepared initially by wet granulation of PD using distilled water. The PD powder (200 g) was loaded into a vessel and granulated using a 4M8 ForMate Granulator (Pro-CepT, Zelzate, Belgium). The powder was subjected to pre-mix conditions of 500 rpm impeller and chopper speeds for 3 min., and finally granulated using 1000 rpm impeller

speed, 120 % impeller torque, 2000 rpm chopper speed, 3 ml/min. dosing speed, 30 mL total dosing quantity, and 22 ^{0}C mixture temperature for 30 min. The granulated samples were dried in vacuum oven at 70 ^{0}C for 12 hours. Moisture content was determined using PMX 60 Moisture analyser (Chromlab Scientific Services, UK), and a mean value of 2.25 % was recorded. The dry granulated samples were sieved (Endecotts, UK) to 850 μm uniform particle size, and stored in a desiccator until further use.

8.3.5.2 Compression

Prior to compression, the contents of PD excipients, Iron (II) sulphate heptahydrate and zinc acetate were formulated (Table 8.1) and mixed uniformly in a low speed mixer at 30 rpm for 30 min. A hydraulic hand press (Specac P/N 15011/25011, UK), set at 200 MPa was used to press the granulated samples into 100, 250 and 500 g tablets as described in subsection 2.4.1 (this study).

Table 8.1. Quantities of cassava PD, Iron and zinc used in excipient development and dissolution studies

Formulation	**Excipient, mg**	**$FeSO_4.7H_2O$, mg**	**$Zn(CH_3COO)_2 \cdot 2H_2O$, mg**	**Tablet size, mg**
Cassava PD	100	0	0	
Cassava PD + Fe	50	50	0	100
Cassava PD + Zn	75	0	25	
Cassava PD	250	0	0	
Cassava PD + Fe	200	50	0	250
Cassava PD + Zn	225	0	25	
Cassava PD	500	0	0	
Cassava PD + Fe	450	50	0	500
Cassava PD + Zn	475	0	25	
Cassava PD + Fe +Zn	425	50	25	

8.3.6 Disintegration and dissolution

8.3.6.1 In vitro dissolution studies

In vitro dissolution was determined simulating U.S. Pharmacopeia (USP) method as described (Chowhan & Chi, 1986) with modifications. The dissolution solvent was 300 mL (pH 6.8) achieved by phosphate buffer and 900 mL (pH 1.2) obtained with 0.1N hydrochloric acid. Both solvents simulated gastric fluid without enzymes were maintained at 37 ^{0}C (range of body temperature).

The PD Excipients-Iron (II) sulphate heptahydrate and zinc acetate tablets were dissolved in the solvent of respective pH at 37 ^{0}C and stirrer (50 rpm, 60 min.). The experiment was setup in such a way that a weighed tablet was placed on a suspended mesh platform inside of a beaker and rotating paddle inserted in the beaker at a height of 25 mm from the tablet. A sample was withdrawn after every 10 min and the undissolved excipients removed by filtration (Whatman no. 1 filter paper). Serial dilutions of the filtrate were made from 10 ml of the initial filtrate, and their UV absorbance recorded at 242 nm using a Biochrom Libra S22 UV/vis spectrophotometer (Cambridge CB4 0FJ, UK). A control containing only PD excipient was run concurrently. Similar quantities of Fe and Zn were dissolved in respective pH 6.8 and 1.2, serially diluted and used to derive standard curves. The experiment was replicated three times, and the data described quantitatively using mathematical models.

.

8.3.6.2 Application of mathematical models for the description of Fe/Zn dissolution mechanism

Fe/Zn dissolution can be best interpreted by kinetic models, similar to what has been used in drug dissolution. The model spells out the quantity (Q) of Fe/Zn dissolved as the function of dissolution time (t), i.e., Q = f (t). However, most excipients are developed in different forms and types resulting in different release mechanisms (slow, medium, fast), and this necessitates a dissection of the more elaborate models, in addition to kinetic model. This helps to understand the behaviour, type of release and angle of application of intact bitter cassava PD. Based on this background and the types of excipients developed in this study, and in addition to kinetics of release, the first order kinetics, Weibull, power, Baker-Lonsdale and Hoffenberg models were applied for the interpretation of dissolution.

When the excipient is dissolved in the test solvent, it undergoes absorption which occurs, first, at the surface. This involves a single reactant-the Fe/Zn release, and thus the First order kinetic model (Gibaldi & Feldman, 1967; Samaha, Shehayeb, & Kyriacos, 2009; Silva & Wagner, 1969), can be applied to describe the dissolution phenomena (Eqn. 8.13)

$$\log C_t = \log C_0 + \frac{kt}{2.303} \quad 8.13$$

where, C_t, micronutrient concentration in solvent at time, t; C_0, initial amount of micronutrient in the solvent; and k, first order release coefficient.
This provides a straight line graph when the c-t graph is developed, and gives the description of proportionality of Fe/Zn release.

In ideal situations, the diffusion and release of nutraceutical should follow the Fickian law. Nonetheless, due to differences in experiments, anomalous behaviour dominates solute motions. Thus, a more generic power law Eqn. 8.14, suggested by Ritger & Peppas, (1987) was used to study behavioural release of micronutrient from the novel intact bitter cassava PD excipients.

$$F_t = kt^n \quad 8.14$$

where, F_t, function of time that is represented by Mt / M_0, the fractional release of micronutrients from the excipient; k, constant defining the structural characteristics of the excipient; and n, release exponent describing the release mechanism. The general dependence of n on the diffusional mechanism (Ritger & Peppas, 1987) is shown in Table 8.2

Table 8.2. Assessment of solute diffusional release mechanisms

Release exponent, n	**Nature of diffusion mechanism**	**Time dependence of fractional release rate (F_t)**
0.5	Fickian	t-0.5
0.5 < n< 1.0	Anomalous (non-Fickian)	tn-1
1.0	Case II	Zero order (time dependent) release
n > 1.0	Super case II	tn-1

Application of Baker and Lonsdale (1974) model was aimed at describing the micronutrient release from the heterogeneous spherical excipient tablets. It is important to note that most nutraceutical excipients are often heterogeneous, and this could have a significant influence on micronutrient release mechanism. Thus, to determine any possible loosening within the tablet matrix such as fissures or streaks, Baker-Lonsdale Eqn. 8.15 was used:

$$F_t = \frac{3}{2}\left[1 - \left(1 - \frac{M_t}{M_\infty}\right)^{\frac{2}{3}}\right] - \frac{M_t}{M_\infty} = kt \qquad 8.15$$

where, M_t and $M\infty$, Fe/Zn quantity released at time t and infinite time; and k, release constant (slope)

In perfect homogeneous excipients, the release of Fe/Zn would assume uniform surface erosion. However, due to anticipated heterogeneous erosion nature of current excipients, a model developed by Katzhendler, Hoffman, Goldberger, & Friedman, (1997) was explored (Eqn. 8.16).

$$\frac{M_t}{M_\phi} = 1 - \left[\frac{k_0 t}{C_0 X_0}\right]^n \qquad 8.16$$

where M_t, quantity of Fe/Zn dissolved in time, t; M_ϕ, total quantity of Iron/zinc dissolved when the excipient tablet is fully exhausted; M_t/M_ϕ, fraction of Fe/Zn dissolved; k_0, erosion rate constant; C_0, initial concentration of Fe/Zn in excipient tablet matrix; X_0, initial radius of excipient tablet matrix; and n = 3 (for spheres). It was assumed that there was no influence of internal and external resistance perpendicular to the erosion.

Tablet excipient dissolution efficiency (E, %) was determined from the area under the curve of C-t plot of Iron/zinc dissolved at time, t or can be derived from Eqn. 8.17 (Khan, 1975).

$$E, \% = \left(\frac{\int_0^t y\ \delta x}{y_{100}\ t}\right) * 100 \qquad 8.17$$

According to Pharmacopoeias, the acceptance dissolution limit is, $t_{45} \geq 80\%$.

8.3.7 Statistics

Statistical significance for the differences between the tensile strengths of the dispersed and agglomerated formulations was evaluated by ANOVA. Dissolution profiles were assessed by calculating the similarity factor f_2 according to the instructions of the FDA (FDA, 1997). Only one time point after 85% of drug released was included in f_2-value calculations. Should the f_2-value be less than 50, the dissolution profiles were considered different (Mäki et al., 2007).

8.4 Results and discussion

8.4.1 Particle size and shape (PSS)

Fabrication of tablet excipients depends on the uniformity of particle sizes in the starting formulations, which makes compaction more effective, and thus regulated delivery matrices. Fig. 8.1 illustrates particle distribution in different samples of PD and compared to microcrystalline cellulose (MCC).

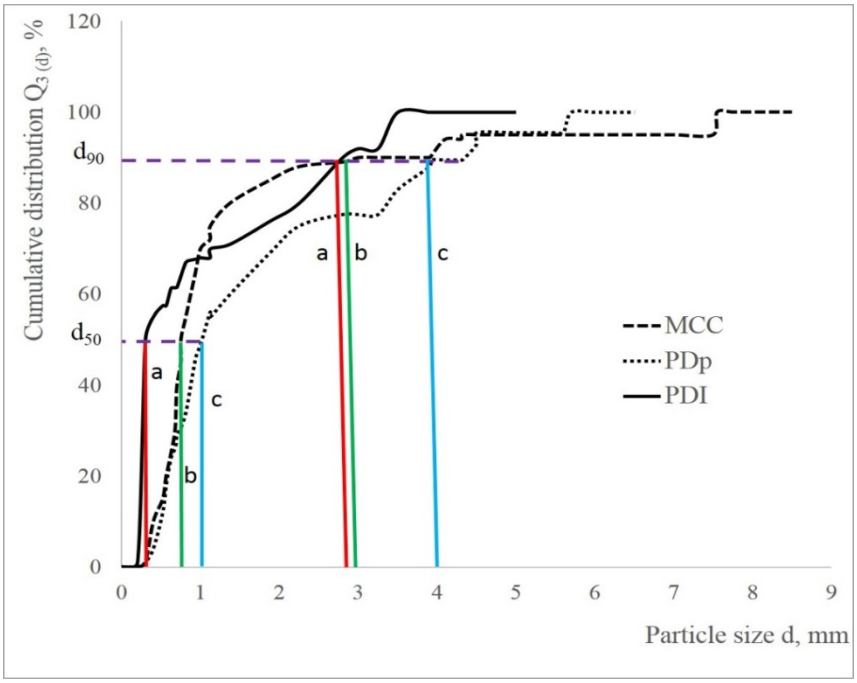


Fig 8.1 Particle size distribution function Q3 (d) analysis of materials used in excipient tablets. Microcrystalline cellulose (MCC, b); from peeled root (PDp, c); and intact root (PDI, a)

Generally, particle size and shape distribution of PDp and PDI followed the same pattern as that of MCC, although MCC showed a more uniform distribution compared with the PDs. The unevenness in distribution might be due to less quantity of PDs used compared with MCC.

The d-values define the diameters of the sphere which divides the samples weight into a specified percentage when the particles are arranged on an ascending mass basis. Thus, d_{50} and d_{90} describe the diameters at which 50 % and 90 % of the sample's weight comprised particles with a diameter less than the respective values. Accordingly, the d_{50} of PDI, PDp and MCC were in the region < 0.3, <0.8 and V1.0 mm, while their respective d_{90} were < 2.8, < 3 and < 4 mm. Thus, it can be concluded that 90% of PDI and MCC particle distribution were within less than 3 mm.

8.4.2 Bulking properties, Carr's Index and Heckel analysis

The intact bitter cassava PD bulking analysis showed that true, tapped and bulk densities of PDI are lower than those of PDp (Table 8.3). The lower values of true, tapped and bulk densities of PDI than for PDp might be due to the nature of their particle size and shape distribution, with PDI revealing a more uniformity in particle size than for the PDp (Fig 8.1). The tap density of a material can be used to predict the flow properties and its compressibility, thereby providing durable solid excipients with the desired strength, porosity and dissolution characteristics. In this study, PDI true density was found to lie within the range reported for microcrystalline cellulose (MCC) reported values (1.52 – 1.668 g/cm^3, and close to a true density of a perfect cellulose crystal (1.582 – 1.512 g/cm^3) (Sun, 2005).

Table 8.3 Bulking properties of intact bitter cassava PD

Cassava PD	Particle density, g/cm^3				
	True	Tapped	Bulk	Hausner ratio	Carr's Index
PD_p	1.75	0.63	0.61	1.03	3.17
PD_I	1.57	0.59	0.55	1.01	16.6

PD_p, derivative from peeled cassava; PD_I, derivative from intact bitter cassava

The associative true densities of PDI and MCC is reflected in their particle and shape distribution as shown in Fig. 8.1, reported in subsection 3.1. By contrast, the higher PDp true density might be due to a more heterogeneous particle size and shape, deviating from that of PDI and MCC. Moreover, the differences between PDI and PDp bulking properties might be a function of their production in the SRRC process and handling (treatment and storage).

The hausner ratios close to 1.0 suggested that the powders were free-flowing. The higher Carr's Index of PDI than that of PDp meant that the inter-particulate and intra-particulate of PDI material interactions were significantly lower than those of PDp. This meant that PDI powder presented better free-flowing capacity compared with PDp, although PDp exhibited the closeness of the bulk and tapped densities than for PDI. This unusual apparent contrast could be attributed to the difficulties in measuring powder bulking properties. Bulk and tapped value closeness defines the best flowing properties of the powder. Thus, it can be concluded that PDI had a better free-flowing ability than PDp.

The effect of elastic deformation of PD and MCC particles on Heckel analysis is presented in Fig. 8.2, indicating that, generally, the void fraction of the three materials was not much different at the initiation of compression. However, detailed analysis showed that the porosity increased in the order, PDp < PDI < MCC. These results imply that the PD inter-particulate bonding seemed to be strong, thereby making PDp and PDI to behave like a powder with minimal free-flowing properties compared to MCC. Moreover, the shapes of the graphs show that particle fragmentation, plasticity and elasticity for the order PDp < PDI < MCC corresponding to increases in compression force.

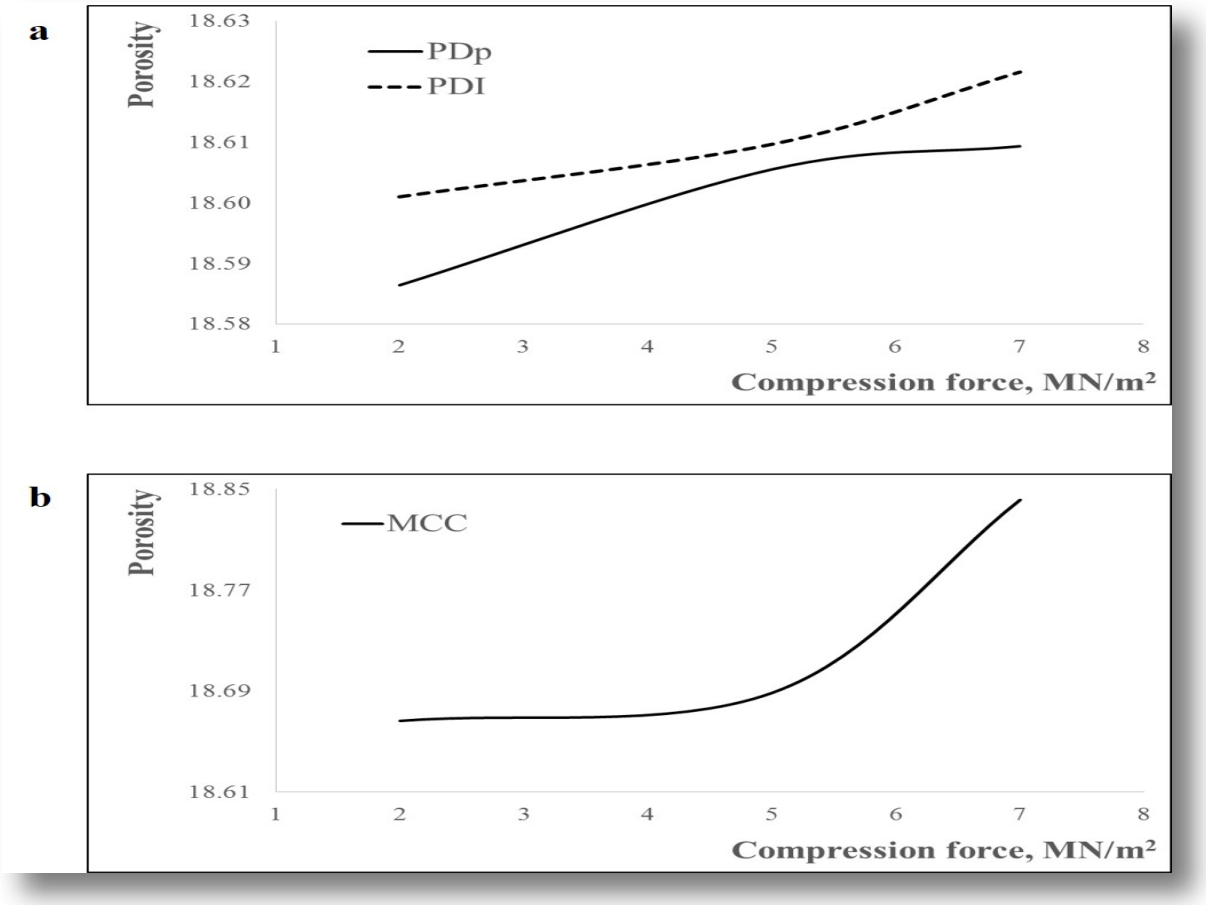


Fig 8.2. Impact of elastic deformation of intact bitter cassava PD particles on Heckel Analysis (a), and as compared to microcrystalline cellulose (b).

Additionally, there appears to be similarities in the way PDI and MCC undergone plastic deformation (horizontal section). However, MCC seemed to show a more systematic compaction than PDI. Apparently, the higher increase in porosity of MCC over short increases in compression pressure than PDI could be attributed to low inter-particulate bonding of MCC particles. The implication of the Heckel analysis result points to the need to tailor intact bitter cassava PD processing to the demands of the tablet excipients. Unfortunately, in this study, the PD was investigated as processed for diverse products. Nevertheless, the analysis highlights promising potential for cassava PD. Conversely, the failure of PDp to compact confirms that employing SRRC on intact roots produce better derivatives than has been conventionally peeled.

8.4.3 Impact of bitter cassava and SRRC on excipient tablet properties

Uniformity of weight of tests carried out on 20 tablets at high pressure (7 MPa) showed that both PDp and PDI had mean weights of 413 mg and 484 mg with mean deviation of 1.56 % and 0.68 % respectively. The deviations for both tablet types were lower than the recommended value of 5 %. The slightly high deviation of PDp could be attributed differences in the bulk densities and particle size distribution during compression.

Physical property analysis of tablets compacted by different pressures showed that PDp yielded tablets at high pressure only, whereas PDI produced tablets when subjected to all pressures (Table 8.4). The crumbling of PDp at medium and high pressures were mainly due to the inability of particles to compact. Generally, PD tablets exhibited lower values of hardness and tensile strength than the MCC. This may be attributed to the nature of initial sample processing. MCC is universally produced by spray drying the neutralized aqueous of strong acid hydrolysed cellulose slurry in order to manipulate the degree of agglomeration (particle size distribution) and moisture content (loss on drying) (Thoorens, Krier, Leclercq, Carlin, & Evrard, 2014). By contrast, PD is a product of weak acid hydrolysis that was oven-dried. Unlike spray-drying, oven drying does not offer the desired agglomeration and controlled moisture loss. Thus, when PD and MC were subjected to direct compaction, MCC had improved compatibility or tabletability of the compression mix. A minimum of 4 KG crushing strength is required for satisfactory hardness. Slow release, oral and hypodermic and chewable tablets have 10-20, 4-10 and 3 KG crushing strength respectively. The slightly lower but insignificant differences in crushing strength of PD might be due particle morphology of the initial materials.

Thus, the desirable physical properties of intact bitter cassava PD can be attained by improvements in the SRRC process, particularly with increased acid hydrolysis, and using a slightly older root (> 12 months maturity). Besides, the drying can be revisited to include spray drying.

Table 8.4. Effect of intact bitter cassava and SRRC on the compaction properties of excipient tablets

Materials	**Pressure, MPa**	**Hardness, KG**	**Diameter, mm**	**Thickness, mm**	**Weight, mg**	**Tensile strength, MPa**
PD_p		-	-	-	-	
PD_I	2	2.32 ± 0.99	13.09 ± 0.04	3.16 ± 0.04	506.36 ± 2.84	0.35
MCC		53.88 ± 1.92	12.96 ± 0.004	3.19 ± 0.05	507.65 ± 8.49	8.3
PD_p		-	-	-	-	
PD_I	5	2.42 ± 0.07	13.08 ± 0.01	3.14 ± 0.07	511.48 ± 9.7	37
MCC		66.04 ± 2.26	12.95 ± 0.004	3.04 ± 0.076	503.78 ± 5.64	10.86
PD_p		2.34 ± 4.43	13.12 ± 0.06	3.10 ± 0.07	512.58 ± 11.52	0.36
PD_I	7	2.64 ± 1.02	13.07 ± 0.004	3.11 ± 0.048	502.62 ± 4.72	0.41
MCC		66.76 ± 3.57	12.96 ± 0.007	3.05 ± 0.08	507.08 ± 12.05	10.75

8.4.4 Evaluation of Fe and Zn excipient tablets

It is evident, from the preceding sections of this study and also widely accepted, that particle size and shape, bulking density/surface area can regulate the tableting properties (e.g. tabletability and flowability) of intact bitter cassava PD. Thus, an understanding of the prior proper processing of the excipient before incorporation of Fe and zinc was necessary. However, since the purpose of the study was to assess the impact of intact bitter cassava and SRRC on the development of Fe and Zn excipients, only granulation was carried out on the intact bitter cassava (PD).

An example of excipient tablet prototypes with and without Fe and Zin produced from intact bitter cassava PD are shown in Fig. 8.3.

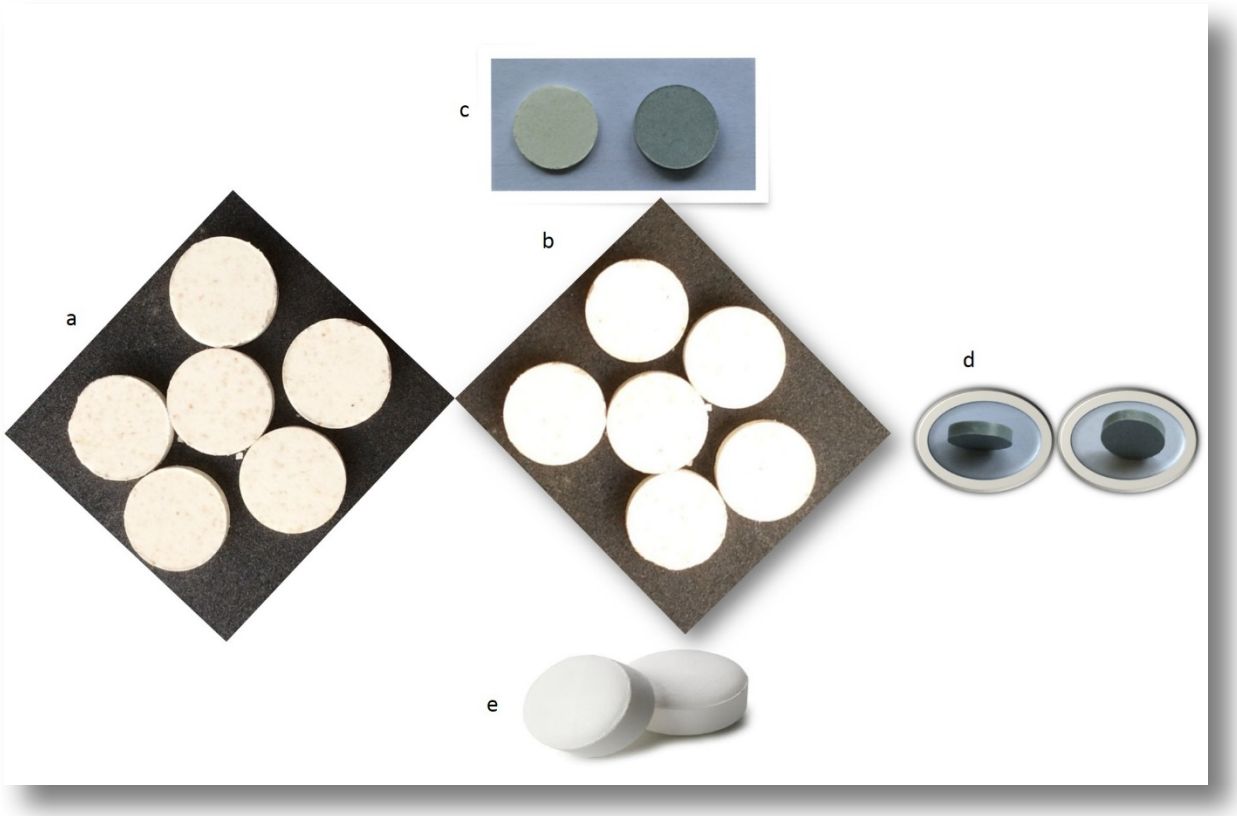


Fig 8.3. Excipient tablet prototypes used in in vitro dissolution: a) from PDp; and b) PDI, without Fe/Zn; c) Fe and Zn; d) combined Fe and Zn; and e) MCC.

8.4.5 Analysis of dissolution and release mechanisms

The results of the release process of intact bitter cassava PD is presented in Fig. 8.4, showing that dissolution time had a highly significant ($p \leq 0.05$) positive impact on Fe and Zn release. This result is expected and attributed to the fast release matrices. Consistently, Zn had a preferential fast release to Fe as far as excipient weights, combined form and solution pH environment were taken into consideration. To gain better understanding of the release nature of the excipient matrix, the dissolution data was fitted to model equations, and the results are presented in Table 8.5 and Fig. 8.5. In all cases, the results correlate inversely with excipient mass, and to a less extent when Fe and Zinc were combined in a single tablet regardless of the weight. By contrast, Fe and Zn were better released in acidic environment (pH 1.2) than the alkaline equivalent (pH 6.8). Nonetheless, taken together, Fe and Zn were highly released in solution medium as verified by their high dissolution efficiency.

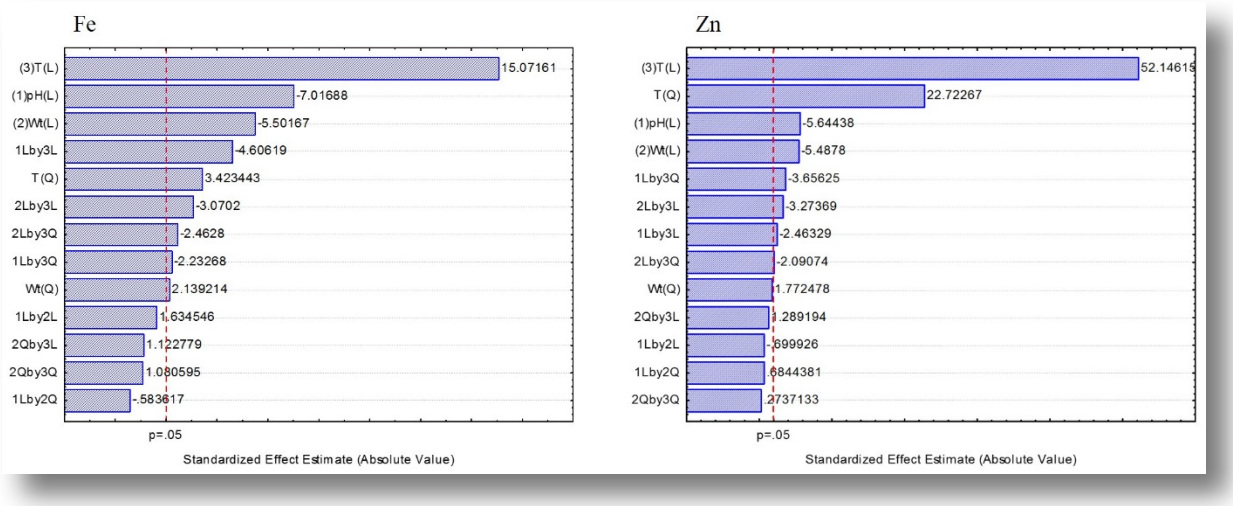


Fig 8.4. Effect of the factors solution pH (pH; 1), weight (Wt; 2), and time (T; 3) on dissolution of Fe/Zn from intact bitter cassava PD tablet excipients.

Regardless of the weight and solution pH, the release exponent, n values demonstrate that the dissolution of Fe and Zn from cassava PD matrix seem to be governed by case II and super case II viscoelastic relaxation mechanism. It is well-known that a desirable mechanism for any release process in various applications should provide zero-order release performance, with n falling around one (n = 1) (Lager & Peppas, 1981; Ritger & Peppas, 1987).

Apart from dissolution due to diffusion, the fast release rates observed in this study could be attributed to bitter cassava PD excipient matrix erosion. As shown in Table 8.5, erosion rates (k_0) seem to be slightly higher compared to k_0 in drug dosage forms (Dürig, Venkatesh, & Fassihi, 1999) and elsewhere (Nep, Asare-Addo, Ghori, Conway, & Smith, 2015). Although erosion phenomena is exploited in drug dosage forms for the design of oral extended-release, it might be of advantage when applied in micronutrient matrices designed specifically with heterogeneous surfaces for fast releases. In this study, surface heterogeneity seemed not to be the major contributor of erosion since the tablets produced had smooth surfaces (Fig. 8.3).
The high erosion rates might be also due to ability of cassava PD to gel quickly, swelled and released the micronutrients as fast as it could. While swelling rate was not determined in this study, the slightly higher erosion values could explain the swelling ability of the tablet excipients.

While there seemed to be no visible heterogeneous surfaces, it seemed to indicate that heterogeneity could be localised within the internal parts of the tablet. As shown in Table 8.5, the slightly higher weight-dependence loosening with 500 mg than for 250 and 100 mg might suggest presence of porous, streaks or crevices with increased solids in the matrix. It might be expected that spaces within the matrix would lead to fast surface erosion by reducing solvent diffusion pathways. This was not likely with intact bitter cassava PD since there is no correlation in the erosion and loosening constants (Table 8.5). This suggests that the fast releases could be a function of swelling of the tablet matrices or due to bulk erosion.
Additionally, in comparison to MCC, it could be hypothesized that the more Powderly PDI, with less porous spaces would form thick gels inside its matrix and delay fast internal erosion. However, this was not possible with fast release rates observed.
Thus, it can be concluded here that if the SRRC processing conditions of intact bitter cassava PD could be regulated to include tailored process for tablets, then it would be possible to balance rate constants, leading to acquiring desired release rates.

Table 8.5. Fitting of intact bitter cassava PD release data to model equations

Excipient system	Tablet mass, mg	Solvent pH	Total mass dissolved	Rate constant, k			Release exponent (n)	Dissolution efficiency, %	R^2
				1st Order	Erosion	Loosening			
Cassava PD/Iron	100	1.2	49.19 ± 0.05	0.017	1.121	0.183	0.865	96	0.922
	250		46.85 ± 0.04	0.016	0.455	0.172	0.866	92	0.913
	500		39.40 ± 0.44	0.029	0.285	0.227	0.889	76	0.948
		6.8	42.30 ± 0.06	0.110	0.914	0.482	1.271	80	0.866
			41.76 ± 0.31	0.111	0.958	0.478	1.273	78	0.864
			36.81 ± 0.12	0.136	1.810	0.434	1.064	70	0.932
Cassava PD/Iron in		1.2	44.58 ± 0.05	0.022	0.371	0.206	0.884	88	0.971
Zinc matrix	100		43.90 ± 0.00	0.021	0.380	0.198	0.919	86	0.989
	250		36.88 ± 0.03	0.078	0.350	0.371	1.033	80	0.949
	500	6.8	42.80 ± 0.01	0.024	0.349	0.207	0.908	81	0.986
			42.43 ± 0.18	0.024	0.343	0.208	0.893	68	0.982
			34.99 ± 0.02	0.095	0.792	0.369	0.920	65	0.980
Cassava/Zinc		1.2	24.87 ± 0.03	0.009	0.876	0.103	1.001	98	0.948

	100		24.93 ± 0.02	0.010	0.611	0.117	0.990	96	0.980
	250		24.21 ± 0.02	0.015	0.498	0.157	1.014	90	0.964
	500	6.8	22.49 ± 0.02	0.011	0.593	0.112	0.966	86	0.946
			22.29 ± 0.01	0.010	0.541	0.110	0.893	84	0.926
			20.20 ± 0.02	0.001	0.468	0.114	0.681	74	0.889
Cassava /Zinc in		1.2	23.62 ± 0.02	0.017	0.449	0.169	1.015	94	0.941
Iron matrix	100		23.41 ± 0.02	0.018	0.372	0.177	0.988	92	0.960
	250		21.20 ± 0.01	0.018	0.379	0.160	1.009	84	0.946
	500	6.8	22.49 ± 0.05	0.022	0.303	0.208	0.898	90	0.971
			22.18 ± 0.02	0.021	0.454	0.203	0.929	89	0.964
			19.19 ± 0.01	0.112	0.623	0.212	0.888	76	0.950

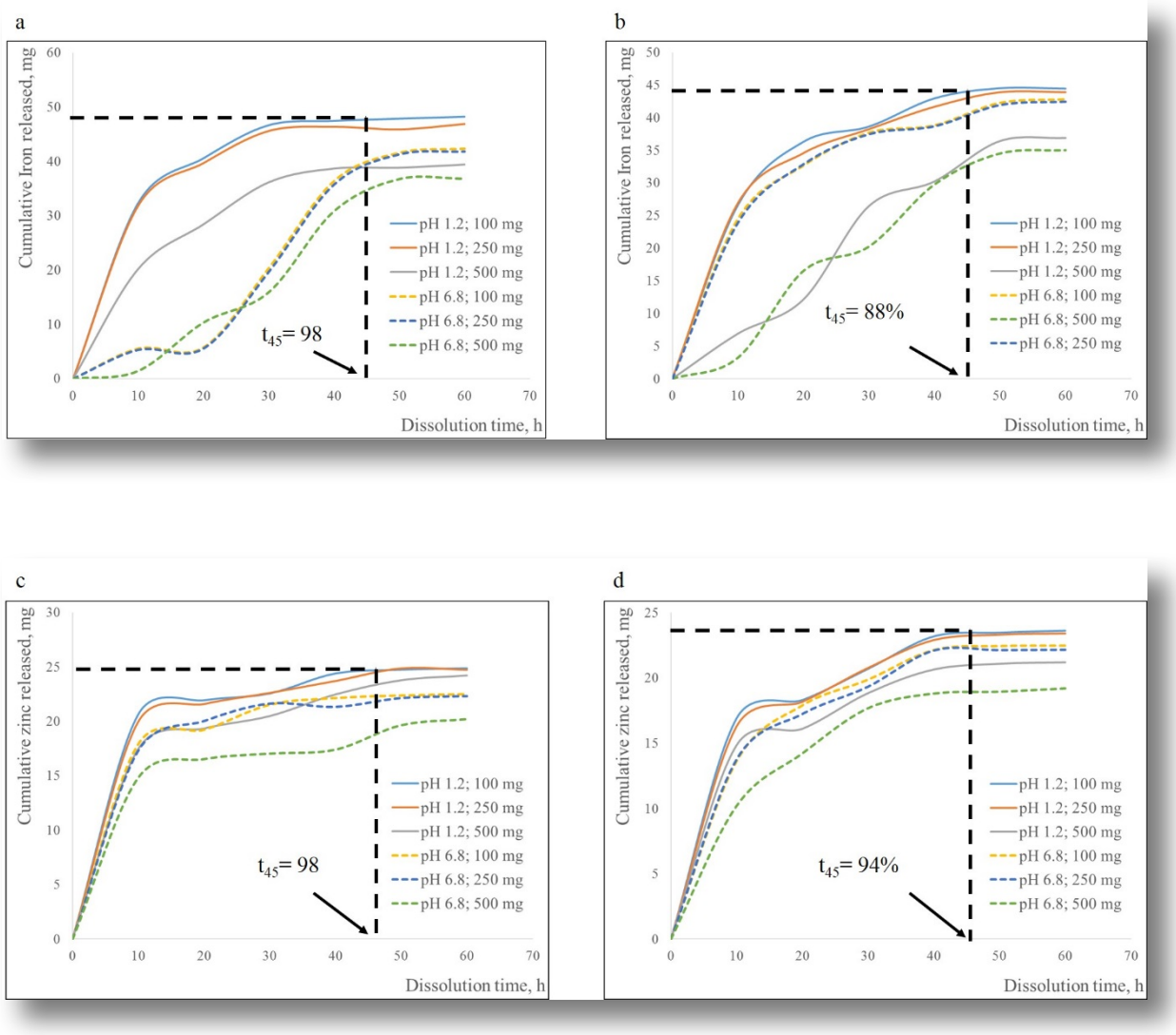


Fig 8.5. Rate profiles of Fe/Zn release from intact bitter cassava PD excipient. Sample aliquots taken from the solution (and replaced with equal amounts) at specified intervals, and absorbance read.

The coefficient of determination, R^2 represents means for all the model fitted. With all R^2 values around 0.900, and this shows a good fitting, and is an indication that they explain the Fe-Zn phenomena from intact bitter cassava PD. Similarly, as exhibited by profile rates (Fig. 8.5), the dissolution efficiency for Fe and Zn was higher for pH 1.2 than in the pH 6.8. In particular, low-weight tablets demonstrated higher dissolution efficiency (DE) than for higher weight ones. Generally, the DE for pH 12-based matrices were within and above the acceptance dissolution limit is, $t_{45} \geq 80\%$ (Saccone, Tessore, Olivera, & Meneces, 2004). The

Fe and Zn micronutrients were incorporated in the tablets in the form of sulphate and acetate, respectively, as they are presented in the body. Ionisation of these nutrients usually occurs when pH of the dissolution is lower (Sharp & Srai, 2007). This probably explains the relatively higher release rates of Fe and Zn in intact bitter cassava PD matrices in solvent at pH 1.2 in contrast to pH 6.8.

Conclusion

Intact bitter cassava (IBC) polysaccharide-rich derivatives, produced with simultaneous release recovery cyanogenesis (SRRC), were investigated as potential nutraceutical tablet excipient for fast delivery of micronutrients Iron and zinc. The tablets were prepared from peeled and intact bitter cassava powders, based on a preliminary screening designed to select the powder derivative, with best tableting properties, capable of formulating nutraceutical excipients for fast Fe and Zn delivery. Intact bitter cassava PD is a better potential biomaterial with superior tableting properties than one obtained from peeled equivalent, and also comparable to known microcrystalline cellulose. The IBC is endowed with properties capable of producing nutraceutical excipients for fast delivery systems as demonstrated in the fast delivery of Fe and Zn in acidic and neutral pH.

The SRRC greatly enhances the tableting properties of IBC PD but cannot alone deliver requisite conditions for full tableting; there is need to further reinforcement PD with standard tableting processes to improve flowability and tableting capacity. Using the preliminary approach of obtaining SRRC-processed powder resulted in effective enhancement of nutraceutical tablet dissolution properties and allowed fast and full releases of Iron and zinc within 30 to 45 min, across all tablet weights.

Overall, this study has demonstrated the potential of intact bitter cassava (IBC) polysaccharide-rich derivatives as an excipient that can enhance fast releases of Iron and zinc. Furthermore, the preliminary strategy of producing the material with SRRC can be employed in production of starting materials meant for developing fast release excipient tablets. The recovered biomaterial from waste cassava may provide broader applications as potential alternative nutraceutical excipients.

Chapter 9. Bitter Cassava Polysaccharide-rich Derivatives as Thymol-encapsulated Coatings in Antifungal Active packaging of Perishable Strawberries

Abstract

Natural-sourced polysaccharides can improve the stability and functionality of plant bioactive extractive carrier coating dispersions by creating a protective covering layer around them. Hypothetically, the encapsulation characteristics of the coating matrices can be regulated by developing them using low-cost and energy-efficient biopolymers rather than assembling them from uncostly multiple enhancer chemicals and polysaccharides. The objective of this study was to evaluate the capacity of intact bitter cassava polysaccharide-rich derivatives (PD) to encapsulate thymol effectively, and evaluate their antifungal effect and strength on stored strawberries using qualitative methods. Four coatings were formulated with intact bitter cassava polysaccharide-rich derivative (2% w/v), glycerol (40% w/w) and thymol (0.25, 0.5, 0.75 and 1.0 % w/v), and analysed by their encapsulation efficiency, permeability to water vapour, surface energy and wetting, and antifungal activity. All the four coatings had higher encapsulation efficiency (> 95%), which was concentration-dependent. Coating permeability to water vapour was in the range of 4.89-0.02 g mm / (M² day kPa), and was inversely proportional to coating concentration. Coating wettability occurred at medium to high contact angles (88.71-111.26^0) and decreased as thymol concentration increased, and this facilitated better and smooth coating of the strawberries. Coatings demonstrated efficient antifungal activity in strawberries, with mould-growth inhibition reaching beyond 14 days of storage.

These results have significant implications for the design of antifungal systems based on intact bitter cassava/natural bioactive-coating dispersions.

Keywords: Bitter cassava; Coating; Thymol-encapsulation; Antifungal; Strawberries

9.1 Introduction

The importance of strawberry fruits as valuable sources of vitamin C, high dietary fibre and potent antioxidant in the daily diets of populations globally cannot be overstated. However, common spoilage issues, attributed to mainly fast deterioration, have been reported as serious and costly problems for strawberries in the supply chain, and specifically during transportation and storage (Chen & Martín-belloso, 2009). The fast loss of quality is associated with high volatilisation of the main components due to the delicate texture, coated by a very thin cuticle and presenting high susceptibility to physical damage, heterogeneity in firmness and a clear relationship between skin strength or fruit firmness and susceptibility to pathogen infection (Dong et al., 2013; Ferreira, Sargent, Brecht, & Chandler, 2008). Apart from loss of volatile compounds, strawberries are susceptible to a large variety of phytopathogenic organisms (Amil-Ruiz, Blanco-Portales, Munoz-Blanco, & Caballero, 2011). Fungi can directly penetrate strawberry fruit epidermal cells, or spread hyphae on top of, between or through cells. Pathogenic and symbiotic fungi and oomycetes ultimately invaginate feeding structures into the host cell plasma membrane, and thus cause fast spoilage particularly in conducive storage conditions. By contrast, strawberries, possess innate sources of inherited resistance to diseases that make them respond efficiently to pathogens due to induced mechanisms, which include cell wall reinforcement, production of reactive oxygen species, phytoalexin generation and pathogenesis-related protein accumulation (Amil-Ruiz et al., 2011). Nonetheless, in today's increased volumes and distribution of commercial strawberries, post-process contaminations that accrue from fungal spore-prone airborne and contact surface environments can override the naturally-inherent defence mechanisms. Ultimately, the control of fungal contamination of strawberry is very crucial.

Non-biodegradable plastic films have been, and are still, the main packaging protectors for most commercial berries, intended to maintain the processing benefits post-process and distribution chain wholesomeness of food products. These films are use-limited due to: (i) being non-degradable; (ii) the fact that fungal contamination could be intensified by moisture condensation on product and package surfaces that favour mould growth, (iii) inability to protect strawberries while exposed to conditions that high temperatures and possibly anoxia conditions in-package. Thus, proactive technological control measures are needed to avoid fungal contamination and create avenues for extending strawberries shelf-life, in particular

those that are subjected to high temperatures before use. In addition, packaging technology must balance food protection with mainly energy and material costs, social and environmental sensitivities, and regulated pollutants and disposed wastes (Marsh & Bugusu, 2007).

Plant bioactive extractives have known outstanding capabilities to preserve most food products, with potential to increase their shelf-life while in storage and distribution (Araújo & Bauab, 2012; Cox, 2012; Palou, Valencia-Chamorro, & Pérez-Gago, 2015; Sultanbawa, 2011; Valdés, Mellinas, Ramos, Garrigós, & Jiménez, 2014). Thymol is among the most popular plant essential oil bioactives for provision of antimicrobial and antioxidant properties (Ahmad, Khan, Yousuf, Khan, & Manzoor, 2010; Ezzat Abd El-Hack et al., 2016; Karoui, Msaada, Abderrabba, & Marzouk, 2016; Nostro et al., 2007; Šegvić Klarić, Kosalec, Mastelić, Piecková, & Pepeljnak, 2007; Zarrini, Delgosha, Moghaddam, & Shahverdi, 2010). Because thymol is known for its post-antimicrobial importance (Zarrini et al., 2010), this makes it suitable for use in fast spoiling strawberries that are destined for extended storage and transportation outside the cold chain. Unfortunately, thymol is limited in its application due to its low solubility character in water (Bilia et al., 2014; Shah, Davidson, & Zhong, 2012). As most matrices use water for their source of initial solutions, the need for alternative efficient thymol carriers has become a priority. Among the alternatives, Nano carriers (NC) have gained a lot of interest, and their use as encapsulating media is currently an exciting alternative strategy (Bilenler, Gokbulut, Sislioglu, & Karabulut, 2015; Blanco-Padilla, Soto, Hernandez Iturriaga, & Mendoza, 2014). The NC have advantages of ensuring antimicrobials security and compatibility in hostile environments, thereby enhancing their activity through controlled delivery and passive cellular absorption mechanism improvement (Blanco-Padilla et al., 2014).

Several encapsulating matrices for the improvement of the functional bioactive incorporation, biocompatibility and stability have been reported, such as: i) food grade colloidal delivery systems comprising of small lipid, phospholipid, and biopolymer particles; and ii) small particle colloidal excipient systems (Z. Zhang et al., 2016). The potential of colloidal systems to improve bioavailability with curcumin (Ting, Jiang, Ho, & Huang, 2014), stability and retention of chitosan films containing basil and thyme essential oil (Perdones, Chiralt, & Vargas, 2016) and thymol/carvacrol-encapsulated zein nanoparticles (Wu, Luo, & Wang, 2012) have been demonstrated. However, studies to validate these carriers/encapsulations of

antimicrobials and antioxidants are mainly limited to development, characterisations, suggestions and recommendations. Their application in active packaging of specific foods is also not significant. Besides, most of the carriers require extra enhancer chemicals and modifications in processes to make them soluble in encapsulations, and this might bring cost and energy implications in their development.

Intact bitter cassava polysaccharide-rich derivatives (PD) are low-cost and energy-efficient materials prepared via improved simultaneous release recovery cyanogenesis, which have potential application in food packaging due to their film-forming ability (Tumwesigye, Oliveira, & Sousa-Gallagher, 2016). However, PD materials have not be investigated for their suitability as carriers of antimicrobial bioactives in active packaging of foods. Their investigations as coating encapsulations of thymol in antifungal protection of strawberries may provide an alternative material for active packaging of food products. Furthermore, the fragility of strawberries to fast spoilage provides the ideal test or avenue to determine the effectiveness and performance of PD as suitable antifungal coatings.

The current study was intended to evaluate the capacity of intact bitter cassava polysaccharide-rich derivatives (PD) to encapsulate thymol effectively, and evaluate their antifungal effect and strength on stored strawberries using qualitative methods. Furthermore, ability of PD-thymol coatings as antioxidant material, their association with permeability to water vapour, and surface hydrophilicity/hydrophobicity were investigated. If the PD successively encapsulated more than 50% of thymol loaded, and protect highly-prone fungal products including those that rapidly undergo oxidation on exposure to air, the coating would be a novel matrix vehicle to encapsulate bioactive compounds for enhanced bioavailability, extended shelf-stability and controlled release.

9.2 Materials and methods

9.2.1 Materials

Intact bitter cassava was obtained from Northern Uganda, and its derivative saccharides, consisting of mainly starch, holocellulose, lignin, and traces of other chemicals, prepared as described in Tumwesigye, Oliveira, & Sousa-Gallagher, (2016). Thymol (≥ 99.0%), and

Ethyl acetate (anhydrous, 99.8%) were purchased from Sigma Ireland. All chemicals were used as received without further purification.

9.2.2 Preparation of PD-thymol coating dispersions

Preparation of PD-thymol coating entailed dispersing thymol (0.25, 0.5, 0.75 and 1.0 % w/v) into 100 ml prepared intact bitter cassava-glycerol solutions. Intact bitter cassava PD (2% w/v) and glycerol (40% w/w %) were mixed while stirring, heated to 70^{0}C for 20 min and cooled back to 37-40^{0}C using a trough of cold water. Thymol was added and the dispersion stirred at high shear speed (1,000 rpm) by overhead stirrer (Eurostar IKA Labortechnik, Germany) for 10 min. The PD and glycerol proportions were based on the optimised formulation for the film production as described in Tumwesigye, Montañez, Oliveira, & Sousa-Gallagher, (2016b). The control sample containing only PD (2% w/v) and glycerol (40% w/w %) was also prepared.

9.2.3 Coating characterisation

8.4.5.1 9.2.3.1 Thymol loading and encapsulation capacity

Thymol-loaded dispersion was dried at 25^{0}C for 9 hours, and milled using IKA Yellowline(R) A10 Analytical Grinder (California, USA) to obtain a powder. The powder (10 mg) was mixed with ethyl acetate (2 ml) under constant stirring in a shaking bath at 37 ^{0}C for I hour. Thymol has been reported to dissolve in ethyl acetate (Wu et al., 2012). The undissolved solids were removed during centrifugation at 3000 rpm for 15 min to obtain the supernatant. Concurrently, a solution containing pure thymol was dissolved in ethyl acetate, diluted into 6 serial solutions and used to obtain the standard curve at 274 nm (Norwitz &Keliher, 1986), defined by Eqn. 9.1.

$$A_{274} = s * T - C \qquad 9.1$$

where, A_{274}, the absorbance at 274 nm, s, slope from the standard curve of serial dilutions, T, the thymol concentration (mg/g) and C, the intercept.

Thymol concentration (T) was determined by measuring the absorbance of the supernatant in a UV-vis spectrophotometer at 274 nm and calculated using the standard curve (Eqn. 9.1).
The loading capacity was calculated as the encapsulated thymol weight fraction of the total solids, and reported as percentage.
The encapsulation capacity was calculated as the ratio of encapsulated thymol to the original thymol incorporated in the PD matrix, and reported as percentage.

8.4.5.2 9.2.3.2 Water vapour permeability

The permeability of the coating to water vapour was determined as described in Tumwesigye et al., 2016b) without modifications. Water vapour permeability (WVP) was determined gravimetrically at 38 °C, 95 % RH according to ASTM E96-05 (2005) method. Films for WVP were obtained from the coating dispersion, cast on 8.4-cm diameter dishes and dried at 25 ^{0}C, 9h, together with coated strawberries (subsection 2.4). Each previously conditioned (54 % RH, 23 ± 2 °C, at least 48 h) film was carefully positioned between acrylic permeation cell containing CaCl2 (0 % RH) and enclosed in a humidity-controlled plastic container partially filled with 1000 mL of KNO_3 salt solution, corresponding to a relative humidity of 95 %. The container was stored in temperature controlled incubator at 38 °C, and cell weight gain was recorded every 2 h for 10 h and used for WVP calculations. WVP was calculated using Eqn. 9.2.

$$\mathrm{WVP} = \frac{\acute{m}\delta}{[\mathrm{AP}(r_{95} - r_0)]} \qquad 9.2$$

where ḿ, mass flow rate (g/day); δ thickness (mm); A, cross-sectional area (m^2); P, saturation partial pressure at 38 °C (kPa) and $r_{95} - r_0$, relative humidity of outside environment (95 %) and cell (0 %). All tests were conducted in triplicate and mean values were used for calculating WVP.

8.4.5.3 9.2.3.3 Coating surface free energy and wettability

Coating surface free energy and wettability (SFEW) were assessed by determining the contact angle according to Tumwesigye et al., (2016a) without modifications. Measurement of contact angle (CA) was achieved using the sessile drop method by Optical tensiometer

(Theta, BiolinScientific Finland) at 25^{0}C, 50% RH. The Theta was equipped with a liquid dispenser holder fitted with a 0.5 mm diameter precision microsyringe steel needle, and OneAttension software for drop shape analysis and live measurements. A rectangular coating film strip (2 cm x 2 cm) was mounted on a pre-cleaned glass slide covered with double-sided tape, then placed on a horizontal holder at 90^{0}C to enable clear observation of film surface and cross-section. In addition to ensure that the correct CA was measured, a film strip was raised a bit from the surface of the slide. The syringe was positioned vertically 10 mm from the film surface and 2 mL deionized water drop automatically dispensed (1.0 ml s^{-1}) on the film. The measurements lasted 180 s and data was analysed for contact angle (θ). All films were conditioned (23 ± 2 ^{0}C, 50% RH, 48 h) prior to measurements and five measurements were carried out. Drop wetting, spreading and beading/shrinking away gives CA of 0, 0–90 and >90 ^{0}C respectively.

A CA of 0^{0}C; 0 < CA <90°C; 90^{0}C ≤ CA < 180^{0}C; and CA = 180^{0}C describe perfectly wetting (strong interaction); high wettability (strong/weak interaction); low wettability (weak interaction; and perfectly non-wetting (weakest interaction) respectively. Super hydrophobic contact surfaces (CA >150°C) demonstrates no contact between the liquid drop and the surface (Zheng & Lü, 2014).

9.2.4 Preparation of strawberry samples for coating, and antifungal analysis

8.4.5.4 9.2.4.1 Strawberry preparation and coating

Freshly purchased strawberries were cleaned of any dirt, disinfected and devoid of free surface water using a filter paper (Whatman no.2). Cleaned strawberries were dipped in freshly prepared PD-thymol coating dispersions (5 min), and air-dried (25^{0}C), while suspended for 6 h. A sample of uncoated strawberry itself was concurrently prepared, and served as a control. The triplicates of each sample were prepared.

8.4.5.5 9.2.4.2 Antifungal analysis

The antifungal impact of PD-thymol coatings was achieved qualitatively by observing the mould growth overtime on strawberries kept at 95% RH and 25^{0}C. In order to ensure the same mould inoculum for all the samples, strawberries were placed on dishes and kept in

controlled chambers. Photographs were taken on the samples every day until 21 days of storage. To ensure that the coated samples were exposed to high mould inoculum, they were kept together with those showing increase mould growth.

9.3 Results and discussion

9.3.1 Influence of bitter cassava and SRRC on thymol loading, encapsulation efficiency and stability

The PD-thymol coating dispersion properties at different thymol loading concentrations are presented in Table 9.1, showing that, regardless of loading level, all the dispersions demonstrated higher encapsulation efficiency, with over 95% explained by encapsulation technique. The encapsulation capacity (EC) showed proportionality to the loading capacity (LC), which was also concentration-dependent. The higher thymol entrapment for all loading levels might be explained by the steric hindrance against thymol droplet aggregation that could have been provided by PD polysaccharide moiety, thereby improving dispersions stability. Thymol is a hydrophobic compound only slightly soluble in water at neutral pH conditions provided by cassava PD, and in practice, overcoming solubility of thymol into cassava PD would require initial dispersion in an emulsifier. Unlike most polysaccharide emulsion systems which require emulsifiers in their industrial application (Glenn et al., 2010; Perdones et al., 2016) and ionic gelation (Avadi et al., 2010), strikingly, in this study, the cassava PD-thymol coating dispersion exhibited conditions of a perfect uniform emulsion system. Specifically, the presence of pectin and perhaps lignin in the PD powder matrix extracted at 12 months could account for the modulation of the emulsification to form stable dispersions. On the other, the pores created by inclusion of other polysaccharides in addition to could have facilitated absorption of thymol, and reduced evaporative loss of thymol during the drying of the PD-thymol coating dispersion.

Improved pore structures in PD are not only crucial permeation to water vapour and gases but the provision of a large surface area throughout the internal matrix compared to the external surfaces. This might also be the for better thymol sequestration within the matrix, and thus the degree of particle agglomeration and facilitating dispersion (Glenn et al., 2010). It can be

concluded that the inclusion of thymol provided strong cassava PD adsorption rather than chemical bonding, although weak bonding of thymol OH groups with the polymer could be possible.

9.3.2 Influence of PD-thymol coating on permeation to water vapour

The permeability to water vapour of cassava PD-thymol coating showed an inverse association with thymol concentration (Table 9.1). The trend observed could be attributed to reduced permeation voids resulting from occupation of the porous area by thymol. The slight decrease in water permeation imply that this could support reduced moisture loss of coated strawberries. Indeed, this was supported by low moisture values observed during the antifungal storage studies. Generally, all the samples showed low water permeation values compared to previous studies on intact bitter cassava films (Tumwesigye et al., 2016a).

Table 9.1. The impact of different thymol contents on coating loading and characteristics

Coating	**ET, mg/g**	**LC, %**	**EC, %**	**WVP, g mm /(M^2.day.kPa)**	**CA, ^{o}**
Cassava PD only	-	-	-	4.89	88.71
Cassava PD with thymol @ 0.25% w/v	0.10	7.4	95.8	3.89	95.48
Cassava PD with thymol @ 0.5% w/v	0.10	14.0	98.1	2.08	101.44
Cassava PD with thymol @ 0.75% w/v	0.09	19.8	98.9	1.66	111.26
Cassava PD with thymol @ 1.0% w/v	0.09	24.8	99.1	0.02	110.07

ET, encapsulated thymol; LC, loading capacity; EC, encapsulation efficiency, WVP, water vapour permeability, CA, contact angle

9.3.3 Effect thymol loading on coating surface free energy and wettability

To enhance the antifungal performances of products, the developed coatings should be compatible with the product surfaces in order to spread evenly and coat the product. The compatibility is assessed by the ability of the coating to enhance or reduce surface wettability (SW). In this study, SW was defined by the contact angle (Table 9.1, Fig 9.1). As was

observed, the contact angle (CA) increased as thymol concentration in the PD matrix increased. Since the degree of surface wetting is an inverse of the size of the CA, it can be said that the wettability decreased as thymol concentration increased. In spite, however, of the surface wetting reduction, all the coating samples still were within the interface of high/low wettability (defined by mid-strength solid/liquid interaction). This might explain the better and smooth coating of the strawberries observed (Fig 9.2 a). Unlike ideal surfaces which are perfectly smooth and chemically homogeneous, strawberries have somewhat rugged surface, and thus the results observed is most likely due to their structural topography.

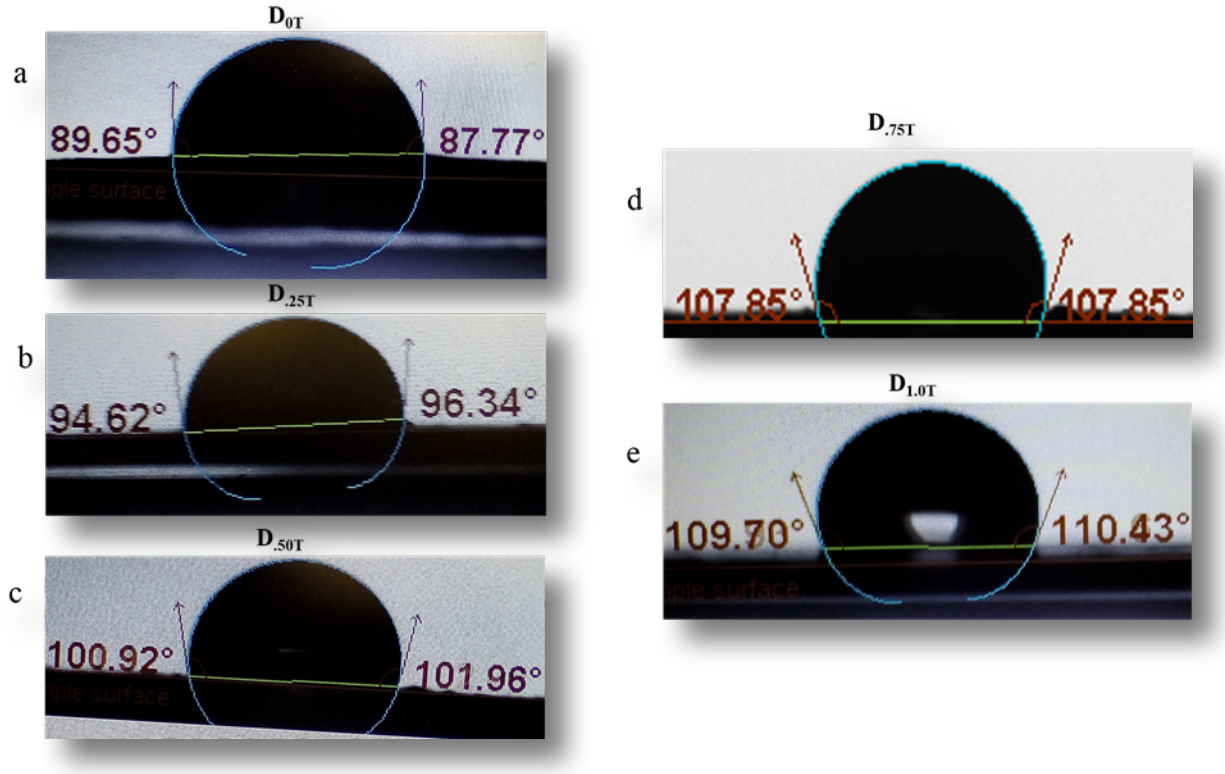


Fig 9.1. Measured contact angles for different thymol loadings: a) control ($D_{0.0T}$); b) 0.25% Thymol ($D_{.25T}$); c) 0.5% Thymol ($D_{.5T}$); d) 0.75% Thymol ($D_{.75T}$); and e) 1.0% Thymol ($D_{1.0T}$).

9.3.4 Impact of PD-thymol coating on mould growth inhibition in storage strawberries

The qualitative results of the mould growth-inhibition by PD-thymol coating on strawberries is illustrated in Fig 9.2b, showing no inhibition on uncoated samples and significant inhibition on coated ones during the 14 days in storage. The two-point (0 day & 14 day)

experiment was used to illustrate the notable inhibition, nonetheless, uncoated strawberries exhibited mould growth after 48 hours of storage at 25^0C, 95% RH.

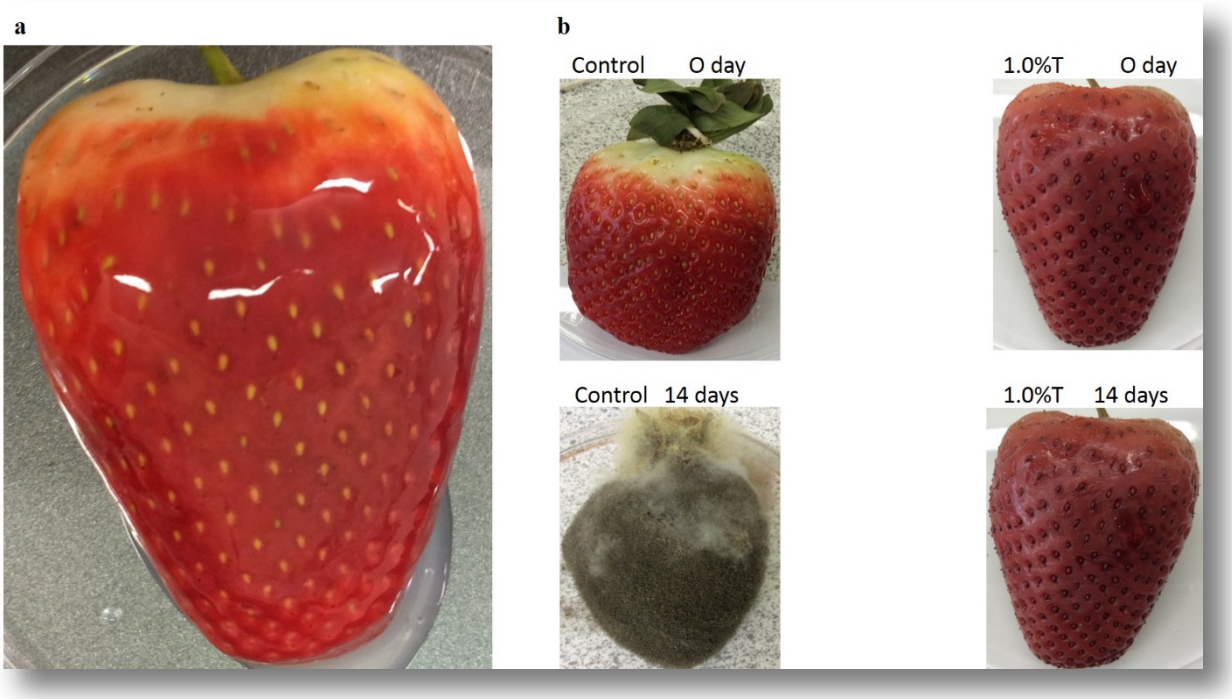


Fig 9.2. An illustrated example of uniform distribution of coating (a) and uncoated (control) and coated with 1.0% Thymol (b) strawberries showing the effect of antifungal activitity.

Qualitative tests give a general indication of a cause, which can be validated with the quantitative tests. Fortunately, in this study, the use of qualitative method is in line with the commercial consumer's initial perception of the spoilage of strawberries.

The significant growth inhibition observed with coated strawberries could be associated with uniformity of coating (Fig 9.2a), but also could be attributed to the better entrapment of thymol in the PD matrix. Equally, the reduced permeation to water vapour due to more hydrophobicity in the coatings might also improve the coatings antifungal capacity. Thus, quantitative studies are essential to analyse the antifungal activity of the coatings, and the spoilage fungi species inhibition, as a function of the thymol loading levels.

Conclusion

Coatings formulated with four intact bitter cassava polysaccharide-rich derivatives and thymol provided exciting results with respect to their encapsulation capacity and stability. All of them exhibited very efficient encapsulation capacity, as shown by higher scores above 95%. Moreover, the steric hindrance phenomenon against thymol droplet aggregation provided the necessary dispersions' stability and uniformity, which governed overall coating patterns.

The coating permeability to water vapour and surface wetting for all concentration levels were intermediate and slightly above medium. A very perfect antifungal inhibition was found for strawberry-coated surfaces, with the result that the fruits remained uninfected beyond 14 days, which was greatly dependent on the stability and reasonable uniformity of surface-wetting during coating.

The stability of the coating, supported by medium water vapour permeability at the hydrophobic-hydrophilic interface and the perfect antifungal ability, can allow their use in broad spectrum antimicrobial applications in commercial systems. These results have significant implications for the design of antifungal systems based on intact bitter cassava/natural bioactive-coating dispersions. Nonetheless, further investigations are needed to address the quantitative analysis, and gain insights into the specific fungi, before full application of the coatings.

General conclusion, outcomes and recommendations for future work

This section highlights the main conclusion that can be drawn from this study, and suggest the future perspectives, with the objective to augment knowledge in the broad area of cassava biobased material research and application.

General conclusion

Sweet cassava has been extensively studied, mostly in the development and improvement of edible films and coatings. The production of its derivative starch using conventional methods is associated with environmental wastes. Different approaches such as fillers, bioactive compounds and chemical modifications have been used to improve structural and functional properties of biobased materials, mainly starch. This has escalated the costs and energy of material production. Together with absence of evaluations for intended application conditions such as in-package environment under real conditions, the exploration of these materials in commercial use, mainly food packaging, has been challenging. Notwithstanding the challenges, there is a great potential of cassava biobased materials in wide-range applications. In particular, if holistic approaches are integrated in the material development towards applications.

Overall, the work in this research focused on developing an integrated sustainable process system for cassava biobased materials intended for broad range applications. Specifically, the research was concentrated on developing an improved downstream cassava processing methodology, known as simultaneous release recovery cyanogenesis (SRRC). Using SRRC, the utilisation of intact bitter cassava has assisted exploitation of intrinsic advantages inherent in cassava for modifying and optimising its polysaccharide-rich derivatives for multifunctional applications in packaging films, coatings as well as nutraceuticals. Further, this created a generic technique/methodology that can be tailored to specific product processing requirements. The selection of SRRC was based on the understanding the challenges faced by conventional methodologies to minimise waste, create quality desired cassava biomaterials, and ensure uniform and polymeric materials for tailor-made applications.

Accordingly, intact bitter cassava (IBC) was studied using SRRC, and compared with the peeled counterpart, which is traditionally used in the development of starch-based products. It was found that IBC and SRRC can be used as sustainable, safe, integrative process solution for high value-added product production from low-cost biobased materials. This resulted in significant waste reduction, safe biopolymer with distinctly white material suitable for any application. Further to this, demonstration of the potential application of IBC derivatives for development of transparent and flexible films was shown. Using SRRC and intact bitter cassava proved that there is no need for peeling prior to processing, and this could save commitment of human and monetary resources and time resulting in cheap materials for food and non-food applications.

A standardised simple, integrated methodology for efficient and low-cost production of biopolymer derivatives (BPD) from novel intact bitter cassava was successfully developed. The methodology showed unique advantages of minimising wastes and providing higher quantities of derivative material compared to a commercial method using sweet cassava. The methodology showed promise as a sustainable choice for use in industrial materials due to the shortening of derivative preparation steps, production, reinforcements and modifications, as separate entities that increase energy. Furthermore, the methodology produced derivatives with desired properties such as uniform microstructure, high thermal stability, and good barrier properties with potential broad range of applications.

The transport phenomenon of fluids and solvents in humidity- temperature-stressed intact bitter cassava (IBC) films was assessed by qualitative and mechanistic techniques, and related to the structural characteristics of interactions. Results showed that (IBC) films possessed wide variable permeability to fluids due to extensive pore size, which can be explored for packaging a broad spectrum of products. Peleg, modified BET, Oswin and Forran-Fontan equations were shown as the best models to describe sorption behaviour of IBC films. Temperature and humidity have more impact on water vapour and oxygen permeation through IBC films. Thus, care need to be taken to avoid exposure at high relative humidity. The mass transfer mechanism of water through IBC films at 75% RH and 95% RH was found to obey case II non-Fickian pattern, which is a good indication of commercial use since water diffusion in most existing commercial materials follow a non-Fickian trend. Similarly, the mass transfer mechanism by toluene and paraffin oil followed Fickian diffusion, meant that the IBC films supports their use in commercial settings. The results

proved that novel BC and SRRC have a significant impact on the IBC films that enhance solvents' ability to induce structural changes in IBC films. Because the integrity of the cassava biobased film packages are dependent on the host environment, extreme care should be ensured to minimise environment effects in the distribution chain.

Packaging films were produced from intact bitter cassava, and optimised in order to obtain desirable properties. Desirability optimisation provided 2 % w/v cassava derivative, 40.0 % w/w glycerol, and 50°C drying temperature as ideal parameters for optimal film development. Optimal film properties are: 0.3 %; transparency, 3.4 %; solubility, 21.8 %; water-vapour-permeability, 4.2 $gmm.M^{-2}.day^{-1}kPa^{-1}$; glass transition, 56°C; melting temperature, 212.6°C; tensile strength, 16.3 MPa; elongation, 133.3%; elastic modulus, 5.1 MPa; puncture resistance, 57.9 J. With optimised parameters and properties, a set of empirical equations can be used to for tailoring films to specific packaging applications.

A new sustainable approach for potential utilisation of cassava waste and reduction of their environment impact using an integrated seven unit process design was developed. Integrating models in the design demonstrated use of intact root and SRRC as an effective tool for green cassava production processes. Moreover, the integrated process design has the advantage of rational use of energy and water through reuse of wastewaters in the reactions and release processes. The strategy allowed integration of non-heat drying with laminar flow hood air systems in the design process. Thus, the integrated process design could be used as a green tool in production of cassava products with near zero environmental waste disposal. It is a promising tool that can be used to improve small-to-medium-scale batch processing of cassava and deliver benefits to commercial trade and environment.

An optimised, standardised and integrated engineering design structural framework for cassava biobased materials has been achieved. This will serve as a design model for disabling cassava toxicity, eliminating waste, providing inexpensive and energy-efficient material production, and ensuring sustainable systems for cassava biomaterial development.

Application of biopolymer flexible films for the development of desired atmosphere packaging to extend shelf life of cherry tomatoes was demonstrated. The attainment of recommended equilibrium headspace O_2 composition indicate that it is not critical to perforate IBC films during EMAP development. The significant unsettling of equilibrium

headspace O_2 composition by temperature and RH suggest that care must be exercised when IBCF packages are placed under real conditions during the distribution chain. The optional requirement of perforations for IBC than OPP films is an advantage of these films to be deployed as alternative film packages for fresh produce. The targeted desirability value of 3.73% headspace oxygen and delayed mould growth on tomatoes showed great capability for application of IBC film in EMAP designs of fresh produce.

The study highlights potential of intact bitter cassava polysaccharide-rich derivatives (IBC PD) as an excipient that can enhance fast releases of Iron and zinc. The study showed that IBC PD possesses superior tableting properties than one obtained from peeled equivalent, and is comparable with commonly used microcrystalline cellulose. The recovered biomaterial from waste cassava may provide broader applications as potential alternative nutraceutical excipients. Furthermore, the IBC PD is compatible with acidic and neutral pH during the delivery of Fe and Zn, but cannot alone deliver requisite conditions for full tableting. Using SRRC-processed powder as tableting starting material greatly enhances dissolution system with fast and full releases of Iron and zinc within 30 to 45 min. The recovered biomaterial from waste cassava may provide broader applications as potential alternative nutraceutical excipients.

Application of biopolymer coatings for antifungal active food packaging was demonstrated with four intact bitter cassava polysaccharide-rich derivatives (IBC PD). The coatings presented thymol encapsulation efficiency above 95%. The IBC PD provided better coating patterns due stable and uniform dispersions, and this resulted into better coating permeability to water vapour and surface wetting. As a result of stability and uniformity of dispersions, IBC PD coatings exhibited better antifungal inhibition beyond 14 days. This is an advantage to traders bearing in mind that non-coated strawberries subjected to real supply chain conditions might not last beyond 48 h. The stability of the coating, supported by medium water vapour permeability at the hydrophobic-hydrophilic interface and the perfect antifungal ability, can allow their use in broad spectrum antimicrobial applications in commercial systems.

The results have significant implications for the design of antifungal systems based on intact bitter cassava/natural bioactive-coating dispersions.

Methodologies designed around standard integrated procedures, matching zero-based approach to contamination elimination, are novel strategies, and if they are used effectively and widely can provide better avenues to eliminate cassava wastes and recover BPD resources as sustainable biomaterials.

Outcomes

1. Mitigating the challenging issue of cyanogens in bitter cassava provides a promise for use in bioderivative development and other applications, but also a paradigm of economic and well-being of communities which use bitter cassava
2. Intact bitter cassava use leads to zero waste, and will help to reshape the current style one-way processing designs into a circular designs modelled on nature's effective approaches. This will also benefit SME processing units achieve a local system that functions efficiently, sustains the environment, and delivers self-sufficiency. Moreover, this will lead to indirect waste elimination instead of waste management.
3. Inclusion of indigenous cassava components as material reinforcements for bioderivatives
4. The SRRC is a novel improvement approach to downstream processing of novel bio-derived products
5. Other potential applications:
    i. In proper by-product's regulation for waste elimination, reduction in costs of waste manage and recycling,
    ii. Generally, in processes which require efficient use of energy resources, reduction in cost of production, and other product integration process designs;
    iii. Development of tailored materials for both food and non-food uses such as:
    iv. Edible and non-edible food packaging films and coatings;
    v. Biobased bags for waste management and replacement of food plastics in the market;
    vi. As ingredients in food industry and excipients in drug delivery;
6. Ultimately, this has initiated a process which may lead to a wider utilisation in broad product research development.
7. Finally, the research contributes to scientific knowledge in material science and engineering process design.

Recommendations for future work

The study demonstrated that the polysaccharide nature and composition of intact bitter cassava derivatives is crucial to customised functional application. Thus, the selection of bitter cassava should be revisited to address maturity, amount of its polysaccharides chemical composition determined, and further improvements in processing using SRRC. In particular, the release stages, polysaccharides require further functionalisation or reduction in order to target the final functions of derivatives.

Biobased materials prepared with intact bitter cassava showed great potential for broad range application in food and non-food, particularly for flexible food packaging materials, coatings for active packaging, and excipients for nutraceutical delivery. While the aim of this study was a proof of concept to develop film prototypes from intact bitter cassava, the film production could be potentially scale up in medium and high scale industrial production of biomaterials. In addition, film individual unique properties such as reasonable mechanical strength, thermal stability, better sealability and resistant to water at low to medium relative humidity. These studies need further in-depth evaluations for their compliance, both in vitro and under supply chain conditions.

The standardised integrated methodology was found to match zero-based approach to contamination elimination when used effectively. In future, and as a follow-up to this study, the methodology can be studied for eliminating wastes and recovering resources as sustainable biomaterials in all systems that generate byproduct wastes to the environment.

Optimisation of films by desirability provided a scope in which tailor-made films can be developed. These require further studies to validate them at commercial level in real conditions.

The successful development of the integrated process design proved that the feasibility of using it in large scale processing can be possible. This would require further studies to improve the efficiency of the integrated process, perhaps using pinch analysis and mathematical optimisations.

A broad range application potential of cassava biobased materials has been demonstrated. An example is the potential application of flexible packaging films in the design of equilibrium atmosphere packaging. Although the films showed compliance in recommended supply chain temperature of 10 ^{o}C for fresh produce, they are prone to high relative humidity. Such conditions, referred to as “abuse” are more often encountered in the supply chain. Thus,

further studies on the validation of the impact of external environments on EMAP of IBCD are necessary. The integrity of the cassava biobased films will depend on the host environment, and maximum care should be ensured to minimise environment effects in the distribution chain.

To ensure compliance of IBC films in the distribution chain, (i) thermal and structural tests should be a must in developing biobased materials; and (ii) validation of films in conditions for their targeted use should be taken as a priority.
The compatibility of IBC films with EMAP design is good news for widening alternative materials for packaging fresh produce. But more research is needed to validate the desirable value under stress conditions of the supply chain.

The SRRC-assisted production of biopolymer derivatives was found to be insufficient to produce materials for nutraceutical excipients, although SRRC provides an advantage of an alternative inexpensive starting material. The deficits might be due to the way recovery stage, particularly drying, is done. Thus, there is need to further reinforcement PD with standard tableting processes to improve flowability and tableting capacity. This can be via controlled drying of derivatives using spray-drying techniques, and subsequent granulation should be investigated.

The study demonstrated significant implications for the design of antifungal systems based on intact bitter cassava/natural bioactive-coating dispersions. Further investigations are needed to address the quantitative analysis, and gain insights into the specific fungi, before full application of the coatings.

The film unique properties such as reasonable mechanical strength, thermal stability, better sealability and resistant to water at low to medium relative humidity should be explored and exploited for application of cassava biobased materials in packaging of dry products, biobased bags and shopping bags. These could have a bigger impact on the current challenges posed to the environment by plastic packaging materials.

Lastly, cassava biobased materials should be improved using a holistic approach reflecting the target products, variable environment, minimising production costs and energy. Use of novel material resources, eliminating waste, and employing a standardised methodology via desirability optimisation, present a promising process integration tool for development of sustainable cassava biobased systems.

References

Abdellatief, A., Butler, J., Teixeira, A., Welt, B., McLamore, E., & Shukla, S. (2015). Predictive Modeling of Oxygen Transmission Through Micro-perforations for Packaging Applications. *Journal of Applied Packaging Research*, *7*(2), 17–31.

Adeola, F. (2011). *Hazardous Wastes, Industrial Disasters, and Environmental Health Risks - Local and Global Environmental Struggles*. (F. Adeola, Ed.) (1st ed.). New York: Palgrave MacMillan: St. Martin's Press LLC.

Adetunji, A. R., Isadare, D. A., Akinluwade, K. J., & Adewoye, O. O. (2015). Waste-to-Wealth Applications of Cassava – A Review Study of Industrial and Agricultural Applications. *Advances in Research*, *4*(4), 212–229.

Aggarwal, A., Singh, H., Kumar, P., & Singh, M. (2009). Simultaneous optimisation of conflicting responses for CNC turned parts using desirability function. *International Journal of Manufacturing Technology and Management*, *18*(3), 319–332.

Ahmad, A., Khan, A., Yousuf, S., Khan, L. A., & Manzoor, N. (2010). Proton translocating ATPase mediated fungicidal activity of eugenol and thymol. *Fitoterapia*, *81*(8), 1157–1162.

Akinpelu, A.O. L. E.F. Amamgbo, A.O. Olojede, A. S. O. (2011). Health implications of cassava production and consumption. *Journal of Agriculture and Social Research*, *11*(1), 118–125.

Alves, V. D., Mali, S., Beléia, A., & Grossmann, M. V. E. (2007). Effect of glycerol and amylose enrichment on cassava starch film properties. *Journal of Food Engineering*, *78*(3), 941–946.

American Society for Testing and Materials. (1998). Standard Test Method for Tensile Properties of Plastics. ASTM.

Amil-Ruiz, F., Blanco-Portales, R., Munoz-Blanco, J., & Caballero, J. L. (2011). The strawberry plant defense mechanism: A molecular review. *Plant and Cell Physiology*, *52*(11), 1873–1903.

Anderson, D. M. (2014). *Design for manufacturability: How to use concurrent engineering to rapidly develop low-cost, high-quality products for lean production*. (D. M. Anderson, Ed.). CRC press.

Araújo, M. G. de F., & Bauab, T. M. (2012). Microbial Quality of Medicinal Plant Materials. *Latest Research into Quality Control*, 67–81.

Argüello-García, E., Solorza-Feria, J., Rendón-Villalobos, J. R., Rodríguez-González, F., Jiménez-Pérez, A., & Flores-Huicochea, E. (2014). Properties of edible films based on oxidized starch and zein. *International Journal of Polymer Science*, Article ID 292404, 1–9.

Arismendi, C., Chillo, S., Conte, A., Del Nobile, M. A., Flores, S., & Gerschenson, L. N. (2013). Optimization of physical properties of xanthan gum/tapioca starch edible matrices containing potassium sorbate and evaluation of its antimicrobial effectiveness. *LWT - Food Science and Technology*, *53*(1), 290–296.

Aro, S. O., Aletor, V. A., Tewe, O. O., & Agbede, J. O. (2010). Nutritional potentials of cassava tuber wastes: A case study of a cassava starch processing factory in south-western Nigeria. *Livestock Research for Rural Development*, *22*(11), 42–47.

Arrhenius, S. A. (1874). *Chambers's encyclopaedia*. (George Newnes, Ed.). London.

ASTM E96/E96M-05. (2005). E96/E96M-05. *Standard Test Method for Water Vapor Transmission of Material. American Society for Testing and Materials, Philadelphia*.

ASTM, F. (2016). Standard Test Method for Seal Strength of Flexible Barrier Materials. In ASTM D (Ed.), *Book of standards*. West Conshohocken, PA USA: Google Patents.

ASTM, S. (2009). D882-09 (2009)." Standard Test Method for Tensile Properties of Thin Plastic Sheeting", ASTM International, West Conshohocken, PA.

Ataeefard, M., Moradian, S., Mirabedini, M., Ebrahimi, M., & Asiaban, S. (2009). Investigating the effect of power/time in the wettability of Ar and O2 gas plasma-treated low-density polyethylene. *Progress in Organic Coatings*, *64*(4), 482–488.

Avadi, M. R., Sadeghi, A. M. M., Mohammadpour, N., Abedin, S., Atyabi, F., Dinarvand, R., & Rafiee-Tehrani, M. (2010). Preparation and characterization of insulin nanoparticles using chitosan and Arabic gum with ionic gelation method. *Nanomedicine: Nanotechnology, Biology, and Medicine*, *6*(1), 58–63.

Azwa, Z. N., Yousif, B. F., Manalo, A. C., & Karunasena, W. (2013). A review on the degradability of polymeric composites based on natural fibres. *Materials & Design*, *47*, 424–442.

Babayemi, O. J., Ifut, O. J., Inyang, U. A., & Isaac, L. J. (2010). Quality and chemical composition of cassava wastes ensiled with Albizia saman pods. *Agricultural Journal*, *5*(3), 225–228.

Barlkani, M., & Hepburn, C. (1992). Determination of crosslink density by swelling in the castable polyurethane elastomer based on 1/4-cyclohexane diisocyanate and para-

phenylene. *Iranian J. of Polym. Sci. & Tech*, *1*(1), 1–5.

Bartz, J. A., Sargent, S. A., & Scott, J. W. (2012). Postharvest Quality and Decay Incidence among Tomato Fruit as Affected by Weather and Cultural, (July), 1–8.

Bedane, A. H., Huang, Q., Xiao, H., & Elc, M. (2012). Mass transfer of water vapor, carbon dioxide and oxygen on modified cellulose fiber-based materials. *Nordic Pulp and Paper Research Journal*, *27*(02), 409–417.

Belibi, P. C., Daou, T. J., Ndjaka, J. M. B., Nsom, B., Michelin, L., & Durand, B. (2014). A Comparative Study of Some Properties of Cassava and Tree Cassava Starch Films. *Physics Procedia*, *55*, 220–226.

Benali, M., & Boumghar, Y. (2015). Supercritical-assisted drying. In A. S. Mujumdar (Ed.), *Handbook of industrial drying* (4th ed., pp. 1261–1270). New York: CRC Press.

Beninca, M., Trierweiler, J. O., & Secchi, A. R. (2011). Heat integration of an Olefins Plant: Pinch Analysis and mathematical optimization working together. *Brazilian Journal of Chemical Engineering*, *28*(1), 101–116.

Bilenler, T., Gokbulut, I., Sislioglu, K., & Karabulut, I. (2015). Antioxidant and antimicrobial properties of thyme essential oil encapsulated in zein particles. *Flavour and Fragrance Journal*, (April), 392–398.

Bilia, A. R., Guccione, C., Isacchi, B., Righeschi, C., Firenzuoli, F., & Bergonzi, M. C. (2014). Essential oils loaded in nanosystems: A developing strategy for a successful therapeutic approach. *Evidence-Based Complementary and Alternative Medicine*, *2014*.

Blanco-Padilla, A., Soto, K. M., Hern??ndez Iturriaga, M., & Mendoza, S. (2014). Food antimicrobials nanocarriers. *Scientific World Journal*, *2014*.

Blazek, J., & Copeland, L. (2009). Effect of monopalmitin on pasting properties of wheat starches with varying amylose content. *Carbohydrate Polymers*, *78*(1), 131–136.

Bodirlau, R., Teaca, C. A., & Spiridon, I. (2013). Influence of natural fillers on the properties of starch-based biocomposite films. *Composites Part B: Engineering*, *44*(1), 575–583.

Bradbury, M. G., Egan, S. V., & Bradbury, J. H. (1999). Picrate paper kits for determination of total cyanogens in cassava roots and all forms of cyanogens in cassava products. *Journal of the Science of Food and Agriculture*, *79*(4), 593–601.

Bradbury, M. G., Egan, S. V, & Bradbury, J. H. (1999). Determination of all forms of cyanogens in cassava roots and cassava products using picrate paper kits. *J. Sci. Food Agric*, *79*(4), 593–601.

Bristow, G. M., & Watson, W. F. (1958). Cohesive energy densities of polymers. Part 1.—

Cohesive energy densities of rubbers by swelling measurements. *Transactions of the Faraday Society*, *54*, 1731–1741.

Brown, Z. K., Fryer, P. J., Norton, I. T., & Bridson, R. H. (2010). Drying of agar gels using supercritical carbon dioxide. *The Journal of Supercritical Fluids*, *54*(1), 89–95.

Brunauer, S. (1943). Adsorption of gases and vapors.

Burke, J. (1984). *Solubility parameters: theory and application*. (J. Burke, Ed.). Waahington DC: The Book and Paper Group of the American Institute for Conservation.

Burns, A., Gleadow, R., Cliff, J., Zacarias, A., & Cavagnaro, T. (2010). Cassava: The drought, war and famine crop in a changing world. *Sustainability*, *2*(11), 3572–3607.

Campos, C. A., Gerschenson, L. N., & Flores, S. K. (2011). Development of Edible Films and Coatings with Antimicrobial Activity. *Food and Bioprocess Technology*, *4*(6), 849–875.

Canning, K., & Co, A. (2000). Edge Effects in Film Casting of Molten Polymers. *Journal of Plastic Film and Sheeting*, *16*(3), 188–203.

Cao, F., Amidon, G. L., Rodriguez-Hornedo, N., & Amidon, G. E. (2016). Mechanistic Analysis of Cocrystal Dissolution as a Function of pH and Micellar Solubilization. *Molecular Pharmaceutics*, acs.molpharmaceut.5b00862.

Cardoso, A. P., Mirione, E., Ernesto, M., Massaza, F., Cliff, J., Rezaul Haque, M., & Bradbury, J. H. (2005). Processing of cassava roots to remove cyanogens. *Journal of Food Composition and Analysis*, *18*(5), 451–460.

Castro de Cruz, E. (2012). Development and characterization of edible films based on cassava starch-glycerol blends to incorporate nutraceuticals. New Jersey: Rutgers University-Graduate School-New Brunswick.

Cereda, M. P., & Mattos, M. C. Y. (1996). Linamarin: the toxic compound of cassava. *Journal of Venomous Animals and Toxins*, *2*(1), 6–12.

Cerqueira, M. A., Sousa-Gallagher, M. J., Macedo, I., Rodriguez-Aguilera, R., Souza, B. W. S., Teixeira, J. A., & Vicente, A. A. (2010). Use of galactomannan edible coating application and storage temperature for prolonging shelf-life of “Regional” cheese. *Journal of Food Engineering*, *97*(1), 87–94.

Chapin, L. J. G., Wang, Y., Lutton, E., & Gardener, B. B. M. (2006). Distribution and Fungicide Sensitivity of Fungal Pathogens Causing Anthracnose-like Lesions on Tomatoes Grown in Ohio. *Plant Disease*, *90*(4), 397–403. http://doi.org/10.1094/PD-90-0397

Chen, C.-C., & Morey, R. V. (1989). Comparison of four EMC/ERH equations. *Transactions of the ASAE*, *32*(3), 983–990.

Chen, F., & Martín-belloso, O. (2009). HANDBOOK OF FRUIT AND Edited by, *25*(C), 2005–2009.

Chen, M. J., Cheng, L. H., Tseng, T. P., Huang, Y. S., Lin, C. H., & Lai, C. H. (2015). Modelling the transport of toluene liquid in protective polymer gloves using a fluorescent dye-tracing technique. *European Polymer Journal*, *66*, 407–418.

Cheng, L. H., Chen, M. J., Cheng, W. H., Lin, C. H., & Lai, C. H. (2012). Mass transfer of toluene vapor through protective polymer gloves. *Journal of Membrane Science*, *409-410*, 180–190.

Chinma, C. E., Ariahu, C. C., & Abu, J. O. (2013). Chemical composition, functional and pasting properties of cassava starch and soy protein concentrate blends. *Journal of Food Science and Technology*, *50*(6), 1179–1185.

Chiwona-Karltun, L., Mkumbira, J., Saka, J., Bovin, M., Mahungu, N. M., & Rosling, H. (1998). The importance of being bitter—a qualitative study on cassava cultivar preference in Malawi. *Ecology of Food and Nutrition*, *37*(3), 219–245.

Chowdhury, M. M. I., Huda, M. D., Hossain, M. A., & Hassan, M. S. (2006). Moisture sorption isotherms for mungbean (Vigna radiata L). *Journal of Food Engineering*, *74(4)*, 462–467.

Chowhan, Z. T., & Chi, L. H. (1986). Drug-excipient interactions resulting from powder mixing. III: Solid state properties and their effect on drug dissolution. *Journal of Pharmaceutical Sciences*, *75*(6), 534–41.

CODEX. (2013). *Proposed draft code of practice to reduce the presence of hydrocyanic acid in cassava and cassava products. Joint Food, W H O Programme, Standards Committee, Codex Contaminantsfoods, O N Session, Seventh Federation, Russian Draft, Proposed Levels, Maximum*. Moscow Russia.

Coombs, J., & Hall, K. (2000). *Non-Food Agro-Industrial Research Information. CD–rom version 1.2, issue 3, 2000 (ISSN 1368–6755, ISBN 1-872691-27-7)* (CD–rom ver). CPL Publishing Services, Newbury, UK.

Cooper, A. I. (2003). Porous materials and supercritical fluids. *Advanced Materials*, *15*(13), 1049–1059.

Costa, S. S., Druzian, J. I., Machado, B. A. S., De Souza, C. O., & Guimaraes, A. G. (2014). Bi-functional biobased packing of the cassava starch, glycerol, licuri nanocellulose and

red propolis. *PLoS ONE*, *9*(11).

Cotten, C., & Reed, J. L. (2013). Mechanistic analysis of multi-omics datasets to generate kinetic parameters for constraint-based metabolic models. *BMC Bioinformatics*, *14*(1), 32.

Cox, S. (2012). An Investigation of the Bioactivity of Irish Seaweeds and Potential Applications as Nutraceuticals . An Investigation of the Bioactivity of Irish Seaweeds and Potential Applications as Nutraceuticals, (June), 377.

Crank, J. (1979). *The mathematics of diffusion*. (J. Crank, Ed.) (2nd ed.). New York: Oxford university press.

Crowe, J., & Bradshaw, T. (2014). *Chemistry for the biosciences: the essential concepts*. Oxford University Press.

Curtzwiler, G., Vorst, K., Palmer, S., & Brown, J. W. (2008). Characterization of current environmentally-friendly films. *Journal of Plastic Film & Sheeting*, *24*(3-4), 213–226.

Tumwesigye, S. K. (2014). Three decades of toxic cyanide management in Uganda. Doing and communicating more with minimal strategies. Has it been possible? Working together to eliminate cyanide poisoning, konzo and tropical ataxic neuropathy (TAN). In *Cassava Cyanide Diseases & Neurolathyrism Network* (p. 12).

Daud, Z., Kassim, A. S. M., Aripin, A. M., Awang, H., & Hatta, M. Z. M. (2013). Chemical Composition and Morphological of Cocoa Pod Husks and Cassava Peels for Pulp and Paper Production. *Australian Journal of Basic and Applied Sciences*, *7*(9), 406–411.

De Meuter, P., Amelrijckx, J., Rahier, H., & Van Mele, B. (1999). Isothermal crystallization of concentrated amorphous starch systems measured by modulated differential scanning calorimetry. *Journal of Polymer Science, Part B: Polymer Physics*, *37*(20), 2881–2892.

de Moraes, J. O., Muller, C. M. O., & Laurindo, J. B. (2012). Influence of the simultaneous addition of bentonite and cellulose fibers on the mechanical and barrier properties of starch composite-films. *Food Science and Technology International*, *18*(1), 35–45.

de Moraes, J. O., Scheibe, A. S., Augusto, B., Carciofi, M., & Laurindo, J. B. (2015). Conductive drying of starch-fiber films prepared by tape casting: Drying rates and film properties. *LWT - Food Science and Technology*, *64*(1), 356–366.

de Moraes, J. O., Scheibe, A. S., Sereno, A., & Laurindo, J. B. (2013). Scale-up of the production of cassava starch based films using tape-casting. *Journal of Food Engineering*, *119*(4), 800–808.

De Pauli, R. B., Quast, L. B., Demiate, I. M., & Sakanaka, L. S. (2011). Production and

characterization of oxidized cassava starch (Manihot esculenta Crantz) biodegradable films. *Starch/Staerke*, *63*(10), 595–603.

de Souza, A. C., Dias, A. M. A., Sousa, H. C., & Tadini, C. C. (2014). Impregnation of cinnamaldehyde into cassava starch biocomposite films using supercritical fluid technology for the development of food active packaging. *Carbohydrate Polymers*, *102*, 830–7.

Debiagi, F., Kobayashi, R. K. T., Nakazato, G., Panagio, L. A., & Mali, S. (2014). Biodegradable active packaging based on cassava bagasse, polyvinyl alcohol and essential oils. *Industrial Crops and Products*, *52*(JANUARY), 664–670.

Denry, I., Holloway, J. A., & Gupta, P. K. (2012). Effect of crystallization heat treatment on the microstructure of niobium-doped fluorapatite glass-ceramics. *Journal of Biomedical Materials Research - Part B Applied Biomaterials*, *100 B*(5), 1198–1205.

Derringer, G. (1980). Simultaneous optimization of several response variables. *Journal of Quality Technology*, *12*, 214–219.

Dias, A. M. A., Braga, M. E. M., Seabra, I. J., Ferreira, P., Gil, M. H., & de Sousa, H. C. (2011). Development of natural-based wound dressings impregnated with bioactive compounds and using supercritical carbon dioxide. *International Journal of Pharmaceutics*, *408*(1-2), 9–19.

Dong, D., Zhao, C., Zheng, W., Wang, W., Zhao, X., & Jiao, L. (2013). Analyzing strawberry spoilage via its volatile compounds using longpath Fourier transform infrared spectroscopy. *Scientific Reports*, *3*(c), 2585.

Doporto, M. C., Dini, C., Mugridge, A., Viña, S. Z., & García, M. A. (2012). Physicochemical, thermal and sorption properties of nutritionally differentiated flours and starches. *Journal of Food Engineering*, *113*(4), 569–576.

Dürig, T., Venkatesh, G. M., & Fassihi, R. (1999). An investigation into the erosion behaviour of a high drug-load (85%) particulate system designed for an extended-release matrix tablet. Analysis of erosion kinetics in conjunction with variations in lubrication, porosity and compaction rate. *The Journal of Pharmacy and Pharmacology*, *51*(10), 1085–92.

E104, A. (2012). Standard practice for maintaining constant relative humidity by means of aqueous solutions. *ASTM. American Society for Testing and L\/laterials*, *2*, 5.

Edama, N. A., Sulaiman, A., & Abd.Rahim, N. S. (2014). Enzymatic saccharification of Tapioca processing wastes into biosugars through immobilization technology. *Biofuel*

Research Journal, *1*, 2–6.

Ehrenstein, G. W. (2001). *Polymeric materials: structure, properties, applications*. (G. W. Ehrenstein, Ed.) (1st ed.). Munich Germany: Carl Hanser Verlag GmbH Co KG.

Embuscado, M. E., & Huber, K. C. (2009). *Edible films and coatings for food applications*. CA USA: Springer.

Emmambux, M. N., Stading, M., & Taylor, J. R. N. (2004). Sorghum kafirin film property modification with hydrolysable and condensed tannins. *Journal of Cereal Science*, *40*(2), 127–135.

Essel, R., & Carus, M. (2014). Increasing resource efficiency by cascading use of biomass. *RURAL21*, *48*(3), 28–29.

Essers, S. (1988). Bitter cassava as a drought resistant crop. *ILEIA-Newsletter*, *4*(4), 10–11.

European Pharmacopoeia. (2015). European Directorate for the Quality of Medicines, Strasbourg, France (8th Edition, pp. 2973–2975).

Ezejiofor, T. I. N., Enebaku, U. E., & Ogueke, C. (2014). Waste to Wealth- Value Recovery from Agro- food Processing Wastes Using Biotechnology : A Review. *Journal, British Biotechnology*, *4*(4), 418–481.

Ezzat Abd El-Hack, M., Alagawany, M., Ragab Farag, M., Tiwari, R., Karthik, K., Dhama, K., … Adel, M. (2016). Beneficial impacts of thymol essential oil on health and production of animals, fish and poultry: a review. *Journal of Essential Oil Research*, 1–18.

Fallis, A. . (2013). Permeability, Diffusivity, and Solubility of Gas and Solute Through Polymers. *Journal of Chemical Information and Modeling*, *53*(9), 1689–1699.

FAO. (2007). *Land evealuation: Towards a revised framework*. Rome.

FAO. (2013). *Food wastage footprint-Impacts on natural resources: summary report*. Rome: Food and Agriculture Organization of the United Nations.

FAOSTAT, F. A. O. (2015). Food and Agriculture Organization of the United Nations Statistics Division. *Rome: FAO*.

Farahnaky, A., Ansari, S., & Majzoobi, M. (2009). Effect of glycerol on the moisture sorption isotherms of figs. *Journal of Food Engineering*, *93*(4), 468–473.

FDA. (1997). Guidance for Industry Dissolution Testing of Immediate. *Evaluation*, *4*(August), 15–22.

Fell, J.T. and Newton, J. M. (1970). Tablet Strength by the Diametral-Compression Test. *Journal of Pharmaceutical Sciences*, *59*(5), 688–691.

Ferreira, M. D., Sargent, S. A., Brecht, J. K., & Chandler, C. K. (2008). Strawberry fruit resistance to simulated handling. *Scientia Agricola*, *65*(5), 490–495.

Finch, C. A. (1983). Chemical Modification and Some Cross-linking Reactions of Water-Soluble Polymers. In C. A. Finch (Ed.), *Chemistry and technology of water-soluble polymers* (pp. 81–111). New York: Springer.

Flores, S., Famá, L., Rojas, A. M., Goyanes, S., & Gerschenson, L. (2007). Physical properties of tapioca-starch edible films: Influence of filmmaking and potassium sorbate. *Food Research International*, *40*(2), 257–265.

Flores, S. K., Costa, D., Yamashita, F., Gerschenson, L. N., & Grossmann, M. V. (2010). Mixture design for evaluation of potassium sorbate and xanthan gum effect on properties of tapioca starch films obtained by extrusion. *Materials Science and Engineering C*, *30*(1), 196–202.

Flory, P. J. (1953). *Principles of polymer chemistry*. (P. J. Flory, Ed.). New York: Cornell University Press.

Forney, C. F., & Brandl, D. G. (1992). Control of humidity in small controlled-environment chambers using Glycerol-water solutions. *HortTechnolgy*, *2*(1958), 52–54.

G. Norwitz & P.N. Keliher, N. N. (1986). Study of the steam distillation of phenolic compounds using ultraviolet spectrometry. *Analytical Chemistry*, 639–641.

Ghorpade, V. M., Hanna, M. A., & Weller, C. L. (1995). Soy Protein Isolate / Poly (ethylene oxide) Films. *Cereal Chemistry*, *72*(6), 559–563.

Gibaldi, B. M., & Feldman, S. (1967). Establishment of Sink Conditions in Dissolution Rate Determinations. *Journal of Pharmacetical Sciences*, *56*(10), 1238–1242.

Gil, M. I., Selma, M. V., López-Gálvez, F., & Allende, A. (2009). Fresh-cut product sanitation and wash water disinfection: Problems and solutions. *International Journal of Food Microbiology*, *134*(1-2), 37–45.

Glenn, G. M., Klamczynski, A. P., Woods, D. F., Chiou, B., Orts, W. J., & Imam, S. H. (2010). Encapsulation of plant oils in porous starch microspheres. *Journal of Agricultural and Food Chemistry*, *58*(7), 4180–4184.

Gonsior, N., Mohr, F., & Ritter, H. (2012). Synthesis of mesomeric betaine compounds with imidazolium-enolate structure. *Beilstein Journal of Organic Chemistry*, *8*, 390–397.

Gourianova, S., Willenbacher, N., & Kutschera, M. (2005). Chemical force microscopy study of adhesive properties of polypropylene films: Influence of surface polarity and medium. *Langmuir*, *21*(12), 5429–5438.

Green, D. W., & Perry, R. H. (2008). Adsorbents and ion exchangers. *Perry's Chemical Engineers' Handbook, Eighth Edition*. New York: McGraw Hill Professional, Access Engineering.

Grip, C.-E., Larsson, M., Harvey, S., & Nilsson, L. (2013). Process integration. Tests and application of different tools on an integrated steelmaking site. *Applied Thermal Engineering*, *53*(2), 366–372.

Guo, C., Zhou, L., & Lv, J. (2013). Effects of expandable graphite and modified ammonium polyphosphate on the flame-retardant and mechanical properties of wood flour-polypropylene composites. *Polymers and Polymer Composites*, *21*(7), 449–456.

Han, J. H. (2005). *Innovations in food packaging*. (Jung H. Han, Ed.) (2nd ed.). Texas USA: Academic Press.

Hayashi, A., & Veiga-santos, P. (2006). Investigation of Antioxidant Activity of Cassava Starch Biobased Materials, (April 2006), 26–28.

Heckel, R. W. (1961). Density-Pressure Relationships in Powder Compaction. *Transactions of the Metallurgical Society of AIME*, *221*, 671–675.

Hermiati, E., Mangunwidjaja, D., Sunarti, T. C., Suparno, O., & Prasetya, B. (2012). Potential utilization of cassava pulp for ethanol production in Indonesia. *Scientific Research and Essays*, *7*(2), 100–106.

Heuzé, V., Tran, G. B., D Archimède, H., Lebas, F., & Regnier, C. (2013). Cassava peels, cassava pomace and other cassava by-products. *Feedipedia. Org. A Programme by INRA, CIRAD, AFZ and FAO*.

Hinterstoisser, B., & Salmén, L. (2000). Application of dynamic 2D FTIR to cellulose. *Vibrational Spectroscopy*, *22*(1-2), 111–118.

Hishinuma, K. (2009). *Heat sealing technology and engineering for packaging: principles and applications*. DEStech Publications, Inc.

Ho, W. S., Tan, S. T., Hashim, H., Lim, J. S., & Lee, C. T. (2015). Waste Management Pinch Analysis (WAMPA) for Carbon Emission Reduction. *Energy Procedia*, *75*, 2448–2453.

Hoffman-Pennesi, D., & Wu, C. (2010). The effect of thymol and thyme oil feed supplementation on growth performance, serum antioxidant levels, and cecal Salmonella population in broilers. *Journal of Applied Poultry Research*, *19*(4), 432–443.

Hood, E. E., Teoh, K. T., Devaiah, S. P., & Requesens, D. V. (2013). Biomass biomass Crops for Biofuels and Bio-based Products biomass crops crops for biofuels and bio-based products. In Robert A. Meyers (Ed.), *Encyclopedia of Sustainability Science and*

Technology (pp. 1268–1298). New York: Springer.

Horev, B., Sela, S., Vinokur, Y., Gorbatsevich, E., Pinto, R., & Rodov, V. (2012). The effects of active and passive modified atmosphere packaging on the survival of Salmonella enterica serotype Typhimurium on washed romaine lettuce leaves. *Food Research International*, *45*(2), 1129–1132.

Hussain, Y., Wu, Y.-T., Ampaw, P.-J., & Grant, C. S. (2007). Dissolution of polymer films in supercritical carbon dioxide using a quartz crystal microbalance. *The Journal of Supercritical Fluids*, *42*(2), 255–264.

Hussein, Z., Caleb, O. J., Jacobs, K., Manley, M., & Opara, U. L. (2015). Effect of perforation-mediated modified atmosphere packaging and storage duration on physicochemical properties and microbial quality of fresh minimally processed "Acco" pomegranate arils. *LWT - Food Science and Technology*, *64*(2), 911–918.

Imam, S., Glenn, G., Chiou, B. S., Shey, J., Narayan, R., & Orts, W. (2008). Types, production and assessment of bio-based food packaging materials. In E. Chiellini (Ed.), *Environmentally Compatible Food Packaging* (pp. 29–62). Cambridge UK: Woodhead Publishing Ltd.

Ioelovich, M. (2012). Study of Cellulose Interaction with Concentrated Solutions of Sulfuric Acid. *ISRN Chemical Engineering*, *2012*, 1–7. http://doi.org/10.5402/2012/428974

Jiménez, A., Fabra, M. J., Talens, P., & Chiralt, A. (2012). Edible and Biodegradable Starch Films: A Review. *Food and Bioprocess Technology*, *5*(6), 2058–2076.

Joffe, R., Rozite, L., & Pupurs, A. (2013). Nonlinear behavior of natural fiber/bio-based matrix composites. In C. L. Bonnie Antoun, H. Jerry Qi, Richard Hall, G.P. Tandon, Hongbing Lu (Ed.), *Challenges in Mechanics of Time-Dependent Materials and Processes in Conventional and Multifunctional Materials, Volume 2* (pp. 131–137). New York: Springer.

John, R. P. (2009). Biotechnological potentials of cassava bagasse. In *Biotechnology for Agro-Industrial Residues Utilisation* (pp. 225–237). Springer.

Juban, A., Nouguier-Lehon, C., Briancon, S., Hoc, T., & Puel, F. (2015). Predictive model for tensile strength of pharmaceutical tablets based on local hardness measurements. *International Journal of Pharmaceutics*, *490*(1-2), 438–45.

Karolewicz, B. (2015). A review of polymers as multifunctional excipients in drug dosage form technology. *Saudi Pharmaceutical Journal*.

Karoui, I. J., Msaada, K., Abderrabba, M., & Marzouk, B. (2016). Bioactive Compounds and

Antioxidant Activities of Thyme- Enriched Refined Corn Oil, *18*, 79–91.

Katzhendler, I., Hoffman, a, Goldberger, a, & Friedman, M. (1997). Modelling of drug release from erodible tablets. *Journal of Pharmaceutical Sciences*, *86*(1), 110–115.

Kechichian, V., Ditchfield, C., Veiga-Santos, P., & Tadini, C. C. (2010). Natural antimicrobial ingredients incorporated in biodegradable films based on cassava starch. *LWT - Food Science and Technology*, *43*(7), 1088–1094.

Kemp, I. C. (2007). *Pinch Analysis and Process Integration*. (I. C. Kemp, Ed.)*Pinch Analysis and Process Integration* (2nd ed.). Oxford,UK: Elsevier.

Khan, K. a. (1975). The concept of dissolution efficiency. *The Journal of Pharmacy and Pharmacology*, *27*, 48–49. http://doi.org/10.1111/j.2042-7158.1975.tb09378.x

Kolawole, O. P. (2014). Cassava Processing and the Environmental Effect. *World Sustainability Forum 2014*, 1–7.

Komatsuka, T., & Nagai, K. (2009). Temperature Dependence on Gas Permeability and Permselectivity of Poly(lactic acid) Blend Membranes. *Polymer Journal*, *41*(5), 455–458.

Kulchan, R., Boonsupthip, W., & Suppakul, P. (2010). Shelf life prediction of packaged cassava-flour-based baked product by using empirical models and activation energy for water vapor permeability of polyolefin films. *Journal of Food Engineering*, *100*(3), 461–467.

Kumar, A. P., & Singh, R. P. (2008). Biocomposites of cellulose reinforced starch: Improvement of properties by photo-induced crosslinking. *Bioresource Technology*, *99*(18), 8803–8809.

Kumar, M. N., & Yaakob, Z. (2011). Biobased Materials in Food Packaging Applications. In Srikanth Pilla (Ed.), *Handbook of Bioplastics and Biocomposites Engineering Applications* (pp. 121–159). Massachusetts USA: Wiley Online Library.

Larotonda, F. D. . S. . (2007). *Biodegradable films and coatings obtained from carrageenan from Mastocarpus stellatus and starch from Quercus suber*. *Engineering*. Universidade do Porto, Portugal.

Lazaridou, A., Biliaderis, C. G., Bacandritsos, N., & Sabatini, A. G. (2004). Composition, thermal and rheological behaviour of selected Greek honeys. *Journal of Food Engineering*, *64*(1), 9–21.

Leroux, J.-C., Allémann, E., De Jaeghere, F., Doelker, E., & Gurny, R. (1996). Biodegradable nanoparticles — From sustained release formulations to improved site

specific drug delivery. *Journal of Controlled Release*, *39*(2-3), 339–350.

Liang, C. Y., & Marchessault, R. H. (1959). Infrared spectra of crystalline polysaccharides. II. Native celluloses in the region from 640 to 1700 cm.− 1. *Journal of Polymer Science*, *39*(135), 269–278.

Lin, C. S. K., Pfaltzgraff, L. A., Herrero-Davila, L., Mubofu, E. B., Abderrahim, S., Clark, J. H., … Luque, R. (2013). Food waste as a valuable resource for the production of chemicals, materials and fuels. Current situation and global perspective. *Energy & Environmental Science*, *6*(2), 426–464.

Liu, Z. (2005). *Edible films and coatings from starch*. (Jung H. Han, Ed.)*Innovations in Food Packaging*. Manitoba R3T 2N2, Canada: Academic Press.

Liu, Z. T., Zhang, L., Liu, Z., Gao, Z., Dong, W., Xiong, H., … Tang, S. (2006). Supercritical CO2 dyeing of ramie fiber with disperse dye. *Industrial and Engineering Chemistry Research*, *45*(26), 8932–8938.

Lundy, M., Ostertag, C. F., & Best, R. (2002). *Value adding, agroenterprise and poverty reduction: A territorial approach for rural business development*. Cali Colombia: Centro internacional de agricultura tropical (CIAT). Rural agroenterprise development project.

MacKerron, C. B., & Hoover, D. (2015). Waste and Opportunity 2015: Environmental Progress and Challenges in Food, Beverage, and Consumer Goods Packaging. *As You Sow*, New York City: The Natural Resources Defense Counc.

Mahalik, N. P., & Nambiar, A. N. (2010). Trends in food packaging and manufacturing systems and technology. *Trends in Food Science & Technology*, *21*(3), 117–128.

Maieves, H. A., Oliveira, D. C. De, Frescura, J. R., & Amante, E. R. (2011). Selection of cultivars for minimization of waste and of water consumption in cassava starch production. *Industrial Crops and Products*, *33*(1), 224–228.

Majozi, T., & Gouws, J. F. (2009). A mathematical optimisation approach for wastewater minimisation in multipurpose batch plants: Multiple contaminants. *Computers and Chemical Engineering*, *33*(11), 1826–1840.

Mäki, R., Suihko, E., Rost, S., Heiskanen, M., Murtomaa, M., Lehto, V. P., & Ketolainen, J. (2007). Modifying drug release and tablet properties of starch acetate tablets by dry powder agglomeration. *Journal of Pharmaceutical Sciences*, *96*(2), 438–447.

Mali, S., Sakanaka, L. S., Yamashita, F., & Grossmann, M. V. E. (2005). Water sorption and mechanical properties of cassava starch films and their relation to plasticizing effect.

Carbohydrate Polymers, *60*(3), 283–289.

Maran, J. P., Sivakumar, V., Sridhar, R., & Thirugnanasambandham, K. (2013). Development of model for barrier and optical properties of tapioca starch based edible films. *Carbohydrate Polymers*, *92*(2), 1335–47.

Marsh, K., & Bugusu, B. (2007). Food packaging - Roles, materials, and environmental issues: Scientific status summary. *Journal of Food Science*, *72*(3).

Marzocca, A. J. (2010). Evaluation of the polymer-solvent interaction parameter λ for the system cured polybutadiene rubber and toluene. *Polymer Testing*, *29*(1), 119–126.

Masaro, L., & Zhu, X. X. (1999). *Physical models of diffusion for polymer solutions, gels and solids*. *Progress in Polymer Science (Oxford)* (Vol. 24).

Matthews, K. R., Sapers, G. M., & Gerba, C. P. (2014). *The produce contamination problem: causes and solutions*. Burlington, USA: Academic Press.

Mensitieri, G., Di Maio, E., Buonocore, G. G., Nedi, I., Oliviero, M., Sansone, L., & Iannace, S. (2011). Processing and shelf life issues of selected food packaging materials and structures from renewable resources. *Trends in Food Science & Technology*, *22*(2-3), 72–80.

Miller-Chou, B. A., & Koenig, J. L. (2003). A review of polymer dissolution. *Progress in Polymer Science (Oxford)*, *28*(8), 1223–1270.

Misra, N. N., Pankaj, S. K., Walsh, T., O'Regan, F., Bourke, P., & Cullen, P. J. (2014). In-package nonthermal plasma degradation of pesticides on fresh produce. *Journal of Hazardous Materials*, *271*, 33–40.

Mistler, R. E., & Twiname, E. R. (2000). *Tape casting: theory and practice*. American ceramic society.

Mu, C., Guo, J., Li, X., Lin, W., & Li, D. (2012). Preparation and properties of dialdehyde carboxymethyl cellulose crosslinked gelatin edible films. *Food Hydrocolloids*, *27*(1), 22–29.

Mudgal, S., Tan, A., Lockwood, S., Eisenmenger, N., Fischer-Kowalski, M., Giljum, S., & Brucker, M. (2012). Assessment of Resource Efficiency Indicators and Targets. *Final Report. European Commission-DG Environment, BIO Intelligence Service*, 87.

Mufumbo, R., Baguma, Y., Kashub, S., Nuwamanya, E., Rubaihayo, P., Mukasa, S., … Kyamanywa, S. (2011). Amylopectin molecular structure and functional properties of starch from three Ugandan cassava varieties. *Journal of Plant Breeding and Crop Science*, *3*(9), 195–202.

Navarro, M., Engel, E., Planell, J. A., Amaral, I., Barbosa, M., & Ginebra, M. P. (2008). Surface characterization and cell response of a PLA/CaP glass biodegradable composite material. *Journal of Biomedical Materials Research - Part A*, *85*(2), 477–486.

Nep, E. I., Asare-Addo, K., Ghori, M. U., Conway, B. R., & Smith, A. M. (2015). Starch-free grewia gum matrices: Compaction, swelling, erosion and drug release behaviour. *International Journal of Pharmaceutics*, *496*(2), 689–698.

Ngo, T. T., Liotta, C. L., Eckert, C. A., & Kazarian, S. G. (2003). Supercritical fluid impregnation of different azo-dyes into polymer: in situ UV/Vis spectroscopic study. *The Journal of Supercritical Fluids*, *27*(2), 215–221.

Ni, W.-M. (2011). *The mathematics of diffusion* (Vol. 82). Philadelphia: siam.

Niemira, B. A. (2012). Cold plasma decontamination of foods*. *Annual Review of Food Science and Technology*, *3*, 125–142.

Nostro, A., Roccaro, A. S., Bisignano, G., Marino, A., Cannatelli, M. A., Pizzimenti, F. C., … Blanco, A. R. (2007). Effects of oregano, carvacrol and thymol on Staphylococcus aureus and Staphylococcus epidermidis biofilms. *Journal of Medical Microbiology*, *56*(4), 519–523.

Nuwamanya, E., Baguma, Y., Wembabazi, E., & Rubaihayo, P. (2013). A comparative study of the physicochemical properties of starches from root, tuber and cereal crops. *African Journal of Biotechnology*, *10*(56), 12018–12030.

Ochs, M., Lothenbach, B., Wanner, H., Sato, H., & Yui, M. (2001). An integrated sorption-diffusion model for the calculation of consistent distribution and diffusion coefficients in compacted bentonite. *Journal of Contaminant Hydrology*, *47*(2-4), 283–296.

Olivato, J. B., Grossmann, M. V. E., Bilck, A. P., Yamashita, F., & Oliveira, L. M. (2013). Starch/polyester films: simultaneous optimisation of the properties for the production of biodegradable plastic bags. *Polímeros*, *23*(1), 32–36.

Oliveira, T. G., Makishi, G. L. A., Chambi, H. N. M., Bittante, A. M. Q. B., Louren??o, R. V., & Sobral, P. J. A. (2015). Cellulose fiber reinforced biodegradable films based on proteins extracted from castor bean (Ricinus communis L.) cake. *Industrial Crops and Products*, *67*, 355–363.

Ollé Resa, C. P., Gerschenson, L. N., & Jagus, R. J. (2013). Effect of Natamycin on Physical Properties of Starch Edible Films and Their Effect on Saccharomyces cerevisiae Activity. *Food and Bioprocess Technology*, *6*(11), 3124–3133.

Orwoll, R. A., & Arnold, P. A. (2007). Polymer–solvent interaction parameter χ. In *Physical*

properties of polymers handbook (pp. 233–257). Springer.

Ospina, B., & Ceballos, H. (2002). *La yuca en el tercer Milenio: Sistemas Modernos de producción, procesamiento, utilización y comercialización* (Vol. 327). CIAT.

Palou, L., Valencia-Chamorro, S., & Pérez-Gago, M. (2015). Antifungal Edible Coatings for Fresh Citrus Fruit: A Review. *Coatings*, *5*(4), 962–986.

Pandey, S. K., & Goswami, T. K. (2012). Modelling perforated mediated modified atmospheric packaging of capsicum. *International Journal of Food Science and Technology*, *47*(3), 556–563.

Pankaj, S. K., Bueno-Ferrer, C., Misra, N. N., Bourke, P., & Cullen, P. J. (2014). Zein film: Effects of dielectric barrier discharge atmospheric cold plasma. *Journal of Applied Polymer Science*, *131*(18), 9541–9546.

Pankaj, S. K., Bueno-Ferrer, C., Misra, N. N., Milosavljević, V., O'Donnell, C. P., Bourke, P., … Cullen, P. J. (2014). Applications of cold plasma technology in food packaging. *Trends in Food Science & Technology*, *35*(1), 5–17.

Pankaj, S. K., Bueno-Ferrer, C., Misra, N. N., O'Neill, L., Tiwari, B. K., Bourke, P., & Cullen, P. J. (2014). Physicochemical characterization of plasma-treated sodium caseinate film. *Food Research International*, *66*, 438–444.

Pankaj, S. K., Bueno-Ferrer, C., Misra, N. N., O'Neill, L., Tiwari, B. K., Bourke, P., & Cullen, P. J. (2015a). Characterization of dielectric barrier discharge atmospheric air cold plasma treated gelatin films. *Food Packaging and Shelf Life*, *6*, 61–67.

Pankaj, S. K., Bueno-Ferrer, C., Misra, N. N., O'Neill, L., Tiwari, B. K., Bourke, P., & Cullen, P. J. (2015b). Dielectric barrier discharge atmospheric air plasma treatment of high amylose corn starch films. *LWT - Food Science and Technology*, *63*(2), 1076–1082.

Paunonen, S. (2013). Strength and barrier enhancements of cellophane and cellulose derivative films: A review. *BioResources*, *8*(2), 3098–3121.

Peleg, M. (1993). Assessment of a semi-empirical four parameter general modelfor sigmoid moisture sorption isotherms. *Journal of Food Process Engineering*, *16*(1), 21–37.

Pelissari, F. M., Andrade-Mahecha, M. M., Sobral, P. J. do A., & Menegalli, F. C. (2013). Optimization of process conditions for the production of films based on the flour from plantain bananas (Musa paradisiaca). *LWT - Food Science and Technology*, *52*(1), 1–11.

Pelissari, F. M., Pelissari, F. M., Grossmann, M. V. E., Grossmann, M. V. E., Yamashita, F., Yamashita, F., … Pineda, E. A. G. (2009). Antimicrobial, Mechanical, and Barrier Properties of Cassava Starch-Chitosan Films Incorporated with Oregano Essential Oil.

Journal of Agricultural and Food Chemistry, 7499–7504.

Perazzo, K. K. N. C. L., Carlos De Vasconcelos Conceição, A., Pires Dos Santos, J. C., De Jesus Assis, D., Souza, C. O., & Druzian, J. I. (2014). Properties and antioxidant action of actives cassava starch films incorporated with green tea and palm oil extracts. *PLoS ONE*, *9*(9), 1–13.

Perdones, Á., Chiralt, A., & Vargas, M. (2016). Properties of film-forming dispersions and films based on chitosan containing basil or thyme essential oil. *Food Hydrocolloids*, *57*, 271–279.

Petrovic, Z. (2008). Polyurethanes from Vegetable Oils. *Polymer Reviews*, *48*(1), 109–155.

Phan The, D., Debeaufort, F., Voilley, A., & Luu, D. (2009). Influence of hydrocolloid nature on the structure and functional properties of emulsified edible films. *Food Hydrocolloids*, *23*(3), 691–699.

Pizarro, C., González-Sáiz, J. M., & Pérez-del-Notario, N. (2006). Multiple response optimisation based on desirability functions of a microwave-assisted extraction method for the simultaneous determination of chloroanisoles and chlorophenols in oak barrel sawdust. *Journal of Chromatography. A*, *1132*(1-2), 8–14.

Polnaya, F. J., Talahatu, J., & Marseno, D. W. (2012). Properties of biodegradable films from hydroxypropyl sago starches. Asian. *Journal of Food Agro-Industry*, *5*(3), 183–192.

Prakash Maran, J., Sivakumar, V., Thirugnanasambandham, K., & Sridhar, R. (2013). Response surface modeling and analysis of barrier and optical properties of maize starch edible films. *International Journal of Biological Macromolecules*, *60*, 412–421.

R.S. Lager & NA Peppas. (1981). Present and Future Applications of Biomaterials in Controlled Drug Delivery Systems. *Biomaterials*, *2*, 201.

Raabe, J., Fonseca, A. D. S., Bufalino, L., Ribeiro, C., Martins, M. A., Marconcini, J. M., … Tonoli, G. H. D. (2015). Biocomposite of Cassava Starch Reinforced with Cellulose Pulp Fibers Modified with Deposition of Silica (SiO 2) Nanoparticles. *Journal of Nanomaterials*, *2015*, 1–9.

Ramirez-Navas, J. S., & Rodriguez de Stouvenel, A. (2012). Characterization of Colombian quesillo cheese by spectrocolorimetry. *Vitae*, *19*(2), 178–185.

Reinas, I., Oliveira, J., Pereira, J., Mahajan, P., & Poças, F. (2016). A quantitative approach to assess the contribution of seals to the permeability of water vapour and oxygen in thermosealed packages. *Food Packaging and Shelf Life*, *7*, 34–40.

Reverchon, E., & Cardea, S. (2012). Supercritical fluids in 3-D tissue engineering. *Journal of*

Supercritical Fluids, *69*, 97–107.

Ritger, P. L., & Peppas, N. A. (1987). A simple equation for description of solute release I. Fickian and non-fickian release from non-swellable devices in the form of slabs, spheres, cylinders or discs. *Journal of Controlled Release*, *5*(1), 23–36.

Rodrigues, D. C., Caceres, C. A., Ribeiro, H. L., de Abreu, R. F. A., Cunha, A. P., & Azeredo, H. M. C. (2014). Influence of cassava starch and carnauba wax on physical properties of cashew tree gum-based films. *Food Hydrocolloids*, *38*, 147–151.

Saccone, C. D., Tessore, J., Olivera, S. a, & Meneces, N. S. (2004). Statistical Properties of the Dissolution Test of USP. *Dissolution Technologies*, (August), 25–28.

Salamone, J. C. (1996). *Polymeric material encyclopedia*. (J. C. Salamone, Ed.)*Polymeric material encyclopedia* (3rd ed.). New York: CRC press.

Salvador, L. D., Suganuma, T., Kitahara, K., Tanoue, H., & Ichiki, M. (2000). Monosaccharide composition of sweetpotato fiber and cell wall polysaccharides from sweetpotato, cassava, and potato analyzed by the high-performance anion exchange chromatography with pulsed amperometric detection method. *Journal of Agricultural and Food Chemistry*, *48*(8), 3448–3454.

Samaha, D., Shehayeb, R., & Kyriacos, S. (2009). Modeling and comparison of dissolution profiles of diltiazem modified-release formulations. *Dissolution Technologies*, *16*(2), 41–46.

Sannino, A., Demitri, C., & Madaghiele, M. (2009). Biodegradable cellulose-based hydrogels: Design and applications. *Materials*, *2*(2), 353–373.

Sayre, R., Beeching, J. R., Cahoon, E. B., Egesi, C., Fauquet, C., Fellman, J., … Zhang, P. (2011). The BioCassava plus program: biofortification of cassava for sub-Saharan Africa. *Annual Review of Plant Biology*, *62*, 251–272.

Scheibe, A. S., De Moraes, J. O., & Laurindo, J. B. (2014). Production and characterization of bags from biocomposite films of starch-vegetal fibers prepared by tape casting. *Journal of Food Process Engineering*, *37*(5), 482–492.

Segat, A., Misra, N. N., Cullen, P. J., & Innocente, N. (2016). Effect of atmospheric pressure cold plasma (ACP) on activity and structure of alkaline phosphatase. *Food and Bioproducts Processing*, *98*, 181–188.

Šegvić Klarić, M., Kosalec, I., Mastelić, J., Piecková, E., & Pepeljnak, S. (2007). Antifungal activity of thyme (Thymus vulgaris L.) essential oil and thymol against moulds from damp dwellings. *Letters in Applied Microbiology*, *44*(1), 36–42.

Shah, B., Davidson, P. M., & Zhong, Q. (2012). Nanocapsular dispersion of thymol for enhanced dispersibility and increased antimicrobial effectiveness against Escherichia coli O157: H7 and Listeria monocytogenes in model food systems. *Applied and Environmental Microbiology*, *78*(23), 8448–8453.

Sharma, G., Wu, W., & Dalal, E. N. (2005). The CIEDE2000 color-difference formula: Implementation notes, supplementary test data, and mathematical observations. *Color Research & Application*, *30*(1), 21–30.

Sharp, P., & Srai, S.-K. (2007). Molecular mechanisms involved in intestinal iron absorption. *World Journal of Gastroenterology : WJG*, *13*(35), 4716–4724.

Silva, M. R., & Wagner, J. G. (1969). Interpretation of Percent Dissolved-Time Plots Derived from In Vitro Testing of Conventional Tablets and Capsules. *Journal of Pharmaceutical Sciences*, *58*(10), 1253–1257.

Simonetto, E. de O., & Borenstein, D. (2007). A decision support system for the operational planning of solid waste collection. *Waste Management (New York, N.Y.)*, *27*(10), 1286–97.

Siracusa, V., Rocculi, P., Romani, S., & Rosa, M. (2008). Biodegradable polymers for food packaging: a review. *Trends in Food Science & Technology*, *19*(12), 634–643.

Sopade, P. a, Halley, P., Bhandari, B., D'Arcy, B., Doebler, C., & Caffin, N. (2002). Application of the Williams – Landel – Ferry model to the viscosity – temperature relationship of Australian honeys. *Journal of Food Engineering*, *56*, 67–75.

Souza, A. C., Benze, R., Ferrão, E. S., Ditchfield, C., Coelho, A. C. V, & Tadini, C. C. (2012). Cassava starch biodegradable films: Influence of glycerol and clay nanoparticles content on tensile and barrier properties and glass transition temperature. *LWT - Food Science and Technology*, *46*(1), 110–117.

Souza, A. C., Goto, G. E. O., Mainardi, J. A., Coelho, A. C. V., & Tadini, C. C. (2013). Cassava starch composite films incorporated with cinnamon essential oil: Antimicrobial activity, microstructure, mechanical and barrier properties. *LWT - Food Science and Technology*, *54*(2), 346–352.

Souza, V. C., Monte, M. L., & Pinto, L. A. A. (2011). Preparation of biopolymer film from chitosan modified with lipid fraction. *International Journal of Food Science and Technology*, *46*(9), 1856–1862.

Stannett, V. (1978). The transport of gases in synthetic polymeric membranes—an historic perspective. *Journal of Membrane Science*, *3*(2), 97–115.

Steele, T. W. J., Huang, C. L., Kumar, S., Irvine, S., Boey, F. Y. C., Loo, J. S. C., & Venkatraman, S. S. (2012). Novel gradient casting method provides high-throughput assessment of blended polyester poly(lactic-co-glycolic acid) thin films for parameter optimization. *Acta Biomaterialia*, *8*(6), 2263–2270.

Sullivan, J. L. (1990). Creep and physical aging of composites. *Composites Science and Technology*, *39*(3), 207–232.

Sultana, N., & Khan, T. H. (2013). Water absorption and diffusion characteristics of nanohydroxyapatite (nHA) and poly(hydroxybutyrate-co-hydroxyvalerate-) based composite tissue engineering scaffolds and nonporous thin films. *Journal of Nanomaterials*, *2013*, 8.

Sultanbawa, Y. (2011). Plant antimicrobials in food applications: Minireview. *Science against Microbial Pathogens: Communicating Current Research and Technological Advances*, *2*, 1084–1093.

Sun, C. (2005). True density of microcrystalline cellulose. *Journal of Pharmaceutical Sciences*, *94*(10), 2132–2134.

Suppakul, P., Chalernsook, B., Ratisuthawat, B., Prapasitthi, S., & Munchukangwan, N. (2013). Empirical modeling of moisture sorption characteristics and mechanical and barrier properties of cassava flour film and their relation to plasticizing–antiplasticizing effects. *LWT-Food Science and Technology*, *50*(1), 290–297.

Tanimoto, Y., Hayakawa, T., Sakae, T., & Nemoto, K. (2006). Characterization and bioactivity of tape-cast and sintered TCP sheets. *Journal of Biomedical Materials Research - Part A*, *76*(3), 571–579.

Tapia-Blácido, D. R., do Amaral Sobral, P. J., & Menegalli, F. C. (2011). Optimization of amaranth flour films plasticized with glycerol and sorbitol by multi-response analysis. *LWT - Food Science and Technology*, *44*(8), 1731–1738.

Teixeira, E. de M., Pasquini, D., Curvelo, A. A. S., Corradini, E., Belgacem, M. N., & Dufresne, A. (2009). Cassava bagasse cellulose nanofibrils reinforced thermoplastic cassava starch. *Carbohydrate Polymers*, *78*(3), 422–431.

Thi, T., & Vuong, P. (2012). *Farmers' perceptions of the "Unleashing the Power of Cassava in Africa in Response to the Food Crisis"- Experiences from Malawi*. Swedish University of Agricultural Sciences, Sweden.

Thoorens, G., Krier, F., Leclercq, B., Carlin, B., & Evrard, B. (2014). Microcrystalline cellulose, a direct compression binder in a quality by design environment - A review.

International Journal of Pharmaceutics, *473*(1-2), 64–72.

Ting, Y., Jiang, Y., Ho, C. T., & Huang, Q. (2014). Common delivery systems for enhancing in vivo bioavailability and biological efficacy of nutraceuticals. *Journal of Functional Foods*, *7*(1), 112–128.

Tokiwa, Y., Calabia, B. P., Ugwu, C. U., & Aiba, S. (2009). Biodegradability of plastics. *International Journal of Molecular Sciences*, *10*(9), 3722–3742.

Torres, A., Romero, J., Macan, A., Guarda, A., & Galotto, M. J. (2014). Near critical and supercritical impregnation and kinetic release of thymol in LLDPE films used for food packaging. *Journal of Supercritical Fluids*, *85*, 41–48.

Trofimchuk, E. S., Efimov, A. V., Nikitin, L. N., Nikonorova, N. I., Volynskii, A. L., Khokhlov, A. R., & Bakeev, N. F. (2014). Preparation of nanoporous polyolefin films in supercritical carbon dioxide. *Russian Journal of Physical Chemistry B*, *8*(8), 1019–1024.

Tumwesigye, K. S., Morales-Oyervides, L., Oliveira, J. C., & Gallagher, M. J. S. (2016). Effective utilisation of cassava bio-wastes through integrated process design: A sustainable approach to indirect waste management. *Process Safety and Environmental Protection*, *2*, 159–167.

Tumwesigye, K. S., Oliveira, J. C., & Sousa-Gallagher, M. J. (2016). New sustainable approach to reduce cassava borne environmental waste and develop biodegradable materials for food packaging applications. *Food Packaging and Shelf Life*, *7*, 8–19.

Tumwesigye, S. K., Baguma, Y., Kyamuhangire, W., & Mpango, G. (2006). Association between accumulation of total cyanogens and progression of cassava mosaic disease in cassava (Manihot esculenta Crantz). *Uganda Journal of Agricultural Sciences*, *12*(1), 13–21.

Tumwesigye, S. K., Montañez, J. C., Oliveira, J. C., & Sousa-Gallagher, M. J. (2016). Novel Intact Bitter Cassava: Sustainable Development and Desirability Optimisation of Packaging Films. *Food and Bioprocess Technology*, *9*(5), 801–812.

Ubalua, A. O. (2007). Cassava wastes: treatment options and value addition alternatives. *African Journal of Biotechnology*, *6*(18), 2065–2073.

Uchechukwu-Agua, A. D., Caleb, O. J., & Opara, U. L. (2015). Postharvest Handling and Storage of Fresh Cassava Root and Products: a Review. *Food and Bioprocess Technology*, *8*(4), 729–748.

UNSD. (1997). Glossary of environment. New York: United Nations Pubns.

USP. (2012). ⟨ 616 ⟩ Bulk Density and. *United States Pharmacopeia and National*

Formulary, *48*, 2011–2013.

Valdés, A., Mellinas, A. C., Ramos, M., Garrigós, M. C., & Jiménez, A. (2014). Natural additives and agricultural wastes in biopolymer formulations for food packaging. *Frontiers in Chemistry*, *2*(February), 6.

Van Boekel, M. A. J. S. (2008). Kinetic Modeling of Food Quality: A Critical Review. *Comprehensive Reviews in Food Science and Food Safety*, *7*, 144–158.

Vásconez, M. B., Flores, S. K., Campos, C. A., Alvarado, J., & Gerschenson, L. N. (2009). Antimicrobial activity and physical properties of chitosan–tapioca starch based edible films and coatings. *Food Research International*, *42*(7), 762–769.

Versino, F., & García, M. A. (2014). Cassava (Manihot esculenta) starch films reinforced with natural fibrous filler. *Industrial Crops and Products*, *58*, 305–314.

Versino, F., López, O. V., & García, M. A. (2015). Sustainable use of cassava (Manihot esculenta) roots as raw material for biocomposites development. *Industrial Crops and Products*, *65*, 79–89.

Vicente, G., Martínez, M., & Aracil, J. (2007). Optimisation of integrated biodiesel production. Part II: a study of the material balance. *Bioresource Technology*, *98*(9), 1754–61.

Weinkauf, D., & Paul, D. R. (1990). Effects of Structural Order on Barrier Properties. *Barrier Polymers and Structures*, *423*, 60–91.

Wicaksono, R., Syamsu, K., Yuliasih, I., & Nasir, M. (2013). Cellulose Nanofibers from Cassava Bagasse: Characterization and Application on Tapioca-Film. *Chemistry and Materials Research*, *313*(13), 2225–956.

World Health Organization. (2014). *Global Status Report on Alcohol and Health 2014*. Geneva, Switzerland.

Wu, Y., Luo, Y., & Wang, Q. (2012). Antioxidant and antimicrobial properties of essential oils encapsulated in zein nanoparticles prepared by liquid-liquid dispersion method. *LWT - Food Science and Technology*, *48*(2), 283–290.

Xu, W., & Que Hee, S. S. (2008). Influence of collection solvent on permeation of di-n-octyl disulfide through nitrile glove material. *Journal of Hazardous Materials*, *151*(2-3), 692–698.

Yoshida, C. M. P., Antunes, A. C. B., Alvear, C., & Antunes, A. J. (2005). An absorption model for the thickness effect in hydrophilic films. *International Journal of Food Science and Technology*, *40*(1), 41–46.

Zainuddin, S. Y. Z., Ahmad, I., Kargarzadeh, H., Abdullah, I., & Dufresne, A. (2013). Potential of using multiscale kenaf fibers as reinforcing filler in cassava starch-kenaf biocomposites. *Carbohydrate Polymers*, *92*(2), 2299–305.

Zarrini, G., Delgosha, Z. B., Moghaddam, K. M., & Shahverdi, A. R. (2010). Post-antibacterial effect of thymol. *Pharmaceutical Biology*, *48*(6), 633–636.

Zhang, X., Heinonen, S., & Levänen, E. (2014). Applications of supercritical carbon dioxide in materials processing and synthesis. *RSC Adv.*, *4*(105), 61137–61152.

Zhang, Z., Zhang, R., Zou, L., Chen, L., Ahmed, Y., Al, W., … Julian, D. (2016). Food Hydrocolloids Encapsulation of curcumin in polysaccharide-based hydrogel beads : Impact of bead type on lipid digestion and curcumin bioaccessibility. *Food Hydrocolloids*, *58*, 160–170.

Zheng, Q., & Lü, C. (2014). Size Effects of Surface Roughness to Superhydrophobicity. *Procedia IUTAM*, *10*, 462–475.

Zhong, Q. P., & Xia, W. S. (2008). Physicochemical Properties of Edible and Preservative Films from Chitosan/Cassava Starch/Gelatin Blend Plasticized with Glycerol. *Food Technology and Biotechnology*, *46*(3), 262–269.

Zhong, Y., & Li, Y. (2011). Effects of storage conditions and acid solvent types on structural, mechanical and physical properties of kudzu starch (Pueraria lobata)-chitosan composite films. *Starch/Staerke*, *63*(9), 579–586.

Zhu, S., Pelton, R. H. &, & Collver, K. (1995). MECHANISTIC M O D E L L I N G OF FLUID PERMEATION, *50*(22), 3557–3572.

Zucca, A., Yamagishi, K., Fujie, T., Takeoka, S., Mattoli, V., & Greco, F. (2015). Roll to roll processing of ultraconformable conducting polymer nanosheets. *Journal of Materials Chemistry C*, *3*(25), 6539–6548.